

Proceedings of the IRE®

continued

	"An Introduction to the Theory of Random Signals and Noise," by W. B. Davenport, Jr., and W. L. Root, <i>Reviewed by W. M. Siebert</i>	1547
	"Atmospheric Explorations," ed. by H. G. Houghton, <i>Reviewed by A. W. Straiton</i>	1547
	"Soviet Education for Science and Technology," by A. G. Korol, <i>Reviewed by Ernst Weber</i>	1548
	"An Introduction to Digital Computers," by R. K. Livesley, <i>Reviewed by W. B. Cagle</i>	1548
	"Principles of Electronic Instruments," by G. R. Partridge, <i>Reviewed by Walther Richter</i> ..	1549
	"Zone Melting," by W. G. Pfann, <i>Reviewed by D. A. Jenny</i>	1549
	"Feedback Control Systems," by O. J. M. Smith, <i>Reviewed by G. S. Axelby</i>	1549
	"Electronic Semiconductors," by Eberhard Spenke, translated by D. Jenny, H. Kroemer, E. G. Ramberg, and A. H. Sommer, <i>Reviewed by G. C. Dacey</i>	1550
	"Photosensitors," by W. Summer, <i>Reviewed by Frederick Koury</i>	1550
	"Control Engineer's Handbook," ed. by J. G. Truxal, <i>Reviewed by J. M. Salzer</i>	1551
	"Van Nostrand's Scientific Encyclopedia," 3rd ed., <i>Reviewed by Gustave Shapiro</i>	1551
	Recent Books	1552
ABSTRACTS	Abstracts of IRE TRANSACTIONS	1552
	Abstracts and References	1556
IRE NEWS AND NOTES	Calendar of Coming Events and Authors' Deadlines	14A
	Call for Papers for the 1959 IRE National Convention	14A
	Professional Group News	16A
	Obituaries	16A
	National Symposium on Telemetry	16A
DEPARTMENTS	Contributors	1543
COVER	Borrowing a leaf from the microwave field, a long range directional antenna has been developed for the 7 to 24 mc range in the form of a giant tapered aperture horn 850 feet long, 500 feet wide and 250 feet high by the U.S. Army Signal Communication Engineering Agency under contract with Developmental Engineering Corp., Washington, D.C., as reported in the article on page 1510.	

BOARD OF DIRECTORS, 1958

*D. G. Fink, *President*
 C. E. Granqvist, *Vice-President*
 *W. R. G. Baker, *Treasurer*
 *Haraden Pratt, *Secretary*
 *J. D. Ryder, *Editor*
 A. V. Loughren,
Senior Past-President
 *J. T. Henderson,
Junior Past-President

1958

A. N. Goldsmith
 H. R. Hegbar (R4)
 E. W. Herold
 K. V. Newton (R6)
 A. B. Oxley (R8)

F. A. Polkinghorn (R2)

D. B. Sinclair
 *Ernst Weber
 J. R. Whinnery

1958-1959

R. I. Cole (R3)
 G. A. Fowler (R7)
 *R. L. McFarlan (R1)
 D. E. Noble
 E. H. Schulz (R5)
 Samuel Seely

1958-1960

G. S. Brown
 W. H. Doherty

*Members of Executive Committee

EXECUTIVE SECRETARY

George W. Bailey
 Evelyn Benson, *Assistant to the Executive Secretary*
 John B. Buckley, *Chief Accountant*
 Laurence G. Cumming, *Technical Secretary*
 Emily Sirjane, *Office Manager*

ADVERTISING DEPARTMENT

William C. Copp, *Advertising Manager*
 Lillian Petranek, *Assistant Advertising Manager*

EDITORIAL DEPARTMENT

Alfred N. Goldsmith, *Editor Emeritus*
 J. D. Ryder, *Editor*
 E. K. Gannett, *Managing Editor*
 Helene Frischauer, *Associate Editor*

EDITORIAL BOARD

J. D. Ryder, *Chairman*
 F. Hamburger, Jr., *Vice-Chairman*
 E. K. Gannett
 Keith Henney
 E. W. Herold
 T. A. Hunter
 G. K. Teal
 W. N. Tuttle



PROCEEDINGS OF THE IRE, published monthly by The Institute of Radio Engineers, Inc., at 1 East 79 Street, New York 21, N. Y. Manuscripts should be submitted in triplicate to the Editorial Department. Responsibility for contents of papers published rests upon the authors, and not the IRE or its members. All republication rights, including translations, are reserved by the IRE and granted only on request. Abstracting is permitted with mention of source.
 Fifteen days advance notice is required for change of address. Price per copy: members of the Institute of Radio Engineers, one additional copy \$1.25; non-members \$2.25. Yearly subscription price: to members \$9.00, one additional subscription \$13.50; to non-members in United States, Canada, and U. S. Possessions \$18.00; to non-members in foreign countries \$19.00. Entered as second class matter, October 26, 1927, at the post office at Menasha, Wisconsin, under the act of March 3, 1879. Acceptance for mailing at a special rate of postage is provided for in the act of February 28, 1925, embodied in Paragraph 4, Section 412, P. L. and R., authorized October 26, 1927. Printed in U.S.A. Copyright © 1958 by The Institute of Radio Engineers, Inc.

Airborne Instruments Laboratory Monograph on page 4A.

Proceedings of the IRE



Poles and Zeros



The "Board". The Board of Directors held its May meeting on the twelfth in Dayton, Ohio, as guests of the Dayton

Section and the PGANE Conference. As hosts the Section officers were especially gracious, and the Conference program (yes, we heard one session) was excellent. We continue to be amazed by the breed of efficient conference managers that IRE programs have developed across the country in Region after Region, while still keeping their amateur standing in good order.

As is almost universally true of our out-of-New York meetings, this one succeeded in accomplishing more than seems possible in New York. This does not necessarily mean that all the accomplishments are recorded in the minutes, however, as much of the progress occurs over the orange juice and griddle cakes, across the steak, or in the hospitable gatherings sponsored by the host groups. As is well known, captive audiences have their value and in our case a captive Board closely associating over forty-eight hours or so studies and discusses many problems of present and future not on the meeting agenda.

Over one dinner table (we had shrimp) the subject of the operations of the Professional Group on Education was discussed, and agreement reached that its purposes might best be served by deliberate study of the *details* of educational problems, rather than by abstract discussion of educational philosophies. At another gathering the National Convention of this year and several problems growing out of it were reviewed, not as subjects requiring action but for guidance in future years.

A prominent point in the meeting itself was the amount of time devoted to Regional Directors' reports, reports of visits, Section problems, finances, events, people, or needed action, giving the Directors a montage of your Section ideas and operations. Included were news of impending new Sections, creation of the South Carolina Section as the 98th, student activities, and discussion of the need for some revision of Regions in order to allow adequate coverage and promotion by the Directors in their Regions.

Again recognizing that the IRE is international in scope, the Board assigned to the Senior Past President in any year the responsibility for coordinating and fostering the activities of our Sections not now included within the boundaries of the

eight Regions, from Tel Aviv to Tokyo. The Editor hopes that this may ultimately repay some of the hospitality given the Senior² Past President and the Senior⁻² Past President on their recent trips abroad.

WESCON Again. Once more it is time for the second major IRE event of the year, WESCON, in Los Angeles on August 19-23. The Editor visited his first WESCON in 1953, when it frankly still retained some of the atmosphere which went with its rented circus tent. He must now truthfully admit that WESCON has eliminated the circus, shown fantastic development and reached a state of maturity exceeded only by the New York Convention. Certainly the combination of West Coast electronic industry, Section vitality, and Hollywood showmanship is well worth a trip to see, and with a chance to absorb a little missile, UHF, or computer technology on the side. Wishwewergoinagin!

TRANSACTIONS, Anyone? The editorial matter served to the readers of Professional Group TRANSACTIONS in the last month seems even a little more diversified than usual, and usual has lately been quite a spread. Note that *Scanning the TRANSACTIONS* in this issue shows coverage from push-button education (pills, not yet) to medical electronics, heat transfer simulators to conductive ceramics, and from industrial electronics to unmanned space ships for orbiting the moon. Such is the timeliness and diversity of material available through the TRANSACTIONS to members of the Professional Groups, now numbering 70,565.

We have previously pointed to the fantastic breadth of the field being enveloped and encompassed by today's electronic engineers and the *Scanning the TRANSACTIONS* page confirms this. Conversely, we can remember when *radio* was not so comprehensive, ceramic materials were used to hang up antennas and were the concern of the ceramic engineer, when heat transfer was what the mechanical engineer had not provided when the plate dripped, when a millisecond was fast, when sidebands were mathematical fiction, when industrial control designers would not tolerate the hint that there was a better way than a contactor, or that a vacuum tube could be trusted to do tomorrow what it had done today, and space ships were out of this world.

Yes, and we can also remember when electronics was concerned with conduction of electrons through gas or space.

—J.D.R.

Glenn A. Fowler

Director, 1958-1959



Glenn A. Fowler was born at Fresno, Calif., on June 1, 1918. He attended the University of California at Berkeley and obtained the Bachelor's degree in electrical engineering in 1941.

From May, 1941 to December, 1943, Mr. Fowler was a member of the staff at the Radiation Laboratory of Massachusetts Institute of Technology, where he engaged in the development of microwave radar systems. The headquarters of the Army Air Forces then utilized his services as a consultant from December, 1943 to November, 1945 in connection with Air Force airborne radar systems. In May, 1945 he undertook a special assignment at the first atomic bomb test site at Los Alamos, N. M. From that date to November, 1949,

he was a member of the staff of Los Alamos Scientific Laboratories and worked at their established field test facilities at Albuquerque, N. M., and Salton Sea, Calif.

When Sandia Corporation was formed in November, 1949, he became its Director of Field Testing and Director of Electronics. He is now Sandia's Vice-President in Charge of Research.

Mr. Fowler, a member of Tau Beta Pi and Eta Kappa Nu, also holds membership in the AIEE. He is a past chairman of the Albuquerque-Los Alamos IRE Section, and a member of the IRE Appointments and Editorial Reviewers Committees. He joined the IRE as an Associate Member, and in 1948 he became a Senior Member.

Scanning the Issue

Batteries (Morehouse, *et al.*, p. 1462)—The PROCEEDINGS presents this month an invited review paper on a subject that is three times as old as radio itself. Despite its venerable age the battery nonetheless represents a field that is currently the center of a surprising amount of important activity. Starting from Volta's discovery of the galvanic cell in 1800, the battery industry has steadily grown to where today it is a husky half-billion dollar industry. Of the many users of batteries, none has a more vital interest in them than the radio engineer. Among all the components he deals with, few can exert such a direct and controlling influence on the design and application of the equipment he builds. His needs, in turn, have been instrumental in greatly stimulating research and development of new and improved types of batteries, especially in the last 15 years. Readers will find in this paper a thorough, yet compact, review of the various types of batteries, how they work, and where they are used. The discussion includes recently developed nuclear and solar-energy power sources as well as the more conventional electrochemical types, and is backed up by an excellent bibliography of over 100 references on the subject.

The Resnatron As a 200-MC Power Amplifier (Tucker, *et al.*, p. 1483)—The tube described in this paper boasts a mighty 3.5 million watts pulsed peak power output at 200 megacycles. It stands 15 feet high, weighs 2½ tons, and its filament draws a mere 7000 amperes. The tube is called a resnatron, which denotes a type of tetrode in which the cavities and tuners are located inside the tube envelope instead of outside. The resnatron was first developed 20 years ago and has an established reputation as a high power tube. Although this type of tube and its operating principles are well known, the development reported here is of more than usual interest because it represents a spectacular jump to megawatt power levels in a frequency range too low to be served by klystrons. While the tube was developed for a very special application—a linear proton accelerator—the problems encountered and techniques used to achieve such a high power output will be of direct interest to designers of high power tubes of all types, as well as of broad interest to systems engineers in general.

Atmospheric Effects on VHF and UHF Propagation (Millman, p. 1492)—The recent advent of earth satellites, guided missiles, and very long range radars has focused considerable attention on the effects of the atmosphere on the propagation of radio waves. Propagation irregularities which formerly were a matter of only academic interest have now become important practical factors in the performance of new long-range systems. For example, it is unlikely that until recently anyone was at all interested in whether the atmosphere would introduce errors in Doppler frequency velocity measurements of objects hundreds of miles away. Yet, in addition to Doppler errors, the ionosphere and troposphere cause changes in the direction of radio waves, time delays, polarization rotations, and attenuation. This paper gives a timely compilation of pertinent theories and data regarding all these effects and presents them in the form of curves and equations which are readily applicable to practical situations.

Atmospheric Noise Interference to Medium Wave Broadcasting (Aiya, p. 1502)—This is one of a series of papers by the same author which investigate various types of electrical discharges associated with thunderstorms and the resulting interference effects they produce. It is a companion to a paper that appeared here last March which dealt with interference in the short wave band. The present paper is concerned with the broadcast band. It differs from the earlier work in that the discharge that gives rise to noise in the broadcast band differs from the one responsible for noise in the short wave band. For example, it is found that lightning discharges within a cloud, which make up 90 per cent of the discharges in a typical storm, do not radiate any significant power below 2.5 megacycles. Thus in the broadcast band, atmospheric interference is due entirely to cloud-to-ground and cloud-to-air discharges, which account for only 10 per cent of the total number of discharges. This study provides a good physical picture and quantitative description of the main source of interference to commercial radio broadcasting.

Suppression of Undesired Radiation of Directional HF Antennas and Associated Feed Lines (Brueckmann, p. 1510)—Many old timers, and perhaps some young timers, too, who find contemporary papers "too mathematical" will have little complaint with this paper which does not contain a single equation. Instead it gives a down-to-earth engineering discussion of the factors responsible for antenna radiation in undesired directions and radiation from balanced open-wire antenna feed lines, and how these causes of interference can be minimized. The discussion is concerned primarily with long range point-to-point communication systems in the 5 to 25-megacycle range, as typified by transoceanic radio stations. In addition to providing broad practical guide lines to good antenna design, two specific developments of interest are reported. One is a novel antenna composed of an array of radiators which form the shape of a giant tapered horn 850 feet long, 560 feet high, and 250 feet wide at the mouth. This antenna has the distinction of outperforming the rhombic antenna, which has been the mainstay of long-range radio stations for a good 30 years. The other development is a wide-band matching transformer which makes feasible the use of coaxial cable in place of open wire feed lines to reduce undesired radiation.

Optimum Noise Performance of Linear Amplifiers (Haus and Adler, p. 1517)—This paper introduces an important new measure of the noise performance of any given type of linear amplifier. This measure takes into account not only the impedance of the source connected to amplifier input and the noise figure of the amplifier, but also the gain of the amplifier stage. By taking gain into account it is able to deal with the case where feedback is applied to an amplifier, a situation in which former measures of noise performance broke down. This new measure of noise thus makes it possible to specify the best noise performance achievable with any type of amplifier. Perhaps the most important property established by the new noise measure is the fact that a cascade of amplifiers of different types cannot have an excess noise figure at high gain that is better than that obtained with amplifiers of the "best" noise class alone.

Scanning the TRANSACTIONS appears on page 1545.



Batteries*

C. K. MOREHOUSE†, R. GLICKSMAN†, AND G. S. LOZIER†

The following paper is one of a planned series of invited papers, in which men of recognized standing will review recent developments in, and the present status of, various fields in which noteworthy progress has been made.—*The Editor*

Summary—A review is given of the chemical compositions, structures, performance characteristics, and applications of various primary and secondary batteries. Both batteries produced presently, and those in the development stages are included.

The following primary batteries have been discussed: dry, solid-electrolyte, wet, reserve, fuel, and EMF standards. The secondary battery section covers a review of lead-acid, nickel-iron, nickel-cadmium, zinc-silver oxide, and cadmium-silver oxide batteries.

Also included is a review of the various nuclear batteries and solar converters showing the relationship to each other and the electrochemical batteries.

I. INTRODUCTION

THE battery industry dates back to Volta's discovery of the galvanic cell in 1800. Prior to the development of the dynamo, batteries were the only practical source of continuous electric current. Although they were replaced as a primary power source toward the end of the nineteenth century, there has been a growing demand for small portable power supplies, resulting in a continued growth in the battery industry through the years. In 1957 about 500 million dollars worth of batteries were produced in the United States alone.

During the first part of the twentieth century, storage batteries for automobiles and dry cells for flashlights were the familiar types. World War II brought a sudden demand for new batteries that greatly stimulated research and development. This led to improved types for existing applications, as well as new batteries to meet new service requirements. Although many of these new batteries may never appear in the civilian market, they nevertheless are important both technically and to our national defense.

Along with new electrochemical batteries, which use chemical energy as their energy source, several new portable power supplies have been developed which use nuclear or solar energy as their energy sources. These devices as yet are not major competitors to the conventional batteries, but are finding some use in specialized applications.

In this paper a review is given of the structures, performance characteristics, and applications of the various electrochemical power supplies. This includes those commercially available, and the important types under development. For completeness, the various nuclear and solar batteries are included and compared with the conventional electrochemical types.

II. DIRECT CONVERSION OF CHEMICAL ENERGY INTO ELECTRICAL ENERGY

Electrochemical processes are the most efficient known for the conversion of one form of energy into usable electrical energy. Batteries, of which a number of different types are produced commercially, are examples of devices which use these processes to convert stored chemical energy directly into electrical energy. They are generally classified into two groups: 1) primary and 2) secondary batteries. The distinction between the two groups is based on the nature of the chemical reactions. Primary batteries are discarded when sufficient electrical energy can no longer be obtained from them (*e.g.*, Leclanché flashlight batteries). Secondary batteries, on the other hand, convert chemical energy into electrical energy by chemical reactions that are essentially reversible. Thus, by passing the current in the reverse direction to that during discharge, the chemicals are restored to their original state (*e.g.*, lead-acid secondary battery).

A battery, of either primary or secondary type, consists of two or more cells connected in either a series, parallel, or series-parallel arrangement to provide different voltages and currents. The cell which is the unit part of the battery consists of five essential components. These are:

Anode—the negative electrode from which electrons flow into the external circuit. Chemically, anodes are reducing agents, characterized by the ease with which they give up electrons and go into solution, forming positive ions.

Cathode—the positive electrode into which electrons flow from the external circuit. Chemically, cathode materials are oxidizing agents, characterized by the ease with which they accept electrons. In so doing, they are reduced to a lower oxidation state.

Electrolyte—a solution that permits ionic conduction between the anode and cathode.

Separator—an inert, porous insulating medium that physically separates the anode and cathode, while permitting the movement of ions in solution between the electrodes.

Seal—means for preventing loss of the electrolyte and water, while permitting gas to escape.

A schematic diagram in Fig. 1 illustrates the electrode processes which occur when electrical energy is with-

* Original manuscript received by the IRE, April 17, 1958.

† RCA Laboratories, Princeton, N. J.

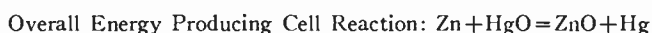
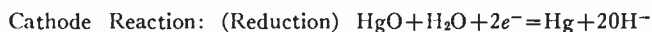
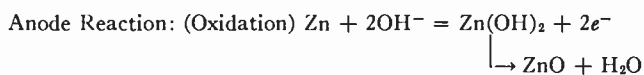
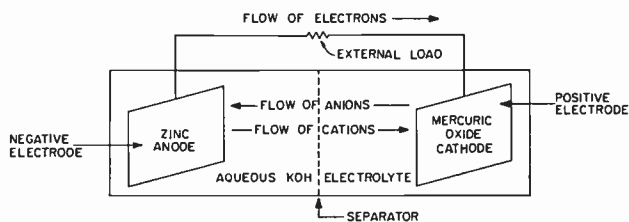
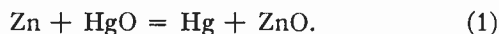


Fig. 1—Electrode reactions and relative flow of electrons and ions during the discharge of a zinc-mercuric oxide dry cell.

drawn from a zinc-mercuric oxide dry cell. Although the chemical reactions vary for each electrochemical cell, the principles are the same for all types.

The theoretical energy that can be obtained from an electrochemical cell of either primary or secondary type is derived from the chemical reactions that occur at the anode and cathode. For example, the chemical reaction which takes place in a zinc-mercuric oxide dry cell is,

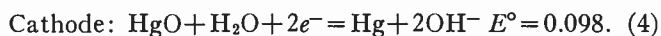


The free energy change (ΔF) for this reaction is related to the potential of this couple by the following equation,

$$-\Delta F = nFE, \quad (2)$$

where F is the Faraday (96,494 coulombs), n the electron change, and E the electromotive force of the cell. From the free energies of the substances involved, the EMF of this cell is calculated to be 1.34 volts.

The EMF of the cell can also be obtained from the half-cell electrode reactions which are shown below along with their reversible potentials (E°):



The potentials at the anode and cathode are also dependent upon the type and concentration of electrolyte (in accordance with the Nernst equation). For the zinc-mercuric oxide cell with a potassium hydroxide electrolyte, the anode potential (E_A) is 1.317 volts, while the cathode potential (E_c) is +0.028 volt.

The EMF of this cell is equal to the sum of the anode and cathode potentials, *i.e.*,

$$E_{\text{cell}} = 1.317 + 0.023 = 1.34 \text{ volts}$$

and the over-all reaction (1) is obtained by taking the sum of the two half-cell reactions, (3) and (4). Thus, from a knowledge of the reversible half-cell potentials, reactions, and electrolyte, the theoretical potential of any electrochemical couple can be calculated.

Table I and Table II (p. 1464) list pertinent data [1], [2] for various anode and cathode materials now used in electrochemical cells. Included in these tables are the theoretical ampere-minute capacities of the various

anode and cathode materials which give the theoretical quantity of electricity available from one gram of material. These values, which are calculated on the basis of Faraday's law, are directly proportional to the number of Faradays per mole involved in the electrochemical reaction and inversely proportional to the molecular weight and volume of the material.

In coupling any of these anode and cathode materials to make an electrochemical cell, it must be kept in mind that they should be compatible with the particular electrolyte used, the extent of compatibility depending upon the particular application. For example, the use of a cathode such as mercuric oxide and an anode such as magnesium in acid solutions would not be advisable due to the high solubility of mercuric oxide and high rate of corrosion of magnesium in acidic electrolytes.

In practice, most electrodes operate at potentials lower than their reversible values, due to polarization effects encountered under load conditions, while their electrode efficiencies also vary with current drain. In addition to the energy losses due to the irreversibility of the electrode reactions, additional losses are encountered in cells due to ohmic IR losses (*i.e.*, resistance of cell components) or deleterious side effects which limit the amount of active material available for the energy producing chemical reactions. Examples of these are the corrosion of metal anodes, or the solubility of the cathode material in the electrolyte, resulting in diffusion to and reaction with the anode material.

Although the principles discussed previously are common to all electrochemical cells, the technical problems will vary from one type of cell to another, due to the use of different electrode materials, constructions, and applications. In the following parts the various primary and secondary cells are discussed in greater detail.

A. Primary Cells

Primary cells include several types designed for different applications. These are subdivided as follows: 1) dry, 2) solid-electrolyte, 3) wet, 4) reserve, 5) fuel, and 6) standard cells.

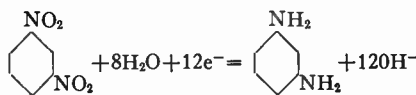
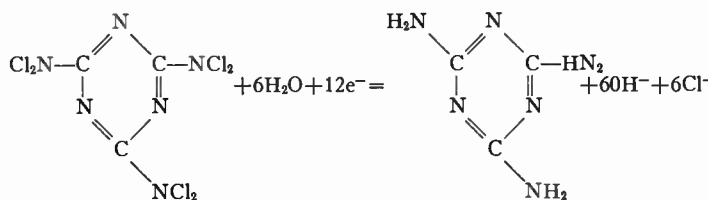
1) *Dry Cells*: The name, dry cells, is a misnomer as the cells actually contain an aqueous electrolyte which is immobilized, and does not spill out when the cells are inverted. Three types of dry cells are presently produced in quantity in this country. The chemical composition of these cells, together with those of the important new cells now under development, are listed in Table III (p. 1465). Also included in the table are the energy producing chemical reactions, approximate average operating voltages, and watt-minute capacities as measured on a light-drain application. In addition, pertinent references are cited in case the reader is interested in more detailed information.

a) *Leclanché cells*: Approximately 90 per cent of the dry cells produced annually in the United States are zinc-manganese dioxide cells, commonly called Leclanché cells after their inventor [22]. The original cells made by Leclanché in 1868 had a spillable electrolyte.

TABLE I
HALF-CELL REACTIONS, POTENTIALS, AND CAPACITY DATA FOR VARIOUS ANODE MATERIALS

Anode Material	Half-Cell Reaction	Half-Cell Potential (volts)		Theoretical Ampere-Minute Capacity	
		E°_{Acid}	E°_{Base}	per gram	per cm^3
Sodium	$\text{Na} = \text{Na}^+ + e^-$	2.71		69.9	67.8
Magnesium	$\text{Mg} + 2\text{OH}^- = \text{Mg}(\text{OH})_2 + 2e^-$		2.67	132.2	230
Magnesium	$\text{Mg} = \text{Mg}^{++} + 2e^-$	2.37		132.2	230
Aluminum	$\text{Al} = \text{Al}^{+++} + 3e^-$	1.67		178.9	483
Zinc	$\text{Zn} + 2\text{OH}^- = \text{Zn}(\text{OH})_2 + 2e^-$		1.245	49.2	351
Zinc	$\text{Zn} = \text{Zn}^{++} + 2e^-$	0.76		49.2	351
Indium	$\text{In} + 3\text{OH}^- = \text{In}(\text{OH})_3 + 3e^-$		1.0	42.0	307
Cadmium	$\text{Cd} + 2\text{OH}^- = \text{Cd}(\text{OH})_2 + 2e^-$		0.81	28.8	248
Iron	$\text{Fe} + 2\text{OH}^- = \text{Fe}(\text{OH})_2 + 2e^-$		0.88	57.6	455
Lead	$\text{Pb} = \text{Pb}^{++} + 2e^-$	0.13		15.6	176
Lead	$\text{Pb} + \text{SO}_4^{--} = \text{PbSO}_4 + 2e^-$	0.37		15.6	176
Hydrogen	$\text{H}_2 = 2\text{H}^+ + 2e^-$	0.00		1596	112
Hydrogen	$\text{H}_2 + 2\text{OH}^- = 2\text{H}_2\text{O} + 2e^-$		0.828	1596	112

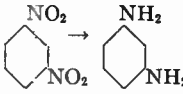
TABLE II
HALF-CELL REACTIONS, POTENTIALS, AND CAPACITY DATA FOR VARIOUS CATHODE MATERIALS

Anode Materials	Half-Cell Reaction	Half-Cell Potential (volts)		Theoretical Ampere-Minute Capacity	
		E°_{Acid}	E°_{Base}	Per Gram	Per cm^3
Manganese Dioxide	$\text{MnO}_2 + 4\text{H}^+ + 2e^- = \text{Mn}^{++} + 2\text{H}_2\text{O}$	+1.23		37.4	188.1
Manganese Dioxide	$\text{MnO}_2 + \text{H}_2\text{O} + e^- = \frac{1}{2} \text{Mn}_2\text{O}_3 \cdot \text{H}_2\text{O} + \text{OH}^-$		+0.17	18.5	93.1
Mercuric Oxide	$\text{HgO} + \text{H}_2\text{O} + 2e^- = \text{Hg} + 2\text{OH}^-$		+0.098	14.8	165
Lead Dioxide	$\text{PbO}_2 + \text{SO}_4^{--} + 4\text{H}^+ + 2e^- = \text{PbSO}_4 + 2\text{H}_2\text{O}$	+1.685		13.4	125
Lead Dioxide	$\text{PbO}_2 + \text{H}_2\text{O} + 2e^- = \text{PbO} + 2\text{OH}^-$		+0.247	13.4	125
Nickel Dioxide	$\text{NiO}_2 + 2\text{H}_2\text{O} + 2e^- = \text{Ni}(\text{OH})_2 + 2\text{OH}^-$		+0.49	32	~110
Silver (II) Oxide	$2\text{Ag}_2\text{O} + \text{H}_2\text{O} + 2e^- = \text{Ag}_2\text{O} + 2\text{OH}^-$		+0.570	26.0*	193*
Silver (I) Oxide	$\text{Ag}_2\text{O} + \text{H}_2\text{O} + 2e^- = 2\text{Ag} + 2\text{OH}^-$		+0.345	13.9	99.2
Silver Chloride	$\text{AgCl} + e^- = \text{Ag} + \text{Cl}^-$	+0.222		11.2	62.5
Cupric Oxide	$2\text{CuO} + \text{H}_2\text{O} + 2e^- = \text{Cu}_2\text{O} + 2\text{OH}^-$		-0.159	40.4*	261*
Cuprous Oxide	$\text{Cu}_2\text{O} + \text{H}_2\text{O} + 2e^- = 2\text{Cu} + 2\text{OH}^-$		-0.357	20.2	121
Cuprous Chloride	$\text{CuCl} + e^- = \text{Cu} + \text{Cl}^-$	+0.137		16.7	58.9
Bismuth Oxide	$\text{Bi}_2\text{O}_3 + 3\text{H}_2\text{O} + 6e^- = 2\text{Bi} + 6\text{OH}^-$		-0.457	20.7	184
Oxygen	$\text{O}_2 + 2\text{H}_2\text{O} + 4e^- = 4\text{OH}^-$		+0.40	201	229
Chlorine	$\text{Cl}_2 + 2e^- = 2\text{Cl}^-$	+1.360		45.3	68.0
m-Dinitrobenzene			-0.15†	114.9	181.5
Hexachlorelemamine			+1.00†	58.0	~92.8

* Calculated on the basis of 2-electron change per mole of oxide.

† Potentials reported are operating potentials, *i.e.*, under load conditions.

TABLE III
CHEMICAL COMPOSITION AND PERFORMANCE CHARACTERISTICS OF VARIOUS DRY CELLS

Type	Cell Components			Energy Producing Reaction
	Anode	Electrolyte	Cathode	
Commercial cells Leclanché	Zn	NH ₄ Cl-ZnCl ₂	MnO ₂	Zn+2MnO ₂ →ZnO·Mn ₂ O ₃ *
Zinc-Mercuric Oxide (RM)	Zn	KOH	HgO	Zn+HgO→Hg+ZnO
Alkaline Zinc-Manganese Dioxide (Crown)	Zn	NaOH	MnO ₂	Zn+2MnO ₂ →Mn ₂ O ₃ +ZnO
New cell developments Magnesium-Manganese Dioxide	Mg	MgBr ₂	MnO ₂	Mg+H ₂ O+2MnO ₂ →Mn ₂ O ₃ +Mg(OH) ₂
Magnesium-Organic	Mg	MgBr ₂	M-Dinitro-ben- zene, etc.†	6Mg+8H ₂ O+  +6Mg(OH) ₂
Magnesium-Bismuth Oxide	Mg	MgBr ₂	Bi ₂ O ₃	3Mg+3H ₂ O+Bi ₂ O ₃ →2Bi+3Mg(OH) ₂
Air	Zn	NaOH	O ₂ (Air)	Zn+½ O ₂ →ZnO
Indium	In	KOH	HgO	2In+3HgO→3Hg+In ₂ O ₃
Aluminum	Al	AlCl ₃ -(NH ₄) ₂ Cr ₂ O ₇	MnO ₂	2Al+3H ₂ O+6MnO ₂ →3Mn ₂ O ₃ +2Al(OH) ₃

Type	Open Circuit Voltage (volts)	Average Operating Voltage‡ (volts)	Capacity Watt-Minutes		References
			Per Gram of Cell‡	Per cm ³ of Cell‡	
Commercial cells Leclanché	1.5-1.65	1.25	4.0	6.1	[3], [4]
Zinc-Mercuric Oxide (RM)	1.34	1.30	7	32	[3], [5]-[8]
Alkaline Zinc-Manganese Dioxide (Crown)	1.52	1.15	2.6	8.1	[9]
New cell developments Magnesium-Manganese Dioxide	1.8-2.0	1.4-1.5	5.8	12	[10]-[12]
Magnesium-Organic	1.65	1.15	8.5	12	[13]-[16]
Magnesium-Bismuth Oxide	1.6	1.03	6.2	12	[17]
Air	1.4-1.5	1.2-1.3	—	—	[3], [18], [19]
Indium	1.15	1.05	—	—	[20]
Aluminum	1.7	1.3	—	—	[21]

* Example of one of several reactions which can occur in a Leclanché dry cell.

† Example of one of many organic cathode materials which can be used.

‡ Approximate results for a light drain application.

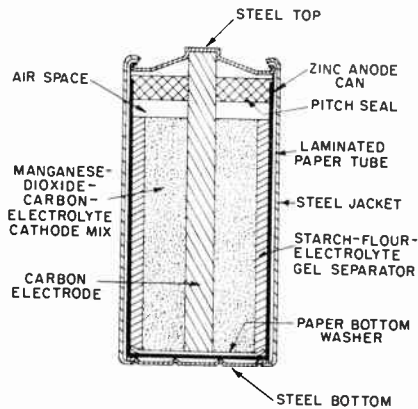


Fig. 2—Cross section of a typical cylindrical flashlight dry cell.

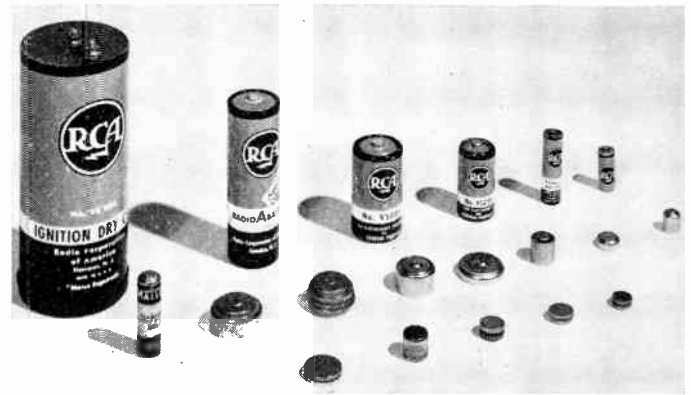


Fig. 4—Various sizes of dry cells. Back row: Leclanché. Middle row: zinc-mercuric oxide (RM). Front row: alkaline zinc-manganese dioxide (crown).

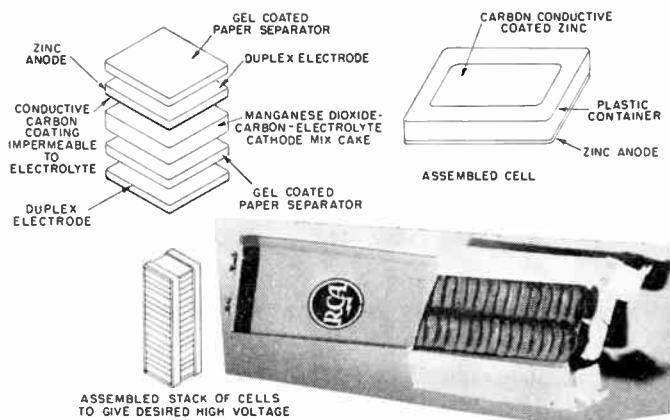


Fig. 3—A typical Leclanché flat-cell construction.

In spite of their large size they were capable of supplying only small currents. At the end of the nineteenth century, improved cell designs [23], [24] appeared with an immobilized electrolyte, thus marking the approximate beginning of the dry cell industry. Today, in the United States, two billion cells are produced annually as compared to 34 million cells produced in 1909 [25].

Along with this growth, there also has been a continued improvement in performance. For example, over the past thirty years performance gains ranging up to 400 per cent have been reported [26], [27]. These gains, which have been the result of a continued research and development effort by the industry, have been due to changes in cell design, elimination of harmful impurities, and the use of higher grade materials which allow for the more efficient conversion of the available chemical energy into usable electrical energy.

Two basic cell designs of the Leclanché type are presently being manufactured. Cross sections of cylindrical, and of flat or layer-built constructions, are shown in Figs. 2 and 3. These two basic designs are made in a number of different sizes, a few of which are illustrated in Fig. 4.

The majority of cylindrical cells contain an amalgamated zinc can which is the negative electrode and functions as the anode and container of the cell. The cylindrical core (positive electrode) is formed from a mixture of manganese dioxide and carbon which is wet with electrolyte. A carbon rod which acts as the positive terminal

is inserted in the center of the cathode mix. The two electrodes are separated by a starch-flour gel also containing some electrolyte.

Some manufacturers use a "metal-clad" construction [28] in which the entire cell, surrounded by an insulating jacket, is encased in a steel tube. This metal construction has the feature of retarding cell leakage caused by zinc can perforation. Others have used modified starch paste separators [29] to make a more leak-resistant cell. In this latter case the starch does not undergo decomposition during cell discharge, and any liquid which escapes from the cell can be readily absorbed in a suitable paper jacket.

Although most of the cylindrical cells are of the previously described construction, one manufacturer makes an "inside-out" cell [30]. This cell has the terminals reversed with the negative zinc anode in the center of the cell. The advantages claimed for this cell are better utilization of zinc and freedom from leakage due to zinc can perforation.

The need for space economy in the high-voltage batteries for radio "B" application has led to the design of flat cells [31]–[33]. The first flat cell battery known as the "minimax" construction [31] was developed by the National Carbon Company. The essential feature of these designs is a duplex electrode, consisting of a flat sheet of zinc, on one side of which is an adherent conductive coating impermeable to the electrolyte composed of carbon mixed with a plastic binder. One side of the zinc serves as the anode of one cell, while the conductive-coated side serves as the positive electrode of the adjacent cell and makes contact with the manganese dioxide cathode. A gel coated paper separates the two cell electrodes. The cells, which are contained in a plastic envelope, as illustrated, are stacked to give the desired voltage, taped to maintain low-contact resistance, and sealed by dipping in wax to prevent moisture loss.

Although the control of all cell components is important from the standpoint of performance, the manganese dioxide cathode is generally considered as the limiting component of Leclanché cells for many applications. For example, the efficiency of the manganese dioxide electrode varies from less than 10 per cent on very heavy current drain applications (D-size flashlight cells dis-

charged continuously at drains greater than 0.5 ampere) to over 90 per cent on light drain applications (radio B).

At present most of the manganese dioxide used in dry cells comes from the African Gold Coast. There is, however, a definite trend to use manganese dioxides which are prepared synthetically by chemical or electrolytic processes as the natural ore supply becomes depleted, and the demand increases for high-cell capacity per unit of weight and volume. The more costly synthetic materials differ from the naturally occurring manganese dioxide in crystal structure, particle size, impurities, and chemical activity. They are used at present in cells designed for high-current drain usage, such as encountered in many industrial and military applications.

The open circuit voltage of Leclanché dry cells ranges between 1.5 and 1.6 volts depending upon the electrolyte composition and type of manganese dioxide used. It decreases about 0.0004 volt per °C over the temperature range of 25°C to -20°C. The ampere-hour and watt-hour capacity or hours of service to the specified end voltages are dependent upon the size of cell, and the rate at which energy is withdrawn from the cell. The lower the rate, the more efficient conversion of the available chemical energy into usable electrical energy. Intermittent type of service is generally preferred, especially for heavy current drain usage. As a rough rule, heavy drain may be defined as meaning any drain which results in a service life of 10 hours or less. In addition, cell capacity is affected by temperature of operation, falling off with decreasing temperature. The cells become inoperative at about -30°C due to freezing of the electrolyte. The low-temperature performance of Leclanché dry cells can be considerably improved and their operation extended to below -40°C by changing to an electrolyte with a lower freezing point [34]-[37].

Shelf life is dependent on quality of manufacturer, cell size, cell formulation, and temperature of storage. In general, for any given manufacturer, the smaller the cell size, the shorter shelf life. Storage temperature has a marked effect on shelf life, the lower the temperature, the longer the shelf life. For example, A-size cells stored for 24 months at 21.1°C gave only 50 per cent of their initial capacity, whereas 70 per cent and 90 per cent capacity retention were obtained from comparable cells stored at 7.2°C and -17.8°C, respectively [27].

The large number of cell sizes and applications has led to the adoption of a considerable number of tests, each intended to simulate some kind of service, as for example, flashlights, portable radios, hearing aids, telephones, or military services. Some of these tests are described in American Standards Specification C 18.1-1954 [38], or the Signal Corps Specification [39]. Most tests involve discharging the cell or battery through a constant resistance simulating the current drain required to power the particular equipment. For example, a flashlight test consists in discharging a single cell through a 2½-ohm resistance until it reaches 0.65 volt. This simulates the drain on each cell in a two cell flashlight containing a 0.5-ampere bulb. As most dry cells are not subjected to exhaustive continuous service, the

majority of the standard tests are intermittent in nature varying from a few minutes of discharge a day to continuous usage. For example, general purpose flashlight cell tests require that the cell be discharged for five consecutive minutes a day, whereas radio battery tests require that the cells or batteries be discharged two or four hours a day. Capacity data, which should be gathered at 21.1°C, are generally reported as hours or minutes of service to specified end voltages. Typical discharge curves and capacity data for Leclanché dry cells compared with other dry cells are shown in Fig. 6 and Fig. 9 through Fig. 11.

b) *Zinc-mercuric oxide cells:* The alkaline zinc-mercuric oxide system was first suggested by Clarke [40] in 1884. Although there were a number of additional attempts made over the years [41]-[44] to design a practical cell using this system, it was not until early in World War II that a commercially usable mercuric oxide dry cell was invented by Ruben [5].

Cells of this general classification contain an amalgamated zinc anode in the form of either a finely divided powder or a coiled corrugated strip. The cathode consists of a mixture of red mercuric oxide with about 5 per cent graphite molded under pressure into a steel cup or pressed as a discrete part and assembled into the cell, depending on the type of cell produced. The electrolyte is an aqueous potassium hydroxide solution containing zinc oxide, and the separator is composed of two materials: a cellulosic material to immobilize the electrolyte, and a barrier material such as microporous plastic interposed between the cathode and the cellulosic material. Two typical constructions which are commercially available are shown in Fig. 5.

The open circuit voltage of mercuric oxide cells is 1.345 volts which is in close agreement with the thermodynamically calculated value for this electrochemical system. These cells have a flat voltage-time discharge curve operating for most of their discharge life between 1.34 and 1.24 volts, depending upon the current drain; the lighter the current drain, the nearer the closed circuit voltage of the cell is to its open circuit voltage. A typical discharge curve for this cell compared with a comparable size Leclanché cell is shown in Fig. 6.

Compared with the Leclanché cell, zinc-mercuric oxide dry cells have several desirable features, namely: 1) a more constant voltage during discharge life, 2) a greater watt-hour capacity per unit of volume and weight, and 3) reportedly better shelf life during storage at elevated temperatures of 45°C and 54.5°C.

In spite of these favorable characteristics, only about 10 per cent of the total dry cells produced annually in this country are of the mercuric oxide type, the reason being the large difference in basic material cost. Mercuric oxide costs approximately six dollars per pound compared to \$0.07 a pound for manganese dioxide. Because of this high cost differential, the mercuric oxide cell has not replaced the Leclanché cell to any appreciable extent in sizes larger than the AA-size (volume 0.43 in³), these sizes are used in the lighting field. For lighting applications the initial cost of the cell or battery

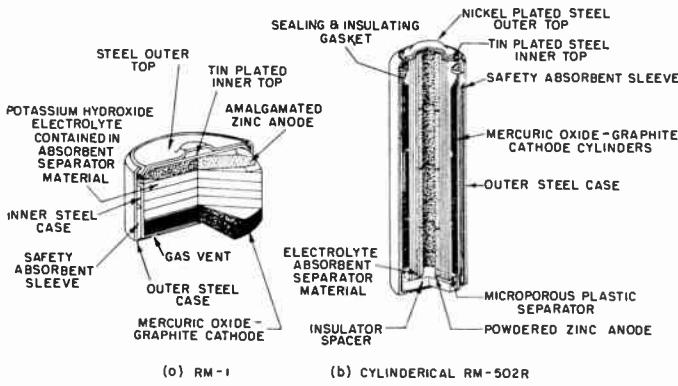


Fig. 5—Cross sections of two typical zinc-mercuric oxide dry cells (manufactured by P. R. Mallory Co.)

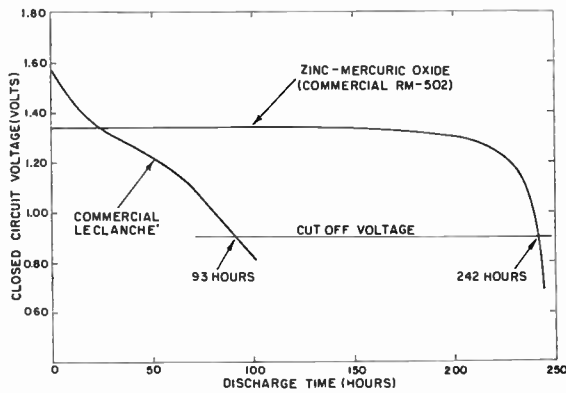


Fig. 6—AA-size penlight dry cells discharged continuously through 150-ohm resistances (simulates current drain encountered in a transistor-operated receiver).

is undoubtedly a more important factor to the consumer than cost or volume per unit of service.

Mercuric oxide cells, however, find use in both military and civilian applications, where capacity per unit of volume and constancy of voltage are important factors. Some of these applications are: hearing aids, small portable radios, portable communication equipment, electrical test apparatus, scientific instruments, and as reference potentials in instruments where the extreme precision of a Weston Standard cell is not required.

Zinc-mercuric oxide dry cells are made in a variety of cell sizes, some of which are illustrated in Fig. 4.

c) *Alkaline zinc-manganese dioxide cells:* A third type, known as "crown cells" because of their crown cap construction [9], is produced in small quantities in this country. These small cells which are similar in construction to the zinc-mercuric oxide cells are composed of a manganese dioxide cathode, an aqueous sodium hydroxide electrolyte, and an amalgamated powdered zinc anode. They have an open circuit potential of 1.52 volts and are most suitable for low-drain applications. Whereas these cells do not give as high a capacity as comparable size mercuric oxide cells, they have a cost advantage in that they contain a cheaper cathode material. Improved performance with a subsequent increase in material cost can be obtained by adding mercuric oxide to the manganese dioxide cathode mix.

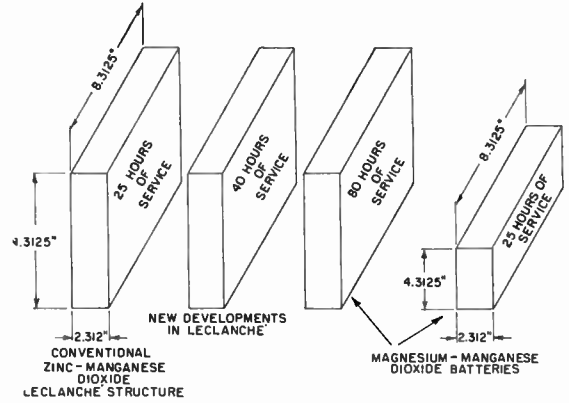


Fig. 7—Relative performance of conventional BA279/U Leclanché as compared to magnesium-manganese dioxide dry cell batteries (BA279/U batteries are used in the Signal Corps handy-talkie AN/PRC-8, 9, 10 transceivers).

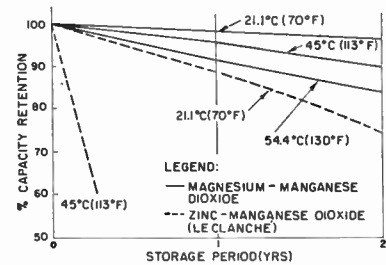


Fig. 8—Shelf life at various storage temperatures of magnesium-manganese dioxide flashlight size cells compared with comparable size commercial Leclanché dry cells.

d) *New dry cell developments:* The zinc-manganese dioxide Leclanché cell has been the dominant dry cell system for over 50 years despite the existence of other theoretically more attractive anode (e.g., Mg, Al) and cathode (e.g., O₂, organic) materials. However, it was not until recently that some of these materials became readily available, and that the electrochemical characteristics were sufficiently understood to enable practical cells to be designed.

In addition, new applications have appeared which require performance characteristics different from those of the conventional cells. This has resulted in several new developments using materials which, although not as attractive on the basis of available energy per unit of weight and volume, have other desirable properties which are important to meet the new requirements.

The status of these new dry cells is briefly reviewed in the following paragraphs.

Magnesium cells: Theoretically magnesium is a more attractive anode material for primary cells than zinc, having a considerably higher reversible electrode potential, and more than twice the ampere-hour capacity per unit of weight. Many attempts [45] have been made over the years to design a practical magnesium electrochemical cell, but it was not until the last ten years that several significant developments have been reported. These have involved the coupling of a magnesium anode and an aqueous magnesium bromide electrolyte with such cathode materials as manganese dioxide, bismuth

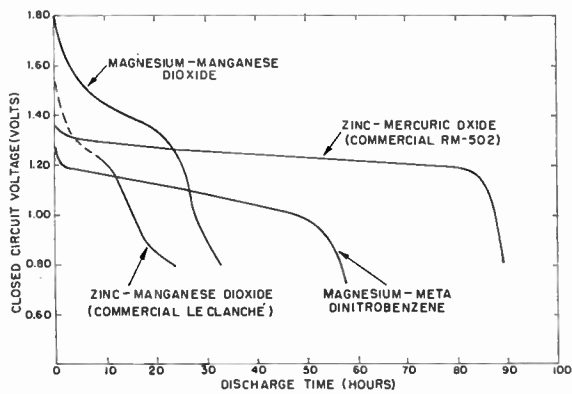


Fig. 9—AA-size penlight dry cells discharged continuously through 50-ohm resistances (simulates current drain encountered in some portable radios).

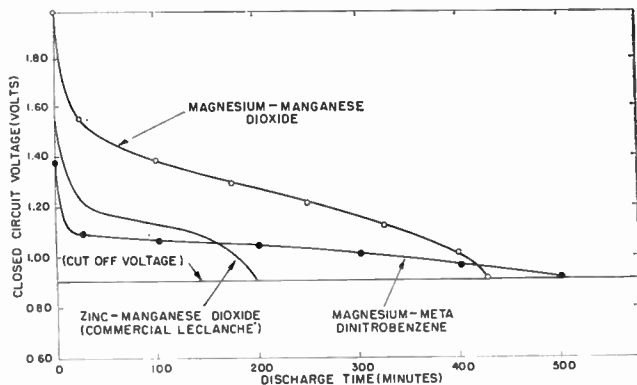


Fig. 10—C-size flashlight dry cells discharged intermittently through 4-ohm resistances (4 minutes per hour, 8 hours per day) (simulates use with 0.25-ampere flashlight bulb).

oxide, and a number of organic compounds. Each of these new dry cells has some desirable characteristics, and offers the possibility of replacing the conventional dry cells for certain applications.

The magnesium-manganese dioxide cells described by Kirk, Fry, and George [10]–[12] are constructed similarly to the Leclanché using an impact extruded magnesium alloy can. They have a sloping voltage-time discharge curve as does the Leclanché cell, but operate at 0.1 to 0.3 volt higher. These cells give double the watt-hour capacity of zinc-Leclanché dry cells on a number of tests corresponding to flashlight, lantern, and radio application. Some of the performance gains on military tests [46] are illustrated in Fig. 7. In addition to the capacity advantages, the magnesium-manganese dioxide cells are reported [46] to have a better shelf life than the Leclanché dry cells, especially at the elevated storage temperatures (Fig. 8).

The second important magnesium cell development involves the use of organic cathode materials, such as aromatic nitro and C-nitroso compounds [13]–[16]. Many of these compounds have from 5–8 times the theoretical ampere-minute capacity of manganese dioxide and mercuric oxide, materials presently used in commercial cells. In addition, the chemical energy derived from these materials can be efficiently converted into

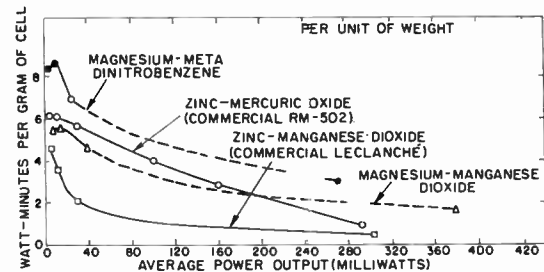
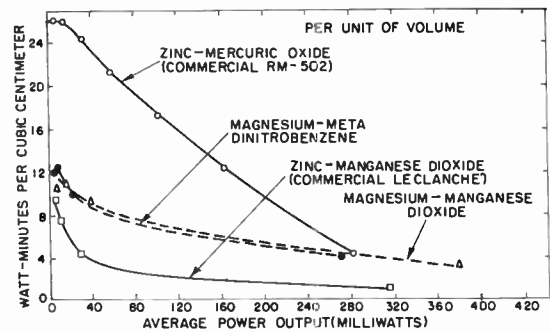


Fig. 11—AA-size dry cells discharged continuously through various resistances (watt-minute capacity and average power output computed to 0.90 volt end voltage).

usable electrical energy. The operating voltage characteristics of the magnesium-organic cells depend upon the structure and types of organic compounds used, but, in general, they have a more constant voltage-time discharge curve than the manganese dioxide cells. For example, the magnesium-meta dinitrobenzene cells operate between 1.00 and 1.20 volts for most of the discharge time, while corresponding cells containing *p*-nitrosodimethylaniline as the cathode material operate between 1.2 and 1.4 volts. Typical discharge curves for AA-penlight and C-size organic cells compared with the Leclanché and magnesium-manganese dioxide cells are shown in Figs. 9 and 10. The C-size cells were discharged intermittently through a 4-ohm resistance simulating flashlight use, while the AA-size cells were discharged continuously through 50-ohm resistances to simulate current drains encountered in portable radio applications. Additional data at various power output levels, showing the relationships between the three cells on the basis of watt-minute capacity per unit of volume and weight at various power output levels, are shown in Fig. 11. These data illustrate the superiority of both types of magnesium cells over the Leclanché on the basis of watt-hour capacity per unit of weight and volume. The desirable features of the organic cells are their constant operating voltage characteristics and their ability to give more hours of service to 1.00 and 0.90 volts than the two manganese dioxide cells.

The organic cell development, aside from the favorable theoretical and proven performance gains, has an additional important feature. It opens the door to a vast supply of new materials, many of which are relatively cheap, and nonstrategic, thus offering the promise of eliminating the country's dependence on foreign ore de-

posits. Further research in this area should result in superior compounds and a better understanding of their efficient utilization.

Another development is the use of a bismuth oxide cathode with a magnesium anode [17]. These cells, because of the cost relationships between bismuth oxide, manganese dioxide, and mercuric oxide, would be expected to be more expensive than the Leclanché, but cheaper than the zinc-mercuric oxide cells. They operate 0.2 to 0.3 volt lower than the zinc-mercuric oxide cells, but have flat voltage-time discharge characteristics similar to this cell. The bismuth oxide cell should not be considered as competitive with the Leclanché for lighting applications, but with further development might compete with the more costly mercuric oxide cell.

With the proven performance gains for these three magnesium dry cells, one might wonder why they have not reached the commercial market. The organic and bismuth oxide cells are relatively new, but the magnesium-manganese dioxide cell has been under extensive research and development for over ten years. There are several technical problems associated with the use of magnesium anodes. These are: cost, "delayed action," high impedance, and loss in capacity on light intermittent tests. These problems are gradually being solved, and it is predicted that magnesium dry cells will achieve commercial significance in the near future.

Air dry cells: Air cells are a class of cells which utilize the oxygen of the air as the cathode component. Several cells of this type have appeared on the market over the years [18], [19]. The most successful of these, the primary wet cell, is discussed in Section II-A, 3.

About 1950 the first air cell of the dry type was produced for a time in this country. These cells contain a zinc anode, an aqueous sodium hydroxide electrolyte, and a special porous water-repellent carbon positive electrode. The carbon electrode is sufficiently porous to permit adequate access of air, and the occlusion of enough oxygen to maintain the intended rates of discharge. They are designed to operate at current drains as high as 0.06 amperes, and for nominal use have an average voltage of about 1.05 volts.

The air dry cells as assembled at the factory are sealed to prevent desiccation during storage. The seal is broken before use to allow oxygen of the air into the porous carbon electrode. For short continuous operation, these cells perform satisfactorily, but for long intermittent types of service, they are subject to drying-out resulting in loss of capacity. It is for this reason that these dry cells have not found wide application. If a membrane can be found which will allow for the efficient transfer of oxygen into the cell without the transfer of water vapor out of the cell, air dry cells should find some commercial application.

Aluminum and indium dry cells: Two other dry cell developments which should be mentioned are the aluminum-manganese dioxide and the indium-mercuric oxide dry cells.

The first is an aluminum counterpart to the Leclanché and magnesium-manganese dioxide cells. It consists of an Alclad aluminum anode can, an aqueous aluminum chloride electrolyte, and a manganese dioxide cathode. Ammonium dichromate is added to the electrolyte to inhibit the corrosion of the aluminum [21]. These cells operate about 0.1 volt higher than the Leclanché with the same sloping voltage discharge characteristics. More research and development is needed on this cell to improve its performance on intermittent tests, as well as to ascertain the shelf life characteristics.

The other development might be considered as an indium counterpart to the zinc-mercuric oxide cell, differing from the latter in the use of an indium anode in place of zinc [20]. The feature of these small cells is that they can be hermetically sealed as the indium anode is more resistant to corrosion than zinc, and thus would liberate less gas. They have a flat voltage-time discharge curve comparable to the zinc-mercuric oxide cell, but have an operating voltage 0.2–0.3 volt lower. These cells were designed specifically for use in an electronic wrist watch. They are more expensive and give less capacity than the zinc-mercuric oxide cell.

2) *Solid Electrolyte Cells:* Solid electrolyte cells are distinguished from other primary cells using liquid electrolytes, as they are composed of solid materials only. A cell of this type, containing a silver anode, a solid silver iodide electrolyte, and an iodine cathode, has an open-circuit voltage of 0.69 volt with a short-circuit current of 20 μ a per square centimeter of electrode area [47]. The silver iodide electrolyte acts as an ionic conductor, permitting the diffusion of silver ions through its crystal lattice.

The most outstanding feature of the solid electrolyte cells is their potentially long shelf life. This is in contrast to cells with liquid electrolytes, in which the shelf life is limited by the reaction of the electrodes with the electrolyte and by the evaporation of the electrolyte itself. Because of their expected 10–20 year shelf life, the solid electrolyte cells are ideal for use in military and other equipment that may be stored for years in a standby condition.

A typical commercial solid electrolyte battery consists of 127 extremely thin cells of the composition Ag/AgBr/CuBr₂, which are stacked in series to produce a potential of 95 volts. This battery which weighs 4.2 grams (0.15 ounce) and measures 0.86 cm (0.34 inch) in diameter and 2.5 cm (0.97 inch) in length, has an available charge of 1 coulomb and furnishes a flash current of 8 μ a. It can be applied as a power source for radiation warning devices and monitoring instruments, and as a charger for low-leakage capacitors. Other potential applications include use as a bias supply for high-impedance circuits, and furnishing low currents to circuits employing electrometer tubes or ionization devices.

Another type of primary cell designed for these applications is the wax electrolyte cell which, like the solid

electrolyte cells, has a predicted long shelf life and sustains low currents only. The cell consists of a zinc anode, a manganese dioxide cathode, and an electrolyte of zinc chloride dissolved in a solid wax of polyethylene glycol [48]. A typical 25-cell wax electrolyte battery, which weighs 0.2 ounce is 0.3 inch in length and 0.5 inch in diameter, has an electromotive force of 37.5 volts and a short-circuit current of 3×10^{-7} amperes at ordinary temperature.

3) *Wet Cells*: Two types of primary wet cells are produced in this country, the zinc-cupric oxide Lalande [3], [18], [19] and the zinc-air cell [3], [18]. These cells find applications where a large capacity, moderately large currents at constant voltage, and long life are the dominant service requirements. Mine, highway, railway, and marine signaling installations, telephone and telegraph circuits, and radio "A" are examples of equipment that are powered by these cells.

The Lalande cell consists of a zinc anode, a caustic soda electrolyte, and a cupric oxide cathode contained in a glass jar. Various electrode shapes and spacings are used depending upon the manufacturer and intended application. A typical construction is shown in Fig. 12. The cells are usually shipped dry, the electrolyte being added prior to usage, and a film of oil added to the top of the electrolyte to prevent evaporation of water and adsorption of carbon dioxide into the solution. In general, Lalande cells are designed to give 500–1000-ampere-hour capacities, and operate between 0.5 and 0.7 volt at current drains as high as 15 amperes. They give capacities of about 2.5 watt-minutes per cm^3 and 1.85 watt-minutes per gram.

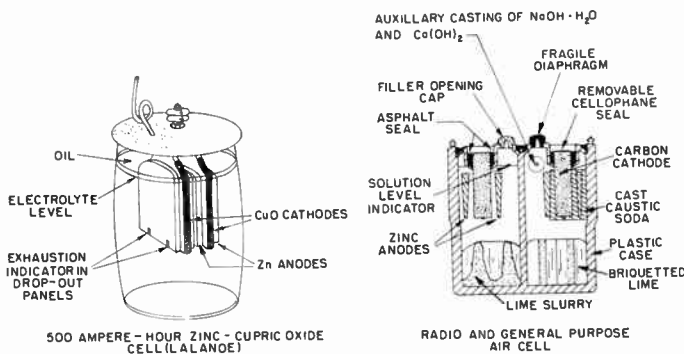


Fig. 12—Cross sections of typical zinc-cupric oxide and zinc-air wet cells. (Schumacher and Heise [18].)

The air cell, which is considered as a replacement for the Lalande cell, differs from the latter in that it contains a porous carbon electrode in place of the cupric oxide. As in the case of the zinc-air dry cell, the porous carbon electrode is designed to absorb oxygen from the air which in turn is reduced in the course of cell discharge. The air cells operate at 1.1–1.2 volts, and have a constant voltage-time discharge curve. Like the Lalande cell, they are designed to be assembled in the field by adding the caustic soda electrolyte. A typical air cell of the Railway type shown in Fig. 12 is designed to operate

at continuous drains as high as 2.0 amperes, or 3.0 amperes on intermittent service. These cells give capacities between 7–11 watt-minutes per cm^3 and 5–9 watt-minutes per gram.

4) *Reserve Cells*: Reserve batteries, sometimes called "one shot" or "delayed action" batteries are primary cells which are assembled in an inactive state and activated prior to use. They are designed to meet some specific application, usually military, and because of their composition and construction have some inherent advantages over the other conventional primary batteries. Some of these are: more active electrochemical systems may be utilized to obtain a higher energy output per unit of weight and volume, long shelf life with a minimum of maintenance, and high over-all performance reliability.

Stimulated by World War II, the development of reserve batteries has involved a study of various electrochemical systems and procedures for activating the cells or batteries. In general, the important cells can be classified into three groups, a) liquid-activated, b) gas-activated, and c) heat-activated as shown in Table IV (p. 1472). The liquid-activated magnesium-silver chloride, magnesium-cuprous chloride, and zinc-silver oxide cells are the most important, the others being in the development stages or used only to a limited extent.

a) *Liquid-activated:*

Magnesium-water activated cells: The water-activated cell systems are among the relatively new power sources which have become important to the military since the beginning of World War II. These cells are stored dry in an inactive condition in hermetically sealed containers and are activated by adding water. They have the advantage over other reserve cell systems in that the electrolyte need not be transported with the battery. One disadvantage is the slow activation time requiring several seconds to minutes for complete activation. They find use in powering airborne equipment, signal lights, emergency lighting, lights for floating buoys, radiosonde equipment, and air-sea rescue equipment.

The magnesium-silver chloride and magnesium-cuprous chloride are two types of water-activated cells commercially available. From the performance data listed in Table IV, it is seen that the silver chloride cells operate at higher voltages and have higher capacities than the cuprous chloride cells. The cuprous chloride cells, however, are cheaper. Both of these cell systems have a constant voltage-time discharge curve and the characteristic of evolving heat during cell discharge which makes them applicable for operation at temperatures as low as -54°C , temperatures encountered in meteorological applications. The heat evolved during cell discharge is due mainly to the corrosion of the magnesium, the energy of this reaction being liberated as heat instead of electrical energy. Typical designs of batteries of this type are illustrated in Fig. 13 (p. 1473).

TABLE IV
CHEMICAL COMPOSITION AND PERFORMANCE CHARACTERISTICS OF VARIOUS RESERVE CELLS

Type	Anode	Electrolyte	Cathode	Activating Agent	Energy Producing Reaction
Liquid-Activated Zinc-Silver Oxide	Zn	KOH	AgO	KOH	$Zn + AgO \rightarrow ZnO + Ag$
Zinc-Lead Dioxide	Zn	H ₂ SO ₄	PbO ₂	H ₂ SO ₄	$Zn + PbO_2 + H_2SO_4 + 2H^+ \rightarrow Zn^{++} + PbSO_4 + 2H_2O$
Cadmium-Lead Dioxide	Cd	H ₂ SO ₄	PbO ₂	H ₂ SO ₄	$Cd + PbO_2 + H_2SO_4 + 2H^+ \rightarrow Cd^{++} + PbSO_4 + 2H_2O$
Lead-Lead Dioxide	Pb	H ₂ SO ₄ , HBF ₄ , H ₂ SiF ₆ , or HClO ₄	PbO ₂	H ₂ SO ₄ , HBF ₄ , H ₂ SiF ₆ , or HClO ₄	$Pb + PbO_2 + 2H_2SO_4 \rightarrow 2PbSO_4 + 2H_2O$ $Pb + PbO_2 + 4H^+ \rightarrow 2Pb^{++} + 2H_2O$
Magnesium-Silver Chloride	Mg	MgCl ₂	AgCl	H ₂ O	$Mg + 2AgCl \rightarrow MgCl_2 + 2Ag$
Magnesium-Cuprous Chloride	Mg	MgCl ₂	CuCl	H ₂ O	$Mg + 2CuCl \rightarrow MgCl_2 + 2Cu$
Magnesium-Organic-N-halogen	Mg	MgCl ₂ , MgBr ₂	Organic-N-halogen (e.g. trichloromelamine)	H ₂ O	$6Mg + 6H_2O + 2 \text{ trichloromelamine} \rightarrow 2 \text{ melamine} + 3Mg(OH)_2 + 3MgCl_2$
Gas-Activated Zinc-Chlorine	Zn	NH ₄ Cl-ZnCl ₂	Cl ₂	Cl ₂	$Zn + Cl_2 \rightarrow ZnCl_2$
Ammonia Vapor Activated	Mg, Zn	NH ₄ SCN-NH ₃	PbO ₂ , MnO ₂	NH ₃	—
Boron Trifluoride	Mg, Al Pb, Zn	HF, H ₃ BO ₃	PbO ₂ , MnO ₂	BF ₃	$Pb + PbO_2 + 4H^+ \rightarrow 2Pb^{++} + 2H_2O$
Heat-Activated	Ca Mg Ca	KCl-LiCl KCl-LiCl KCl-LiCl	ZnCrO ₄ Basic ZnCrO ₄ WO ₃	heat to melt LiCl-KCl	— —

Operating Characteristics of Cells Discharged Under Optimum Conditions

Type	Average Operating Voltage (Volts)	Capacity		References
		Watt Minutes per Gram	Watt Minutes per cm ³	
Liquid-Activated Zinc-Silver Oxide	1.4-1.5	6.6-7.4	11.4-13.2	[54], [55]
Zinc-Lead Dioxide	2.1-2.4	3.4	13.9	[56], [57]
Cadmium-Lead Dioxide	1.8-2.1	1.8	4.0	[57], [58]
Lead-Lead Dioxide	1.6-2.1	2.1-2.6	5.5-7.7	[57]
Magnesium-Silver Chloride	1.3-1.6	up to 10.6	up to 29.3	[26], [49]-[51]
Magnesium-Cuprous Chloride	1.1-1.3	2.6-4.0	5.1	[26], [49], [52]
Magnesium-Organic-N-halogen	1.9-2.3	up to 8.0	up to 8.4	[53]
Gas-Activated Zinc-Chlorine	1.3-1.9	—	—	[59], [60]
Ammonia Vapor Activated	—	2.0-2.6	3.7	[61]
Boron Trifluoride	1.6-2.1	—	—	[62]
Heat-Activated	3.28 2.23 2.48	— — —	— — —	[63], [64] — —

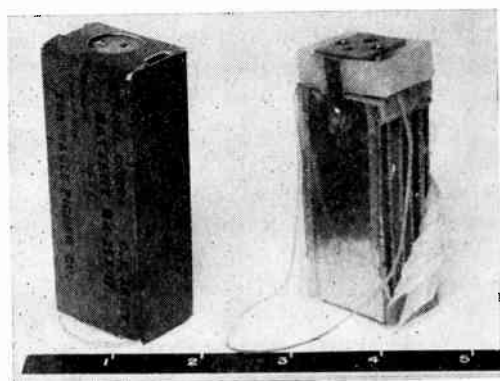
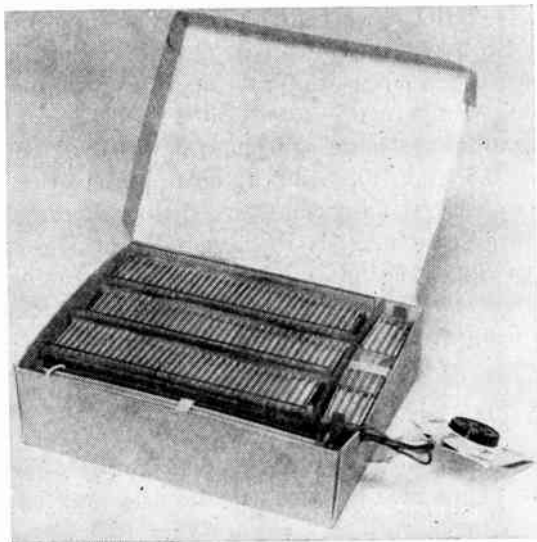


Fig. 13—Magnesium-cuprous chloride water-activated reserve batteries.

An important new water-activated reserve cell system under development utilizes a magnesium anode and organic N-halogen compounds, such as trichloro-melamine [53]. The N-halogen compounds are attractive as they operate at 0.6–0.7 volt higher than the silver chloride electrode, approaching the potential of the chlorine electrode. In addition, many of these materials have a greater theoretical ampere-minute capacity per unit of weight than any of the inorganic materials. To date, it has been shown that batteries can be made which will give nearly twice the watt-hour capacity per unit of weight and volume of the magnesium-cuprous chloride battery on certain military tests.

Zinc-silver oxide cells: Zinc-silver oxide reserve cells have been developed to meet the need for high-rate batteries capable of delivering their rated capacities in one to ten minutes. They find application in missiles, radio-controlled model planes and boats, emergency power, etc.

The valuable features of these cells are their high watt-hour capacities per unit of weight and volume and constancy of voltage during discharge at high-power output levels. An example of a typical battery is the Signal Corps BA-467/U which occupies a volume of about 0.16 m³ (960 inches³), weighs 22.7 kg (50 pounds)

and delivers 180 amperes for 10 minutes at a voltage of 28 ± 2 volts.

These batteries, which are designed primarily for military applications are stored dry and are automatically activated. One activation method is to apply an electric pulse to a squib which ruptures a diaphragm holding back the potassium hydroxide electrolyte. This forces the electrolyte into the battery. Activation times on the order of a few tenths of a second for the battery to reach operating voltage have been attained. In order to achieve operation at low temperatures (-54°C), electric heaters are incorporated in the batteries.

Lead dioxide cells: Several lead dioxide reserve cells [56]–[58] have been described, consisting of a lead dioxide cathode and a zinc, cadmium, or lead anode. These cells which are designed for high rate applications, are activated by adding aqueous solutions of fluoroboric acid, sulfuric acid, or fluorosilicic acid. They have a limited life after activation due to the rapid attack of the zinc and cadmium anodes by the electrolyte. The interest in these cell systems has been due to their superior low-temperature performance without the use of external heaters, and their low cost.

b) Gas-activated cells: Three different gas-activated cells now under development are shown in Table IV. Although they differ from each other in performance characteristics, they have one common feature in that they are activated by adding a gaseous component. In the case of the zinc-chlorine cell, the cell is activated by introducing chlorine into a porous carbon electrode. The chlorine gas is contained under pressure in a cylinder with an electrically operated valve. The other two cells are activated by adding an electrolyte component, such as ammonia or boron trifluoride. Various anode and cathode materials have been investigated for the latter type cells.

These cells are being designed for high rate applications of the type for which the zinc-silver oxide batteries are presently used. The potential advantages of these new systems are high capacity, favorable low temperature characteristics, and low cost.

c) Heat-activated (thermai) cells: In these cells the electrolyte is a nonconductive solid at ordinary temperatures. They are activated by applying heat which melts the solid electrolyte making it conductive and enabling current to be withdrawn from the cells. Calcium and magnesium have been used as anode materials, various metallic chromates and oxides as cathodes, and alkali halides as electrolytes [63], [64]. The favorable features of these cells are: high-operating cell voltages (e.g., over 3.00 volts); ability to withstand high current drains; long shelf life in the inactivated condition; operation over wide temperature range; no maintenance; and ruggedness. These cells have a relatively short operating life which limits their use to specialized military applications requiring a few minutes of service.

5) Fuel Cells: For many years, investigators have been attracted to the problem of converting the energy

TABLE V
REPORTED EFFICIENCIES OF VARIOUS ENERGY CONVERTERS

Energy Source	Conversion Processes	Reported Efficiency (per cent)
Chemical	Electrochemical	90
Chemical, Nuclear, or Solar	Heat→Mechanical (e.g., steam-turbine)	40
Chemical, Nuclear, or Solar	Heat→Thermionic	8
Chemical, Nuclear, or Solar	Heat→Thermoelectric	7
Solar	Photovoltaic	12
Nuclear	Dielectric Charging	1
Nuclear	Contact Potential	0.01
Nuclear	Electron Voltaic	2.5

of fuels directly to electrical energy without passing through the intermediate thermal and mechanical stages. In principle, the conversion of carbonaceous fuels such as coal to electrical energy could be more efficiently carried out in an electrochemical cell than by the conventional steam-turbine cycle, as the efficiency of the latter cycle is limited by more severe thermodynamic restrictions. As seen from the data in Table V, electrochemical processes are the most efficient known for the conversion of chemical energy into electrical energy. Fuel cells are electrochemical cells. They differ from conventional batteries in that the chemicals which enter into the anode and cathode reactions are fed into the electrodes at a rate proportional to the rate at which electrical energy is withdrawn.

Two types of fuel cell systems have been extensively investigated within the past ten years. The first involves the use of carbonaceous fuels, the objective being to efficiently realize the energy that can be derived from coal. In order to avoid some of the difficulties associated with feeding coal directly into a cell, coal is first converted into carbon monoxide or water gas, these gases are fed into the negative electrode of the cell. At the same time, oxygen is fed into the positive electrode, the over-all energy producing cell reaction being $\text{CO} + 1/2\text{O}_2 \rightarrow \text{CO}_2$. It has been reported [65] that cells containing perforated-iron electrodes with a mixed carbonate electrolyte impregnated in a porous magnesia diaphragm can be made to operate continuously for several months at a conversion efficiency of 55 per cent. These cells which were designed to operate at 600°C had an operating potential of 0.8 volt at a current density of 55 ma/cm² of electrode surface area. Although this is a remarkable advance, it is still not competitive with the conventional methods for producing large quantities of electrical energy. However, it has been calculated that an over-all efficiency of 75 per cent should be possible if water gas is used in an integrated system and the electrochemical cell operated at a high temperature such that the waste can be utilized to effect the endothermic water gas reaction. If such a goal is realized, and the cells can be shown to operate within a minimum of maintenance, fuel cells of this type will be increasingly important.

The other class of fuel cells utilize hydrogen as the fuel, the over-all energy producing cell reaction being:

$2\text{H}_2 + \text{O}_2 \rightarrow 2\text{H}_2\text{O}$. Two cells of this type have been reported. Both types use a caustic electrolyte but differ in their electrode composition and operating temperature. The high temperature (200–250°C) cell designed by Bacon and his associates [66] has an operating potential between 0.5 and 1.05 volts at current densities up to 1 ampere/cm². It has been claimed that these cells can be operated continuously for several months at an efficiency of 70 per cent giving power outputs ranging up to 22,000 watts/m³ (6000 watts/foot³) of cell volume. A cell, developed by National Carbon Company, which operates at room temperature utilizes porous carbon electrodes and gives comparable efficiencies to the Bacon cell.

Although the hydrogen-oxygen cells probably will not compete economically with the large power stations, the advantages of such cells are that they serve as a source of silent power, and give greater watt-hour capacities per unit of weight and volume at higher power rates than the conventional batteries.

6) EMF Standards:

a) *Weston cell*: The Weston or standard cells, are examples of electrochemical cells which are used as standards of electromotive force. They consist of an amalgamated cadmium anode, an aqueous solution of cadmium sulfate as the electrolyte, and a mercurous sulfate cathode. There are two types, saturated and unsaturated, the terminology referring to the concentration of the cadmium sulfate in the electrolyte. The saturated cells are more constant in EMF, but require careful control of temperature for accurate measurements. These are used primarily as reference standards. The unsaturated cells which are commercially available have a temperature coefficient close to zero, and are suitable for work requiring no greater accuracy than 0.01 per cent. The average EMF of new unsaturated cells is about 1.01916 absolute volts and should not change more than 71 μv per year [67].

Standard cells are delicate instruments made from very high purity chemicals, and should not be subjected to strong light and temperatures above +40°C or below 4°C. They also can be damaged if anything but negligible currents are withdrawn from them.

b) *Grid-bias cells*: Cells of this type serve as a source of potential rather than of current, finding use in electronic equipment as a bias on the control grid. They are small, hermetically-sealed cells composed of a vanadium pentoxide cathode, a weak-acid electrolyte such as a viscid ammonium glycol borate paste, and either a zinc or cadmium anode. The cadmium cells have an electromotive force of 1.05 volts, and zinc cells 1.2 volts. If properly used, the life of these cells may be 10 years or more without more than a negligible change in EMF [68].

B. Secondary Cells

Secondary or storage cells are electrochemical cells which after discharge can be restored to their original

TABLE VI
CHEMICAL COMPOSITION AND PERFORMANCE CHARACTERISTICS OF VARIOUS SECONDARY BATTERIES

Type	Anode	Electrolyte	Cathode	Current Producing Reaction Discharge → Charge ←	Average Operating Voltage on Light Drains (Volts)	Capacity on Light Drains*		References
						Whr/lb	Whr/in ³	
Lead-Acid	Pb	H ₂ SO ₄	PbO ₂	$\text{Pb} + \text{PbO}_2 + 2\text{H}_2\text{SO}_4 \rightleftharpoons 2\text{PbSO}_4 + 2\text{H}_2\text{O}$	1.95-2.05	16-20	1.5-2.1	[26], [69]-[71]
Nickel-Iron (Edison)	Fe	KOH	Ni(OH) ₂ , Ni ₂ O ₃	$\text{Fe} + \text{NiO}_2 \rightleftharpoons \text{FeO} + \text{NiO}$	1.10-1.30	12-13	0.98-1.05	[26], [69]-[71], [78]
Nickel-Cadmium (Junger)	Cd	KOH	Ni(OH) ₂ , Ni ₂ O ₃ , & NiO ₂	$\text{Cd} + \text{NiO}_2 \rightleftharpoons \text{CdO} + \text{NiO}$	1.10-1.30	10-12	0.75-0.95	[26], [69]-[71], [79]-[82]
Zinc-Silver	Zn	KOH	AgO	$\text{Zn} + \text{AgO} + \text{H}_2\text{O} \rightleftharpoons \text{Ag} + \text{Zn(OH)}_2$	1.40-1.50	50-55	3.1-3.6	[26], [69], [83]-[85]
Cadmium-Silver	Cd	KOH	AgO	$\text{Cd} + \text{AgO} \rightleftharpoons \text{Ag} + \text{CdO}$	1.05-1.10	~33	~2.7	[26], [86]
Lead-Silver Oxide	Pb	KOH	Ag ₂ O	$\text{Pb} + \text{Ag}_2\text{O} \rightleftharpoons \text{PbO} + 2\text{Ag}$	0.80-0.85	13.6	1.8	[87]
Cadmium-Mercuric (Oxide)	Gd	KOH	HgO	$\text{Cd} + \text{HgO} \rightleftharpoons \text{CdO} + \text{Hg}$	0.9	—	—	[88]

* These data were calculated from large capacity batteries under optimum conditions.

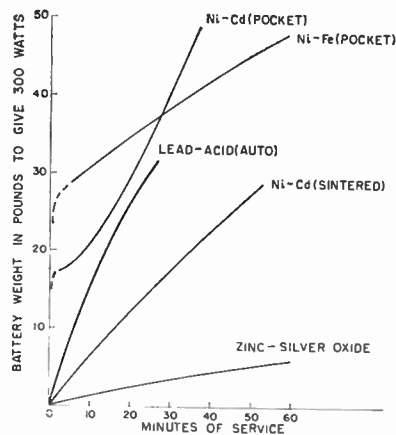


Fig. 14—Relative performance of various secondary systems of special construction designed to deliver 300 watts for a specified time interval.

chemical state by passing the current in the reverse direction. Although they have the same set of basic components as primary cells, the anodes and cathodes of secondary cells have a more stringent requirement, in that the electrode reactions have to be reversible. This requirement immediately limits the number of electrode materials available for secondary cells. At present, lead, cadmium, iron, and zinc anode materials, and lead dioxide, nickel dioxide, and silver oxide cathode materials are the only ones used in commercial secondary cells.

The secondary battery business dates back to Planté's discovery of the lead-acid system in 1860. Over the years there has been a continuous growth in this business, reaching a total of about 300 million dollars in 1956 in the United States alone. They are used for a wide variety of applications ranging from megawatt power supplies for submarines to small milliwatt power supplies for portable radios.

At present five types of batteries are produced commercially. The chemical composition and some of their performance characteristics are listed in Table VI, and

Fig. 14. Each are discussed in greater detail in the following paragraphs.

1) *Lead-Acid Batteries:* Lead-acid secondary batteries, the most important of the five classes, are made in a variety of sizes and shapes for many applications. Three major types are produced, automotive, motive, and stationary [69]-[71]. The applications for which each are designed and their performance characteristics are listed in Table VII and Fig. 15. Whereas the basic energy-producing chemical reaction is the same for all lead-acid cells, these types differ from each other in construction and performance characteristics.

Automotive batteries [72], the most important class in terms of total value of product and general availability, are made in a limited number of standard sizes on automatic equipment with emphasis on low cost. They are designed to furnish high currents (200 to 300 amperes for a 6-volt system) for a few seconds or minutes over a wide range of temperatures. These requirements have led to a thin plate construction (Fig. 16). The electrodes are comprised of grids cast from high-purity lead containing about 10 per cent antimony which are filled with a paste consisting of a mix of lead oxide, water, and sulphuric acid. The paste of the negative plates contains about 1 per cent of "expander" to improve the high rate discharge and low-temperature characteristics. The expander contains two important ingredients, barium sulfate on which lead sulfate can crystallize, and an organic material, such as the derivative of the lignin fraction of wood, which prevents lead sulfate from crystallizing on the sponge lead surface. No expander is used in the positive plates. After the plates have been formed, dried, and assembled, they are immersed in a weak sulphuric acid solution and charged, the lead oxide of the negative plate being converted to sponge lead, and lead dioxide being formed at the positive plates. Acid-resistant porous wood or microporous rubber separators are generally used to separate the anodes and cathodes from each other. Performance data for a typi-

TABLE VII
TYPICAL APPLICATIONS AND PERFORMANCE CHARACTERISTICS OF VARIOUS SECONDARY BATTERIES

Type	Application	Life Characteristics		Charge Retention	References
		Cycle Service Life	Float Charging Life		
Lead Acid Automotive	High currents for a few seconds or minutes: engine cranking	250-400 cycles	Up to 4 years in automotive service with good care	20% to 30% drop per month	[69]-[72]
Motive	Discharge rate of 3 to 10 hours with nearly complete discharge: electric trucks, air conditioning and lighting of railroad cars	3-6 years (see text)	—	—	[69]-[71], [73]
Stationary Lead-Antimony grid Lead-calcium grid Planté Positive	Designed for long service life, in particular on float type charging: emergency power, railway signals, telephone exchanges	6-8 years	14 years	30% drop per month	69-[71], [74]
		Not determined	25 years (estimated)	6% drop per month	[74], [76]
		10-14 years	25 years	—	[74]
Low Discharge	Specially designed stationary for low discharge rates and low self-discharge rates: recording, warning, and control devices: industrial and laboratory instruments	10-20 cycles with 6 months to a year between cycles	20 years	15% drop per year	[75]
Electrolyte Retaining	Designed to have nonspillable electrolyte for portable high-rate power in place of dry cells: radio, photographic flash units, guided missiles	200-300 cycles	—	30% drop per month	[77]
Nickel-Iron (Edison)	Heavy duty industrial and railway applications:	1800 cycles	7-12 years heavy Industrial; 14-25 years standby	25% to 35% drop per month	[69]-[71], [78]
Nickel-Cadmium Pocket Plate	General purpose cell with wide applicability where mechanical and electrical abuse and long life are important factors	As good as sintered plate if not better	25 years	20% to 40% drop per year	[69]-[71], [79]
Sintered Plate	High rate and low temperature	Several thousand cycles*	20-25 years (estimated)	Less than 50% drop per year	[69]-[71], [80]-[82]
Zinc-Silver Oxide High Rate	Discharge rates of 1 minute to 30 minutes	10-20 cycles over 3-6 months	—	—	[69], [83]-[85]
Medium Rate	Discharge rates of 30 minutes to 5 hours	40-50 cycles over 6-9 months	—	20% to 30% drop per year	
Low Rate (1 hour and over)	Discharge rates over 1 hour	150 cycles over a year; 300 cycles with special construction	—	—	
Cadmium-Silver Oxide	Low-rate and long-life applications	600-700 cycles, 3000 cycles on a 40% discharge	Estimated to be good	Estimated as good as zinc-silver oxide	[86]

* One manufacturer claims 5000 cycles.

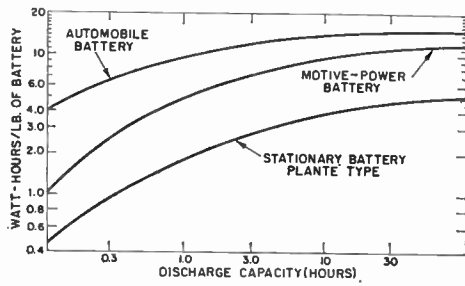


Fig. 15—Power output of various types of lead-acid batteries. (Courtesy of *Encyclopaedia Britannica*.)

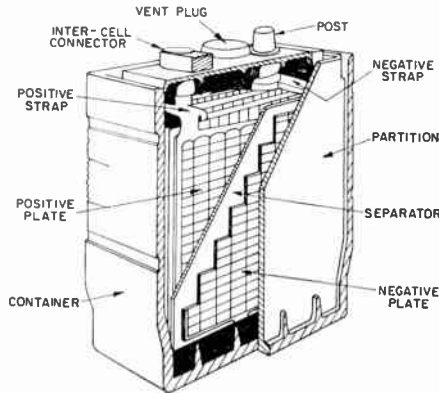
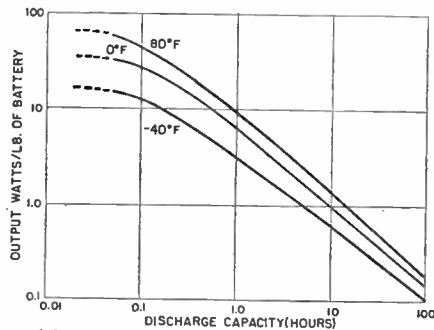
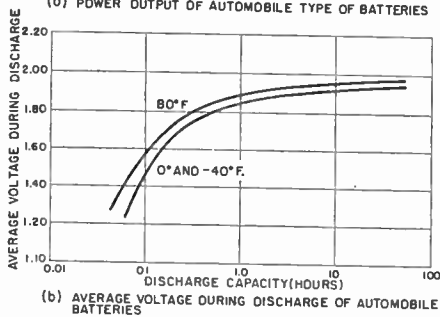


Fig. 16—Cutaway of automotive battery showing the pasted plate construction. (Courtesy of Electric Storage Battery Company.)



(a) POWER OUTPUT OF AUTOMOBILE TYPE OF BATTERIES



(b) AVERAGE VOLTAGE DURING DISCHARGE OF AUTOMOBILE BATTERIES

Fig. 17—Performance data for a typical automotive battery. (Willihnganz [72].)

cal automotive battery are shown in Fig. 17. It should be noted that the main effect of temperature is on the current output and not the voltage.

The second major class of lead-acid batteries is used for motive-power service [73]. They are required to supply power for three to ten hours, and are designed to withstand frequent deep discharges instead of remaining

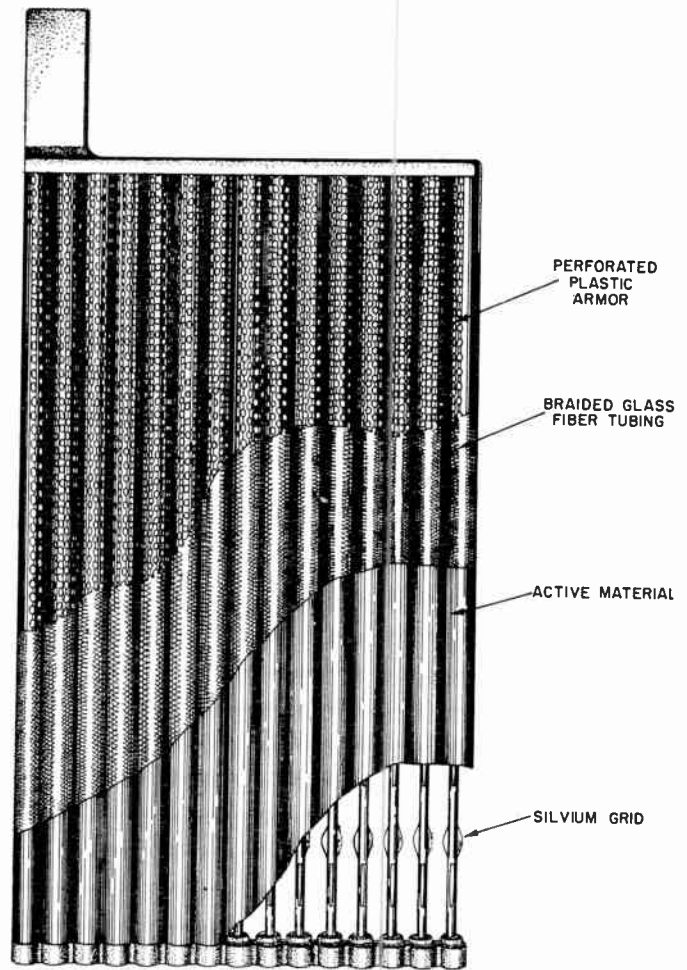


Fig. 18—Positive plate of an oxide-iron clad battery. (Courtesy of Electric Storage Battery Company.)

almost fully charged as in the case of automotive batteries. The negative plates of motive batteries although thicker are similar to automotive batteries. The most important difference between the two types is that the positive plates are protected to prevent loss of active material which would otherwise occur in batteries that are alternatively charged and discharged. One method is to incorporate the active material in slotted cylindrical sleeves which have antimonial lead or silver-lead spines in the center to allow for the passage of electrons to the active material. A positive plate consists of an assembly of these tubes as shown in Fig. 18. Another design comprises the use of thicker pasted plates with several layers of strong separator material to prevent the loss of active material during use. These changes in positive plate construction along with the use of thicker grids have led to batteries which give three to six years of service in applications where automotive batteries would last less than six months. However, they are more expensive than comparable size automotive batteries.

Stationary batteries [74], [75]; unlike the automotive and motive types, are designed for long life applications which do not require the mechanical ruggedness or high current output. Low self-discharge, sta-

bility, and high efficiency are the important features. Most of the stationary batteries use the pasted positive plate construction similar to the motive battery. A Planté positive plate type construction is also used. In this case, the active material is derived from the plate itself. In addition to a different positive plate construction, the grid material and design are also constructed differently to decrease the self-discharge rate encountered in the other two battery types. This has been accomplished by using grid materials, such as pure lead or a lead-calcium alloy [76], in place of the lead-antimony alloy. Antimony, which is needed for structural reasons, causes a high self-discharge rate. Antimony also causes gassing at lower charging voltages.

A fourth class of lead-acid batteries are those which have been designed with an electrolyte-retaining separator to prevent loss of electrolyte when the batteries are inverted [77]. These batteries are generally smaller in size than the other types and are designed for portable high-rate power applications for which the conventional dry cells would not be suitable.

2) *Nickel-Iron (Edison) Batteries*: The nickel-iron-alkaline batteries [69]–[71], [78] as they exist today are essentially the same as discovered by Edison around 1900 and marketed in 1908. The negative electrode consists of pockets of active material grouped together to form a plate, while the positive plate is an assembly of perforated nickel tubes filled with nickel hydroxide and nickel. A cutaway view of the nickel-iron cell is given in Fig. 19. These batteries find their widest use in heavy duty industrial and railway applications, e.g., 1 to 8-hour discharge rates.

The nickel-iron cell on a five hour rate has a slightly greater capacity on a weight basis while occupying a little larger volume than a lead-acid motive-power battery.

A second interesting property of this battery is that its ampere-hour capacity remains close to its rated capacity at high discharge rates. However, at high discharge rates the voltage of nickel-iron batteries drops considerably and hence is not recommended for automotive applications.

These batteries have other advantages in that they are mechanically strong and resist electrochemical abuse. For example, they may be overcharged, and completely discharged for long periods of time. In addition, they operate at higher temperatures and have a longer life than the lead-acid batteries.

There are several disadvantages to the use of these batteries. One is their poor low-temperature performance. Also, they consume more water, develop more heat, and are more expensive than lead-acid batteries. Also, their charge retention is poor; a typical battery after one month storage loses approximately 42 per cent of its initial capacity.

3) *Nickel-Cadmium Batteries*: The nickel-cadmium battery [69], [70] discovered by Junger and Berg about

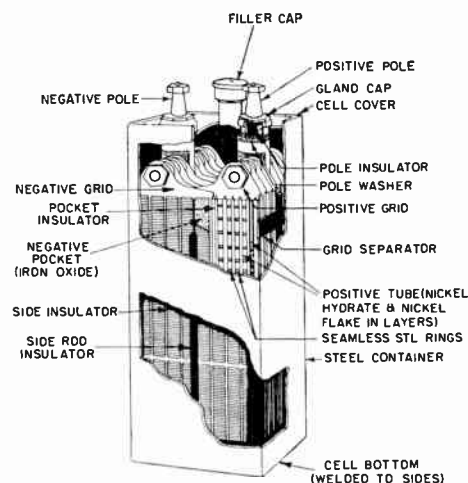


Fig. 19—Cutaway view of nickel-iron cell. (Anderson [78].)

1900 is closely related to the nickel-iron Edison battery. Both are mechanically rugged and will withstand electrochemical abuse in that they can be overcharged, overdischarged, or stand idle in a discharged condition. The nickel-cadmium battery differs from the Edison battery in the use of cadmium anodes in place of iron. Although the nickel-cadmium batteries operate at slightly lower voltages than the nickel-iron batteries, they show very little self-discharge. They can be trickle-charged, and when standing idle they evolve practically no gas, so that for some purposes they can be hermetically sealed. The nickel-cadmium batteries can be operated over a temperature range of -54°C (-65°F) to 82°C (180°F) and they are characterized by an excellent service life under both cycle and float operation. Initially, they are more expensive than comparable lead-acid batteries, which has limited their use for some applications.

The two nickel-cadmium cell constructions in use are the pocket type [79], similar to the nickel-iron construction, and the sintered-plate construction [80]–[82]. The sintered-plate construction differs from the pocket type in the method of support. Plates are made from nickel powder which is molded into shape and heated at an elevated temperature in a nonoxidizing atmosphere. This gives a strong, porous plate which contains about 80 per cent pore volume. The active material is impregnated in the pores of these plates by soaking them in a solution of nickel salts to make positive plates, and a solution of cadmium salts to make negative plates.

The sintered-plate design, because of the thinner plate construction and larger electrode surface area, offers advantages over the pocket-type construction in that they operate at higher current drains and are more efficient at low temperatures. For example, specially designed sintered plate batteries can be discharged and charged at -54°C . These properties are desirable for automotive use, and except for cost, the nickel-cadmium sintered-plate batteries are competitive

TABLE VIII
PERFORMANCE CHARACTERISTICS OF VARIOUS NUCLEAR BATTERIES

Type	Energy Source (millicuries)	Conversion Process	Voltage (volts)	Current (amperes)	Impedance (ohms)	Efficiency (per cent)	References
High-Vacuum Charger	250 Sr—Y-90	direct charging	to 350,000	10^{-9}	10^{15}	25	[89]–[91]
Dielectric Charger	50 Sr—Y-90	direct charging	to 10,000	10^{-11}	10^{13}	up to 1	[92], [93]
Contact Potential	ionizing radiation	contact potential	1 per cell	10^{-11}	10^8 – 10^{11}	0.01	[95], [96]
Semiconductor Junction	250 Sr—Y-90	electron voltaic	0.3 per cell	10^{-5}	10^2 – 10^4	2.5	[97], [98]
Thermojunction	150×10^3 Po—210	thermoelectric	0.75	25×10^{-3}	—	0.2	[99], [100]
Photovoltaic	4.5×10^3 Pm-147	photovoltaic	1	10^{-5}	—	1	[101]

with the lead-acid automotive batteries. On light drain application the pocket and sintered-plate batteries have similar characteristics. Since the sintered-plate construction is relatively new, the life characteristics of these batteries have not been completely determined.

4) *Zinc-Silver Oxide Batteries*: Zinc-silver oxide batteries [83]–[85] represent a new class of secondary batteries which have become commercially available since World War II. The theoretical possibilities of using this electrochemical system have been recognized for many years. However, it was not until H. G. André demonstrated in the early thirties that the active anode and cathode materials could be kept separated during the charging and discharging processes that a practical zinc-silver oxide secondary battery was realized. This was accomplished by using a semi-permeable membrane separator.

These batteries can furnish higher currents and give three to five times greater watt-hour capacities per unit of weight and volume than the lead-acid, nickel-iron, or nickel-cadmium storage batteries. They are particularly adapted for delivering high watt-hour capacities at discharge rates less than 30 minutes, which makes them attractive for many special military applications. However, because they are more expensive and have a shorter cycle life than the conventional storage batteries, they have not found wide commercial usage.

5) *Cadmium-Silver Oxide Batteries*: The recently announced cadmium-silver oxide battery [86] combines the high capacity features of the silver oxide cathode with the favorable cycling and low-rate discharge characteristics of the cadmium anode. Other than the replacement of the zinc sponge anode with a cadmium sponge, the construction of these batteries is similar to the zinc-silver oxide batteries.

These batteries at the present stage of development give about 2.5 times the watt-hour capacity per unit of weight and volume of comparable nickel-cadmium batteries. However, not enough data are available on cycle life to make an over-all performance comparison of these two batteries. Compared with the zinc-silver

oxide battery, they give about 40 per cent less capacity and are not suitable for high rate discharge. They are recommended for low rate and long cycle life applications.

6) *New Developments*: Several new battery systems under development are lead-silver oxide [87], cadmium-mercuric oxide [88], zinc-nickel dioxide [26], and iron-silver oxide [26]. The properties of some of these are given in Table VI. Two of these cells, lead-silver oxide and cadmium-mercuric oxide, have been designed for specialized applications.

III. CONVERSION OF NUCLEAR ENERGY TO ELECTRICAL ENERGY

The direct conversion of nuclear energy to electrical energy has recently attracted considerable attention. The immediate interest lies in the possible application of such processes to produce simple, reliable, long-life power sources.

At the present stage of development, nuclear batteries cannot be used for conventional power demands such as encountered in lighting and automotive applications, as they are not suitable for supplying more than microwatts of power. However, for uses which require long shelf life, for continued use of low current over long periods of time as in earth satellites, or for equipment in inaccessible regions, nuclear cells have merit. Another advantage of these cells is that they are temperature independent and can operate at extremes of temperature, where other conventional cells fail.

The future usefulness of the nuclear batteries depends upon the solution of several problems, such as the high cost of radioactive material, radiation shielding, and the low-energy conversion efficiency.

The various nuclear batteries are summarized briefly in the following parts and their performance characteristics in Table VIII.

A. Direct Charging

This method of conversion uses only charged radiation and involves the simple collection of charged

carriers by an electrode to create a voltage. These direct charging devices consist of three principal parts; a radioactive source, an insulating medium between the electrodes, and a metal collector. This type of cell is capable of producing high voltages if enough time elapses to build up a charge of electrons. They are limited in their usefulness by low currents and high impedances, as seen by the data in Table VIII. The current and the impedance depend upon the amount of radioactive material used; however, the use of large amounts is not feasible due to the present high cost of such materials and the need for shielding.

Commercial batteries of this type are available [94] with voltage ratings from 1 to 10,000 volts and current ratings from 5×10^{-12} to 5×10^{-9} amperes.

B. Contact Potential Difference

This method utilizes both charged and uncharged radiation, and operates by using contact potential fields [95], [96] to separate charges and to produce currents. The basic principle of this cell is illustrated in Fig. 20. Here are shown two electrodes of dissimilar metals or surfaces, between which there is enclosed an atmosphere of gas, for example argon. Radiation of any type having sufficient energy to ionize the gas produces carrier pairs. These are acted upon by the field due to the contact potential difference of the metal surfaces, the positive ions flowing in one direction and the negative electrons in the opposite. This produces an electric current which may pass through an external load R and do useful work.

In this cell, which has an especially low efficiency due mainly to the small absorption coefficient of gases for radioactive radiation, the maximum output voltage is the contact potential difference.

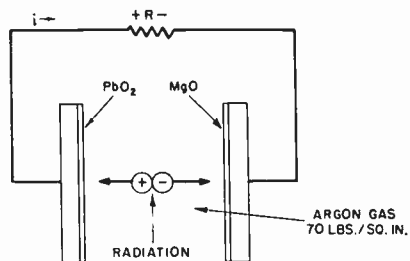


Fig. 20—Diagram of contact potential device.

C. Semiconductor Junction

When beta particles are absorbed by a semiconductor they dissipate most of their energy by ionizing the atoms of the solid. The carriers generated in this fashion are in excess of the number permitted by thermodynamic equilibrium and if they diffuse to the vicinity of a rectifying junction, they induce a voltage across the junction.

A power generating device [97], using this phenomenon (electron-voltaic effect), is shown schematically in Fig. 21. The junction consists of silicon, with p type

on the left and n type on the right, with a source of ionizing radiation placed near this junction.

Because of the high multiplication accompanying the absorption of beta particles in the semiconductor, this type of device gives a higher current and lower impedance than the direct charging types. The disadvantage of this cell, which uses high energy beta particles, is its short life which results from the radiation damage of the silicon crystals.

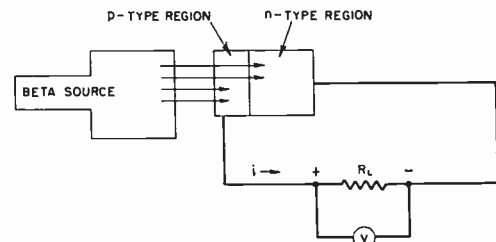


Fig. 21—Schematic diagram of semiconductor converter and circuit.

D. Thermojunction

This type of nuclear cell makes use of a thermopile which converts the heat from radioactive decay into electricity [99], [100]. The battery, developed by Birden and Jordan [99] uses 150 curies of polonium 210 as the source of nuclear radiation, and maintains a temperature difference of about 232°C (450°F) between the hot and cold junctions of 40 thermocouples. The disadvantages of this particular cell is that polonium decays with a relatively short half life of 138 days and is quite expensive.

E. Photovoltaic

The application of the photovoltaic effect to the conversion of radioactive energy to electrical energy consists of two steps, 1) converting the radioactive energy to photons by the use of scintillating media, and then 2) utilizing these photons to eject electrons from a suitably prepared surface. The electrons flow to a collecting electrode and through an external load.

A cell of this type [101], which uses a silicon photocell and a light source consisting of a mixture of promethium oxide and a phosphor, has recently been announced. The voltage of this cell remains essentially constant, while the current decays exponentially with the decay of the radioactive material. Thus, for this particular cell, the power output drops to about one-half of its initial value after two and one half years, which is the half life of promethium 147.

IV. CONVERSION OF SOLAR ENERGY TO ELECTRICAL ENERGY

As an outgrowth of the extensive work on solid-state materials, silicon photovoltaic converters have been developed [102]–[104] which make use of a special type of barrier layer between two semiconductors known as a p - n junction. When radiant energy strikes this junction,

a potential disturbance occurs which can be utilized to deliver electric power to an external circuit.

A typical set of curves for this cell is shown in Fig. 22, in which the open-circuit voltage V_0 is plotted as a function of the sunlight intensity, and where the power output and efficiency for full sunlight (100 mw/cm²) is plotted as a function of the voltage, which varies due to a variation of load resistance.

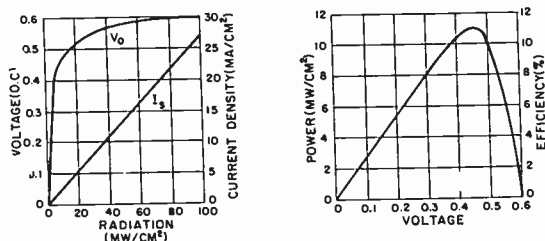


Fig. 22—Typical curves showing current-voltage and power relations of silicon solar battery.

The over-all efficiency of this device, which is 11 per cent in full sunlight, is limited by the following factors [104]: 1) some of the radiant energy is lost by reflection from the silicon surface, 2) up to 30 per cent of the hole-electron pairs may be lost by recombination, and 3) the internal resistance of the cell itself.

Another type of solar converter is the cadmium sulfide cell [105] which has an open-circuit voltage of 0.45 volt, a short-circuit current of 15 ma/cm², and an efficiency of 5 per cent. This material, which has a band gap of 2.4 ev as compared to 1.1 ev for silicon, shows an anomalous photovoltaic response in that it responds to light energies below the band gap energy at about 1.8 to 2.0 ev, depending upon impurity content.

More recently, solar cells were made using CdTe, InP, and GaAs [106]. Conversion efficiencies ranging from 2 per cent to 6.5 per cent have been achieved. Considerable improvement in these results is expected as the technology of these new semiconductors is advanced.

Selenium and silicon photovoltaic cells are commercially available. For selenium, the maximum efficiency for conversion of full sunlight is between 0.5 per cent and 1 per cent. Thus a cell of this type will produce about 0.5 mw/cm² in average sunlight and have an open-circuit voltage about 0.5 volt, and a short-circuit current about 2 ma. For silicon cells, the efficiency of conversion is about 8.8 per cent for the average production unit. However, selected units with efficiencies above 10 per cent are also available at higher cost. To be cost competitive with a Leclanché dry cell, a solar cell must last ten years, assuming it operates at an efficiency of 8 per cent [107].

The chief problems associated with solar cells is the high cost of materials, and the need for a simple, cheap storage cell having a life equal to the solar cell itself, so that the power source can continue to operate in the absence of adequate light [108].

BIBLIOGRAPHY

- [1] Latimer, W. M. *Oxidation Potentials*. New York: Prentice-Hall, Inc., 1952.
- [2] Walkley, A. "The Potential and Coulombic Capacity of Some Galvanic Cell Systems," *Journal of the Electrochemical Society*, vol. 99 (August, 1952), pp. 209C-214C.
- [3] Vinal, G. W. *Primary Batteries*, New York: John Wiley and Sons, Inc., 1950.
- [4] Heise, G. W., and Cahoon, N. C. "Dry Cells of the Leclanché Type, 1902-1952—A Review," *Journal of the Electrochemical Society*, vol. 99, August, 1952, pp. 179C-187C.
- [5] Ruben, S.; "Balanced Alkaline Dry Cells," *Transactions of the Electrochemical Society*, vol. 92 (1947), pp. 183-193.
- [6] Friedman, M., and McCauley, C. E., "The Ruben Cell, A New Alkaline Primary Dry Cell Battery," *Transactions of the Electrochemical Society*, vol. 92 (1947), pp. 195-215.
- [7] Booe, J. M. "The Alkaline-Mercury Oxide Cell," *Journal of the Electrochemical Society*, vol. 99 (August, 1952), pp. 197C-200C.
- [8] Dalfonso, J. L., "Alkaline Dry Batteries," *Proceedings of the Tenth Annual Battery Research and Development Conference*, Power Sources Division, Signal Corps Engineering Laboratories, Fort Monmouth, N.J., pp. 11-14, 1956.
- [9] Herbert, W. C., "The Alkaline Manganese Dioxide Dry Cell," *Journal of the Electrochemical Society*, (August, 1952), pp. 190C-191C.
- [10] Kirk, R. C., and Fry, A. B., "Magnesium Dry Cells," *Journal of the Electrochemical Society*, vol. 94 (1948), pp. 277-289.
- [11] Fry, A. B., Kirk, R. C., and George, P. F. (to Dow Chemical Co.) U.S. Pat. 2,547,907, April 3, 1951; U.S. Pat. 2,547,908, April 3, 1951; U.S. Pat. 2,547,909, April 3, 1951.
- [12] Kirk, R. C., George, P. F., and Fry, A. B. "High Capacity Magnesium Dry Cells," *Journal of the Electrochemical Society*, vol. 99 (August, 1952), pp. 323-327.
- [13] Glicksman, R. and Morehouse, C. K. "Investigations of the Electrochemical Characteristics of Organic Compounds. I. Aromatic Nitro Compounds," *Journal of the Electrochemical Society*, vol. 105 (June, 1958), pp. 299-305.
- [14] Morehouse, C. K., and Glicksman, R. "Dry Cells Containing Various Aromatic Nitro Compounds as Cathode Materials," *Journal of the Electrochemical Society*, vol. 105 (June, 1958), pp. 306-311.
- [15] Glicksman, R., and Morehouse, C. K. "Investigation of the Electrochemical Characteristics of Organic Compounds. II. Aromatic Nitroso Compounds," the *Journal of the Electrochemical Society*, submitted for publication.
- [16] Morehouse, C. K., and Glicksman, R. "Dry Cells Containing Various Aromatic C-Nitroso Compounds as Cathode Materials," *Journal of the Electrochemical Society*, submitted for publication.
- [17] —, —. "Magnesium-Bismuth Oxide Dry Cells," *Journal of the Electrochemical Society*, submitted for publication; U.S. Pat. 2,809,225, October 8, 1957 (to Radio Corporation of America).
- [18] Schumacher, E. A., and Heise, G. W. "The Alkaline Cell with Copper Oxide or Air Depolarization (1902-1952)," *Journal of the Electrochemical Society*, vol. 99 (August, 1952), pp. 191C-196C.
- [19] Schumacher, E. A. "Air Depolarized Batteries," See [8], pp. 14-19.
- [20] Boswell, T. L. (to Elgin National Watch Company). U.S. Patent 2,683,184, July 6, 1954.
- [21] Stokes, J. J., Jr. "The Aluminum Dry Cell," unpublished paper presented at the Electrochemical Society Meeting, Pittsburgh, Pa., October, 1955.
- [22] Leclanché, G. *Les Mondes*, vol. 16 (1868), pp. 532-535. Also *Comptes rendus*, vol. 83 (1876), p. 54.
- [23] Gassner, C. German Patent 37,758, April 8, 1886; U.S. Patent 373,064, November 15, 1887.
- [24] Tomassi, D. *Traite des Piles Electriques*. Paris: Georges Corre, pp. 267-271, 1889.
- [25] Vinal. See [3], p. 45.
- [26] Hamer, W. J. "Modern Batteries," IRE TRANSACTIONS ON COMPONENT PARTS, vol. CP-4 (September, 1957), pp. 86-96.
- [27] Birdsall, C. G. "Leclanché Batteries." See [8], pp. 1-3.
- [28] Anthony, H. R. C. U.S. Patent 2,198,423, April 23, 1940.
- [29] Morehouse, C. K., and Welsh, J. Y. (to Olin-Matheson Chemical Corporation). U.S. Patent 2,748,183, May 29, 1956.
- [30] Adams, P. H. "Developments in Dry Batteries and Associated Electronic Equipment," *PROCEEDINGS OF THE INSTITUTE OF RADIO ENGINEERS*, vol. 12 (August, 1951), pp. 167-178.
- [31] Huntley, A. K. "A Radio 'B' Dry Battery of Flat Type Construction," *Transactions of the Electrochemical Society*, vol. 68 (1935), pp. 219-230.
Reid, C. J., and Morrill, M. T. U.S. Patent 690,772, January 7, 1902.

- [32] French, H. F., "Improvements in B-Battery Portability," PROCEEDINGS OF THE INSTITUTE OF RADIO ENGINEERS, vol. 29 (June, 1941), pp. 299-303. U.S. Patent 2,272,969.
- [33] Franz, A. O., Martinez, J. M., and Koppelman, M. D. (to Olin Industries). U.S. Patent 2,416,576, February 25, 1947.
- [34] Vinal, See [3], pp. 127-159.
- [35] Otto, E., Morehouse, C. K., and Vinal, G. W. "Low Temperature Dry Cells," *Transactions of the Electrochemical Society*, vol. 90 (1946), pp. 419-432.
- [36] Kameyama, M. and Naka, A. "Investigation of Low Temperature Dry Cells," *Journal of the Society of the Chemical Industry, Japan*, vol. 39 (1936), pp. 871.
- [37] Wilke, M. E. "Dry Cell Designed to Operate at -40°C Containing Lithium Chloride in the Electrolyte," *Transactions of the Electrochemical Society*, vol. 90 (1946), pp. 433-440.
- [38] *American Standard Specification for Dry Cells and Batteries*. National Bureau of Standards Circular 559, 1955.
- [39] U.S. Military Specifications, Batteries, Dry, MIL-B-18R, Amendment No. 2, September 20, 1956.
- [40] Clarke, C. L., U.S. Patent, 298,175, May 6, 1884.
- [41] Aron, H., German Patent 38,220, December 13, 1886.
- [42] Edison, T. A., U.S. Patent, 704,303, July 8, 1902.
- [43] Morrison, W. U.S. Patent 916,575, March 30, 1909; 975,885, 975,980, and 976,092, November 15, 1910. German Patent 273, 143, April 24, 1914.
- [44] Bronsted, J. N., German Patent 296,397, February 7, 1917, U.S. Patent 1,219,074, March 13, 1917.
- [45] Morehouse, C. K. "Magnesium Primary Batteries," *Journal of the Electrochemical Society*, vol. 99, (August, 1952), pp. 187C-189C.
- [46] Hovendon, J. M. "Magnesium Batteries." See [8], pp. 8-10.
- [47a] Lehovik, K. "Solid Electrolyte Batteries." See [8], pp. 50-53.
- [47b] Shapero, S. J. "Solid Electrolyte Batteries," *Proceedings of the Eleventh Annual Research and Development Conference*, Power Sources Branch, U.S. Army Signal Engineering Laboratories, Fort Monmouth, N.J., pp. 3-5, 1957.
- [48] Wood, R. E. "Punched-Cell Batteries with Polyethylene Glycol Electrolytes," *Journal of the Electrochemical Society*, vol. 103 (1956), pp. 417-420.
- [49] Morse, E. M. "Water-Activated Batteries." See [8], Also, See [47b], pp. 69-72.
- [50] *Water-Activated Batteries*. General Electric Technical Brochure, No. GEA 6238A, 12/55 (9 M).
- [51] Blake, I. C. "Silver Chloride-Magnesium Reserve Battery," *Journal of the Electrochemical Society*, vol. 99 (August, 1952), pp. 202C-203C.
- [52] Pucher, L. E. "The Cuprous Chloride-Magnesium Reserve Battery," *Journal of the Electrochemical Society*, vol. 99 (August, 1952), pp. 203C-204C.
- [53] Morehouse, C. K., and Glicksman, R. "N-Halogen Organic Compounds as Cathode Materials for Primary Batteries," *Journal of the Electrochemical Society*, vol. 104 (1957), pp. 467-473.
- Lozier, G. S., Cutler, L. H., and Morehouse, C. K. "Organic N-Halogen-Magnesium Reserve Batteries," Extended Battery Abstracts of the Electrochemical Society Meeting, Buffalo, N.Y., pp. 52-53, October, 1957.
- [54] Howard, P. L. "The Silver Peroxide-Zinc Alkaline Cell," *Journal of the Electrochemical Society*, vol. 99 (1952), pp. 200C-201C.
- [55] Wilburn, N. T. "Zinc-Silver Oxide Batteries," See [8], pp. 20-22.
- , "Development and Reliability Investigations of Zinc-Silver Oxide Missile Batteries," See [47b], pp. 58-61.
- [56] Schlotter, W. J. "The Lead Dioxide-Zinc Reserve Type Cell," *Journal of the Electrochemical Society*, vol. 99 (1952), pp. 205C-206C.
- [57] Schrodtt, J. P., Otting, W. J., Schoegler, J. G., and Craig, D. N. "A Lead Dioxide Cell Containing Various Electrolytes," *Transactions of the Electrochemical Society*, vol. 90 (1946), pp. 405-417.
- [58] Pucher, L. E. "The Lead Dioxide-Cadmium Reserve Type Cells," *Journal of the Electrochemical Society*, vol. 99 (1952), pp. 204C-205C.
- [59] Kilmer, S. B., Lawson, H. E., and Randolph, C. L. "Chlorine-Depolarized Battery," See [8], pp. 29-32.
- Langworthy, E. M., Randolph, C. L., and Lawson, H. E. "Chlorine-Depolarized Battery." See [47b], pp. 67-69.
- [60] Howard, P. L. "The Chlorine-Zinc Primary Cell," *Journal of the Electrochemical Society*, vol. 99 (1952), pp. 206C-207C.
- [61] Gleason, H. S., and Freund, J. M. "Amonia Vapor Activated Batteries," Extended Battery Abstracts of the Electrochemical Society Meeting, Buffalo, N.Y., pp. 31-32, October, 1957.
- Gleason, H. S., and Minnick, L. J., "Amonia Vapor Activated Batteries." See [47b], pp. 13-16.
- [62] Evans, G. E. "Boron Trifluoride Batteries." See [47b], pp. 11-13.
- [63] McKee, E. "Thermal Cells." See [8], pp. 26-28, 1956.
- [64] Goodrich, R. B., and Evans, R. C. "Thermal Batteries," *Journal of the Electrochemical Society*, vol. 99 (1952), pp. 207C-208C.
- [65] Gorin, E., and Recht, H. L. "Fuel Cells. See [8], pp. 53-56, 1956.
- [66] Adams, A. M. "Electrochemical Cells as Energy Converters," AIEE Conference Paper, No. C. P. 56-266, pp. 1-16, January, 1956.
- [67] Vinal. See [3] pp. 160-213.
- [68] Vinal. See [3], pp. 321-323.
- [69] Vinal, G. W. *Storage Batteries*. New York: John Wiley and Sons, Inc., 4th ed., 1955.
- [70] Willihnganz, E. "Batteries (In Part)," in *Encyclopaedia Britannica*, vol. 3, pp. 217E-218, 1956.
- [71] Lord, E. L., and Anderson, F. C. *Batteries—Standard Handbook for Electrical Engineers*. Edited by A. E. Knowlton, 9th ed. New York: McGraw-Hill Book Company, Inc., pp. 1891-1940, 1957.
- [72] Willihnganz, E., "The Lead-Acid Automotive Battery," *Journal of the Electrochemical Society*, vol. 99 (1952), pp. 234C-236C.
- [73] Riggs, N. C. "Lead-Acid Motive Power and Carlighting Batteries," *Journal of the Electrochemical Society*, vol. 99 (1952), pp. 236C-238C.
- [74] Thomas, U. B. "Lead Acid Stationary Batteries," *Journal of the Electrochemical Society*, vol. 99 (1952), pp. 238C-241C.
- [75] Rose, C. C., and Zachline, A. C. "Low Discharge Cells," *Journal of the Electrochemical Society*, vol. 99 (1952), pp. 243C-244C.
- [76] Jensen, H. E. "Calcium-Lead Grid Batteries," See [47b], pp. 73-77.
- [77] Endress, C. N., and Rose, C. C. "Plastic Container-Electrolyte Retaining Lead-Acid Storage Batteries," *Journal of the Electrochemical Society*, vol. 99 (1952), pp. 241C-243C.
- [78] Anderson, F. C. "The Edison Nickel-Iron-Alkaline Cell," *Journal of the Electrochemical Society*, vol. 99 (1952), pp. 244C-248C.
- [79] Bergstrom, S. "Nickel-Cadmium Batteries," *Journal of the Electrochemical Society*, vol. 99 (1952), pp. 248C-250C.
- [80] Ellis, G. B., Mandel, H., and Linden, D. "Sintered Plate Nickel-Cadmium Batteries," *Journal of the Electrochemical Society*, vol. 99 (1952), pp. 250C-252C.
- [81] Fleischer, A. "Vented Ni-Cd Batteries," See [47b], pp. 83-86.
- [82] Belove, L., and Schulman, I. M. "Sealed Sintered Plate Ni-Cd Batteries," See [47b], pp. 41-44.
- [83] Eidensohn, S. "The Zinc-Silver Peroxide Alkaline Storage Battery," *Journal of the Electrochemical Society*, vol. 99 (1952), pp. 252C-254C.
- [84] Howard, P. L. *Zinc-Silver Oxide Batteries*, Technical Bulletin, Yardney Electric Corporation.
- [85] —. *The Silver-Zinc Rechargeable Battery*. Technical Bulletin, Yardney Electric Corporation.
- , "Zinc-Silver Oxide Batteries," See [8], pp. 4144.
- [86] —. *The Silver Oxide-Cadmium Alkaline Secondary Battery*. Technical Bulletin, Yardney Electric Corporation.
- , "Cadmium-Silver Oxide Batteries." See [47b], pp. 78-80.
- [87] Goldberg, M. B., and Reed, H. B., Jr. (to U.S. Government). U.S. Patent 2,697,736, December 21, 1954.
- [88] —, —, (to U.S. Government). U.S. Patent 2,697,737, December 21, 1954.
- , —, "A New Rechargeable Dry Cell," Extended Abstracts of the Electrochemical Society Meeting, Buffalo, N.Y., pp. 31-35, 1957.
- [89] Linder, E. G. "Nuclear Electrostatic Generator," *Physical Review*, vol. 71 (1947), pp. 129-130.
- [90] Linder, E. G., and Christian, S. M. "The Use of Radioactive Material for the Generation of High Voltages," *Physical Review*, vol. 83 (1951), p. 233.
- [91] —, —, "The Use of Radioactive Material for the Generation of High Voltage," *Journal of Applied Physics*, vol. 23 (1952), pp. 1213-1216.
- [92] Linder, E. G., and Rappaport, P. "Radioactive Charging Through a Dielectric Medium," *Physical Review*, vol. 91 (1953) pp. 202.
- [93] Rappaport, P., and Linder, E. G. "Radioactive Charging Effects with a Dielectric Medium," *Journal of Applied Physics*, vol. 24 (1953), p. 1110.
- [94] *Nuclear Batteries*. Patterson-Moos Division, Universal Winding Company, Technical Brochure.
- [95] Kramer, J. B. "A New Electronic Battery," *The Electrician*, vol. 93 (1924), p. 479.

- [96] Ohmart, P. E. "A Method of Producing and Electric Current from Radioactivity," *Journal of Applied Physics*, vol. 22 (1951), pp. 1504-1505.
- [97] Rappaport, P. "The Electron-Voltaic Effect in *P-N* Junctions Induced by Beta-Particle Bombardment," *Physical Review*, vol. 93 (1954), pp. 246-247.
- [98] Rappaport, P., Loferski, J. J., and Linder, E. G. "The Electron-Voltaic Effect in Germanium and Silicon *P-N* Junctions," *RCA Review*, vol. 17 (1956), pp. 100-128.
- [99] "Radioactive Heat to Electricity," *Chemical Engineering News*, vol. 32 (1954), p. 4183.
- [100] Blanke, B. C., "Thermoelectric-Type Nuclear Batteries," See [47b], pp. 109-110.
- [101] Miller, R. C. "The Elgin-Kidde Nuclear Battery," See [47b], pp. 102-105.
- [102] Chapin, D. M., Fuller, C. S., and Pearson, G. L. "A New Silicon *P-N* Junction Photocell for Converting Solar Radiation into Electrical Power," *Journal of Applied Physics*, vol. 25 (1954), pp. 676-677.
- [103] —, —, —. "The Bell Solar Battery," *Bell Laboratories Record*, vol. 33 (1955), pp. 241-246.
- [104] Pearson, G. L. "Conversion of Solar to Electrical Energy," *American Journal of Physics*, vol. 25 (1957), pp. 591-598.
- [105] Reynolds, D. C., Leies, G., Antes, L. L., and Marburger, R. E., "Photovoltaic Effect in Cadmium Sulfide," *Physical Review*, vol. 96 (1954), pp. 533-534.
- [106] Rappaport, P., and Loferski, J. J. "New Solar Converter Materials." See [47b], pp. 96-99.
- [107] Linder, "Solar Batteries." See [8], pp. 59-62.
- [108] Lunz, "Sealed Cells with Solar Converters." [47b], pp. 89-92.

The Resnatron as a 200-MC Power Amplifier*

E. B. TUCKER†, H. J. SCHULTE‡, E. A. DAY§, AND E. E. LAMPI||

Summary—Tetrode amplifiers (resnatrons) used to power the Minnesota Linear Proton Accelerator are described. These demountable tubes are continuously pumped, grid pulsed 202-mc amplifiers capable of a peak power output of 3.5 megw during 300- μ sec pulses with two per cent duty cycle. A transconductance of 0.12 mho and power gains of 10 have been observed. Reliability has been surprisingly good. Life limitation is due to crystallization of the pure tungsten filaments. The average time between pull-downs because of filament trouble varies from 700 to 1140 hours of operation. The lower life corresponds to higher power service conditions.

INTRODUCTION

THE RESNATRON originated about 1938 when Sloan and Marshall developed an oscillator which depended upon the relationship between transit time and frequency to provide the proper feedback phase.^{1,2} During World War II, resnatrons were developed for jamming purposes as noise-modulated cw oscillators.³ Subsequent to the war years, Collins Radio Company of Cedar Rapids, Iowa, carried on some resnatron work both as oscillators and as amplifiers. In general, the objective of all these tubes was the development of high cw power, and power outputs of the order

of 60 kw were obtained.^{4,5} It should be noted that as an amplifier it is not necessary and is, in fact, undesirable for the transit time to play the same role that is played in the original oscillator. The name resnatron when it is used today appears to denote a tetrode with a particular tube construction in which the cavities and tuners are all contained in the vacuum envelope, rather than a particular type of tube. The resnatron herein described is a tetrode in which the screen operates at the same dc potential as the anode.

When the Minnesota Linear Proton Accelerator was first contemplated, there was an obvious need for an amplifier capable of very high peak powers; in this case 200 mc appeared to be an optimum frequency. It was estimated that in order for the fields in the large accelerator cavities to be built up within a reasonable length of time, it would be ideal to use a shaped rf pulse so that the power available during the first 50 μ sec of the pulse would be 8 megw and the power for the remainder of the 300- μ sec pulse would be such that the average power during the pulse would be 4 megw. The high rf drive at the first of the pulse would serve to build the rf level in the tank up to the 4-megw operating level faster than the usual rectangular pulse. There was not at that time (1949-1950), nor is there today, a commercially available tube capable of providing such power. The resnatron-type tube, with its reputation for high average power, seemed the most logical choice, with various ring circuit arrangements being the only alternatives. In 1950, the Collins Radio Company was given a contract to develop and build five tubes with

* Original manuscript received by the IRE, November 25, 1957; revised manuscript received, March 10, 1958. This work was supported by the Atomic Energy Commission.

† General Electric Res. Lab., Schenectady, N. Y., formerly with Univ. of Minn., Minneapolis, Minn.

‡ Bell Telephone Labs., Murray Hill, N. J., formerly with Univ. of Minn., Minneapolis, Minn.

§ Midwestern Universities Res. Assn., Madison, Wis., formerly with Univ. of Minn., Minneapolis, Minn.

|| Bell Telephone Labs., Allentown, Pa., formerly with Univ. of Minn., Minneapolis, Minn.

¹ D. H. Sloan and L. C. Marshall, *Phys. Rev.*, vol. 58; 1940.

² D. H. Sloan, U. S. Patents Nos. 2,404,541; 2,404,542; 2,405,762; and 2,405,763.

³ W. G. Dow and H. W. Welch, "Very High Frequency Techniques," McGraw-Hill Book Co., Inc., New York, N. Y., vol. 1, ch. 19; 1947.

⁴ W. W. Salisbury, "The resnatron," *Electronics*, vol. 19, p. 92; February, 1946.

⁵ D. B. Harris, "New UHF resnatron designs and applications," *Electronics* vol. 24, pp. 86-89; October, 1951.

specifications similar in outline to those given above. The general design was made by W. W. Salisbury. In April, 1953, the contract was canceled by mutual agreement and the final development and testing of the tubes were carried out in Minneapolis by the accelerator staff of the University of Minnesota.

It should be emphasized that a minimal number of changes was made at Minnesota in both mechanical and rf design. Therefore, there are, in the final tube, many design details for which Collins Engineers should have full credit.

GENERAL DESCRIPTION

The Minnesota resnatrons are massive structures of copper and iron. The top of the tube stands some fifteen feet above the floor on which the iron base plate is supported by four iron legs. Because of the large area of rubber gasketing used in the vacuum joints, the tubes are continuously pumped by means of a 1400 C.F.M. oil-diffusion pump operated with a freon refrigerated baffle (which cuts the pumping speed by a factor of two). Exclusive of the vacuum pump, the tube weighs about $2\frac{1}{2}$ tons. In addition to the usual elements necessary for a tetrode, the vacuum enclosure contains all of the rf cavities, tuners, water-cooling coils, and a 100-kv dc isolation choke. The tube is readily dismantled for filament replacement or other repairs.

The resnatron is a coaxially arranged beam tetrode with screen and anode operated at the same dc potential. Due to the far-from-ideal vacuum conditions, a pure tungsten filament is used. The cathode consists of 36 strands of tungsten with approximately five inches of emitting length per strand. Thus the tube in reality consists of 36-unit tetrodes operating in parallel. The 60-cycle filament power of 7000 amperes at 6 volts is provided by a step-down transformer with a single-turn secondary of sheet copper with a cross section of 12 square inches. One side of the secondary is operated at ground potential.

All elements of the tube, with the exception of the filament itself, are water cooled. This necessitates the provision of three purified-water supplies at potentials different from ground. The tubes are operated class C with grounded grid circuits. The grid is driven by an rf pulse of the appropriate shape. The only unusual feature of this operation is that here we have a continuously pumped tube standing off voltages in the range of 70 kv both during and between pulses. Of course the 300- μ sec pulse is long enough so that, with the exception of power dissipation, the operation is essentially cw.

The rf power-distribution system of the accelerator (see Fig. 1) is, for the high-power portion, aluminum waveguide with dimensions 40 by 12 inches. There is need for transition from waveguide to coaxial line at both input and output of the resnatrons, since the tubes are coaxial by design. Three of the four tubes used in the system drive individual cavities of the linear accelerator while the fourth acts as the driver for the other three.

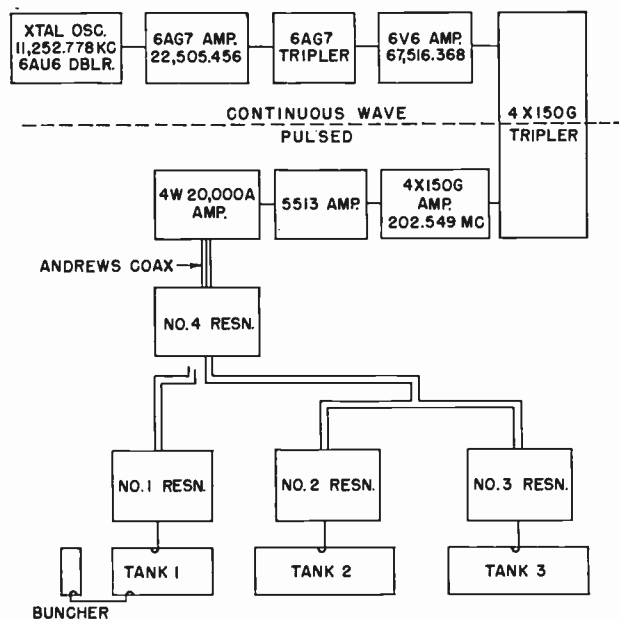


Fig. 1—Block diagram of the radio frequency system of the Minnesota Linear Accelerator. The distribution system between resnatrons and from resnatrons to tanks is aluminum waveguide.

The input to the latter tube is provided by a frequency multiplier and amplifier chain which produces a pulse power of 200 kw at a frequency of 202.55 mc.

ELECTRODE CONFIGURATION AND CHARACTERISTICS

Each individual sector of the tube has the typical beam tetrode electrode arrangement. Cross-section drawings of these 10° sectors are given in Fig. 2, while the vertical section for the final design of Fig. 2(b) is given in Fig. 3.

The indentations in the anode are secondary electron traps which are often used in tubes operating with screen and anode at the same dc potential. The operation of these secondary traps depends on transit time. The fields of the output cavity are concentrated between the screen bars and the anode fins. Electrons passing through the gap in such phase as to excite the fields will, therefore, lose most of their energy in this strong field region, and then will proceed toward the anode wall. Even though these primary electrons strike the anode wall with reduced velocity, they will, in general, have enough energy to produce secondaries. The phase of the fields in the output cavity (assuming it unchanged) is such as to accelerate these secondaries toward the grid, but they will travel relatively slowly and be accelerated by weak fields until the anode fin tips are reached. The traps are made deep enough so that the phase of the fields in the anode cavity reverses before the secondaries reach the strong field region. Secondaries are thus prevented from returning to the screen and loading the output cavity in this undesirable fashion. Proper behavior of these traps requires that the electron beam be narrow enough so that none of the electrons strikes the fin tips, where transit time cannot provide the suppression required. The space charge

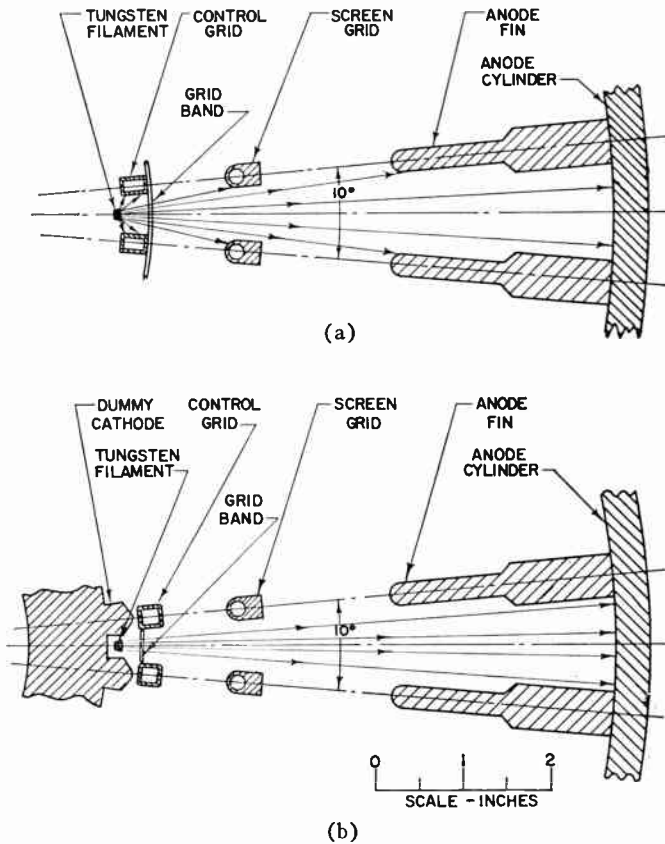


Fig. 2—Cross section of two resnatron designs. The arrows indicate possible electron trajectories for positive grid voltage. (a) Old model. (b) New model.

forces tend to help suppress the secondaries as well.

The shaping of the electrodes is in general such as to enhance the beam formation. The banding in the position shown in Fig. 2(a) is, however, an anomaly. Tubes without this banding derive their focussing properties from the screen-field penetration between the grid bars. Such tubes suffer from screen cathode feedback through the grid bars to the extent that a triode oscillation is set up with the screen acting as the anode. This oscillation appears to be the same mode for which the original resnatrons were designed; *i.e.*, there is a half-cycle transit from the cathode to the screen, and the feedback (because of the screen-cathode capacity) produces the correct feedback phasing. This type of oscillation should be voltage sensitive, but the oscillation was so violent that the tubes could not be pushed through the region of instability. In order to suppress the oscillations, the banding was added to the grid. However, the presence of the banding means that the beam begins to blow up as soon as the grid goes positive with respect to the cathode. Thus, one expects that such an electrode configuration would show the above mentioned anode cavity loading due to electrons striking the anode fins, and secondaries being accelerated back to the screen. Such was indeed the case.

Electrolytic tank measurements were made to test the suitability of the proposed geometries in regard to cut-off μ and the beam properties in the absence of

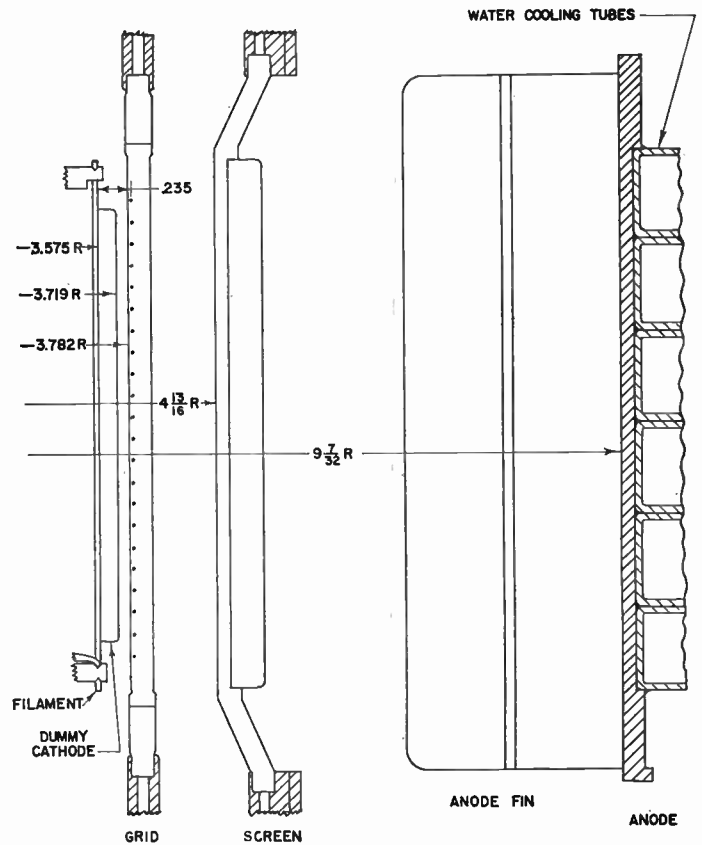


Fig. 3—Vertical section of Pierce gun design. Dummy cathode is the focussing element at ground potential. The anode water cooling tubes are soft soldered in place.

space charge. For the geometry of Fig. 2(a), cut-off μ was 50, the mutual conductance turned out to be 0.193 mho, and of course the potential plots were such as to indicate beam blow up. In the case of the rf measurements this trouble manifests itself in a limiting of the power output at a plate current which corresponded to the grid just being driven to cathode potential. An increase of the drive power increased the plate current, but failed to increase the power output. In the actual resnatron there is no method of measuring the screen current separately from the plate current, but there is good indirect evidence that the screen current increases as the grid reaches ground potential. Incorrect loading of the plate cavity can cause a similar effect, but changes in the output coupling did not improve the situation, and the beam blow-up hypothesis is confirmed by other tests in which the screen current could be monitored.

The output power limit for the configuration of Fig. 2(a) is too low to provide sufficient power for the accelerator at reasonable plate voltages. The final configuration adopted to remedy this situation was that of Fig. 2(b), consisting of a Pierce gun in which a four-thirds power dependence of the voltage on radial distance from the cathode (as required for rectilinear flow) was approximately achieved in the grid-cathode vicinity. The actual geometry is modified somewhat from the ideal Pierce configuration to satisfy the requirements of

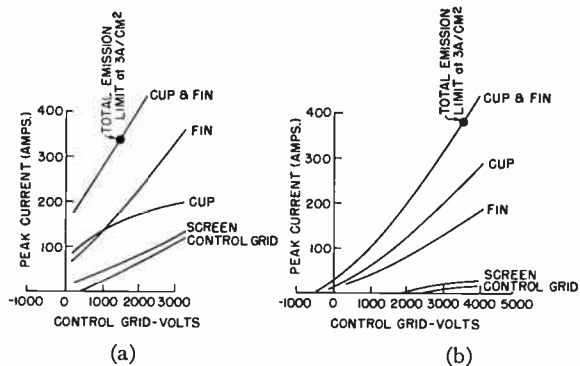


Fig. 4—Triode transfer characteristics measured under dc conditions in full scale model. Voltages and currents have been scaled to values characteristic of full resonatron at 75-kv anode potential. (a) Old model. (b) New model.

reproducibility and assembly clearance. Because of mechanical difficulties, the grid-cathode spacing of the new design is greater than in the old, and thus the mutual conductance and gain are expected to be down.

In order to check the behavior of the various configurations under consideration a full-scale model of a 30° sector of the resonatron was constructed. Only the middle section of the three units was fitted with a cathode, the other sectors serving to provide the proper boundary conditions for the single beam. Since only dc tests were contemplated, the test section was only long enough to include the actual lengths of the tube elements. The model was built so that the currents to the screen, anode fins, and anode cylinder were separately monitored as contrasted to the case in the actual resonatron where the three currents are all measured as plate current.

The main objective of the model tests was to check beam characteristics. Fig. 4 gives the triode transfer characteristics for the two designs with screen and anode operated at the same potential. Under this condition, it can be seen that the screen and control grid currents are both low for the final design, whereas the old design shows a marked increase in screen and control grid currents as the grid goes positive. It should also be noted that the current to the anode cylinder drops off in the old design while in the new one this same current increases steadily. The real test of the electrode configuration is that mode of operation where the anode potential is depressed below that of the screen. This corresponds to that part of the rf cycle when electrons will deliver power to the output cavity and also when secondaries will be accelerated back to the screen. If secondaries do not return to the screen under dc conditions with the anode depressed, there is no reason to believe that they will during rf operation. Thus the screen current measured under such dc conditions is the maximum possible, and will in practice be reduced by the effectiveness of the transit-time suppression. Fig. 5 shows the useful currents measured for the two electrode configurations in the dc tests.

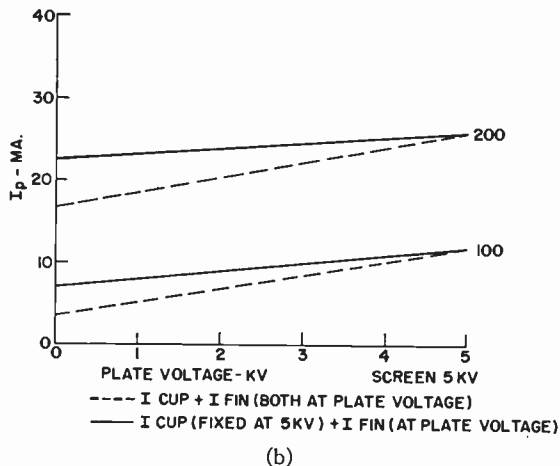
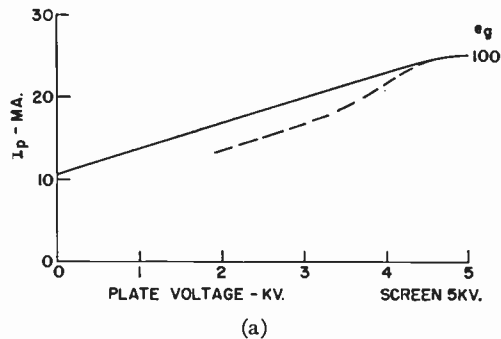


Fig. 5—Comparison of useful currents in two resonatron designs. Dotted lines represent current collected with anode fin and cylinder at anode potential. The solid lines show current collected with cylinder and screen both at 5 kv, and fins at potential shown as anode potential. Note that new design gives much larger fraction of useful current. (a) Old model. (b) New model.

The tube constants from the above curves are cut-off μ of 76 and a mutual conductance of 0.12 mho. The lower mutual conductance results in lower gain, but the grid can now be driven positive and the net result is that a higher power output is available. Figs. 6 and 7 give triode characteristics and estimated tetrode characteristics for the two designs. Only the Pierce gun design will be considered during the remainder of this paper.

CATHODE

One of the greatest problems in a continuously pumped tube is that of the cathode. Because of the relatively poor vacuum attained, the filaments presently in use are of pure tungsten.⁶ The details of the tensioning device which is necessitated by the thermal expansion of the five-inch length of the tungsten filament are given in Fig. 8. Fig. 9 shows the assembled cathode with a heat shield covering the tensioning springs. This flexibility is provided at the lower end of the filament; the upper end is held by a fixed support. In order to provide the emission of 3 amperes per square cm required for the higher power tubes, the filament temperature must be in the vicinity of 2700°K. The water-cooled focussing electrode which partially surrounds

⁶ The filaments and pantograph blocks were manufactured by RCA.

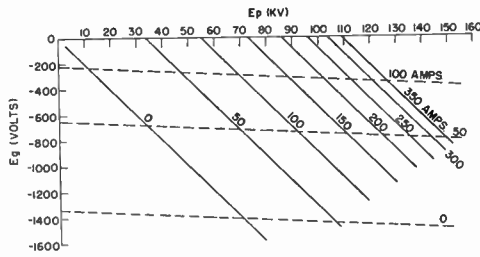


Fig. 6—Constant current characteristics for old design. Solid lines: triode characteristics, dotted lines: tetrode characteristics assuming screen 70,000 volts, gm=0.193, cathode anode mu 2000.

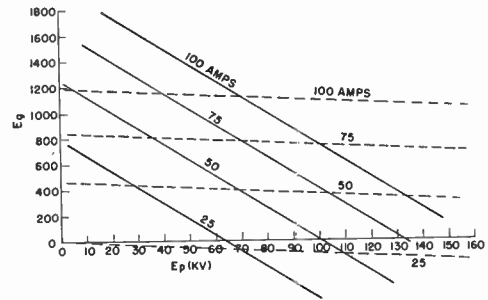


Fig. 7—Constant current characteristics of Pierce gun design resnatron. Solid lines: triode characteristics, dotted lines: estimated tetrode characteristics using 70,000 volts on screen, cathode anode mu of 2000.

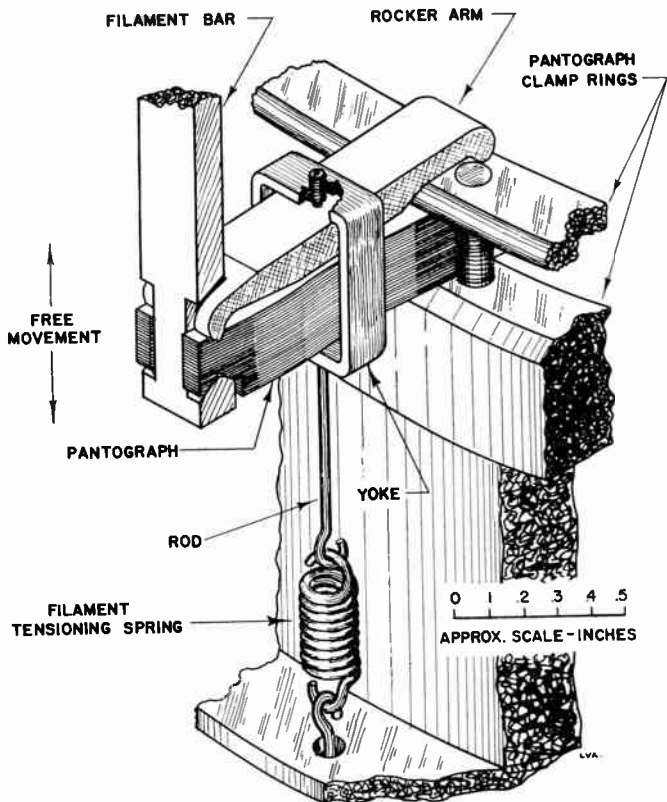


Fig. 8—Filament tensioning system. Pantograph leaves are of chrome copper, rocker arm and springs of high temperature tool steel. The temperature is around 400°C in this vicinity.

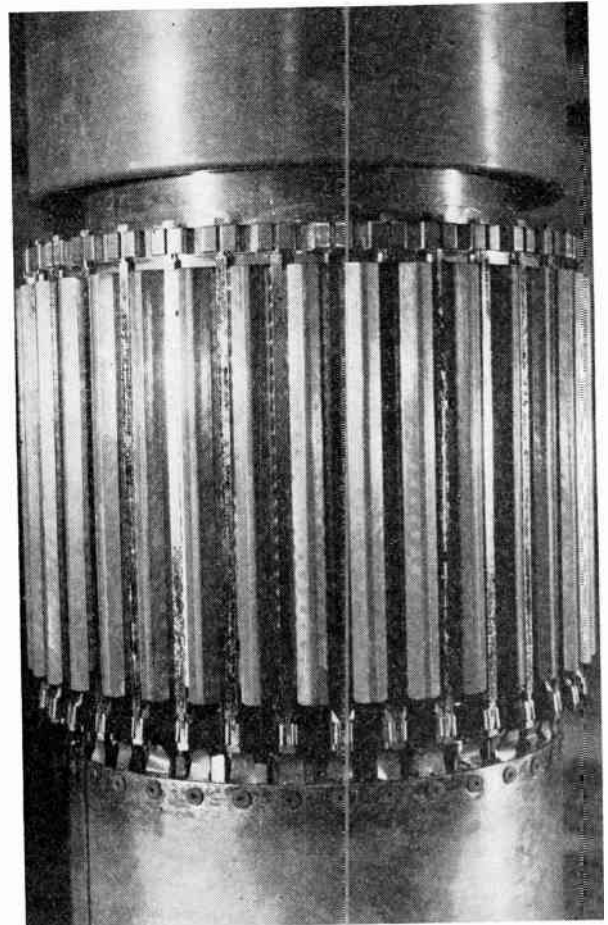


Fig. 9—Assembled cathode showing tungsten filaments in place with the fixed support at top and the pantographs below. Note that two of the pantograph leaves are used to provide rf contact from the lower end of the filament to the heat shield around the tensioning springs.

the cathode in the new design, increases the radiation loss from the filaments and hence raises the filament power required.

The temperature is kept constant over the whole length of the filament emitting area by "necking down" near the end of the filament. Trial and error tests of various lengths and neck sizes produced the final design in which the temperature variation along the active length of the filament was less than 50°K. The only connection between the filament and the copper pantograph block is a pressure contact. It appears that this behaves as a self-seating device since, if the contact is bad, the junction heats and the filament beds itself better in the copper until a good contact is made and heating stops. The centering of the filament between the supports is important and must be carefully checked during assembly. It is obvious that the proper balance

between radiation and conduction will be achieved only for a good contact.

In most applications, the life of a tungsten filament is limited by weakening due to evaporation. This does not seem to be the case in this tube; instead, life is limited by filament breakage due to crystal growth and subsequent slipping along crystal planes. The majority of filaments that have failed show no measurable evaporation, but the surface shows distinct signs of crystal formation. It appears that at the operating ten-

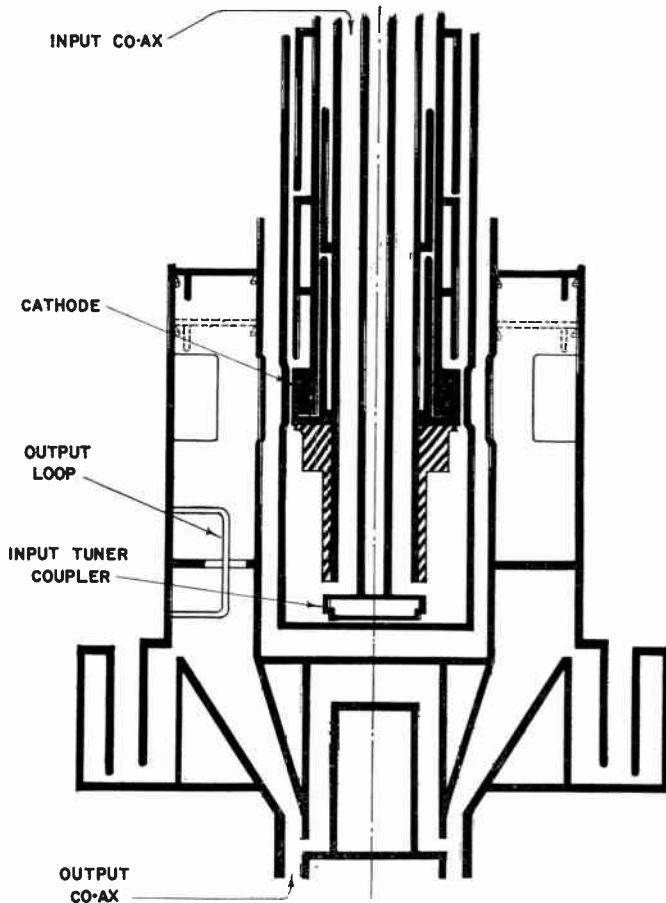


Fig. 10—Circuits for resnatron. This is all enclosed in the vacuum system.

sion and temperature, the filaments part at a crystal boundary long before evaporation has any effect. The life span, however, varies greatly. Certain of the tungsten filaments have very respectable lives of over 1000 hours; others last only a few hours. So far, no method has been found of determining, before use, which filaments will fail early. The reason was thought first to be connected with the heat and rolling treatment used to shape and work the tungsten during manufacture. Recent work, however, seems to indicate that the flexibility of the pantographs may be the unknown variable. In spite of the fact that all filaments have the same nominal treatment and look identical at the time of assembly, their behaviors vary considerably.

The filament voltage is controlled by a motorized gang of transtats which provide continuous variation from zero to full voltage. It is absolutely essential that the voltage be run up slowly enough to allow the filaments to heat gradually.

Tests are being carried out to determine whether some of the lower temperature cathodes (matrix, thoriated tungsten, etc.) will be satisfactory. So far, the rate of poisoning has been such that it precludes the use of any of these low-temperature cathodes in the existing vacuum system.

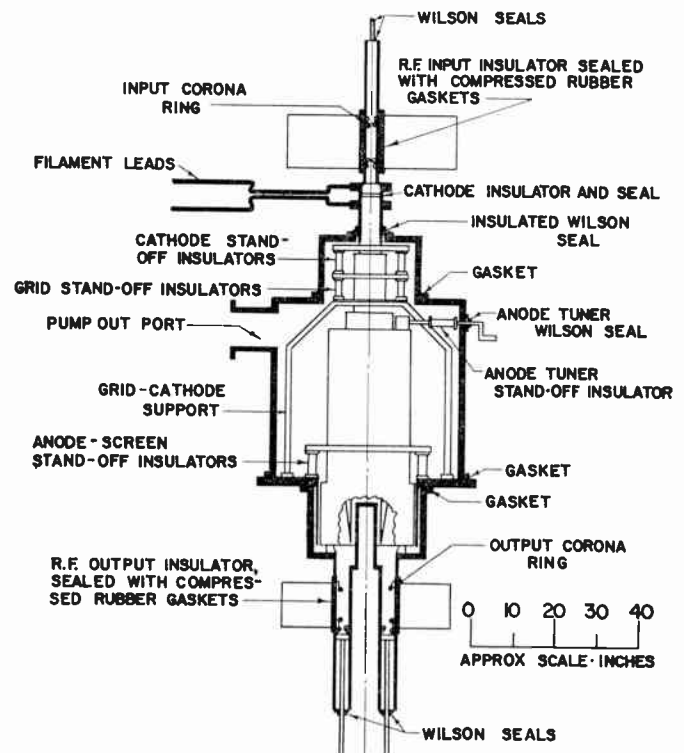


Fig. 11—Mechanical layout. The legs which support the base plate are not shown.

CIRCUITRY

A description of the resnatron cannot be complete without some discussion of the circuitry enclosed in the vacuum shell. The high-power rf distribution system for the accelerator is 40 by 12 inches aluminum waveguide. Since the resnatron structure is coaxial, a waveguide-coaxial transition section is necessary at both input (top) and output (bottom). Fig. 10, which illustrates the rf circuits, does not show these transitions. But Fig. 11 does include them, since the vacuum seal is made at this junction. For tuning purposes, stub tuners are used on both coax and waveguide, the former being in vacuum and the latter in air.

Power from the input transition section flows down the input coax line to the combined coupler tuner and thence into the cathode grid cavity. The coupling to the $3/4 \lambda$ cavity is capacitive, and the filaments are situated $1/4 \lambda$ from the upper end which is effectively shorted by the double rf chokes. A second set of rf chokes prevents loss of power between the coaxial filament leads.

The grid screen cavity should provide a low impedance at the beam elevation for all frequencies. This is frequently approximated by utilizing one end of the cavity to adjust the impedance at the fundamental and odd harmonics, while the other end can be used to provide a low impedance for the even harmonics. This procedure was used here, but for some frequencies not related in any simple fashion to the fundamental, the screen grid impedance was high enough to build up

sufficient voltage so that feedback to the cathode via the screen-cathode capacity caused uncontrollable oscillations. This mode of oscillation, in which electrons require a transit time $T/2$ from cathode to anode, is precisely that envisaged in the original resnatron. Such an oscillation should be voltage sensitive, and a high enough voltage should suppress it. However, in this case, the oscillation was so violent that it was impossible to get a voltage high enough so that the feedback was not in phase. The grid was banded to reduce the screen cathode capacity, and the oscillations were successfully controlled in this manner. In principle, the length of the screen can be adjusted to change the properties of the grid screen cavity, but such changes were ineffective in controlling the oscillation and were abandoned. In order to help control low frequency oscillation (connected with the grid bias supply) an $8 \mu\text{f}$ condenser is used to bypass the dc grid bias lead near the tube.

The anode cavity is a $\lambda/2$ cavity with a movable shorting plunger at the upper end for tuning. This tuner is adjustable from outside the tube, the gear drive having an insulating section to couple the motion to the parts operating at the high dc voltage. In the lower part of the cavity, three loops feed the output coaxial line. The dc isolation choke, which accounts in part for the large tube dimensions, has in some of its outer components, diameters such that circumferential modes are possible. Whereas single loop excitation normally leads to excitation of the first θ mode, the three loops avoid the problem. Correct phasing of the loops at 200 mc was accomplished by maintaining reasonable mechanical accuracy.

Although the existence of the large isolation choke increases the vacuum volume and the area to be out-gassed, it has the advantage that any power leaking from the isolation chokes is still contained in the vacuum shell. With the more usual construction in which isolation is accomplished by means of a choke joint in the external waveguide, the rf leakage would probably have been too high to tolerate.

All major parts of the chokes and cavities are solid OFHC copper with the exception of the control grids which are nickel for purely mechanical reasons. (The copper proved to be so soft that it was difficult to handle the grid assembly without deforming it.) All joints are hard soldered, copper welded or bolted. No special care was taken to polish the surfaces. No rf heating problems have been encountered. Fig. 12 shows the control grid under construction.

MECHANICAL

It has been said that once the tube dimensions have been set, the remainder of the problem involves mechanical engineering. We were most fortunate in having excellent cooperation both in the engineering and in the construction of parts.

The anode is cooled by means of water circulating in copper tubes wound outside and soft soldered to the

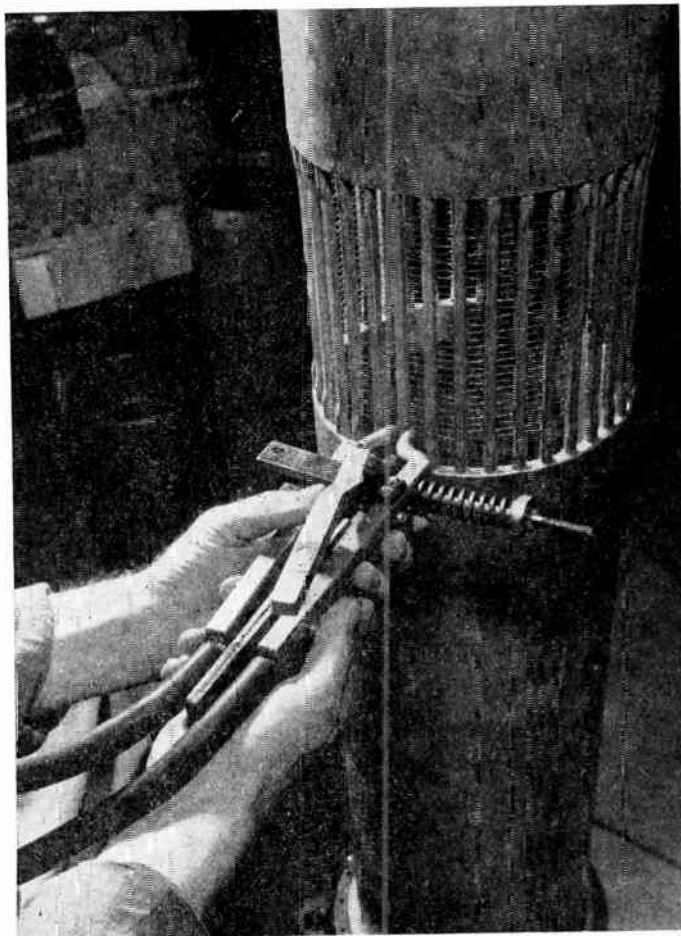


Fig. 12—Control grid under construction—tungsten wire spot welded to nickel grid bars.

anode cylinder. (Hard solder would have been used had it been feasible.) The other tube elements are made of two coaxial cylinders baffled in such a way as to allow water to flow down one side, around the bottom and back up the other side. In the case of the control and screen grids, the grid bars form part of the flow circuit. There is, on the average, a temperature difference across the cylinder due to the in-out temperature difference of the water. In practice the water flow is high enough so that this differential is not troublesome. Water leaks are, however, a real problem with this type of construction.

As mentioned above, no special surface treatment is used other than a reasonably smooth machine finish. A polish would be worthwhile if it eliminated arcing during dc high-voltage outgassing. It is felt, however, that low-energy high-voltage arcing will condition the surface itself, and the length of time required is not appreciably lessened by polishing, since if a single arc occurs on a polished surface, a number of arcs will be needed to clean up the surface. In this tube, the arcing is fairly evenly split between the screen grid cylinders and the isolation choke. It is thought that the arcing in the choke takes place mainly during dc outgassing, whereas the arcing during operation occurs preponderantly near the beam in the screen grid region.

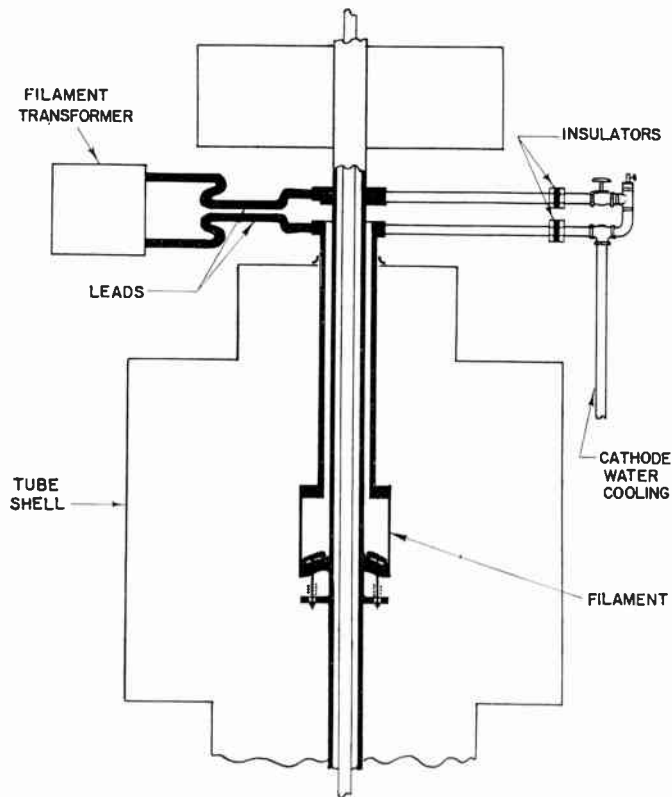


Fig. 13—Filament supply schematic.

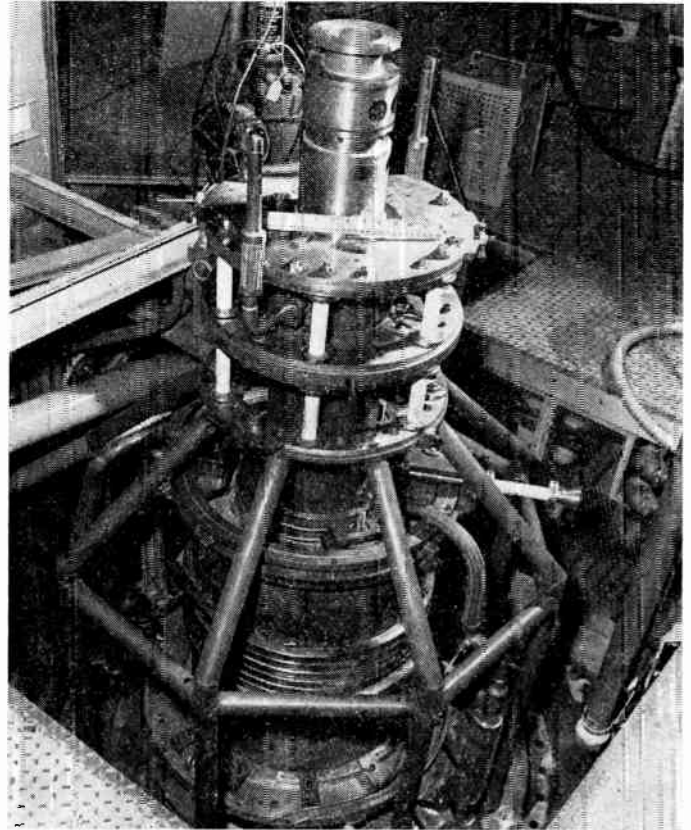


Fig. 14—Assembled tube without vacuum housing and part of the input coaxial line.

The filament connectors shown in Fig. 13 are heavy-bolted clamp-type connectors which not only provide contact through which 7000 amperes flow with negligible voltage drop, but also act as the water connectors to both ends of the cathode.

The vacuum system for each resonator consists of a 1400 C.F.M.⁷ oil-diffusion pump with a freon baffle. Each tube has its own diffusion pump but a common fore line is used. Air-operated manifold valves can isolate the tube from pumps and baffle, and are automatically set to do so in case of vacuum trouble. Up until now, Litton oil has been used in the diffusion pumps. After the system has been pumped for several weeks, the cold pressure is in the vicinity of 5×10^{-7} mm Hg. There is some indication that other pump oils are more desirable for use with lower-temperature filaments. All of these pressures are measured in the vacuum manifold, and the operating pressures in the vicinity of the filament are doubtless higher. O-rings, flat gaskets and Wilson seals are used depending on size and function. Periodic defrosting of the refrigerators (every two or three months) has been found necessary to prevent too much oil accumulating on the cold baffles.

The type of construction precludes any real bakeout. One might consider a steam-temperature bakeout by using steam in the water systems and such a treatment was used once. Normal O-rings (neoprene) are not

cured sufficiently to withstand this treatment without deforming, and subsequent vacuum troubles completely nullify any gain made by the bakeout. Some tests indicated that a curing procedure for the O-rings and gaskets could be worked out, but it is not thought worthwhile at present.

The cleaning techniques are not complicated and cannot be greatly successful because of the contaminated atmosphere in the building. The standard procedure is to wipe all parts with a clean cloth soaked in acetone (or vythene), flush with C.P. acetone (or vythene) and then flush with alcohol. When it is necessary to handle parts, cloth gloves are used.

ALIGNMENT

The anode and screen are presumed to be perpendicular to the base plate. The anode can be rotated to align the fins with the screen bars. This procedure is carried out using, as alignment criteria, sights through holes drilled in the anode midway between the fins. (See Fig. 14.) The cathode and grid are aligned as a unit using gauges to determine concentricity and spacing; then the whole assembly is lowered into the tube and aligned with the screen by sighting through the holes in the anode. Adjustments are provided between the cathode and grid, and between the grid and screen, to adjust for vertical position as well as rotation. Because of the weights involved, assembly of all these

⁷ Consolidated Vacuum Corp., M.C.F. 1400.

units is accomplished by means of heavy cranes and great care must be taken to avoid damage to cathodes, grid bars, etc.

WATER-LOAD TESTS

During construction, and prior to using the resnatrons to drive the accelerator tanks, they were tested by running them into waveguide water loads. These loads were constructed from a 40-inch length of guide with a diagonal lucite sheet to contain the water. The water flow was directed so as to prevent hot spots and to insure adequate mixing. Several precautions were found to be necessary before the loads would take the 3.5 megw of peak power which was eventually measured. It was found that the city water corroded the aluminum casing so badly that hot spots would develop at underwater surfaces and little steam explosions would occur. The surface of the aluminum was thoroughly cleaned and painted to prevent corrosion. The end plate had to be welded in place because of the difficulty of obtaining a waterproof joint and good electrical contact at the same time. Because of the short length of the water load, a susceptible post tuner was needed to match the load to the guide.

All tests were conducted with the load matched to the guide. Resnatron tuning adjustments were made to maximize the power to the load. After calibration, many of the measurements were made using resistive loop directional couplers rather than waiting for the water load to come to equilibrium.

Since we were concerned with power at only one frequency, the bandwidth was unimportant as long as the 300- μ sec pulse was amplified with moderate fidelity. No measurements of loaded Q 's were made. Although a certain amount of testing was required to determine that the loop size was satisfactory, this was essentially a cut and try method in which loops of various areas and shapes were tried until the ones giving maximum power were obtained. As a matter of fact, the original set of loops, based on very simple calculations (suggested by W. W. Salisbury) of fields in the cavity and the field induced in the loop, turned out to be the most satisfactory.

Typical power outputs and the operating conditions for the two electrode configurations are given in Table I.

TABLE I

	E_p kv	i_p amps	E_a kv	i_a amps	Power Gain	Power Output watts
Old design	40	33	-3.5	3.3	15	0.85×10^6
New design	70	81	-1	1.65	10	3.5×10^6

In practice, of course, the resnatrons are operated into the high- Q tanks. There was some question as to whether the tubes would operate as well into the high- Q load as they did driving the water load. For example,

the effect of the substantial mismatch which is inevitable sometime during the tank buildup was unknown. Since the tanks were readily available and the coupling waveguide was already laid out, once the resnatrons produced power into the water load, it was very easy to connect the power output of the resnatrons to the cavity to be driven. Because of their size, the resnatrons were initially installed in the positions they would occupy when powering the accelerator. Leaving the resnatron tuning at the resistive load positions and tuning the transitions to the tank to the matched positions (determined with CW), it was found that the resnatron would deliver quite reasonable power to the high- Q circuit. To optimize the power, it was necessary to retouch the tuning. An automatic frequency control was available to keep the tanks in tune.⁸

The waveguide from the resnatron output involved one right-angle turn before a transition back to coax line, in order to feed a loop whose resistive component had been matched to the tank. No care had been taken to make the electrical distance from the tube to the tank a multiple of a half wavelength which is sometimes considered to be the ideal for such a system.

In general, it was found that the main gain in tuning was the change in build-up time that one could achieve by detuning the load. In general, the build-up is faster if the high- Q tank is detuned, and, in spite of the fact that the final level is not as high as for the on-tune case, it may be the most desirable mode of operation. Operation into the high- Q load was uneventful, and although no thermal power measurements were made into this water-cooled load, the power obtained was not far from that into a resistive load under the same conditions (using measured rf field strengths and the estimated shunt impedance to calculate power). For us the main criterion is whether protons of the correct energy are obtained from the accelerator, and not the absolute power output of the tube. From the tube engineering point of view, this may be undesirable, but from the accelerator point of view, it is the measure of success.

MAINTENANCE AND RELIABILITY

In operation, there are three resnatrons operating into high- Q tanks with a fourth acting as a driver for the other three. The power outputs required are approximately 3.5, 2.2, 0.6, and 0.6 megw. The tubes all operate off a common dc plate supply, and each is individually biased so that operation is class B or just on the class C side of this point. An arc in an individual tube will trip off the power supply and interrupt operation. From work done with the individual resnatrons, it has been observed that by far the greatest number of arcs occur during the rf pulse, and it is not felt that the use of dc on the plate decreases the re-

⁸ E. A. Day, Featherstone, Johnson, E. E. Lampi, E. B. Tucker, and Williams, submitted to *Rev. Sci. Instr.* on Minnesota Linear Accelerator.

liability to any great extent. Each arc trips off the plate supply⁹ and the outage time depends on how fast the vacuum recovers from the arc-produced gas. Normally the outage will not be more than 20 seconds. The principal rf arcing trouble has occurred at the output vacuum seal, and the addition of the shields indicated in Fig. 11 corrected the trouble. No multipactoring has been observed, perhaps because the most probable places are biased with dc voltages.

The loss of an individual filament makes disassembly necessary only if a cathode-grid short results. Resnatrons have been operated with as many as nine filament strands broken, no cathode grid shorts having developed; at other times we have not been so fortunate. Careful records of voltage and current for each resnatron filament show steps indicating loss of filament strands. Very recently, however, a tube with a new pantograph assembly operated for 900 hours without loss of a single filament strand. To date the operation of the resnatron has been a pleasant surprise.

⁹ R. P. Featherstone, C. Ling, and P. A. Cartwright, *Trans. AIEE*, vol. 72, pt. I, pp. 145-152; 1953.

ACKNOWLEDGMENT

The early work on the resnatron at Collins Radio Company was done by W. W. Salisbury, Drs. R. L. McCreary, P. I. Corbell, and W. J. Armstrong, while E. Phillips was responsible for design of some waveguide components. Much of the credit for the filament and pantograph design is directly attributable to the excellent cooperation of the RCA Power Tube Division, Lancaster, Pa. Dr. L. Garner, W. Parker, and W. Harbaugh were most cooperative in providing design information and samples.

This work was carried out as part of the accelerator program and was aided considerably by the advice, cooperation, and understanding of the Minnesota Linear Accelerator Group headed by Prof. J. H. Williams. The construction of parts was supervised by R. B. Thorness. The majority of the numerous assemblies and disassemblies were the responsibilities of L. Rawson, K. Menafee, W. Eckman, and D. E. Service. R. P. Featherstone aided in many ways. The encouragement and advice of Prof. D. H. Sloan has been of great value. To these and others who aided both directly and indirectly we acknowledge our indebtedness.

Atmospheric Effects on VHF and UHF Propagation*

GEORGE H. MILLMAN†, SENIOR MEMBER, IRE

Summary—This paper is mainly concerned with the effects of the troposphere and ionosphere on the propagation of vhf and uhf radio waves.

Tropospheric refractive index profiles and ionospheric electron density models representative of average atmospheric conditions are presented.

Mathematical relationships are derived for calculating refraction effects, time delays, Doppler errors, polarization changes, and attenuation experienced by radio waves traversing the entire atmosphere.

I. INTRODUCTION

THE ADVENT of man-made satellites projected into outer space focuses attention on the problem of determining their true orbital paths as they circumsolve the earth. The prediction of orbital positions necessitates that a satellite must first be detected

and then tracked. These functions can be performed either by optical means or by radio wave transmissions.

With regard to the use of radio waves in long-range detection and prediction, the limiting factor of system performance and capability is largely dependent upon the medium, or atmosphere, through which the waves are propagated. In the atmosphere, the regions which greatly influence and affect radio wave propagation are the troposphere and the ionosphere.

The effects brought about by the passage of waves through these regions manifest themselves as angular refraction, time delays, Doppler errors, polarization rotations, and attenuation. In the ensuing discussion, these phenomena are described and assessed with application to frequencies in the vhf and uhf range.

II. ATMOSPHERIC MODELS

A study of the effects of the atmosphere on radio wave propagation necessitates a knowledge of the height variation of the dielectric constant, or refractive index,

* Original manuscript received by the IRE, November 27, 1957; revised manuscript received, March 20, 1958. This work was supported by the Rome Air Dev. Center under Contract AF 30(602)-1514.

† General Electric Co., Syracuse, N. Y.

in the tropospheric and ionospheric regions. Since the magnitude of the dielectric constant is a function of such parameters as the geographic location on the earth, weather, time of day, and season of the year, it would be an overwhelming task to analyze completely atmospheric propagational effects under all parametric conditions. To simplify the analytical problem, atmospheric models representative of average conditions are employed.

The Troposphere

In the troposphere, the index of refraction which is a function of meteorological variables such as water vapor, air temperature, and air pressure, can be represented by

$$(n - 1) \times 10^6 = \frac{a}{T} \left(p + \frac{b\epsilon}{T} \right) \tag{1}$$

where n is the refractive index; T , the air temperature in degrees Kelvin; p , the total pressure in millibars; and ϵ , the partial pressure of water vapor in millibars. The first term, ap/T , applies to both optical and radio frequencies, while the second term, $ab\epsilon/T^2$, is the explicit water vapor relationship required only at radio frequencies.

According to Kerr,¹ the constants, a and b , are approximately equal to 79°K/mb and 4800°K, respectively. Campen and Cole² quote 74.4°K/mb and 4973°K as the values of a and b . Through consideration of various propagation experiments, Smith and Weintraub³ arrive at the values of 77.6°K/mb and 4810°K.

The expression for the refractivity of air is independent of frequency in the 100–10,000-mc range. According to Smith and Weintraub,³ this expression is considered to be valid to 0.5 per cent in $(n - 1) \times 10^6$ units for frequencies up to 30,000 mc and normally encountered ranges of temperature, pressure, and humidity.

The analytical expressions of refractive index for a standard atmosphere utilized in this study were derived by Campen and Cole.² The refractive index of a completely wet (100 per cent relative humidity at all levels) standard atmosphere is approximated by the polynomial expression

$$N_w = 338 - 50.9Z + 4.39Z^2 - 0.245Z^3 + 0.0071Z^4 - 0.00006Z^5 \tag{2}$$

where

$$N_w = (n_w - 1) \times 10^6. \tag{3}$$

¹ D. E. Kerr, "Propagation of Short Radio Waves," M.I.T. Rad. Lab. Ser., McGraw-Hill Book Co., Inc., vol. 13; 1951.

² C. F. Campen and A. E. Cole, "Tropospheric Variations of Refractive Index at Microwave Frequencies," Geophysical Res. Directorate, Air Force Surveys in Geophysics, No. 79, October, 1955.

³ E. K. Smith, Jr. and S. Weintraub, "The Constants in the Equation for Atmospheric Refractive Index at Radio Frequencies," Central Radio Propagation Lab., Natl. Bur. of Standards, Boulder, Colo., Rep. No. 1938; September, 1952.

For a completely dry (zero per cent relative humidity at all levels) standard atmosphere, the refractive index is given by

$$N_d = 262 - 25.1Z + 0.92Z^2 - 0.016Z^3 + 0.0001Z^4. \tag{4}$$

Eqs. (2) and (4) are valid for $0 \leq Z \leq 10$ km. Above 10-km altitude, the refractive index is assumed to decay exponentially as

$$N_{w,d} = N_{ow,od} e^{-h/25} \tag{5}$$

where h is the altitude in thousands of feet, and N_{ow} and N_{od} are the values of N_w and N_d , respectively, at the earth's surface.

The Ionosphere

According to the theory of Eccles and Larmor,⁴ the refractive index of a medium containing free electrons is given by

$$n = \sqrt{1 - \frac{4\pi N_e e^2}{m\omega^2}} \tag{6}$$

where

- N_e = electron density (electrons/cm³),
- e = electron charge (4.8×10^{-10} esu)
- m = electron mass (9.1×10^{-28} gm),
- ω = angular frequency of the incident wave (radians/second).

This relationship is valid when the earth's magnetic field and the collisions of electrons with ions and neutral particles are neglected.

The distribution of electron density with height under equilibrium conditions, as formulated by Chapman,⁴ is

$$N_e = N_m e^{1/2[1-Z-e^{-Z}]} \tag{7}$$

where N_m is the electron density at the level of maximum ionization and Z is the normalized height.

The normalized height is given by

$$Z = \frac{h - h_m}{H} \tag{8}$$

where h_m is the height of maximum ionization density and H , the scale height which is defined as the height of the homogeneous atmosphere at a given temperature.

The distribution of electron densities under consideration is assumed to follow the Chapman form. The assumed magnitudes and levels of maximum ionization and scale heights given in Tables I and II are for both the daytime and nighttime ionospheric models.

⁴ S. K. Mitra, "The Upper Atmosphere," The Asiatic Soc. of Calcutta, Calcutta, India, 1952.

TABLE I
DAYTIME PARAMETERS OF ELECTRON DENSITY

Layer	H-(km)	h _m -(km)	N _m -(electrons/cm ³)
E	10	100	1.5 × 10 ⁶
F ₁	40	200	3.0 × 10 ⁶
F ₂	50	300	12.5 × 10 ⁶

TABLE II
NIGHTTIME PARAMETERS OF ELECTRON DENSITY

Layer	H-(km)	h _m -(km)	N _m -(electrons/cm ³)
E	10	120	0.8 × 10 ⁴
F	45	250	4.0 × 10 ⁶

In the upper atmosphere, electron collisions occur due to the presence of neutral particles and heavy ions and ultimately cause absorption of energy from the electromagnetic waves traversing the ionized medium. If it is assumed that the atmosphere is chemically homogeneous and isothermal, the angular collisional frequency of the electrons, ν , with the particles should obey the exponential law

$$\nu = \nu' e^{-(h'-h)/H} \tag{9}$$

where ν' is the collision frequency in radians per second at the altitude, h' , and H is the scale height in the region.

The parameters which describe the electron collision frequency model utilized in this study are presented in Table III.

TABLE III
COLLISION FREQUENCY PARAMETERS

Layer	H-(km)	h'-(km)	ν' -(radians/second)
E	10	100	3 × 10 ⁶
F	45	134	10 ⁴

III. ATMOSPHERIC REFRACTION OF RADIO WAVES

When electromagnetic waves are propagated through a medium whose dielectric constant or index of refraction is a varying function of the path, the waves undergo a change in direction or refraction. Since the earth's atmosphere is such a medium, errors are evidently introduced in the radar angular measurements of target position.

In the following analysis, only elevation-angle errors have been considered, even though horizontal refraction effects are definitely a source of azimuthal angle error.

To simplify the analytical problem, the troposphere and ionosphere are stratified into layers of constant refractive index. It is fully realized that this approach will render only approximate answers. However, since the profiles of refractive index in the atmosphere are not precisely known, a more exact mathematical solution appears unnecessary at this time.

A typical ray path trajectory of radio waves traversing the atmosphere in the vertical plane is shown in Fig.

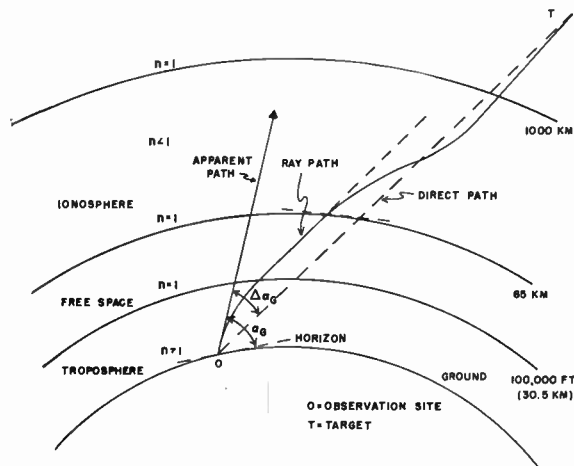


Fig. 1—Typical ray path trajectory.

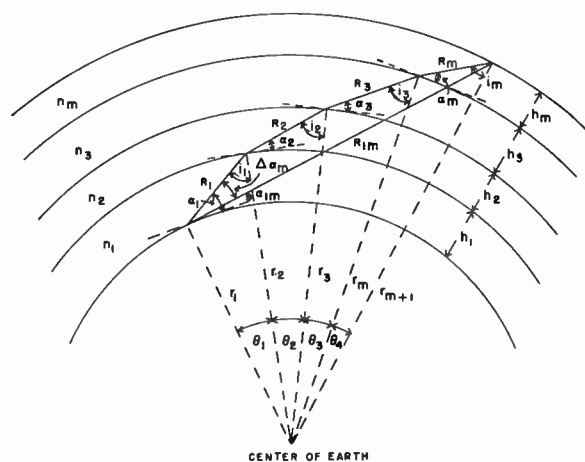


Fig. 2—Atmospheric layer stratification.

1. It is assumed that 1) the troposphere extends to approximately 100,000 feet, with refractive index decreasing uniformly with height; 2) the ionosphere lies between 85–1000 km with a minimum refractive index at the level of maximum electron density; 3) free space or the region of unity refractive index prevails between the tropospheric and ionospheric regions. The elevation-angle error due to refraction, $\Delta\alpha_G$, is the angle between the apparent path direction and the direct line-of-sight path.

Tropospheric Refraction

Consider the stratified atmosphere, shown in Fig. 2, to consist of m layers of thickness, h_m . The index of refraction is assumed constant in each layer. A ray elevated at an angle, α_1 , in layer 1 is incident at an angle, i_1 , at layer 2.

From the law of sines, the angle of incidence, i_1 , is found to be

$$\sin i_1 = \frac{\sin\left(\frac{\pi}{2} + \alpha_1\right)}{r_2 / r_1} \tag{10}$$

where r_1 is the radial distance from the center of the earth to the lower edge of layer 1 and $r_2=r_1+h_1$.

The angle that the ray makes with the horizon in layer 2, α_2 , is readily obtainable from Snell's Law for a spherically symmetrical surface which states that

$$n_1 r_1 \cos \alpha_1 = n_2 r_2 \cos \alpha_2. \tag{11}$$

From (10) and (11) it is seen that the general expressions for α_m and i_m are therefore given by

$$\alpha_m = \cos^{-1} \left[\frac{n_{m-1} r_{m-1}}{n_m r_m} \cos \alpha_{m-1} \right] \tag{12}$$

and

$$i_m = \sin^{-1} \left[\frac{r_m}{r_{m+1}} \cos \alpha_m \right] \tag{13}$$

where

$$r_{m+1} = r_1 + \sum_{j=1}^m h_j. \tag{14}$$

Applying the law of sines again for the direct path, it follows that

$$\alpha_{1m} = \cos^{-1} \left\{ \frac{r_{m+1}}{R_{1m}} \sin \left[\sum_{j=1}^m \theta_j \right] \right\} \tag{15}$$

where

$$R_{1m}^2 = r_1^2 + r_{m+1}^2 - 2r_1 r_{m+1} \cos \left[\sum_{j=1}^m \theta_j \right] \tag{16}$$

and

$$\theta_j = \frac{\pi}{2} - \alpha_j - i_j. \tag{17}$$

The refraction-angle error, $\Delta\alpha_m$, which is the difference between the apparent elevation angle, α_1 , and the true elevation angle, α_{1m} , is therefore given by

$$\Delta\alpha_m = \alpha_1 - \alpha_{1m}. \tag{18}$$

In the case of the troposphere, α_1 corresponds to the ground elevation angle, α_G , and r_1 corresponds to r_0 , the radius of the earth.

The constants employed in the computation of refraction errors for the two tropospheric models were based on an assumed 18-layer stratified atmosphere. The layer thickness varied from 500 to 2500 feet below the 5000-foot level. Between this height and 50,000 feet and between the 50,000-100,000-foot region, the stratification thicknesses were 5000 and 10,000 feet, respectively.

As shown in Fig. 3, the refraction error increases with altitude and is a maximum for the standard atmosphere with 100 per cent relative humidity. For a target at 100,000 feet altitude and a propagating angle of 5° , an error of about 2.3 milliradians is obtained. For a 25° elevation angle, the refraction error decreases by a factor

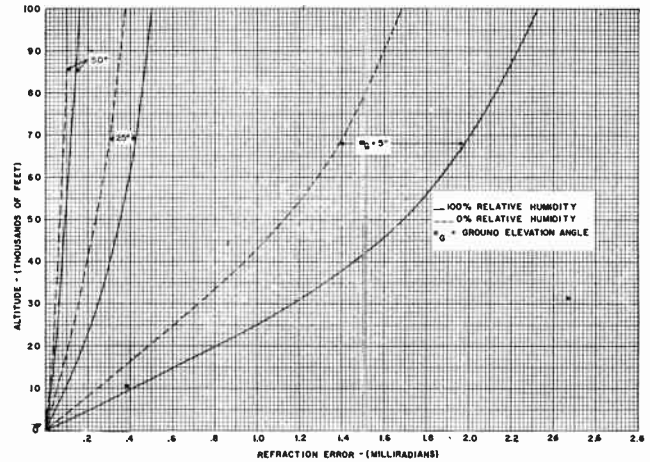


Fig. 3—Tropospheric refraction errors for a standard atmosphere.

of 4.5. Comparing errors calculated for zero per cent with 100 per cent relative humidity, it is seen that under identical conditions the latter are about 1.5 times greater than the former.

Ionospheric Refraction

The preceding mathematical development is applicable to the ionospheric problem. It is necessary, however, to redefine the angle, α_1 , as the ionospheric elevation angle, α_I , and the distance, r_1 , which now corresponds to the distance from the center of the earth to the bottom edge of the ionosphere. Actually, $r_1=r_0+h_0$, where h_0 is the height of the ionosphere above the earth's surface.

For the daytime electron density model, the ionosphere was stratified into 11 layers varying in thickness from 5 to 50 km between the 85-250-km heights and from 100 to 200 km between the 250-1000-km region. In the case of the nighttime model, a 10-layer stratification was employed with thicknesses varying from 15 to 35 km between the 85-200-km level and from 100 to 300 km between 200-1000 km.

The refraction errors for the daytime and nighttime models of electron density are presented in Figs. 4 and 5 for 200 and 400-mc transmission frequency. It is evident that for identical propagating conditions the angle error decreases with the square of frequency.

It is noted that the angular error is a maximum in the vicinity of the maximum ionization. The effect of the E layer on refraction in comparison to the F layer, where the greatest deviation takes place, appears to be very slight. The daytime refraction error is approximately 2.7 times greater than the nighttime error. This compares favorably with the value of 3.1, which is the ratio of daytime-to-nighttime maximum density.

The realistic electron densities have been substituted by an idealistic model in which the electron densities are constant above the levels of maximum ionization. Thus, for the daytime model, 12.5×10^5 electrons/cm³ are assumed to be present above 300 km and, for the

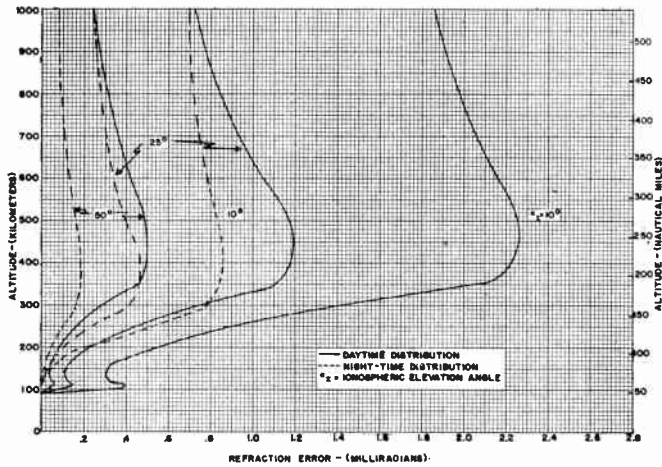


Fig. 4—Ionospheric refraction errors at 200 mc—decaying distribution of electron density above F-layer maximum.

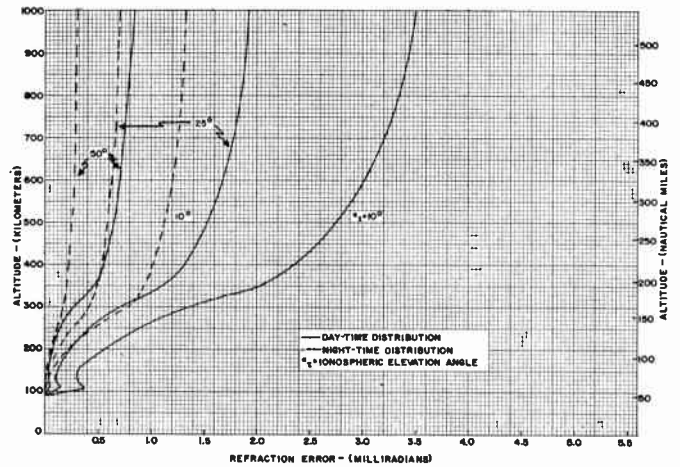


Fig. 6—Ionospheric refraction errors at 200 mc—constant distribution of electron density above F-layer maximum.

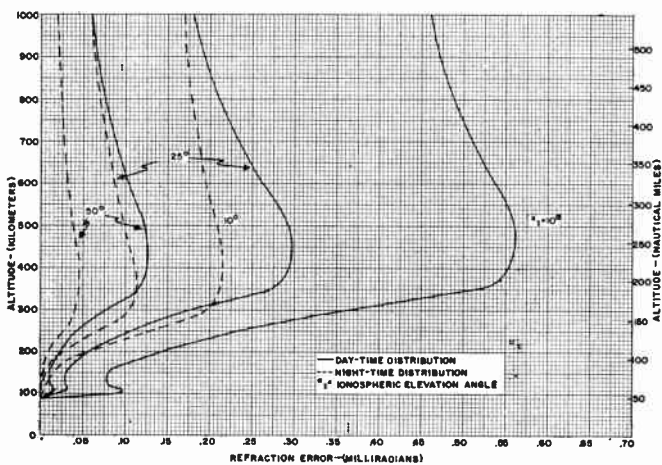


Fig. 5—Ionospheric refraction error errors at 400 mc—decaying distribution of electron density above F-layer maximum.

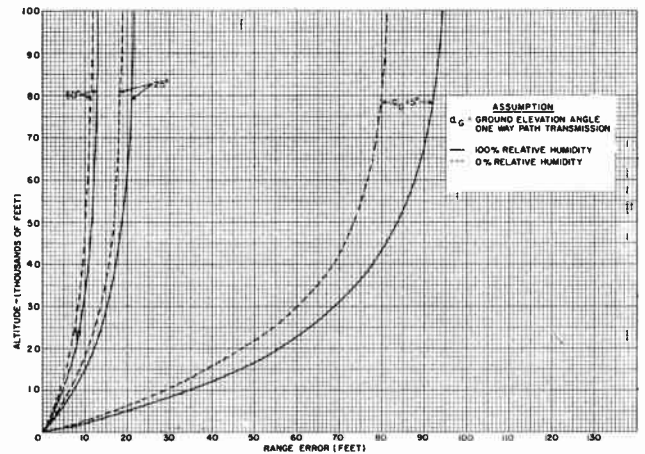


Fig. 7—Tropospheric range errors for a standard atmosphere.

nighttime model, 40.0×10^4 electrons/cm³ above 250 km.

As indicated in Fig. 6, the refraction error increases with altitude, while, for the models of decaying electron density, the error is found to decrease at the high altitudes. Since the true electron density distribution above the F-layer maximum is not known, there is evidently a region of uncertainty in theoretically predicting ionospheric refraction errors.

IV. TIME DELAYS IN THE ATMOSPHERE

Since the velocity of electromagnetic propagation in the troposphere and ionosphere is slightly less than the assumed free space velocity, an error is produced in the range measurements of radar target positions. An additional source of error is the increase in the ray path length brought about by refraction. Both factors are taken into account in this investigation of tropospheric and ionospheric range errors.

Tropospheric Time Delay

Referring to Fig. 2, it is seen that the time of travel along ray path, R_1 , is

$$t_1 = \frac{R_1}{V_{p1}} \tag{19}$$

where V_{p1} is the phase velocity in the first layer defined by

$$V_{p1} = \frac{c}{n_1} \tag{20}$$

and where c is the free space propagation velocity.

It follows, therefore, that the total time of flight of the refracted beam in the stratified layers becomes

$$t_i = \frac{1}{c} \sum_{j=1}^m n_j R_j \tag{21}$$

Since the free space travel time of the unrefracted ray is

$$t_{1m} = \frac{R_{1m}}{c} \tag{22}$$

the range error reduces to

$$\Delta R = \sum_{j=1}^m n_j R_j - R_{1m} \tag{23}$$

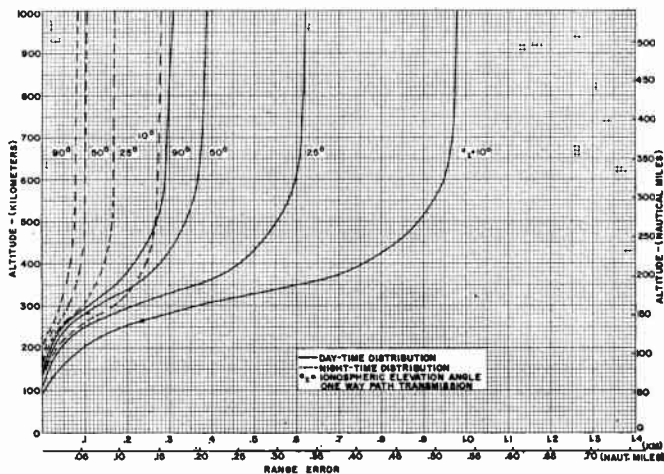


Fig. 8—Ionospheric range errors at 200 mc—decaying distribution of electron density above F-layer maximum.

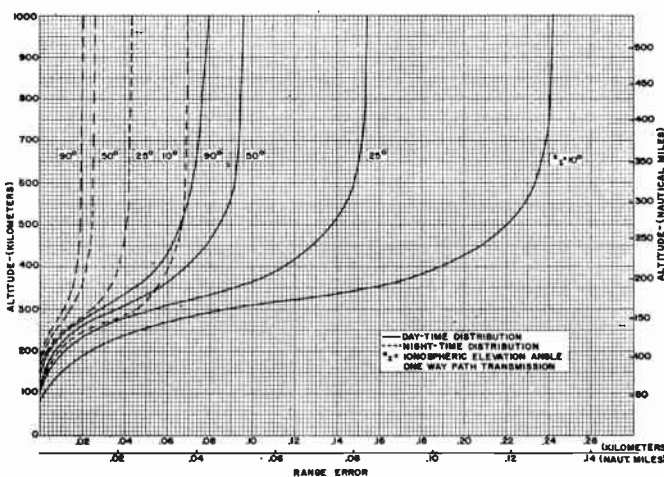


Fig. 9—Ionospheric range errors at 400 mc—decaying distribution of electron density above F-layer maximum.

where the distance, R_j , is given by

$$R_j^2 = r_j^2 + r_{j+1}^2 - 2r_j r_{j+1} \cos \theta_j \quad (24)$$

and where R_{1m} , α_j , and θ_j are the parameters previously defined in Section III.

The tropospheric range errors plotted in Fig. 7 for the two standard atmospheric models are a direct function of the amount of relative humidity in the air, the value at zero per cent relative humidity being about 85 per cent of the value at 100 per cent relative humidity. Since the maximum, two-way path transmission, range error is on the order of 195 feet for a target elevated at an angle of 5° , it is therefore concluded that the troposphere has very little effect on propagational time delays.

Ionospheric Time Delay

The group velocity of a wave packet must be used when problems of pulsed electromagnetic waves are concerned. In the troposphere, the group and phase velocity are synonymous since, in the frequency range of interest, the index of refraction is independent of frequency. For the ionosphere, however, the refractive

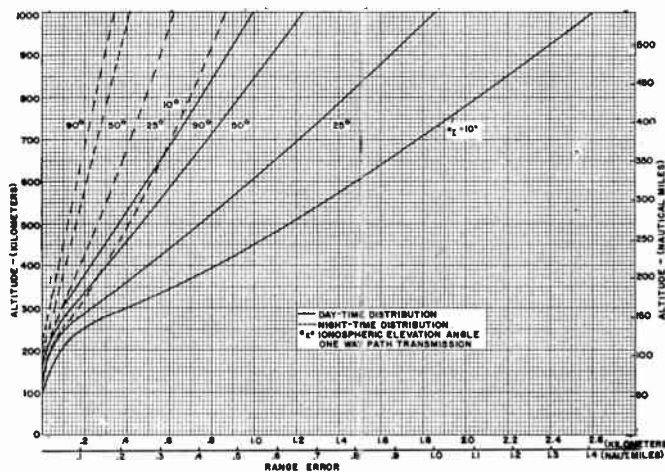


Fig. 10—Ionospheric range errors at 200 mc—constant distribution of electron density above F-layer maximum.

index of the medium is a function of the transmitted frequency.

In the simple case when the earth's magnetic field and electron collisions are neglected, the group velocity, V_g , is related to the phase velocity by

$$V_p V_g = c^2. \quad (25)$$

Since

$$V_g = \frac{1}{nc} \quad (26)$$

the total time of travel in the deviating medium becomes

$$t_t = \frac{1}{c} \sum_{j=1}^m \frac{R_j}{n_j}. \quad (27)$$

It follows that the range error is given by

$$\Delta R = \sum_{j=1}^m \frac{R_j}{n_j} - R_{1m}. \quad (28)$$

Figs. 8 and 9 are graphs of range error for the daytime and nighttime models of electron densities previously described. It is seen that: 1) the range error is a maximum during the daytime, increasing with low elevation angles; 2) the error is inversely proportional to the square of frequency; 3) the majority of the time delay occurs below the 500–600-km height. At 200 mc, for a two-way path transmission, the maximum error is on the order of 1.1 nautical miles. As shown in Fig. 10, this value is increased to 2.8 nautical miles when the distribution of electron density is assumed constant above the F-layer maximum.

V. DOPPLER EFFECTS DUE TO THE ATMOSPHERE

Due to the propagational anomaly of refraction of radio waves traversing the atmosphere, an error is introduced in the determination of the line-of-sight or radial velocity of a moving target. This error results from the fact that the direction of the refracted ray at the target differs slightly from the fictitious line-of-sight or apparent path direction. The Doppler error, introduced

by the incorrect assumption of the magnitude of the refractive index at the target location in the deviating medium, is believed to be indeterminate and is therefore not considered in this analysis.

It should be mentioned that, unlike the refraction and range errors, the Doppler errors are not cumulative. In other words, the total Doppler error, for a target traversing the ionosphere, is only the localized error at the specific point in the medium. The troposphere merely acts as a refractive medium.

Tropospheric Effect

A target, T , is traveling with a velocity, V , in an arbitrary direction in the refractive medium. The components of target velocity for the various orientations shown in Fig. 11 are

$$V_r = V \cos (\psi + \Delta\alpha_T) \tag{29}$$

$$V_d = V \cos \psi \tag{30}$$

$$V_a = V_d \cos (\Delta\alpha_G) \tag{31}$$

where V_r , V_d , and V_a are the components of V in the ray path direction, in the direct path direction, and in the apparent path direction, respectively. The angle, $\Delta\alpha_G$, is the refractive error angle while $\Delta\alpha_T$ is the angle between the ray path and the direct path at the target location.

The error introduced in the measurement of the target Doppler velocity, ΔV , is given by

$$\Delta V = V_a - V_r. \tag{32}$$

Expanding the cosine term of (29) and then substituting the resulting expression, together with (30) and (31), in (32), it follows that the velocity error can be written in the form

$$\Delta V = V \cos \psi [\cos (\Delta\alpha_G) - \cos (\Delta\alpha_T)] + V \sin \psi \sin (\Delta\alpha_T). \tag{33}$$

Since $\Delta\alpha_G$ and $\Delta\alpha_T$ are very small angles, the trigonometric functions can be expanded in a series. Neglecting higher order terms, it follows that

$$\Delta V \cong V \cos \psi \left[\frac{(\Delta\alpha_T)^2}{2} - \frac{(\Delta\alpha_G)^2}{2} \right] + V \sin \psi (\Delta\alpha_T). \tag{34}$$

Since the magnitudes of $(\Delta\alpha_T)^2$ and $(\Delta\alpha_G)^2$ are of the order of microradians, the target radial velocity component, $V \cos \psi$, can be neglected. Thus, to a first approximation

$$\Delta V \cong V \sin \psi (\Delta\alpha_T). \tag{35}$$

It is seen that the Doppler velocity error in the radial direction attributed to refraction is composed only of the tangential velocity component of target velocity, $V \sin \psi$. The error is a maximum when the velocity vector is perpendicular to the direction of the direct path, and is a minimum when the target is moving along the direct line-of-sight path.

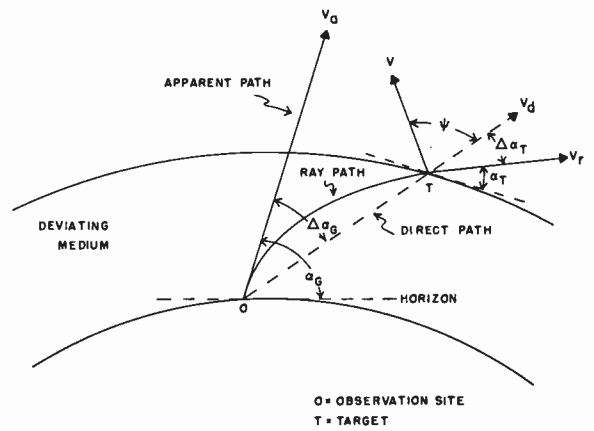


Fig. 11—Geometric orientation of target velocity components.

It is of interest to note that the identical expression for the Doppler velocity error, given by (35), would have been obtained if ΔV had been defined by

$$\Delta V = V_d - V_r. \tag{36}$$

In other words, the magnitude of the refraction error angle is not significant and can be neglected in this analysis.

According to the general concept of the Doppler effect, the reflection of a radio wave from a moving object results in a signal being returned to a fixed transmitting-receiving system whose frequency differs from the transmitted frequency. Analytically, this phenomenon is written as

$$f_d = - \frac{2V \cos \psi}{c} f \tag{37}$$

where f_d is the difference between the apparent reflected frequency, f' , and the transmitted frequency, f .

The error, encountered in the measurement of the Doppler frequency, is, therefore, merely

$$d(f_d) = - \frac{2f}{c} \cos \psi dV \tag{38}$$

where it is assumed that f and ψ are errorless quantities. The term $\cos \psi dV$ is the component of target velocity error in the radial direction.

Substituting (35) in this relationship, it follows that the Doppler frequency error due to refraction is

$$d(f_d) = - \frac{2f}{c} V \sin \psi (\Delta\alpha_T). \tag{39}$$

With regard to the angle, $\Delta\alpha_T$, it can be readily shown from simple geometric considerations that

$$\Delta\alpha_T = \cos^{-1} \left[\frac{r_0}{r_0 + h} \cos (\alpha_G - \Delta\alpha_G) \right] - \cos^{-1} \left[\frac{n_G r_0}{n_T (r_0 + h)} \cos \alpha_G \right] \tag{40}$$

where n_G and n_T are the refractive indexes at the ground

and target, respectively, and h is the target height above the earth's surface. To a first approximation, the refraction error, $\Delta\alpha_G$, can be neglected for elevation angles greater than 3° .

For an assumed target speed of 20,000 feet/second and $\psi=90^\circ$, the maximum Doppler frequency errors are plotted in Fig. 12, for the two tropospheric models of refractive index. The values of $\Delta\alpha_T$ used in these calculations are derived for a target at an altitude of 100,000 feet where n_T is approximately unity. It is seen that the greatest error occurs for the standard atmosphere with 100 per cent relative humidity. The error is directly proportional to frequency and, at 200 mc and 5° elevation angle, the maximum error is approximately 21 cps.

Ionospheric Effect

The mathematical derivation of the Doppler frequency error presented above is valid for the ionospheric problem. However, in applying (40) to conditions in the ionosphere, the following modifications are required: 1) the radius of the earth, r_0 , is replaced by r_0+h_0 where h_0 is the height of the lower edge of the ionosphere above the earth's surface; 2) the target height, h , is measured vertically from the lower edge of ionosphere; 3) the ground refractive index, n_G , now becomes n_I , the index of refraction at the entrance into the ionosphere, which, for all practical purposes, is unity; 4) the ground elevation angle, α_G , is replaced by the ionosphere elevation angle, α_I . An evaluation of the angle, $\Delta\alpha_T$, reveals that it is a maximum at the level of maximum ionization density and is frequency dependent, its magnitude varying approximately with the inverse square of frequency.

From the results given in Fig. 13, it is seen that the Doppler frequency error is a maximum during the daytime and at low elevation angles. For an assumed target speed of 20,000 feet/second and $\psi=90^\circ$, the error, at 200 mc and at an ionospheric elevation angle of 10° (this is the minimum angle that a ray makes with the tangent at an ionospheric stratified surface) is about 33 cps. For the nighttime, under similar conditions, the error is only 11 cps. It should be noted that, for the ionosphere, the Doppler error is inversely proportional to frequency.

VI. IONOSPHERIC POLARIZATION EFFECTS

When a plane polarized radio wave enters the ionosphere, it separates into two independent wave components, both, in the general case, elliptically polarized with opposite senses of rotation. This phenomenon is the result of the electromagnetic waves interacting with the electrons in the ionosphere, which is encompassed in the earth's magnetic field. The two waves progress inside the ionized medium with different speeds. The phase relationship between the two waves is continuously changing as the ionosphere is traversed. On leaving the ionosphere, the waves recombine. The one signifi-

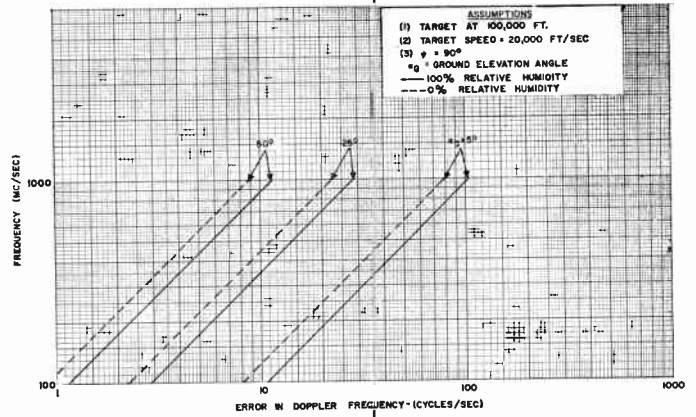


Fig. 12—Doppler frequency error in the troposphere for a standard atmosphere.

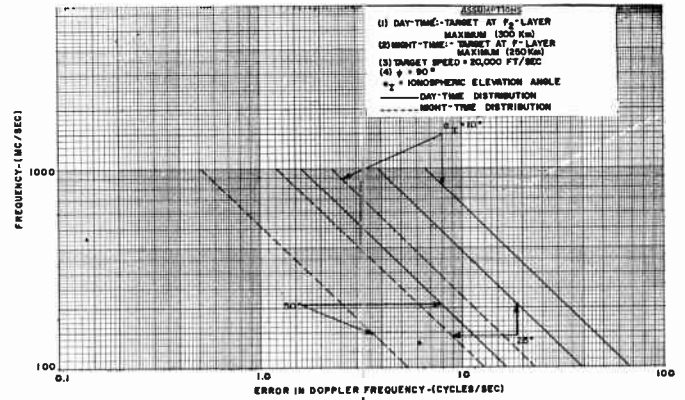


Fig. 13—Doppler frequency error in the ionosphere.

cant alteration in the physical properties of the resultant wave is that the polarization of the emergent wave is different from the original wave.

Mathematical Derivation

Consider two sinusoidal progressive waves of the form

$$a_1 e^{j(\omega t - \gamma_1 s)} \quad | \quad a_2 e^{j(\omega t - \gamma_2 s)}$$

where γ_1 and γ_2 are the phase constants defined by

$$\gamma_{1,2} = \frac{\omega}{V_{p1,2}} \quad (41)$$

The difference in phase between the two waves traversing a distance, ds , is given by

$$d\phi = (\gamma_1 - \gamma_2) ds \quad (42)$$

Utilizing (20) and (41), it follows that the total phase shift for a two-way propagating path is

$$\phi(s) = \frac{2\omega}{c} \int_{s_1}^{s_2} \Delta n ds \quad (43)$$

where s_1 and s_2 are the limits of the path, and where $\Delta n = n_1 - n_2$. In terms of a vertical height variable, this expression becomes

$$\phi(h) = \frac{2\omega}{c} \int_{h_1}^{h_2} \Delta n f(h) dh \quad (44)$$

where

$$f(h) = \frac{r_0 + h_0 + h}{\sqrt{(r_0 + h_0 + h)^2 - [(r_0 + h_0) \cos \alpha_1]^2}} \quad (45)$$

According to the theory of propagation of electromagnetic waves through an ionized medium in the presence of an external magnetic field (Magneto-Ionic Theory), the refractive index of the medium is a complex function of such parameters as the frequency of the wave, the electron density, and the electron collisional frequency.⁴ For transmission frequencies above 100 mc the effects of electron collisions and layer critical frequencies can be neglected. Thus, based on these assumptions, the difference in the refractive indexes for transverse propagation (*i.e.*, the earth's magnetic field is perpendicular to the direction of propagation), becomes

$$\Delta n \cong \frac{\omega_c^2 \omega_H^2}{2\omega^4} \quad (46)$$

where

$$\omega_H = \frac{\mathcal{H}e}{mc}, \quad \omega_c^2 = \frac{4\pi N_e e^2}{m} \quad (47)$$

and where \mathcal{H} is the magnitude of the magnetic field in gauss. The other quantities in these expressions are defined by (6).

Substituting (46) and (47) in (44), the total phase shift simplifies to

$$\phi(h) = \frac{e^4}{2\pi^2 m^3 c^3 f^3} \int_{h_1}^{h_2} N_e f(h) \mathcal{H}^2 dh \quad (48)$$

Similarly, for longitudinal propagation (*i.e.*, the earth's magnetic field is parallel to the direction of propagation), it can be shown that

$$\Delta n \cong \frac{\omega_c^2 \omega_H}{\omega^3} \quad (49)$$

It follows that the total phase shift becomes

$$\phi(h) = \frac{2e^3}{\pi m^2 c^2 f^2} \int_{h_1}^{h_2} N_e f(h) \mathcal{H} dh \quad (50)$$

It should be noted that the limits of integration are in the same units as the free space velocity, c , and that the frequency, f , is in cps. Eqs. (48) and (50) can be readily integrated by numerical methods.

The phase change between the two magneto-ionic components, or polarization shift, for the two modes of propagation, are plotted in Figs. 14 and 15. The calculations were based on an assumed constant \mathcal{H} of 0.6 gauss.

It is evident that the greatest polarization shifts occur, 1) when the direction of propagation is parallel to the

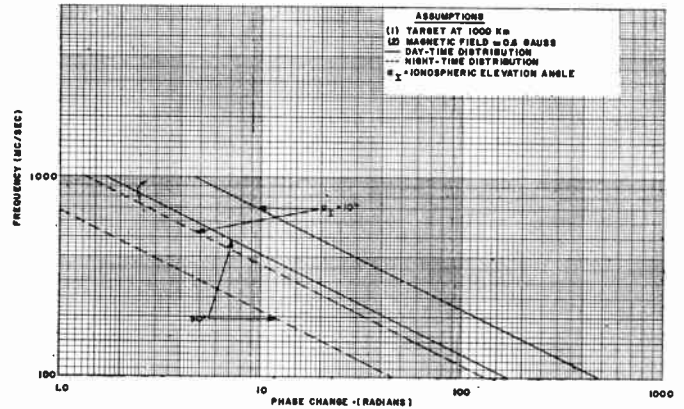


Fig. 14—Phase change between two magneto-ionic components—two-way path transmission—longitudinal propagation.

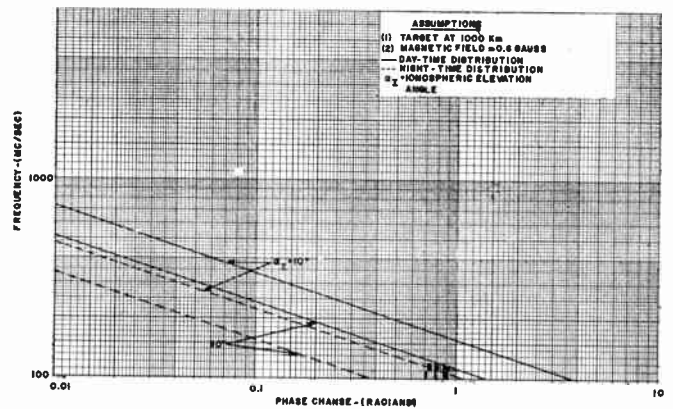


Fig. 15—Phase change between two magneto-ionic components—two-way path transmission—transverse propagation.

earth's magnetic field, 2) during the daytime when the total electron content in the ionosphere is a maximum, 3) at low angles of propagation. In addition, it is seen that, for longitudinal propagation, the ionospheric polarization shift is inversely proportional to the square of frequency.

At 200 mc, a maximum phase change of approximately 120 radians can be anticipated as compared to a value of 0.5 radian for propagation perpendicular to the earth's magnetic field.

Assuming identical propagational conditions, the polarization shift during the daytime is approximately 3.5 times greater than during the nighttime.

VII. ATMOSPHERIC ATTENUATION OF RADIO WAVES

Tropospheric Attenuation

The absorption of radio waves in the lower atmosphere is the result of the presence of both free molecules and suspended particles such as dust grains and water drops condensed in fog and rain. In a noncondensed atmosphere, oxygen and water vapor are the substances which cause absorption.

Theoretical calculations of the anticipated absorption of electromagnetic waves by oxygen and water vapor have been made by Van Vleck.¹ His values of

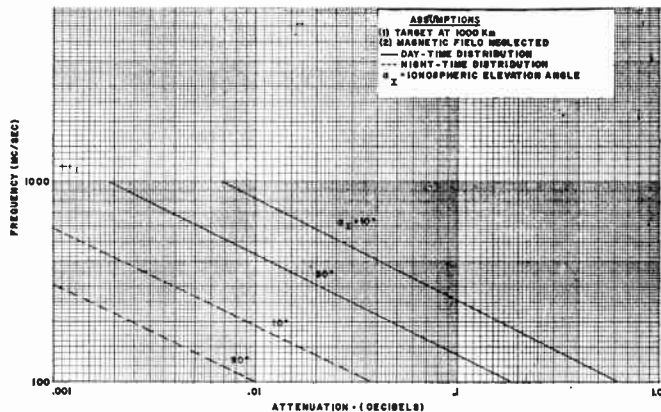


Fig. 16—Ionospheric attenuation—one-way path transmission.

the decay constant of oxygen at frequencies of 300 mc, 1000 mc, 3000 mc, and 10,000 mc are 0.0014 db/km, 0.0050 db/km, 0.0066 db/km, and 0.0072 db/km, respectively. The amplitude of the radio wave decreases at the rate of $10^{-0.06\gamma L}$ where L is the effective path length and γ is the decay constant. Assuming that the oxygen content is effective to an altitude of 50,000 feet and that the radar antenna beam is elevated at an angle of 5°, then the radiation traverses a distance of 156 km in this medium. This results in a two-way path attenuation, at 300 mc, of about 0.44 db, which is in addition to the free space attenuation.

At temperate latitudes, the water vapor decay constant at 3000 and 10,000 mc may be as high as 0.00004 db/km and 0.00066 db/km, respectively. It is therefore quite apparent that, for frequencies in the vhf and uhf range, the absorption by water vapor is insignificant.

Ionospheric Attenuation

An electromagnetic wave passing through an ionized medium imposes a periodic force on the electrons, causing them to vibrate. The absorption of signal energy occurs when the electrons, colliding with other particles, are forced to give up some of their energy to these particles.

The total attenuation, A , is given by the integral

$$A = \int_{s_1}^{s_2} k ds \tag{51}$$

where the limits of integration are the limits of the path

and where k is the absorption coefficient of the medium defined by

$$k = \frac{N_e e^2 \nu}{2\pi c n m f^2} \tag{52}$$

This expression is based on the assumption that the earth's magnetic field is neglected and that the transmitted frequency is much greater than the electron collision frequency,⁴ the latter being valid for frequencies in the vhf range.

Substituting (9) and (52) in (51) and assuming non-deviation type of absorption, $n \cong 1$, the total attenuation becomes

$$A = \frac{e^2 \nu'}{2\pi c m f^2} \int_{h_1}^{h_2} f(h) N_e e^{-(h'-h)/H} dh \tag{53}$$

where the path differential is expressed in terms of the height differential.

The total attenuation for waves traversing the ionosphere is plotted in Fig. 16. It is seen that the attenuation is inversely proportional to the square of frequency, with daytime absorption being considerably greater than the nighttime effect. The maximum total daytime attenuation, at a frequency of 100 mc, is approximately 1.28 db. It thus appears that, under normal conditions, ionospheric attenuation should be negligible at frequencies above 100 mc.

VIII. CONCLUSIONS

The propagational errors considered in this study are representative of average atmospheric conditions. These errors can be compensated for when the distribution of electron density in the ionosphere and the variation of dielectric constant in the troposphere are known. Although the general magnitude of these parameters can be obtained through the use of vertical incident ionospheric soundings and meteorological observations taken in the near vicinity of a radar installation, such measurements do not describe the true conditions along the path travelled by the radio waves. It is fully realized that utilization of these data will only partially correct for the slowly-varying component of atmospheric errors. The instantaneous fluctuations about the mean of propagational errors which are the result of inhomogeneities in the atmosphere do not appear to be compensative at this time.



Atmospheric Noise Interference to Medium Wave Broadcasting*

S. V. CHANDRASHEKHAR AIYA†, SENIOR MEMBER, IRE

Summary—A brief description is given of the typical tropical thundercloud and the electrical discharges associated with it. The discharge that contributes significantly to noise in the medium waveband is described in greater detail. There follows a systematic physical analysis of how the atmospheric noise impulse as heard by the ear arises and how it causes annoyance to the listener of broadcast programs. Hence, criteria are developed both for the measurement and estimation of atmospheric noise in the band. The method of analysis is similar to the one adopted by the author in a previous communication on atmospheric noise interference to short wave broadcasting.

The results of the investigation are expected to hold over the frequency range, 0.23 to 2.5 mc.

INTRODUCTION

THE medium waveband, as ordinarily understood, extends from 0.3 to 3.0 mc. In this band, atmospheric noise is the principal source of interference to signaling systems. This is particularly so in the tropics, where atmospheric noise is high and man-made noise is low due to the under-developed nature of the countries situated therein. Broadcasting is the most important service for which frequencies are at present allocated in the band, and this paper examines the interfering effect of atmospheric noise on this one specific service.

The method of analysis adopted in the paper is similar to what has been reported in a previous communication.¹ Problems already discussed are briefly described when absolutely necessary. Detailed discussion has been restricted to those aspects of analysis in which this paper differs from the previous one. Such differences arise because the discharge that gives rise to noise in the medium waveband differs from the one responsible for noise in the short waveband.

NOISE INTERFERENCE

Discharges associated with lightning radiate impulses. The different Fourier components of the impulses travel through space like other radio waves and those lying within a bandwidth, B , at a frequency, f , are picked up by the receiver and finally produce the acoustic impulse that is heard through the loudspeaker. The waveform of this acoustic impulse gets superposed on the waveform of the actual program and causes annoyance to the listener.

As the physical parameters associated with lightning discharges show statistical variations, both the meas-

urement² and the estimation³ of atmospheric noise must have a suitable statistical basis. An idealized statistically valid representation of the phenomenon has already been defined as the one obtained by the assignment of median values to the different physical parameters associated with the phenomenon and this has been called a "typical" case.¹ This concept is adopted for this paper also.

An objective noise meter which simulates the typical human ear, and thus properly measures the interfering acoustic impulse, has already been described and discussed.^{1,2,4} Its essential characteristics are summarized in Table I.

TABLE I
CHARACTERISTICS OF THE OBJECTIVE NOISE METER

1) Receiver	a) superheterodyne receiver with a bandwidth of 6 kc at 6 db down b) efficiency of rectification of modulation to be 0.9
2) Output unit	c) af output to be fed to the output unit a) charging time constant = 0.01 second b) discharging time constant = 0.5 second c) meter time constant = 0.2 second d) flat frequency response from 100 to 5000 cps e) logarithmic response for overload protection
3) Calibration	a) continuous signals b) modulation—30 per cent c) modulating af to be 400 cps

If E_{30} is the noise field strength as obtained with the calibration described in Table I, it can be converted to the noise field strength E_m , corresponding to a calibration using signals modulated to a depth, m , by the following equation:⁵

$$E_m = E_{30} \cdot \frac{0.3}{m} \quad (1)$$

The noise field strength is measured by the noise meter described in Table I. The data are collected and assessed on a statistical basis to deduce the median value of noise at a particular frequency for a particular sector of day for a season, and this is called the noise level. This noise level can be estimated by knowing the

* S. V. C. Aiya, "Measurement of atmospheric noise interference to broadcasting," *J. Atmos. Terr. Phys.*, vol. 5, pp. 230-242; September, 1954.

† L. D. College of Engineering, Ahmedabad 9, India.

¹ S. V. C. Aiya, "Atmospheric noise interference to short-wave broadcasting," *Proc. IRE*, vol. 46, pp. 580-589; March, 1958.

² S. V. C. Aiya, "Measurement of atmospheric noise interference to broadcasting," *J. Atmos. Terr. Phys.*, vol. 5, pp. 230-242; September, 1954.

³ S. V. C. Aiya, "Noise power radiated by tropical thunderstorms," *Proc. IRE*, vol. 43, pp. 966-974; August, 1955.

⁴ S. V. C. Aiya and K. R. Phadke, "Atmospheric noise interference to broadcasting in the 3 mc band at Poona," *J. Atmos. Terr. Phys.*, vol. 7, pp. 254-277; October, 1955.

⁵ S. V. C. Aiya, "Conversion data for atmospheric noise interference measurements," (to be published).

mean center of thunderstorm activity and the laws of propagation, if the power which corresponds to the equivalent acoustic impulse can be calculated from lightning discharge data.⁴ In evaluating the acoustic impulse and the equivalent power radiated from lightning discharges, it is necessary to take note of the fact that, so far as the ear is concerned, it is the maximum amplitude of sound, averaged for 0.001 second that measures impulsive noise and that the over-all effect observed over a period of 0.2 second is equivalent to continuous sound.¹

In view of what has been explained above, the principal objects of this paper are 1) to indicate clearly the type of discharge associated with lightning that radiates noise in the medium frequency band, 2) to evaluate the characteristics of the interfering acoustic impulse that the noise meter measures and, hence, 3) to calculate the equivalent source power corresponding to the measured acoustic impulse. The sections that follow are devoted to examining the three problems in the order indicated. Finally, a concluding section briefly reviews the entire problem.

THUNDERSTORMS

Thunderstorms are localized thermodynamic processes in the atmosphere accompanied by electrical discharges. The growth and decay of thunderstorms as noise radiators have been investigated⁶ in the tropics. It is found that a thunderstorm gradually builds up after local noon and reaches its peak activity by evening. This peak activity lasts three to six hours over land masses and longer over the sea. After peak activity, there is a drop and then a decay prior to sunrise. Generally, the activity is over within two hours after sunrise except for thunderstorms over the sea. Further discussion here is restricted to the period of peak activity of a thunderstorm.

During peak activity, a thunderstorm radiates at least ten flashes per minute and each flash lasts 0.2 second. In any typical thunderstorm, all flashes are intermittent and consist of four separate strokes. In between such strokes, slow electrical processes occur but they are not of importance for noise radiation in the short and medium wavebands. The physical nature of a stroke is as follows. There is probably a pilot streamer. This is followed by a leader streamer which is referred to here as the leader. This leader is followed by a recoil of low intensity and long duration when the discharge occurs in the cloud only. When the discharge strikes the ground, there is a return stroke of great intensity and short duration in place of the recoil occurring in cloud discharges.

All leaders in cloud discharges are discontinuous and consist of a number of steps following each other in

time sequence. The growth of current during a discharge in a step gives rise to the radiation of an impulse and a stepped leader, therefore, radiates a train of impulses. The first leader in a cloud-to-ground stroke is a stepped leader but the greater part of the subsequent leaders is not stepped and they are often called dart leaders. The return stroke, the recoil, and the unstepped portion of dart leaders do not radiate any significant power in the short and medium wavebands.⁷ It follows that the steps in the stepped leaders are the principal sources of noise in the short and medium wavebands. For a clear understanding of the distinction between the discharges responsible for noise in these two bands, it is necessary to examine the processes involved in the different types of stepped leaders. For this purpose, a description of the typical tropical thundercloud and the associated leaders is essential; this is given in the following sections.

THE TROPICAL THUNDERCLOUD

The data collected on the several aspects of lightning discharge by several methods in different parts of the world during different periods of the day have been critically examined and the essential characteristics of importance to noise deduced.⁷ This section and the two that follow contain a factual summary of the results to the extent necessary for this paper.

Electrical discharges associated with lightning are basically discharges in the air at certain pressures and with a certain percentage of moisture. In certain cases, this discharge takes place in an atmosphere of charged particles and so on. But, the phenomenon is essentially the same at all latitudes. Differences, if any, arise from the fact that the height of the cloud base above mean sea level varies with latitude due to the variation of the height of tropopause. The condition necessary for a discharge to strike the ground is that the cloud base is within a certain maximum distance from the ground. This implies that, for a discharge to strike the ground, the height of the cloud base above mean sea level depends on the altitude of the place.

A pictorial view of a typical tropical thundercloud is given in Fig. 1. The cloud base is about 4 km above mean sea level and the actual cloud extends to a height of about 14 km. Accumulation of positive and negative charges is as shown in the figure. Positively charged regions are not well defined and the spread of positive charge is diffuse. The negatively charged region is well defined and there is practically uniform concentration of charge.

Ordinarily, cloud discharges occur from the negatively charged regions and involve a length of about 1 km of the negatively charged region per stroke. It must be pointed out that this cloud discharge does occur even when the discharge is from the cloud to the air or to ground, but, in such cases, it is mostly a discharge from the negative region to the bottom positive region. That

S. V. C. Aiya, C. G. Khot, K. R. Phadke, and C. K. Sane, "Tropical thunderstorms as noise radiators," *J. Sci. Ind. Res. (India)*, vol. 14B, pp. 361-376; August, 1955.

⁷ S. V. C. Aiya, "Atmospheric noise radiators," (to be published).

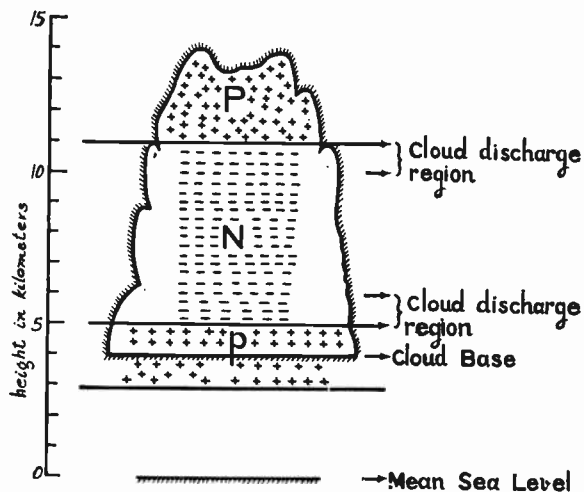


Fig. 1—A typical tropical thundercloud.

is, the cloud discharge is always there, either as part or whole of the discharge in all discharges.

A cloud discharge involves a length of about 1 km of the negatively charged region and $1/\sqrt{2}$ of this length, *i.e.*, 0.71 km, disappears after each stroke and this process goes on until the middle of the negatively charged region is reached. Since the latter is about 3 km from the ends, ordinarily, four strokes should be expected per typical flash as observed.⁸ Since the negatively charged region extends over a length of 6 km or more, there is always a possibility of 10 strokes per flash in very exceptional cases. These statements hold for all discharges.

We now proceed to examine the details of a cloud discharge. It has already been pointed out that a stroke in such a discharge consists of a leader followed by a recoil. All such leaders are stepped and probably involve a length of 1 km of the negatively charged region, the successive leaders in a flash arising ordinarily from higher and higher regions. In each step, it is the growth of current in a discharge that gives rise to significant radiation. This growth can be represented by

$$I = I_0(1 - e^{-\delta t}) \tag{2}$$

where, I_0 is the peak current. δ is *similar* to the inverse of the relaxation time as defined by Gunn⁹ and is given by

$$\delta = 4\pi\lambda \cdot 10^9 \tag{3}$$

where λ is the electrical conductivity of the region in electrostatic units (esu). It follows, therefore, that δ varies and is not constant. However, in calculations involving total vertical lengths of 1 or 2 km, it is reasonable to assume an average value for δ . As reliable conductivity measurements within the cloud are not

available, it becomes difficult to calculate δ for cloud discharges.

Peak electric fields arise from the maximum rate of change of current, X , and this is given by

$$X = (dI/dt) \max = I_0 \cdot \delta. \tag{4}$$

The different parameters associated with a step in a cloud discharge have been discussed and given elsewhere.⁸ A step radiates an impulse and, therefore, a stepped leader radiates a train of impulses. Since there are four strokes to a flash, a cloud discharge radiates four trains of impulses. A Fourier analysis of an impulse radiated by a step shows that it consists of a large number of components of different amplitudes and frequencies. The most important question to be examined is whether all the Fourier components of the impulse travel out of the small region in which the step makes its appearance. This is discussed briefly below.

A cloud discharge is confined to the negatively charged region in the cloud marked *N* in Fig. 1. An intense electric field, exceeding the disruptive strength of the dielectric, initiates the discharge and the appearance of steps. Because of these disturbed conditions, parts of the *N* region around the step have characteristics different from the rest of the *N* region. This is best described by saying that a "pocket" is created in the *N* region when a step appears. This pocket exists for a very short time but the important point to remember is that it exists for a period longer than the time taken by the step to radiate an impulse. In the Appendix it is shown that this pocket behaves in a manner *similar* to a waveguide and cuts off radiation at all frequencies below 2.5 mc. It follows, therefore, that a cloud discharge contributes to noise only at frequencies above 2.5 mc.

CLOUD-TO-GROUND DISCHARGE

When the height of the cloud base is of the order of 2.2 km from the ground, conditions are favorable for a cloud-to-ground stroke. In such a case, each of the four strokes consists of a leader and a return stroke. The first leader to ground is shown in Fig. 2. The literature on lightning discharges is full of terms like alpha leaders, beta leaders, etc. To avoid confusion, an entirely new nomenclature is adopted here. A typical stepped leader to ground has three distinct stages which are given below.

Stage I

This occurs in the negatively charged region and is identical with what has already been described as a cloud discharge. This stage does not contribute to noise in the medium waveband up to 2.5 mc.

Stage II

This occurs in the lower positively charged region; *i.e.*, partly in the cloud and partly in the air. The different parameters associated with steps in this stage are identical with those of stage I. But this stage lasts

⁸ B. F. J. Schonland, "The lightning discharge," in "Handbuch der Physik," ed. S. Flugge/Marburg, Springer-Verlag, Berlin, Germany, vol. 22, pp. 576-628; 1956.

⁹ R. Gunn, "The electrification of precipitation and thunderstorms," Proc. IRE, vol. 45, pp. 1331-1358; October, 1957.

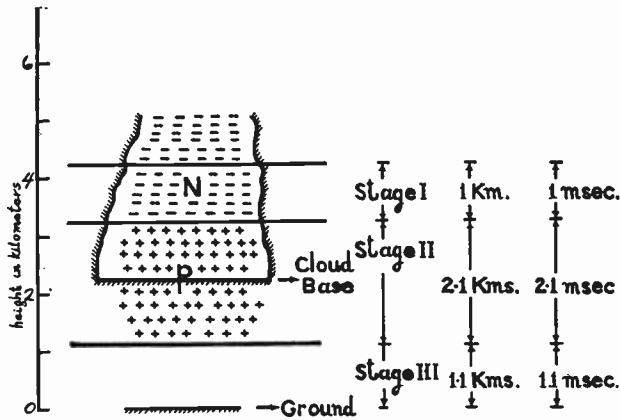


Fig. 2—First leader to ground and its stages.

0.0021 second. The "pocket" created by a step in this stage does not cut out any radiation in the medium and short wavebands (see Appendix). As it occurs at a lower height, δ is probably lower in value.

Stage III

This occurs from the end of the positive region to ground, and probably corresponds to what is often called alpha leader in lightning discharge literature. Steps are formed in charge-free air at definitely lower heights from ground and near ground. Steps are short and the intervals between steps are shorter. Because of the charge-free nature of air and the lower altitude, δ is distinctly of lower value and it appears that X for this region is about 1/10 of its value for stage I or stage II. The lower values of X and the step length considerably reduce the amplitude of radiation so that the radiation from this region becomes negligible compared to that from stage II for the medium waveband.

In the second and subsequent leaders to ground, stage III is generally absent; *i.e.*, there is no stepped nature for this length of the leader path. Similarly, the greater portion of stage II is not stepped. That is, for practical purposes, the few indeterminate steps if they occur at all in stage II of second and subsequent leaders, can be neglected in calculations. But stage I is always stepped in all the four leaders to ground.

When the height of the cloud base above ground is between 2.2 and 4 km, there is the possibility of stage I and part or all of stage II for the first leader, and stage I and a negligible part of stage II for the second and subsequent leaders. Each leader is followed by a process similar to recoil described earlier. All these correspond to what is generally called an air discharge. When the height of the cloud base is less than 2.2 km from ground, part or all of stage II may disappear.

MEDIUM WAVE NOISE RADIATOR

From the discussion in the preceding sections, it is clear that the electrical processes accompanying cloud discharges do not contribute noise in the medium waveband. The author's observations in Poona and Ahmeda-

bad show that discharges within the cloud constitute 90 per cent of all discharges. Cloud-to-ground discharges and cloud-to-air discharges together appear to constitute the remaining 10 per cent, of which the majority are cloud-to-ground strokes. These facts appear to hold for the tropics and, it follows, therefore, that only 10 per cent of the tropical thunderstorm discharges can contribute noise in the medium waveband.

In the cloud-to-ground or cloud-to-air discharges, it is only stage II of the stepped leader that can radiate noise in the medium frequency band. Stage II exists for the first leader of all cloud-to-ground strokes and, to a great extent, for cloud-to-air discharges. Part of stage II may exist for the second and subsequent leaders. Therefore, stage II of the first leader to ground or into the air is the principal source of noise in the medium waveband. There may be a small effect of part of stage II that may appear in the second and subsequent leaders, but it is not necessary to take account of this in calculations. This stage II differs from stage I in the following three characteristics only: 1) It is of longer duration, *viz.* 0.0021 second. 2) The "pocket" associated with a step does not cut out radiation in the medium and short wavebands. 3) The value of δ is lower.

About half of stage II is in the cloud and the other half is outside the cloud. Assuming that the value of δ at 2.1 km from ground corresponds to the average value for the whole of stage II, and using the conductivity value for air at an altitude of 2.1 km as given by Gunn,⁹ δ can be calculated from (3). This procedure is reasonably correct as we are below the cloud base at 2.1 km altitude. The value of δ so obtained is $4.6 \times 10^6 \text{ sec}^{-1}$.

The data required for a discussion of atmospheric noise in the medium waveband are reproduced in Table II. We are now in a position to summarize how

TABLE II
DATA FOR TYPICAL CLOUD-TO-GROUND OR AIR DISCHARGES

T_f	= over-all duration of a flash = 0.2 second
N	= minimum number of flashes per minute during peak activity = 10
n	= number of strokes per flash = 4
	= number of leaders
n_1	= number of leaders having the entire stage II = 1
T_s	= time interval between strokes in a flash = 0.04 second
T_L	= over-all duration of stage II of the first stepped leader = 0.0021 second
T	= time duration of a step = less than a microsecond
T_i	= time interval between steps = 0.000074 second
ν	= recurrence frequency of the steps = 13500 cps
l	= length of a step in a stepped leader = 67 meters
δ	= constant in the expression for the exponential rise of current in the discharge in a step in stage II of the leader = $4.6 \times 10^6 \text{ sec}^{-1}$.
X	= maximum rate of change of current in a step = 10^{10} amperes per second

noise in the medium waveband arises. A thunderstorm in which a discharge occurs in the air or to ground radiates at least 10 flashes¹⁰ per minute during peak

¹⁰ All the flashes need not necessarily strike the ground.

activity. A typical flash consists of four strokes and it is only stage II of stepped leaders that radiates noise in the medium frequency band. Hence, stage II of the first leader radiates a train of impulses for 0.0021 second. Each impulse lasts a fraction of a microsecond and the time interval between the impulses is 0.000074 second. This may be followed at intervals of 0.04 second by the radiation of a few similar impulses thrice. The Fourier components of all these impulses travel through space like other radio waves and those lying within a bandwidth, B , at a frequency, f , are picked up by the receiver and produce the acoustic impulse heard by the ear. The characteristics of this interfering acoustic impulse are examined in the next section.

THE INTERFERING ACOUSTIC IMPULSE

It has already been pointed out that the maximum value of the amplitude of sound averaged over 0.001 second gives a proper measure of the apparent loudness of an impulse as assessed by the ear.¹ As per discussion in the previous section, stage II of the first stepped leader in the discharges to ground or into the air radiates a train of impulses for 0.0021 second. It is difficult to evaluate the maximum average amplitude for 0.001 second during this period of 0.0021 second. Further, it appears that this value will not differ significantly from the average value for 0.0021 second. Hence, the latter will be taken as a proper measure of the apparent loudness of the impulse as assessed by the ear. That is, we will regard the average amplitude arising from a train of impulses lasting 0.0021 second, as the quantity we are interested in and hence confine our discussion to the equivalent rectangular pulse lasting 0.0021 second.

Such a rectangular pulse can be regarded as roughly corresponding to half of a complete 100 per cent modulated envelope. It follows that the equivalent modulating frequencies probably correspond to 238 cps; *i.e.*, roughly 240 cps, and their harmonics. The corresponding modulating frequencies evaluated for short-wave broadcasting were 500 cps and their harmonics. The predominant frequency in the noise impulse is lower for the medium waveband than for the short waveband. This fact is fully consistent with the author's observations during the last decade that the noise impulse as heard in the medium waveband has a lower AF than the one in the short waveband.

Since the predominant AF corresponds to 240 cps, this frequency should be used as the modulating frequency in the standard signal generator used for calibrating the noise meter. As there is no essential difference between 240 and 400 cps either theoretically or from the practical standpoint, the use of 400 cps as the modulating frequency appears to be a scientifically justifiable step.

A time plot of the actual radiation from a flash that gives rise to noise in the medium waveband and the corresponding acoustic impulses are given in Fig. 3. There is a full train of impulses from the first leader. From the second, third, and fourth leaders, there *may* be radiation

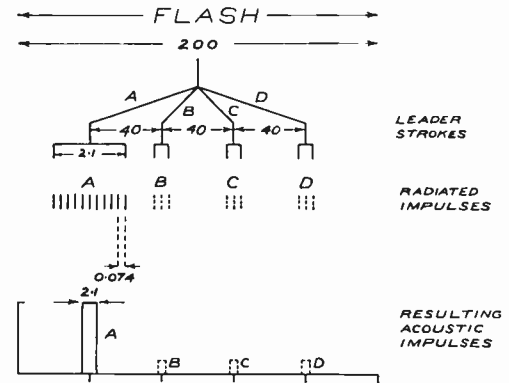


Fig. 3—Acoustic impulses from stage II of cloud to ground leaders. (Time intervals shown in milliseconds)

of a few impulses but this will always be indeterminate. The duration of such trains, however, will be for less than 0.001 second and as the average value for such trains has to be deduced for 0.001 second, it will obviously be very small. There being no certainty of radiation from leaders subsequent to the first, the impulses radiated and the equivalent acoustic impulses arising therefrom are shown in Fig. 3 by use of dotted lines.

From Fig. 3, it is obvious that the trains of impulses are *equivalent* to rectangular pulses and that they produce such rectangular pulses after rectification. The pulse at *A* is of the highest magnitude and longest duration but the pulses at *B*, *C*, and *D*, if they occur at all, are only of 0.001 second duration and of very small amplitude. The integrated effect of the pulses at *A*, *B*, *C*, and *D* over a period of 0.2 second is what produces the effect equivalent to continuous sound on the ear and the calculation has to be carried out by taking note of the charging and discharging time constants of the noise meter. The pulse at *A* produces the effect at *A* and its amplitude gradually decays. The effect of the small pulses at *B*, *C*, and *D* is to superpose the decay curves of their amplitudes on that of the pulse at *A*. Therefore, the actual acoustic impulse as heard by the ear becomes ill-defined and gives the impression of being rather drawn out. If, at any time during 0.2 second, the net effect of the pulses at *B*, *C*, and *D* increases the amplitude of the pulse at *A* by 3 db or more for 0.001 second, this effect will be noticed by the ear and can be regarded as a hump in the decay curve of the amplitude of the pulse produced at *A*. Experimental observations of the acoustic noise pulse as heard by the ear and also as measured by the meter, indicate that this does occur. Therefore, the maximum effect on the ear may be at *A* or at any point between *A* and *D*. Further, observations indicate that this increases the amplitude corresponding to that at *A* by 3 to 6 db, 3 db being the more common. However, this hump producing effect is not "typical."

From the discussion in the previous paragraph, the following conclusions can be drawn. For practical purposes, it is best to discuss the problem by considering the pulse at *A* only and ignoring the effects of the pulses

at *B*, *C*, and *D*. But, in considering the higher decile values of the noise levels, an allowance of 3 db may be made for the possible hump producing effect of the pulses at *B*, *C*, and *D*. On the basis of this simplified approach, we now proceed to deduce the equivalent amplitude of the corresponding continuous wave carrier, its level of the modulation, etc., in exactly the same manner as before.¹

Suppose the carrier amplitude corresponding to a rectangular pulse like the one at *A* in Fig. 3 is *Y*. Then, taking account of the efficiency of rectification of modulation, 0.9, the duration of the pulse, 0.0021 second, and the charging time constant of the noise meter, 0.01 second, the amplitude of the equivalent continuous wave carrier, *Z*, is given by

$$Z = (0.9) \cdot (0.0021/0.010) \cdot Y = (0.189) \cdot Y \quad (5)$$

$$\cong (0.19) \cdot Y. \quad (6)$$

A point worth noting here is the fact that the discharging time constant, 0.5 second, does not come into the calculation as we are dealing with one pulse only.

As before,¹ it follows that the noise impulse produces an effect on the ear that corresponds to a depth of modulation of 0.19 of this equivalent continuous wave carrier. The depth of modulation chosen for the noise meter calibration is 0.3. Hence, in comparing measured noise levels with estimates, it is necessary to reduce either of the two by use of (1). In evaluating standards of satisfactory service in the medium waveband, due account must be taken of the fact that the depth of the equivalent modulation of the noise impulse is 0.19 and not 0.30 as in the case of the short waveband.

POWER RADIATED BY A FLASH

The discussion of the previous sections makes it clear that a flash to ground or into the air radiates principally one train of impulses which gives rise to noise in the medium waveband. These impulses occur at random and the recurrence frequency is ν (see Table II). The bandwidth of the receiver, *B*, is 6000 cps. For such a case, the root mean square amplitude arising from the train of impulses has been calculated.³ In this calculation, it has been assumed that δ is much less than ω_0 and δ is neglected. If this assumption is removed, we get the following expression:

$$\begin{aligned} S(\omega_0) &= \text{root mean square amplitude due to a stroke} \\ &\quad \text{in a flash} \\ &= \sqrt{2\nu B} \cdot \frac{X \cdot l}{\sqrt{\omega_0^2 + \delta^2}} \end{aligned} \quad (7)$$

where,

$$\omega_0 = 2\pi f \quad (8)$$

and *f* is the frequency to which the receiver is tuned.

The train of impulses arises from stage II of the first leader to ground or into the air and each impulse is radiated by a step. Since all these steps are in stage II

of the leader, they can be considered to be high above ground. They are of short length and practically vertical. Therefore, the radiator can be regarded as a short vertical dipole in free space. Taking account of these facts and the gain factor of the antenna, the following expression has been deduced³ for the peak electric field intensity due to a stroke in a flash in $\mu V/m$:

$$E_1 = \frac{30}{cr} \cdot S(\omega_0) \sqrt{(1.5) \sin^2 \theta} \quad (9)$$

where

c = velocity of light in meters per second,

r = distance of the point from the source in 10^6 meters,

θ = angle the direction of radiation makes with the axis of the dipole.

As before,¹ the average value of the electric field due to a train of impulses is given by

$$E_2 = (0.85) \cdot E_1. \quad (10)$$

*E*₂ corresponds to *Y* in (6) but we require *E* which corresponds to *Z* in the same equation and, hence,

$$E = (0.85) \cdot (0.19) \cdot E_1. \quad (11)$$

In noise estimations, we calculate the field, *E*, in $\mu V/m$ at a point distant, *r*, from the source from the following expression:

$$E = 212 \cdot \sqrt{P/1000} \frac{\sin \theta}{r} \quad (12)$$

where

P = statistical median value of the equivalent power radiated by the noise source in watts.

From (7), (9), (11), and (12), the value of *P* can be deduced and after substituting the numerical values for the quantities involved from Tables I and II, we get

$$P = \frac{16.1}{f^2} \cdot \frac{1}{1 + \frac{\delta^2}{4\pi^2 f^2 \cdot 10^{12}}} \quad (13)$$

$$= \frac{16.1}{f^2 + \frac{\delta^2}{4\pi^2 \cdot 10^{12}}} \quad (14)$$

where

f = frequency in mc,

$\delta = 4.6 \times 10^6 \text{ sec}^{-1}$.

In (14), δ can be neglected when

$$\frac{\delta^2}{4\pi^2 \cdot 10^{12}} < \frac{1}{10} \cdot f^2, \quad (15)$$

i.e., when

$$f > 2.3 \text{ mc.} \quad (16)$$

Similarly, in (14), *f* can be neglected when

$$f^2 < \frac{1}{10} \frac{\delta^2}{4\pi^2 \cdot 10^{12}}, \quad (17)$$

i.e., when

$$f < 0.23 \text{ mc.} \quad (18)$$

Below 0.23 mc, the power radiated is practically independent of f and has a constant value of 30 watts. This question will not be discussed here as the problem of noise radiation below 0.23 mc is the subject matter of a separate communication.

From (18), it follows that (13) holds for all frequencies above 0.23 mc. But, beyond 2.5 mc, the radiation from discharges within the cloud becomes much more important and since such discharges are much more frequent, (13) is of no significance. It is, therefore, concluded that (13) holds from 0.23 to 2.5 mc.

It is necessary to emphasize that the frequency limits for the validity of (13), *viz.*, 0.23 and 2.5 mc, should not be taken too rigidly. The lower limit depends on δ , which is estimated from conductivity measurements. The higher limit has been evaluated in the Appendix. The limits have been evaluated with some care and have the support from the author's preliminary noise measurements, but detailed investigations may lead to a slight revision of these values.

A preliminary report of the sequence of experimental work which led to the calculations reported in this paper and the actual equation as given in (13) has already been made.¹¹ A detailed report of the actual experimental work and its comparison with the estimates deduced from (13) will shortly be published elsewhere.¹²

CONCLUSION

This paper gives a brief summary of the physical picture of a typical tropical thundercloud and some of the electrical discharges, etc., associated with it. This has been deduced from lightning discharge data. It will be seen that the first stepped leader to ground has four parts roughly of the same length, *viz.*, 1 km. Two of these parts together constitute stage II as defined. Both these parts occur in the lower positive region, but, one part is within the cloud and the other outside the cloud. Photographic methods may often get only this lower part of stage II. Similarly, only the upper part of stage II may be regarded as a cloud discharge. The possibility of confusion is increased by the fact that stage I and the whole of stage II have the same values for the length of the stepped leader, interval between steps, etc. Detailed discussions are undertaken elsewhere⁷ but it is sufficient to state here that this typical tropical thundercloud as described appears to represent facts in their essentials. Since the paper is restricted in scope to a discussion of "typical" cases, uncommon cases have been entirely eliminated.

¹¹ S. V. C. Aiya, "Noise radiation from tropical thunderstorms in the standard broadcast band," *Nature*, vol. 178, p. 1249; December, 1956.

¹² S. V. C. Aiya and C. G. Khot, "Atmospheric noise interference in the standard broadcast band at Poona," (to be published).

The concept of the interfering acoustic impulse and the calculation of the equivalent power radiated by the source have been discussed in detail earlier¹ and a review of these becomes unnecessary here.

It has been stated that cloud discharges do not radiate any significant power below 2.5 mc. The author carried out some preliminary experiments by changing the tuning and listening to the noise impulse when only cloud discharges were taking place and found an abrupt change of noise magnitude in the region, 2 to 3 mc. When local thunderstorms were followed by noise measurements simultaneously at a number of frequencies, the result was confirmed. An explanation for this has been attempted in the Appendix.

The statement that cloud-to-ground strokes are the principal sources of noise in the medium waveband is based on actual observations but the statement that cloud-to-air discharges also give rise to noise in this band is based on inference.

Systematic noise measurements were carried out for a complete year, 1954–1955, in the standard broadcast band and repeated again in 1955–1956. The two sets of data were carefully examined to confirm consistency and every possible care was taken in carrying out measurements in 1955–1956. The noise levels, deduced on the basis of such measurements, can only be explained, and explained satisfactorily, on the basis of deductions in this paper. The estimates agree well with measured values. This is perhaps the most striking indication that the approach to the problem as given in this paper is probably in the right direction.

APPENDIX

POCKETS IN ACTIVE THUNDERCLOUDS

Experimental results indicate that cloud discharges do not radiate noise below a certain frequency and that this frequency lies between 2 and 3 mc. An attempt is made here to explain these results and calculate the actual cutoff frequency.

Cloud Characteristics for Step Formation

A typical tropical thundercloud is shown in Fig. 1. It has certain electrical characteristics. These change when the thundercloud becomes active and lightning discharge commences. An active thunderstorm thus can be regarded to exist under disturbed conditions. Conditions that exist in a thundercloud prior to its becoming active can be called normal conditions. For understanding the changes that take place with the commencement of activity of a thunderstorm, we require the electrical characteristics of a thundercloud under normal conditions. The closest approach to such conditions is probably a mild cold front with no lightning activity. Data for such a case are given in Table III of Gunn's paper.⁹ This table can be used for a tropical thundercloud provided we abstract from it data corresponding to the same isotherm.

We now consider the mechanism of a cloud discharge. Physical processes occur leading to the development of intense electric fields. This is followed by the initiation

of the flash. The first leader stroke appears to always commence approximately at the freezing level or zero degree isotherm. Subsequent strokes commence from higher regions. The first step in the first leader stroke occurs on the zero degree isotherm. Subsequent steps occur at lower levels but under disturbed conditions. Similarly, steps of subsequent leader strokes occur at other levels but again under disturbed conditions. Therefore, it is reasonable to assume that typical conditions existing in the cloud prior to the formation of a step are those corresponding to the first step of the first leader stroke. On this basis, the data in Table III of Gunn's paper corresponding to 0°C represent the normal electrical characteristics of a tropical thundercloud prior to the appearance of a step. The relevant information is reproduced in Table III.

TABLE III
CLOUD CHARACTERISTICS FOR STEP FORMATION

1) Temperature = 0°C
2) Charge on a positive drop = +0.042 esu
3) Charge on a negative drop = -0.100 esu
4) Positive particle space-charge density = 1.0×10^{-5} esu/cm ³
5) Negative particle space-charge density = -4.6×10^{-6} esu/cm ³
6) Excess negative particle space-charge density = -3.6×10^{-6} esu/cm ³

Pocket Formation

The zero degree isotherm will be across the *N* region of Fig. 1. This region contains electrons, ions, and charged drops. The drops are so heavily charged that, in any approximate calculations involving charges, we can neglect the electrons and ions. Consider the negatively charged drop. As in Table III, it has a negative charge of 0.1 esu, *i.e.*, a considerable number of electrons are attached to it. It is well known that, under the action of intense electric fields, such electrons attached to the drop can get separated from it. The free electrons so produced go to form an electron gas.

An intense electric field exceeding the disruptive strength of the dielectric initiates the discharge and the appearance of steps. We are not interested here in the actual step formation but in the phenomena accompanying it. The effect of the intense field is felt not only in the portion of the cloud where the step appears but also in the space immediately surrounding it. We describe this space immediately surrounding the step as a pocket. In this pocket, electrons are liberated from the negatively charged drops by the action of the intense electric field. The pocket thus gets filled with an electron gas. The physical condition of this pocket is thus different from the conditions prevailing in the *N* region of the cloud elsewhere. (Such pockets account for the observed reflections from active thunderclouds in radar studies of cloud behavior.)

The creation of the pocket precedes the appearance of the step as it commences with the production of electric fields of much lower value. This pocket, once created, gradually disappears and traces of it exist practically until the commencement of the next stroke. During pocket formation, positive and negative charges get

neutralized and the excess negative space-charge density appears in the form of an electron gas. Therefore, the electron density in the pocket is given by

$$n = \frac{3.6 \times 10^{-5}}{4.77 \times 10^{-10}} \quad (19)$$

$$= 7.548 \times 10^4 \text{ electrons/cc} \quad (20)$$

(4.77×10^{-10} is the electronic charge in esu).

Wave Propagation through the Pocket

It follows from the previous section that the pocket is equivalent to a medium containing free electrons. Propagation of electromagnetic waves through such media is well known. The refractive index of such media is given by

$$\mu = \sqrt{1 - \frac{81 \cdot n}{f^2 \cdot 10^6}} \quad (21)$$

where

$$f = \text{frequency in mc.} \quad (22)$$

The refractive index depends on the frequency of the wave and the electron density in the medium. There is propagation of waves when the refractive index is real. When the refractive index is imaginary, attenuation takes place and the pocket will not transmit the waves; this happens when

$$f < \sqrt{\frac{81 \cdot n}{10^6}}, \quad (23)$$

i.e.,

$$f < 2.47 \text{ mc,} \quad (24)$$

i.e.,

$$f < 2.5 \text{ mc approximately.} \quad (25)$$

This shows that the pocket behaves in a manner similar to a waveguide and cuts out radiations from the step of the leader for all frequencies below 2.5 mc.

General

The behavior of the pocket as explained in this note is applicable to the *N* region of the cloud where there are excess negatively charged drops and electron gas formation is possible. Cloud discharges occur in the *N* region and hence, the discussion holds for cloud discharges. In the *p* region of the cloud or below it, there is excess of positively charged drops and, therefore, there are no possibilities for the electron gas formation in the pocket and the discussion of this note does not apply. If the pocket is full of charged ions, the cutoff frequency will be very much lower as it depends on the mass of the ions and the ion density. Hence there is no waveguide action for radiations from stage II in Fig. 2 for the frequencies in the medium and short wavebands.

A detailed discussion of the problems examined here will be found elsewhere.⁷

Suppression of Undesired Radiation of Directional HF Antennas and Associated Feed Lines*

H. BRUECKMANN†, FELLOW, IRE

Summary—An analysis of the situation in point-to-point radio communication circuits at frequencies below MUF with respect to radiation in undesired directions brings to the fore some aspects which are useful as guide lines in antenna research, design, and application engineering.

In many cases, the interference experienced in operating receivers in the high-frequency range can be attributed primarily to the relatively high side lobes of the radiation pattern of rhombic antennas. Progress has been made in suppressing these side lobes through the development of antenna arrays employing nonuniform amplitude distributions and, more recently, through the advent of modified horn-type antennas. Other sources of interference which are usually overlooked are associated with balanced open-wire lines which are not operated properly. Recently, it has become feasible to replace these lines by coaxial cable using broad-band balun transformers.

INTRODUCTION

THIS discussion is concerned with only one category of applications of HF antennas, though it is one of great importance: long-range fixed-point-to-point radio communication at frequencies below MUF. It is exemplified in the Army Global Communication System of strategic circuits operated by the Army Communications and Administrative Network (ACAN), mostly at frequencies between 5 and 25 mc. Ionospheric scatter propagation, mobile stations, or short-range circuits are not discussed, although some of the considerations here apply equally well. We are faced here with applications in which the usable signals carrying the desired information depart from the transmitting antenna and arrive at the receiving antenna in a relatively narrow solid angle (between about 5 and 15 degrees elevation angle, depending on the range, layer height, number of hops, etc., and between \pm about 5 degrees azimuth angle relative to the azimuth of the Great Circle through receiver and transmitter). The deviations from the Great Circle path depend on the range, irregularities of the ionospheric layers, etc. Other paths for the desired signal outside this solid angle may exist, but they are not usable or dependable and may be even harmful. Capability of the receiving antenna to receive from other directions makes the radio circuit only more susceptible to interference. There is an analogy between spurious frequency responses, or generations of electronic equipment, and spurious side lobes of directional antennas. Frequency

allocation corresponds here to geographical location. A typical situation at a receiving station is depicted in Fig. 1(a) for the horizontal plane. Actually, the problem is a three-dimensional one. For the sake of simplicity the third dimension is omitted in Fig. 1(a), but has to be taken into account in a thorough investigation, as illustrated in Fig. 1(b). For subsequent considerations, it is useful to introduce a number of short terms which permit describing quantitatively either a particular application or a particular antenna.

GENERAL CONSIDERATIONS

In general, the bearing of the direction of arrival of the usable signal varies with time. The variations are statistical. The sector which encompasses all variations in the bearing of the direction of arrival of the useful signal with time for a specified percentage of the total circuit time shall be called "sector of arrival of the desired signal." For a typical circuit, it is less than 10 degrees for 80 per cent of the total circuit time. This sector, in general, is not symmetrical about the direction of the Great Circle through transmitter and receiver due to the propagational effects of the auroral zone.

In many cases, the likely source of strong interfering signals is known, or at least the place is known where no strong interference is to be expected. The sector (or sectors) which covers all bearings from which strongly interfering signals (usually a multiplicity of them) arrive, or are likely to arrive, may be called "critical sector." It is also a value of a statistical nature, rather than a constant, and has to be handled accordingly. For many reasons, advantage should be taken of the knowledge of the geographical situation, if at all possible.

The designation of "horizontal half-power beam-width" for the azimuthal angle between the extreme bearings of the half-power points of the main beam has been generally accepted. It is a property of the particular antenna used. The two terms discussed below are also properties of the antenna.

The capability of a given antenna to reject interference can be expressed by the ratio of the gain in a specified direction, as seen from the antenna, to the gain in the direction from which the desired signal arrives. It shall be called "rejection ratio." This term is an abstraction which purposely disregards the existence of the ionosphere. It is identical with the radiation pattern only if the desired signal arrives in the direction of the maximum of the main beam.

* Manuscript received by the IRE, November 28, 1957. This paper was presented at the Symposium on Electromagnetic Interference, Asbury Park, N. J., November 20, 1957.

† U. S. Army Signal Res. and Dev., Fort Monmouth, N. J.

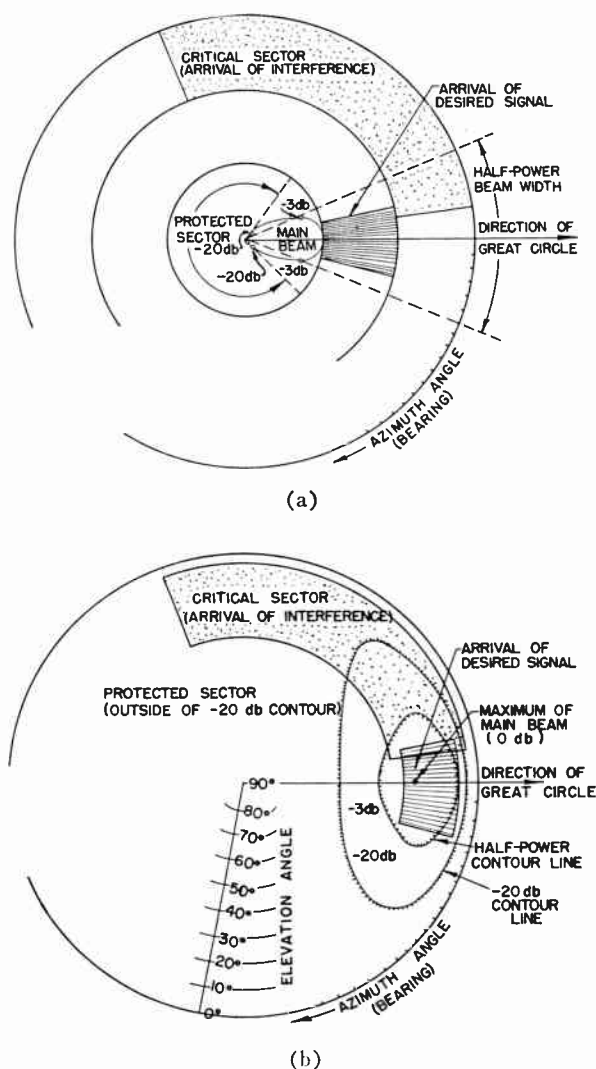


Fig. 1—(a) Plan view presentation of various sectors involved in the operation of typical radio communication receiving antenna affected by interference (schematic). Inner circle shows the antenna pattern, middle ring the desired signal, and the outer rings show the interference. (b) Contour-map presentation of the same situation as the one depicted in (a).

The sector or sectors within which the radiation of a given antenna is a specified ratio (for example -20 db), or less than the radiation in the maximum of the main beam, shall be called the "protected sector." In other words, within this sector the rejection is higher than a specified minimum.

With this nomenclature, it is possible to make some general statements on receiving antennas. They are useful as guide lines for research and development as well as application engineering.

The protected sector is always smaller than 360 degrees minus the half-power beamwidth, because the beamwidth between directions for which the gain is lower than -3 db is larger. The factor by which it is larger corresponds to the so-called "form factor" of receiver-selectivity characteristics and does not greatly

depend upon whether, say, 20 or 30 -db rejection ratio is specified. Provided the side lobes are lower than is necessary to meet the required minimum-rejection ratio, the protected sector is always about 360 minus 3 times the half-power beamwidth. In other words, decreasing the half-power beamwidth by a certain amount increases the protected sector by 3 times that amount and vice versa, if only the side lobes can be kept low enough.

If the critical sector of interference overlaps completely with the sector of arrival of the desired signal, little can be gained by using low-side-lobe antennas, assuming that the interference is stronger than thermal and static noise. Of course, a simple antenna will then perform operationally almost as well as an elaborate one. If, however, the critical sector overlaps only partially with the sector of arrival of the desired signal, the rejection ratio can be improved by slewing the main beam by an angle equal up to about half of the half-power beamwidth in the proper sense.

Since an antenna approaching the ideal is always difficult and costly to build, a possible compromise is an antenna which has a high rejection ratio for signals arriving from directions within the critical sector, at the sacrifice, if necessary, of a low rejection ratio for directions outside this sector. This approach has not yet been given much attention, but has the potentiality of leading to simple and relatively inexpensive solutions. Such a statement will become clearer when recent approaches aiming at the ideal antenna are considered.

If we consider transmitting antennas now, we can see that the above terms and conclusions about receiving antennas apply equally well, after substituting "depart" for "arrive." The protection relates then to other circuits, rather than to the circuit under consideration. Yet the suppression of undesired radiation from transmitting antennas has been given, in the past, much less importance than that from receiving antennas. The reasons for this are obvious and are not discussed here. It is believed, however, that sooner or later a stage of development will be reached at which both are given equal importance.

RECEIVING ANTENNAS

Efforts, reported below, to improve receiving antennas had to start from the state of the art established by the rhombic antenna which has been dominating the appearance of overseas radio stations for the last 30 years. For some years, the rhombic has become more widely recognized as the compromise solution which it is with respect to frequency range and directivity. Extensive measurements¹ of the radiation patterns of an operational typical rhombic antenna 756 feet long and 260 feet wide have provided precise information on the

¹ H. Brueckmann, "Analysis of Measured Radiation Patterns of Two HF Antenna Arrays and One Rhombic," U. S. Army Signal Engineering Labs., Rep. E-1198; January, 1957.

magnitude of the side lobes. The chart of Fig. 2 gives their direction and magnitude relative to the main lobe at four frequencies. This chart lists the horizontally polarized side lobes up to elevation angles of about 30 degrees only. Although the other polarization and higher elevation angles are not included, the chart gives a fairly complete picture of the performance of rhombics. It shows that: 1) azimuthal direction of all side lobes at all frequencies measured agrees excellently with theory whereas agreement of calculated and measured elevation angles of side lobe maxima may be called reasonable; 2) magnitude of the side-lobe maxima in the front sector, as far as determined, agrees fairly well with theory; and 3) agreement of the magnitude of the side-lobe maxima in the rear sector with theory is poor. (This is plausible in view of the fact that small reflections at the termination and the side poles are bound to affect the pattern in the rear section profoundly.)

The measurements have again demonstrated that rhombics poorly reject interfering signals arriving from the forward sector over the entire frequency range. At all frequencies, some side lobes exist which are only about 6 to 10 db down from the main lobe. The back lobe varies between -6 and -20 db, decreasing gradually in strength with increasing frequency, as do the other side lobes in the rear sector.

About four years ago, a reappraisal of the situation with respect to interference in strategically important circuits of the Army, led to the conclusion that some of these circuits had to be equipped with low-side-lobe receiving antennas immediately. However, the state of the art at that time did not permit reducing side lobes and at the same time satisfying the frequency range requirements. In order to break the deadlock, the concept of covering the required minimum frequency range from 6 to 18 mc with one antenna was abandoned. Two different prototype antennas were built under this program, for which the design information² was supplied by this laboratory. Both were designed for a narrow band, one centered around a frequency below 10 mc., and the other one centered around a frequency above 10 mc. Fig. 3 shows an over-all view of the antenna for lower frequencies which was built by Developmental Engineering Corporation under Signal Corps contracts.^{3,4} It consists of a vertical plane wire-grid acting as a parasitic reflector, seven wavelengths or over-all 950 feet wide, and $3/4$ wavelength or 104 feet high, with 12 vertical

LOBE NO.	FREQ 4.932 MC MAIN LOBE			FREQ 7.465 MC MAIN LOBE			FREQ 12.2525 MC MAIN LOBE			FREQ 17.465 MC MAIN LOBE		
	MAX POWER GAIN	ELEVA. DEG.	AMPLI. db	MAX POWER GAIN	ELEVA. DEG.	AMPLI. db	MAX POWER GAIN	ELEVA. DEG.	AMPLI. db	MAX POWER GAIN	ELEVA. DEG.	AMPLI. db
1	31	15.5	-13.1	42	10	-5.5	19	9.2	-10.2	15	8.5	-11.4
2	55	27	-7.0	59	5.7	-14.8	29	9.2	-11.5	32	5.8	-9.6
3	88	27	-13.0	79	10	-14.5	42	9.2	-7.5	41	8.5	-10.6
4	123	21.6	-16.5	180	30	-13.6	65	9.2	-17.7	50	8.5	-13.2
5	180	27	-5.9				78	9.2	-17.5	59	8.5	-18.0
6							177	9.2	-22.8	66	8.5	-18.8
7										76	8.5	-18.5
8										180	8.5	-19.3

* Main lobe maximum power gain figure is relative to isotropic radiator.

Fig. 2—Orientation and magnitude relative to main lobe of measured horizontally polarized side lobes of RD-4 rhombic at four frequencies.

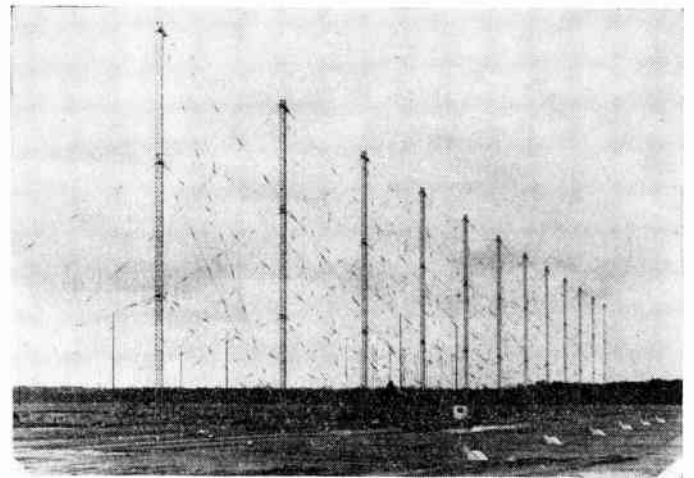


Fig. 3—Vertical antenna array employing nonuniform amplitude distribution.

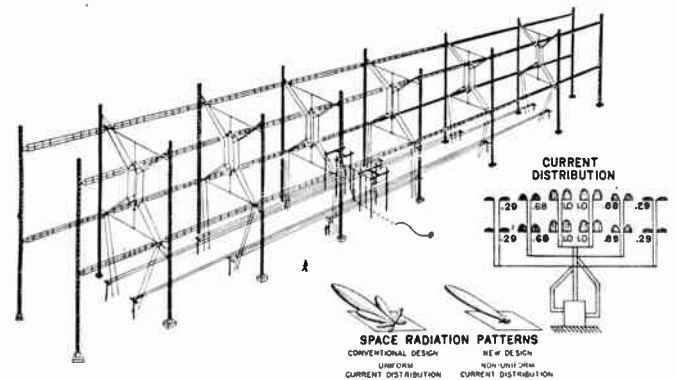


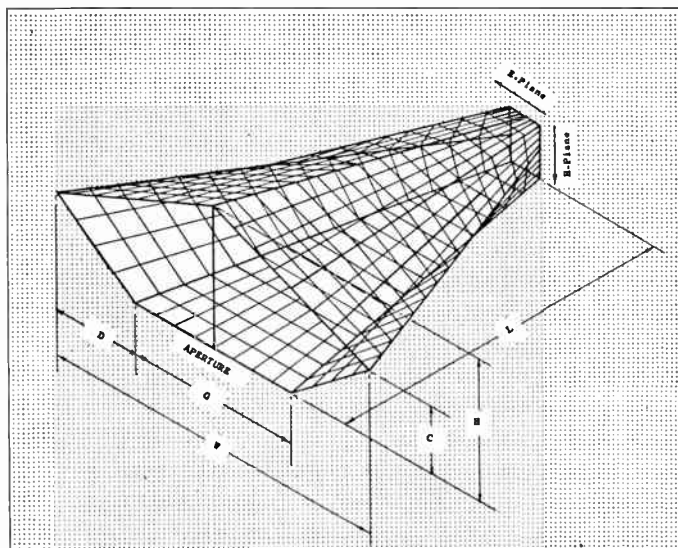
Fig. 4—Arrangement of supports of final category A1 antenna.

elements in front of it. Fig. 4 shows the antenna for higher frequencies which was built by a Signal Corps construction company under the direction of the U.S. Army Signal Communication Engineering Agency. It consists of two vertical curtains of 12 horizontal full-wave dipoles each of which is fed. The over-all width of this array is also seven wavelengths or about 560 feet, its height is $1\frac{1}{2}$ wavelengths or 123 feet. In both arrays

² H. Brueckmann, "HF Broadside Antenna Arrays with Non-Uniform Amplitude Distribution," U. S. Army Signal Engineering Labs., Rep. E-1214; September, 1957.

³ D. F. Bowman, "Broadside Antenna Array of 12 Vertical Elements with Non-Uniform Current Distribution," Developmental Engineering Corp., Leesburg, Va., Signal Corps Contract DA-36-039 SC-56762, Final Tech. Rep.; September, 1954.

⁴ H. A. Ray and B. G. Hagaman, "HF Vertically Polarized Directional Antenna Array," Developmental Engineering Corp., Leesburg, Va., Signal Corps Contract DA-36-039 SC-64670, Interim Tech. Rep.; December, 1955.



	L	W	H	C	D	G
FULL-RANGE TAHA AT 7 Mc.	844' 6A	506' 3.6A	253' 1.8A	88' 0.6A	189' 1.2A	169' 1.2A
LOW-RANGE TAHA AT 8 Mc.	798' 4.1A	798' 4.1A	399' 2A	188' 1A	288' 1.2A	288' 1.2A
HIGH-RANGE TAHA AT 12 Mc.	534' 4.1A	354' 4.1A	187' 2A	84' 1A	110' 1.2A	110' 1.2A

Fig. 5—Characteristic dimensions of TAHA.

the amplitude distribution of the excitation of the dipoles with respect to each other is nonuniform in contrast to conventional arrays. The particular taper employed is the so-called Dolph-Tchebycheff distribution. It is believed that these arrays are the first ones in the high-frequency range and in the field of radio communication which employ nonuniform amplitude distribution. The half-power beamwidth of both arrays is 10 degrees, the gain 24 db. The side lobes of the vertical array were measured to be 23 db, or more, down from the main lobe. The horizontal array was in faulty condition during the last measurements, which was discovered only afterward. The measured side-lobe level of -20 db is not representative, therefore. All indications are that eventually a side-lobe level of -26 db, or less, can be achieved. In summarizing, it can be said that these arrays reduce the side lobes, compared to a rhombic of comparable gain, by about 20 db, a spectacular improvement from the interference-suppression point of view. But this improvement is bought at the expense of the width of the frequency range of a single antenna and necessitates a separate antenna for each operating frequency, not to speak of the increase in cost, complexity, and required real estate.

Faced with this serious shortcoming of arrays and stimulated by the experience gained in designing them, a new approach to the problem of the broad-band directional antenna with low side lobes was taken at the beginning of 1956. This approach was along the line of horn-type antennas. It culminated in the design of TAHA (Tapered Aperture Horn Antenna) by Boynton G. Hagaman, Developmental Engineering Corporation,

Leesburg, Va., under contract with these laboratories.⁵ Fig. 5 gives an idea of its configuration. Construction of a full-scale prototype is at present under way. Its overall dimensions are: length 850 feet, height 250 feet, width 560 feet. The performance data determined so far by model measurements are impressive. Side-lobe level is -20 db, or less, over the entire frequency range. Fig. 6 shows that the horizontal beamwidth of TAHA can be made to equal that of a rhombic over the entire frequency range of the latter.

It is believed that, at long last, a substitute for the rhombic antenna has been found which is, for a given gain or beamwidth, equal if not better with respect to bandwidth and, at the same time, much superior with respect to side-lobe suppression by a factor in the order of 15 to 20 db. No doubt, this technical advance has to be paid for. The development which is still in progress has not gone far enough, however, to permit a fair comparison of costs.

ANTENNA FEED LINES

Antenna feed lines of the balanced open-wire transmission line type are still used almost exclusively in HF transmitting installations, in contrast to receiving installations which are using mostly coaxial cable. One aspect of balanced open-wire lines which has been given little attention is that they act as rather efficient directive radiators if excitation is unbalanced with respect to ground. Such unbalanced excitation can occur unintentionally if the transmitter or the line are not carefully constructed or operated. Relatively small deficiencies suffice to cause strong unbalanced excitation. Yet the provisions presently made for detecting such deficiencies are totally inadequate in almost all installations, both commercial and military, to the knowledge of this author.

This contention is borne out by the vector diagrams of Fig. 7 which show the voltage and current vectors involved in an elementary section of open-wire line for both the left and right-hand side. Fig. 7 illustrates how any given excitation can be split into a perfectly balanced excitation and a pure unbalanced excitation superimposed on each other. From this illustration it becomes obvious, for example, that the left-side currents and right-side currents can be exactly equal in amplitude satisfying one condition for balanced excitation, and that notwithstanding, the unbalanced current component can be strong. A small deviation of the currents from the 180-degree phase relationship suffices for this end. This proves that two ammeters, one in each side of the line, are not sufficient to detect such a situa-

⁵ R. E. Ankers, B. G. Hagaman, and others, "Reliable High-Frequency Communications," Developmental Engineering Corp., Leesburg, Va., Signal Corps Contract DA-36-039 SC-64486; July, 1956. (See also Sixth through Ninth Progress Reports; November, 1956, through December, 1957.)

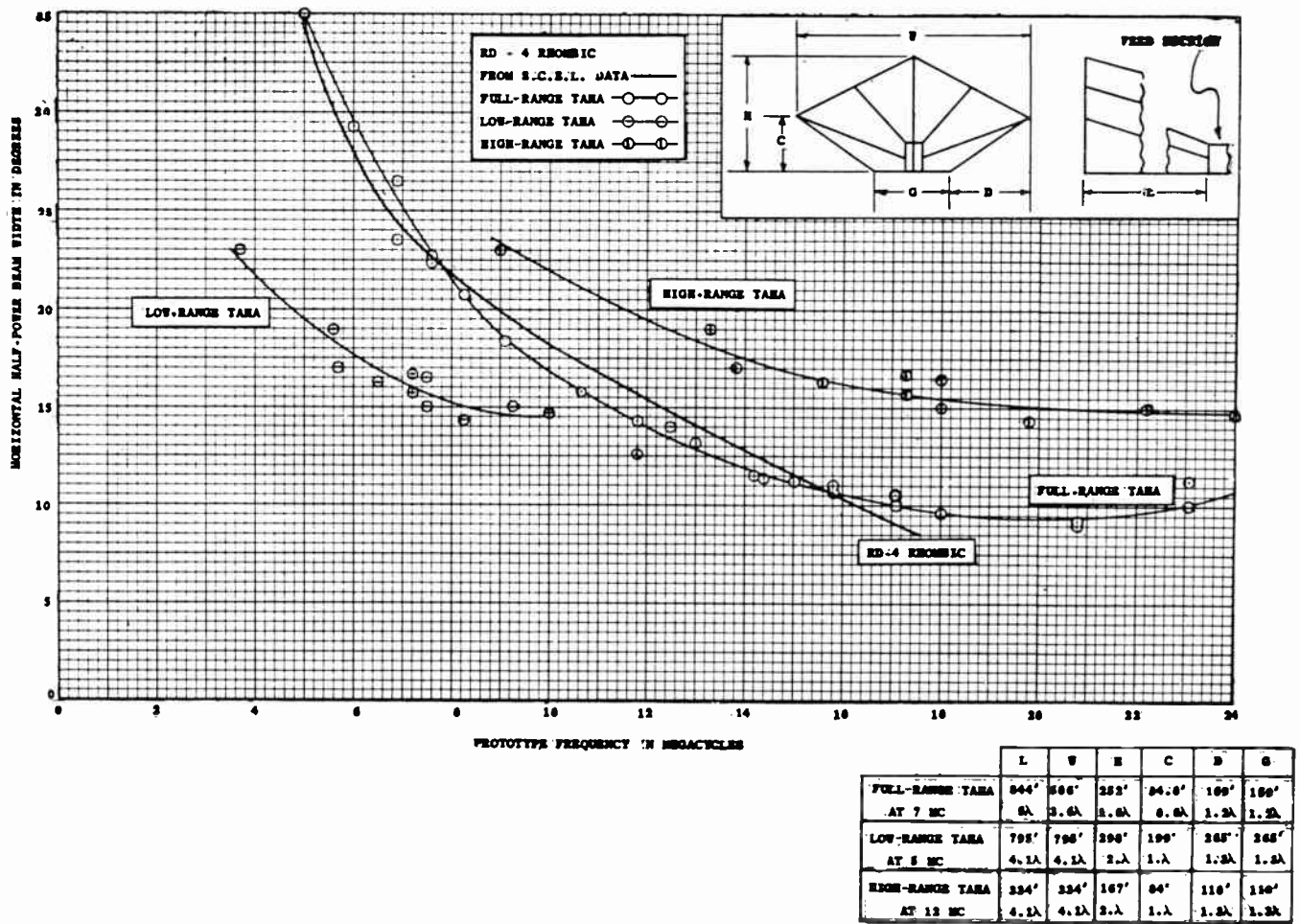


Fig. 6—Horizontal half-power beam width as a function of frequency for TAHA and RD-4 rhombic.

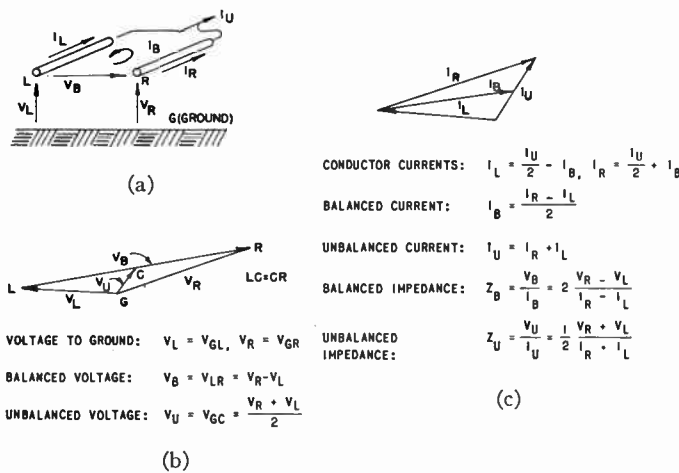


Fig. 7—Relationships in a two-wire line. (a) Assumed directions of voltages and currents. (b) Vector voltages. (c) Vector currents and impedances.

tion. Yet, two ammeters are presently standard equipment for monitoring. The large inaccuracy of RF ammeters, especially when the currents are lower than the full-scale value, permits a strong unbalance to go undetected even if the 180-degree-phase condition is satis-

fied. With this kind of monitoring equipment it is conceivable that most of the output power of a transmitter is radiated from the line or absorbed in the ground underneath and only little is radiated from the antenna in the normal way, without being noticed. In any case this radiation may greatly exceed the unavoidable radiation of the line originating from the balanced component of the excitation.

The reason why presently used monitoring equipment is inadequate is, by the way, not that adequate equipment is unavailable or too expensive. Fig. 8 shows the circuit diagrams of a commercially available voltmeter in the switch positions "balanced" and "unbalanced" which permit measuring both voltage components directly and separately. Two such instruments a quarter wavelength apart along the line, or one such instrument together with a corresponding one measuring the balanced and unbalanced current components, are necessary to detect unbalanced excitation under all circumstances. However, one instrument alone already would minimize the chances of strong unbalanced excitation going undetected.

Monitoring the degree of balance of the excitation of a line is, of course, only a first step in suppressing radia-

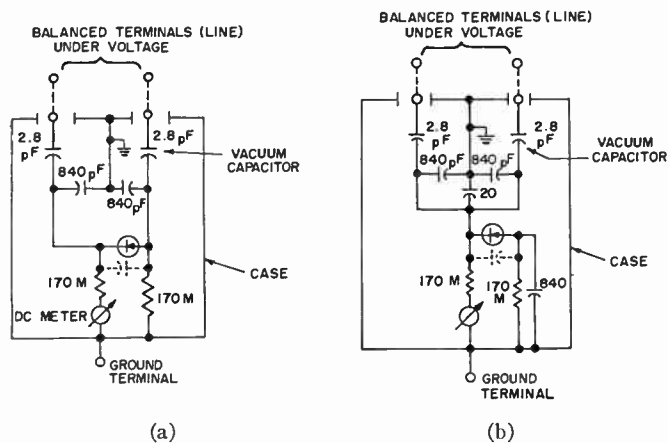


Fig. 8—Voltmeter for measuring degree of balance of the voltage in a three-terminal network. (a) Measurement of balanced voltage component. (b) Measurement of unbalanced component.

tion from it. The next step would be to take corrective measures if the unbalanced excitation exceeded a specified percentage of the balanced excitation. In principle, provisions for adjustment are required in both line and transmitter, although probably in most cases adjustment of the transmitter will suffice. At present, provisions for adjustment do not exist or are not adequate. Incorporating such provisions is not technically difficult, but not a minor modification either from the overall engineering point of view.

It should be mentioned that unbalanced excitation of an open-wire line can also occur through coupling to an adjacent perfectly balanced line, as illustrated in Fig. 9.

In determining the tolerable unbalanced excitation at the line input, one has to consider the resulting radiation from the line together with the antenna in relation to the radiation from the antenna for balanced excitation. It is obvious that the radiation from the line in the direction of the maximum of its radiation pattern at least should not exceed the radiation in the strongest side lobe of the antenna radiation pattern for normal operation. This means that the RF power in the unbalanced excitation should be at least 6 db down from the power in the balanced excitation if a rhombic antenna is used, assuming that the maximum directivity gain of the line together with the antenna for unbalanced excitation is the same as that of the antenna for balanced excitation, and that the power absorbed in the ground is negligible. Higher directivity gain of the line would tend to lower the tolerable unbalance, and strong absorption would permit raising it. Though 6-db minimum required suppression seems to be a very modest goal, it is not sure whether this requirement is met in existing installations. On the other hand, it would be unreasonable to require the radiation of the line resulting from the unbalanced excitation to be lower than that from the balanced excitation. Presently-available in-

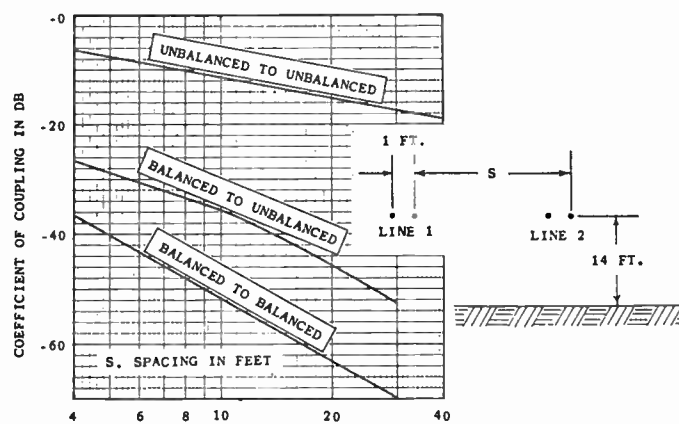


Fig. 9—Coupling between parallel quarter-wave sections of standard 600-ohm line.

formation is not sufficient to permit definite conclusions in this respect. It is certain, however, that radiation from open-wire lines due to unintentional unbalanced excitation will become a critical factor when, at some time in the future, effective side-lobe suppression will be required of transmitting antennas. As an indication of how critical it is, it is mentioned that the radiation of conventional lines due to the balanced component of the excitation at 50 mc is only about 20 db down from the radiation in the main beam of an antenna with 25-db gain.

In view of these anticipated difficulties in preventing open-wire lines from radiating, it appears to be simpler and more effective to replace them with shielded lines, which, for the purpose of this discussion, include coaxial cable as well as balanced shielded lines. Two reasons have prevented the adoption of this solution up to now. One was that reliable wide-band transformers for matching the antenna to shielded lines were not available. The other reason was the relatively high cost of shielded lines.

The engineering approach to the economy of feed lines is to compare the annual interest and amortization plus maintenance of different types of lines to the annual ac-power cost, based on a given antenna input power. Into this comparison enter the period of amortization, the interest rate, the absolute value of the antenna power, the efficiency of the transmitter, and the line length. In a recent survey by Developmental Engineering Corporation under contract with these laboratories,⁵ it has been shown that, in the case of high antenna power, the shielded balanced line is more economical in the long run than the open-wire line. This survey dispels a prejudice of many radio engineers against shielded lines for feeding transmitting antennas. Although at lower antenna power the shielded line is usually still less economical than the open-wire line, it is believed that the difference is outweighed in many cases by the differences in reliability under severe environmental conditions and in other respects which

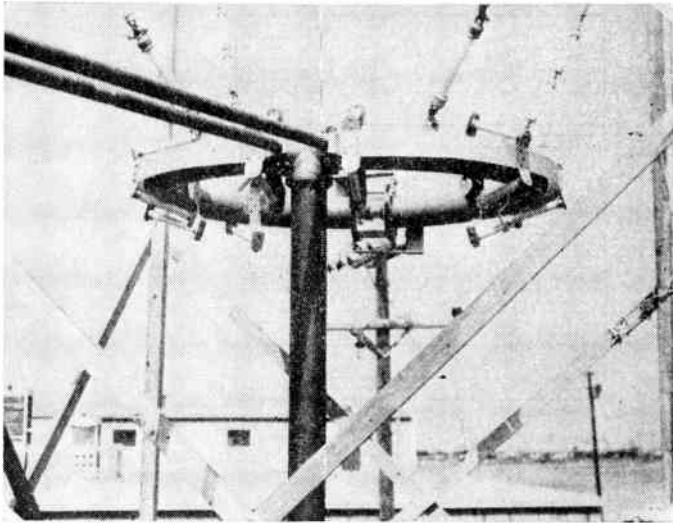


Fig. 10—Experimental broadband balance-unbalance transformer (DECO).

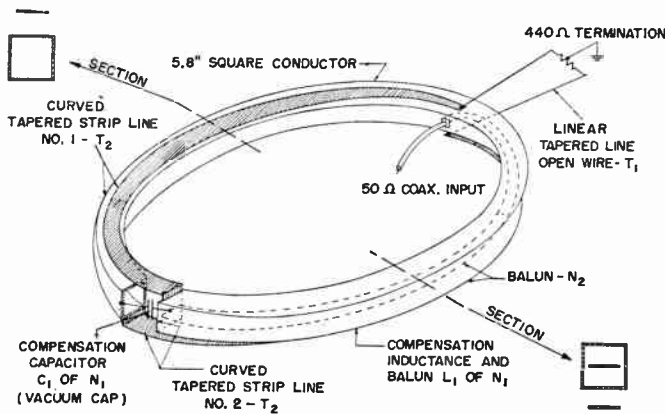


Fig. 11—Pictorial view of wide-band matching transformer.

favor shielded lines apart from the interference suppression aspect.

The decisive factor is, of course, the technical feasibility of broad-band matching of shielded lines to the antennas. It can now safely be said that this problem has been solved. Figs. 10 and 11 show a broad-band transformer developed by Developmental Engineering Corporation under contract with these laboratories.⁶ It is a modification of a transformer widely used in

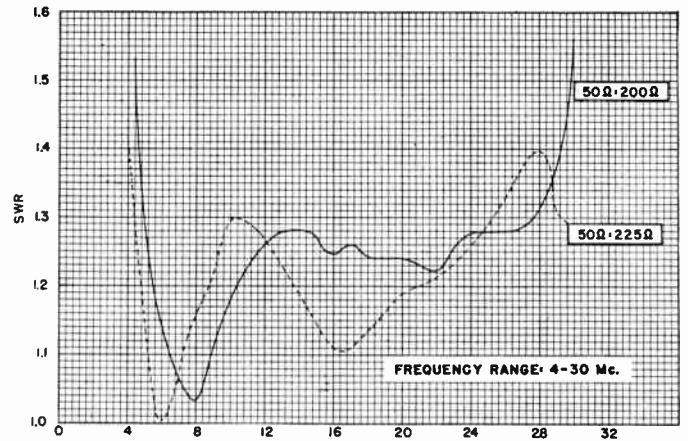


Fig. 12—Standing-wave characteristics of the DECO balun.

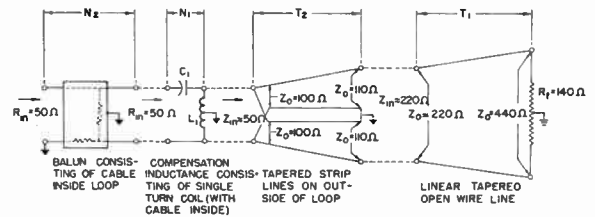


Fig. 13—Functional analysis of wide-band transformer.

Germany⁶ and designed to match 50 ohms unbalanced to 225 ohms balanced over the frequency range from 4 to 30 mc without any readjustment. It can handle a power of 500-kw cw. Fig. 12 shows that the SWR is less than 1.4 to 1 over the entire range. Transformation to higher impedances can be obtained with an additional section of exponential line relatively short in length, as illustrated in Fig. 13. This example is an extreme case in the sense that it combines an extremely wide frequency range of 1:7.5 and a very high power-handling capability. It has been cited here in order to show that such stringent requirements can be met without difficulty. Of course, even less difficulty is encountered where we have the requirements of smaller frequency ranges and lower-power handling capabilities.

⁶ W. Berndt, "Transportation of energy to the antennas of shortwave overseas stations," *Telefunken Zeitung*, vol. 27, nos. 104, 105; July, 1954.



Optimum Noise Performance of Linear Amplifiers*

H. A. HAUS†, ASSOCIATE MEMBER, IRE, AND R. B. ADLER†, SENIOR MEMBER, IRE

Summary—A single quantitative measure of amplifier spot noise performance is established. It removes difficulties heretofore associated with the effect of feedback upon spot noise performance. This measure, $(M_e)_{opt}$, is a function of the amplifier noise and circuit parameters alone. It determines the lowest spot noise figure achievable at high gain with a given amplifier, which is used either alone or in a passive interconnection with other amplifiers of the same $(M_e)_{opt}$. Moreover, passive interconnection of amplifiers with different $(M_e)_{opt}$ cannot lead to a spot noise figure at high gain better than that obtainable by using only amplifiers of the smallest $(M_e)_{opt}$. $(M_e)_{opt}$ is, therefore, a valid measure of the absolute quality of amplifier noise performance.

In many important cases the best noise performance attainable with a particular type of amplifier is actually achieved by a simple cascade in which the input of each stage is properly mismatched. The mismatch conditions for each stage do not in general coincide with those normally used to “minimize” its noise figure.

In the case of a two-terminal-pair negative resistance amplifier, a limiting form of which is the maser, optimization may always be obtained using an ideal circulator.

I. INTRODUCTION

IT IS common practice to describe the single-frequency noise performance of an amplifier in terms of its “spot noise figure,” and it is well known that this figure is a function of the impedance of the source connected to the amplifier input. Thus, in giving an adequate conventional description of amplifier noise performance, the source impedance, as well as the noise figure, must be specified.

Usually, when regarded as a function of source impedance alone, the noise figure has a minimum value for some particular choice of this impedance. If with this source impedance the gain of a given amplifier remains sufficiently large, its noise figure will prescribe the noise figure of any amplifier cascade in which it is used as the first stage. In this way, it is possible to build an amplifier cascade with any desired high gain, and with a noise figure set by the minimum (with respect to source impedance) of the noise figure of the original amplifier.

If a cascade is to be composed of several individual amplifiers, each of which alone has a “high enough” gain when driven from the source impedance that yields its minimum noise figure, the previous argument shows that the amplifier with the lowest minimum noise figure should be used as the first stage. Any other choice would result in a higher over-all noise figure for the cascade.

* Original manuscript received by the IRE, June 17, 1957. This work was supported in part by the U. S. Army (Signal Corps), the U. S. Air Force (Office of Scientific Res., Air Res. and Dev. Command), and the U. S. Navy (Office of Naval Res.).

† Dept. of Elec. Eng. and Res. Lab. of Electronics, Mass. Inst. Tech., Cambridge, Mass.

The foregoing discussion seems to suggest that the minimum value (with respect to source impedance) of the noise figure of an amplifier may be used as an adequate criterion of its noise performance, and as a basis for comparison with other amplifiers. The validity of the argument, however, is based upon the two previously mentioned restrictions:

- 1) each stage has “high enough” gain when driven from the “optimum” source that yields the minimum noise figure; and
- 2) only the source impedance of each stage is varied in controlling the noise performance.

Unfortunately, stage variables other than source impedance, and stage interconnections other than the simple cascade, may be important in amplifier applications. The question of the quality of noise performance then becomes much more complicated. For example, when degenerative feedback is applied to an amplifier, its noise figure can be reduced to as close to unity as desired (*e.g.*, by-passing the entire amplifier with short circuits yields unit noise figure). But its gain is also reduced in the process. Indeed, if identical stages with the feedback are cascaded to recover the original single-stage gain before feedback, the resulting noise figure of the cascade cannot be less than that of the original amplifier [1]. Moreover, with degenerative feedback the gain may easily be so greatly reduced that, as a first stage in a cascade, this amplifier alone no longer determines the over-all noise figure of the cascade. The criterion considered above as a measure of amplifier noise performance breaks down. It appears that the characterization of amplifier quality must include, in addition to the specification of noise figure and source impedance, at least the specification of the gain.

The purpose of this paper is to develop a reasonable single quantitative measure of amplifier noise performance, which must involve both noise figure and gain. Our suggested criterion for characterizing amplifier quality is based on the plausible premise that, basically, amplifiers are supposed to provide “gain building blocks” without adding excessively to system noise. On this basis the following criterion is adopted.

Suppose that n different types of amplifiers are compared. An unlimited number of amplifiers of each type is presumed to be available. A general lossless (possibly nonreciprocal) interconnection of an arbitrary number of amplifiers of each type is then envisioned, with terminals so arranged that in each case an over-all two-terminal-pair network is achieved. For each amplifier type, both the lossless interconnecting network and

the number of amplifiers are varied in all possible ways to produce two conditions simultaneously:

- 1) a very high available gain (approaching infinity) for the over-all two-terminal-pair system when driven from a source having a positive real internal impedance; and
- 2) an absolute minimum noise figure F_{\min} for the resulting high-gain system.

The value of $(F_{\min} - 1)$ for the resulting high-gain two-terminal-pair network is taken specifically as the "measure of quality" of the amplifier type in each case. The "best" amplifier type will be the one yielding the smallest value of $(F_{\min} - 1)$ at very high gain.

The justification for this quality criterion hinges upon four theorems, the demonstration of which forms the body of this paper.

- 1) F_{\min} at arbitrarily high gain exists under the above required conditions for any amplifier type, and can be calculated in a direct manner from the amplifier noise and circuit parameters.
- 2) Passive dissipative interconnection of several given amplifiers never yields a lower F_{\min} (at arbitrarily high gain) than that achievable with lossless interconnections.
- 3) The F_{\min} achievable at large gain with an interconnection of amplifiers of different types can never be lower than that achievable when only amplifiers of best quality are used.
- 4) Circuit connections exist for achieving F_{\min} at high gain with any amplifier type. They depend to some extent upon the class of amplifier in question, and are not necessarily unique.

Before we can prove the theorems, however, certain rather new concepts must be introduced [2]–[4]:

- 1) Exchangeable power, P_e ;
- 2) Exchangeable power gain, G_e ;
- 3) Modification of the noise figure definition to conform with concepts 1 and 2; and
- 4) Noise measure, M (or M_e).

We shall first consider some elementary cascading ideas leading to the notion of noise measure, and next the question of exchangeable power and related quantities. A matrix formulation of the foregoing new concepts will then be carried out, which will lead to the four major theorems.

II. CASCADING OF AMPLIFIERS AND NOISE MEASURE

The simplest interconnection of amplifiers for achieving high gain is the cascade connection. A brief review of the conventional theory of noise performance in a cascade connection, when the component amplifiers do not necessarily have large gain, actually furnishes a major clue to introducing the noise measure concept and to solving the entire problem of characterizing the quality of amplifier noise performance.

Suppose that two amplifiers with noise figures F_1 and F_2 and available gains $G_1(>1)$ and $G_2(>1)$ are to be cascaded. The question is: Which amplifier should be used as the input stage in order to achieve the smallest over-all noise figure of the cascade? For simplicity, suppose that the noise figures F_1 and F_2 and the available gains G_1 and G_2 are independent of the order of cascading. When amplifier 1 is at the input, the over-all noise figure is

$$F_{12} = F_1 + \frac{F_2 - 1}{G_1}. \quad (1)$$

When amplifier 2 is at the input, we find

$$F_{21} = F_2 + \frac{F_1 - 1}{G_2}. \quad (2)$$

The condition $F_{12} < F_{21}$ dictates that amplifier 1 should be first in the cascade. For this condition,

$$F_1 + \frac{F_2 - 1}{G_1} < F_2 + \frac{F_1 - 1}{G_2},$$

or, if we subtract 1 from both sides and rearrange, we have

$$\frac{F_1 - 1}{1 - \frac{1}{G_1}} < \frac{F_2 - 1}{1 - \frac{1}{G_2}}.$$

Thus, the cascade connection of the two amplifiers will have the smaller noise figure when the amplifier with the smaller value, not of F , but of the quantity

$$M = \frac{F - 1}{1 - \frac{1}{G}} \quad (3)$$

is placed first in the cascade.

It is reasonable to expect from the above result, and from the considerations set forth in the Introduction, that M will play an important role in determining the quality of amplifier noise performance. Indeed, it is essentially M that we have called the "noise measure."

The cascading formula expressed in terms of M , rather than F , has the form

$$M_{12} \equiv \frac{F_{12} - 1}{1 - \frac{1}{G}} = M_1 + (M_2 - M_1) \frac{G_2 - 1}{G_2 - 1}, \quad (4)$$

where $G = G_1 G_2$ is the gain of the cascaded pair. The noise measure, from (4), has the significant property that two amplifiers of equal M (but possibly different gains) connected in cascade result in an over-all amplifier with the same M . Therefore, if an amplifier has a noise measure M , an available gain $G > 1$, and a positive output impedance, a cascade of many identical amplifiers with suitable matching transformers leads to an over-all amplifier of arbitrary large gain and the

same M . The excess noise figure of the over-all amplifier is $F - 1 = M$. In these cases the physical significance of M is: the excess noise figure at large gain. It is through an extension of this property of M to more general cases that we shall be able to deal analytically with the noise performance criterion introduced in Section I.

It will also be necessary to know that: the noise measure M of a passive two-terminal-pair network in thermal equilibrium at temperature T is just -1 . This is proved by the following argument. On thermodynamic grounds, the total noise power available at the output terminals must be $kT\Delta f$, if a passive impedance at equilibrium temperature T is at the input. But the available noise power at the output is also $FGkT\Delta f$, from the definition of F . Therefore, $FG = 1$ and $M = -1$.

III. EXTENDED DEFINITIONS OF GAIN, NOISE FIGURE, AND NOISE MEASURE

Any general theory of linear active networks must include situations involving negative resistance. However, the conventional notion of the "available power" of a source leads to singular values or complete indeterminacy in the theory of cases that are perfectly meaningful in the final outcome.

We therefore propose to use a new concept, the *exchangeable power* of a source, to replace the conventional term "available power." An obvious modification of "available power gain" to *exchangeable power gain*, and a corresponding revision of the noise figure definition (on the basis of exchangeable gain and exchangeable power) follow immediately from the new concept. The underlying needs, and the reasons for our choice of the specific definition of exchangeable power given below are discussed elsewhere at length [4]; here we present only a summary to make the present paper self-contained.

A. Exchangeable Power

Definition: The *exchangeable power* $P_e (\leq 0)$ of a two-terminal linear network is the *stationary* value of its power output, regarded as a function of its terminal current (or voltage).

In terms of the Thévenin representation of this network, comprising an rms open-circuit terminal voltage E_s and an internal (source-free) impedance $Z_s = R_s + jX_s$, our definition can be shown to yield

$$P_e = \frac{|E_s|^2}{4R_s}; \quad R_s \neq 0. \quad (5)$$

When $R_s > 0$, (5) gives for $P_e (> 0)$, the conventional available power of the network, which is also the greatest power obtainable from it by arbitrary variation of the load impedance. The optimum load for this purpose is the (passive) impedance Z_s^* . When $R_s < 0$, however, $P_e (< 0)$ represents in magnitude the greatest power that can be pushed into the "source" network by arbitrary variation of the (possibly nonpassive) "load" imped-

ance. The optimum load for this purpose is the (nonpassive) impedance Z_s^* , which actually pushes power into the original network (hence the negative value of P_e).

We note, incidentally, that the conventional available power of a network with any value of $R_s < 0$ (and $E_s \neq 0$) would always be infinite [achieved under (passive) load conditions $-Z_s$]. This is an awkward singular result; and it is at variance with both our present definition of P_e and the corresponding equation (5). One obvious advantage of the exchangeable power concept is that it retains an invariant analytical expression in all cases for which it is defined.

B. Exchangeable Power Gain

The *exchangeable power gain* G_e of a two-terminal-pair network is now defined from the exchangeable power P_{es} of the input source and the exchangeable power P_{eo} at the network output. Specifically,

$$G_e = \frac{P_{eo}}{P_{es}}. \quad (6)$$

If $Z_s = R_s + jX_s$ is the source impedance, and $Z_o = R_o + jX_o$ is the output impedance of the network with the source impedance Z_s connected at the input, we find that

$$G_e > 0 \quad \text{if} \quad R_s/R_o > 0 \quad (7a)$$

$$G_e < 0 \quad \text{if} \quad R_s/R_o < 0. \quad (7b)$$

Observe that when $R_s > 0$ and $R_o > 0$, G_e becomes the conventional available gain of the two-terminal-pair network.

C. Extended Noise Figure and Noise Measure

The foregoing ideas lead to an extended definition F_e of the noise figure of a two-terminal-pair network

$$F_e = 1 + \frac{N_{ei}}{G_e kT\Delta f}, \quad (8)$$

where N_{ei} is the exchangeable noise power at the network output when the source has a given (noiseless) impedance Z_s . Thus N_{ei} contains only the effect of *internal* network noise sources. The use of $kT\Delta f$ in (8) represents merely an arbitrary (but convenient) normalization factor for cases in which the source impedance has a *negative* real part. Otherwise it represents physically the available noise power from a passive impedance at thermal equilibrium temperature T .

From (5)–(8), it is clear that

$$F_e - 1 > 0 \quad \text{if} \quad R_s > 0 \quad (9a)$$

$$F_e - 1 < 0 \quad \text{if} \quad R_s < 0. \quad (9b)$$

If $R_s > 0$ and $R_o > 0$, F_e becomes the standard noise figure F . It is easy to show that cascading formulas (1) and (2) always remain valid when F and G are replaced by F_e and G_e [4].

The generalized form of the noise measure M introduced in (3) becomes

$$M_e = \frac{F_e - 1}{1 - \frac{1}{G_e}} \tag{10}$$

The algebraic sign properties of M_e are summarized in Table I. With reference to Table I it should be pointed out that with $R_S > 0$, conventional available gain greater than 1 occurs in only two ways

- 1) $G_e > 1$, and
- 2) $G_e < 0$.

TABLE I
ALGEBRAIC SIGNS OF EXCHANGEABLE GAIN AND DERIVED QUANTITIES

R_S	R_O	G_e	$F_e - 1$	$ G_e $	M_e
>0	>0	>0	>0	>1	>0
>0	>0	>0	>0	<0	<0
>0	<0	<0	>0	$\gg 1$	>0
<0	>0	<0	<0	$\gg 1$	<0
<0	<0	>0	<0	>1	<0
<0	<0	>0	<0	<1	>0

Case 1 holds whenever the amplifier has an output impedance with positive real part and an available (or exchangeable) gain greater than one. Case 2 corresponds to an amplifier with an output impedance having a negative real part. Such an amplifier has an infinite available gain in the conventional sense. In both cases M_e is found to be greater than zero. Since we are only interested in amplifiers driven from positive source resistance and with a conventional available gain greater than one, only positive values of M_e are of interest.

Suppose therefore that the amplifier has some value of $M_e > 0$. Let us relate the excess noise figure to M_e . In case 1, we find that the excess noise figure is

$$F_e - 1 = F - 1 = \left(1 - \frac{1}{G}\right) M_e$$

Thus, the excess noise figure of the amplifier is less than M_e by a gain-dependent factor $1 - (1/G)$. Cascading of identical amplifiers of this type leads to an amplifier of large gain, with the excess noise figure $F - 1 = M_e$ (see Section II).

In case 2, we obtain, since $G_e < 0$,

$$F_e - 1 = F - 1 = \left(1 + \left|\frac{1}{G_e}\right|\right) M_e$$

Now the excess noise figure is greater than M_e by the factor $(1 + 1/|G_e|)$. The conventional available gain of the amplifier is infinite, and cascading is unnecessary. The above expression is already the excess noise figure at high gain.

The argument that follows is based upon the aforementioned properties of M_e . It will be shown (among

other things) that under a very general class of external passive circuit operations upon the terminals of a given amplifier, the possible positive values of M_e for the resulting system have a lower bound $(M_e)_{opt}$. It will also be shown that this lower bound can always be achieved with suitable auxiliary passive networks, in such a way that the output impedance of the altered amplifier has a positive real part. Thus, by repeated cascade, with suitable interstage coupling, the available gain can be increased arbitrarily and the final excess noise figure at large gain becomes just $(M_e)_{opt}$. We will also show that no other arrangement of this type of amplifier can yield a lower value of noise figure at large gain.

IV. MATRIX FORMULATION OF EXCHANGEABLE POWER AND RELATED QUANTITIES

In order to deal effectively with the envisaged general network interconnections of amplifiers, it is necessary to put into matrix form important amplifier quantities: exchangeable power, exchangeable power gain, and noise measure.

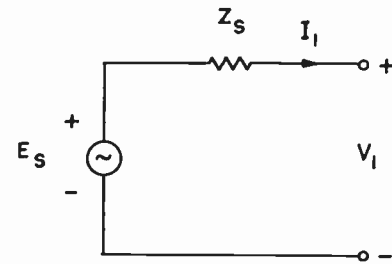


Fig. 1—Thévenin equivalent of two-terminal linear source.

A. Exchangeable Power

A linear two-terminal source of power can be represented by its Thévenin rms open-circuit voltage E_s , in series with its internal impedance Z_s . Let V_1 and I_1 be the terminal voltage and current of the source (see Fig. 1), so that

$$V_1 + Z_s I_1 = E_s \tag{11}$$

To express (11) in matrix form suitable for cascade applications, define column vectors (matrices) v and x

$$v = \begin{bmatrix} V_1 \\ I_1 \end{bmatrix}; \quad x = \begin{bmatrix} 1 \\ Z_s^* \end{bmatrix} \tag{12}$$

and let the “dagger” (†) designate the complex conjugate of the transpose of any matrix. Then, for (11), we have

$$x^\dagger v = E_s \tag{13}$$

Since multiplication of (13) by a constant c does not alter it, we can, purely as a matter of form, always make a new column vector

$$y = \begin{bmatrix} y_1 \\ y_2 \end{bmatrix} = cx = \begin{bmatrix} c \\ cZ_s^* \end{bmatrix}$$

and a new scalar

$$\gamma = cE_s,$$

so that the source equation (13) becomes

$$\mathbf{v}^\dagger \mathbf{v} = \gamma \tag{14a}$$

with

$$y_2/y_1 = Z_S^*, \tag{14b}$$

where Z_S is still the internal impedance of the source. This formal multiplication feature of the source equation is sometimes helpful in interpreting the following analyses.

Now the exchangeable power P_e of the source may be written in matrix form

$$P_e = \frac{|E_s|^2}{2(Z_S + Z_S^*)} = \frac{|E_s|^2}{2(\mathbf{x}^\dagger \mathbf{P} \mathbf{x})} = \frac{|\gamma|^2}{2(\mathbf{y}^\dagger \mathbf{P} \mathbf{y})} \tag{15}$$

where the square "permutation" matrix \mathbf{P} is defined as

$$\mathbf{P} = \begin{bmatrix} 0 & 1 \\ 1 & 0 \end{bmatrix} \tag{16}$$

with properties $\mathbf{P}^\dagger = \mathbf{P}$ and $\mathbf{P}^{-1} = \mathbf{P}$. The usefulness of the last expression in (15) lies in the fact that it can be written by inspection for any two-terminal source with a source equation in the form of (14).

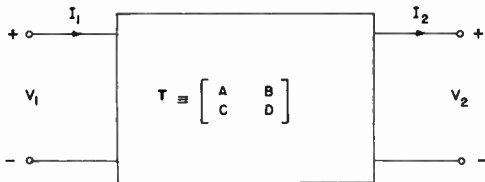


Fig. 2—Two-terminal-pair linear source-free network.

B. Exchangeable Power Gain

Consider a linear source-free two-terminal-pair network, described by its general-circuit constants A, B, C, D (see Fig. 2). If \mathbf{v} is the "input" column vector defined by (12), and we let \mathbf{u} be the "output" column vector,

$$\mathbf{u} = \begin{bmatrix} V_2 \\ I_2 \end{bmatrix}, \tag{17a}$$

and \mathbf{T} is the general circuit matrix,

$$\mathbf{T} = \begin{bmatrix} A & B \\ C & D \end{bmatrix}, \tag{17b}$$

the network equations are expressed in matrix form as

$$\mathbf{v} = \mathbf{T} \mathbf{u}. \tag{18}$$

When the network of Fig. 2 is driven by the source of Fig. 1, the exchangeable output power P_{e0} from terminal pair 2 can be obtained at once from a source equation in the form of (14) written with \mathbf{u} as column variable. Multiplication of (18) by \mathbf{y}^\dagger , with the use of (14), yields

this new relation,

$$(\mathbf{y}^\dagger \mathbf{T}) \mathbf{u} = \gamma. \tag{19}$$

Accordingly, by applying the steps of (14)–(16) to (19), we find that

$$P_{e0} = \frac{|\gamma|^2}{2\mathbf{y}^\dagger \mathbf{T} \mathbf{P} \mathbf{T}^\dagger \mathbf{y}} \tag{20}$$

and with (15) and (6), for the exchangeable gain we have

$$G_e = \frac{\mathbf{y}^\dagger \mathbf{P} \mathbf{y}}{\mathbf{y}^\dagger \mathbf{T} \mathbf{P} \mathbf{T}^\dagger \mathbf{y}}. \tag{21}$$

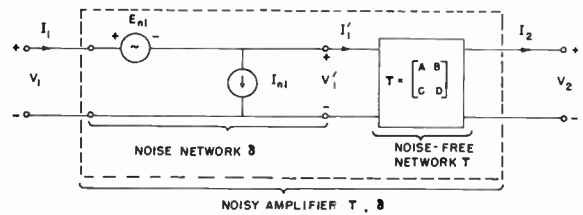


Fig. 3—Two-terminal-pair linear network with internal sources.

C. Extended Noise Figure and Noise Measure

To apply the matrix formulation of exchangeable power to the calculation of the (extended) noise figure of a two-terminal-pair noisy network, we still describe the network by its general-circuit constants, but we also allow for noise voltages or currents at the terminals in the absence of external sources. With reference to Fig. 3, the network equations for the dotted box [5] would be

$$\mathbf{v} = \mathbf{T} \mathbf{u} + \boldsymbol{\delta} \tag{22}$$

with $\boldsymbol{\delta}$ a "noise column vector,"

$$\boldsymbol{\delta} = \begin{bmatrix} E_{n1} \\ I_{n1} \end{bmatrix}. \tag{23}$$

Actually, for noise processes, the complex amplitudes E_{n1} and I_{n1} are only of formal significance, the important physical concepts being the self- and cross-power density spectra, which are summarized in the convenient matrix form

$$\overline{\boldsymbol{\delta} \boldsymbol{\delta}^\dagger} = \begin{bmatrix} \overline{E_{n1} E_{n1}^*} & \overline{E_{n1} I_{n1}^*} \\ \overline{I_{n1} E_{n1}^*} & \overline{I_{n1} I_{n1}^*} \end{bmatrix} \tag{24}$$

which is Hermitian and positive definite (or semidefinite).

Now (22) can be rewritten as two relations:

$$\mathbf{v}' = \mathbf{T} \mathbf{u} \tag{25a}$$

$$\mathbf{v} = \mathbf{v}' + \boldsymbol{\delta}. \tag{25b}$$

If we visualize

$$\mathbf{v}' = \begin{bmatrix} V_1' \\ I_1' \end{bmatrix}$$

as referring simultaneously to the input terminals of a noise-free network T and the output terminals of a pure noise network δ , the cascade division of the system is represented in Fig. 3. The noiseless part T does not affect the noise figure of the system. Thus, for noise figure calculations, we need only consider the noise network δ driven by a source of internal impedance Z_S [5].

The source equation appropriate to the right-hand terminals in Fig. 4 can be obtained from (25b) and (14) with $E_S=0$.

$$v^{\dagger}v' = -y^{\dagger}\delta. \tag{26}$$

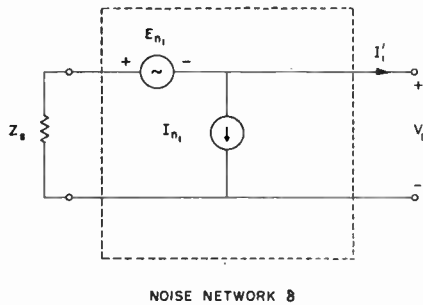


Fig. 4—Essentials of Fig. 3 for determination of noise figure.

Therefore, the output exchangeable power, N_{ei} , produced by the internal noise only, is given by

$$N_{ei} = \frac{y^{\dagger}\delta\delta^{\dagger}y}{2y^{\dagger}Py} \tag{27}$$

and, since $G_e=1$ for this network, we have

$$F_e - 1 = \frac{N_{ei}}{kT\Delta f} = \frac{y^{\dagger}\delta\delta^{\dagger}y}{y^{\dagger}Py(2kT\Delta f)}. \tag{28}$$

Finally, in view of (10), (21), and (28) the noise measure becomes

$$M_e = \frac{y^{\dagger}\delta\delta^{\dagger}y}{y^{\dagger}(P - TPT^{\dagger})y} \left(\frac{1}{2kT\Delta f} \right). \tag{29}$$

V. EXTREMAL PROPERTY OF THE NOISE MEASURE

The properties of the noise measure M_e are the bases upon which we build the quality criterion of amplifier noise performance given in the Introduction. Recall that only positive values of M_e are of interest (see Section III-C). We shall first show that M_e , for a two-terminal-pair network, has a minimum positive value with regard to *all* lossless (possibly nonreciprocal) transformations that can be performed on the original network so as to obtain a new two-terminal-pair network from it.

The most general lossless transformation of the kind described above is shown in Fig. 5. It consists of an "imbedding" of the original network into a four-terminal-pair network. Such a network can be represented conveniently in a modified general-circuit matrix notation, by using two matrix equations (see Appendix 1):

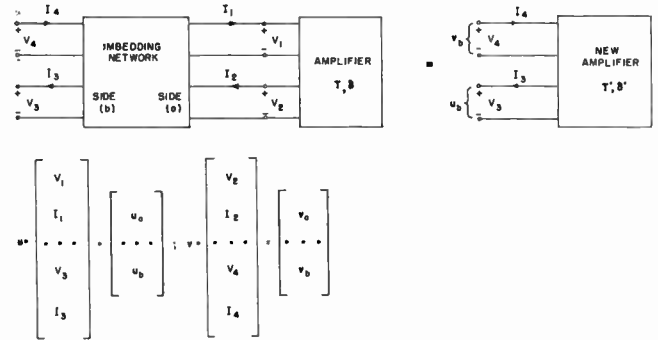


Fig. 5—Imbedding of two-terminal-pair amplifier for production of a new two-terminal-pair amplifier.

$$v_a = T_{aa}u_a + T_{ab}u_b \tag{30}$$

$$v_b = T_{ba}u_a + T_{bb}u_b. \tag{31}$$

If the imbedding network is lossless, it cannot contain internal noise, and therefore (30) and (31) contain no terms representing internal sources.

The original two-terminal-pair amplifier imposes a relation upon the column vectors v_a and u_a . If we observe, from Fig. 5, that for this amplifier network the meanings of T and δ will only be consistent with our previous definition of them (see Figs. 2-4), and if we now regard v_a as an *output* and u_a as an *input*, we have

$$u_a = Tv_a + \delta. \tag{32}$$

If (32) is introduced into (30) and (31), we can find a relation between v_b and u_b . This is the relation characterizing a new two-terminal-pair amplifier with output u_b , input v_b , general-circuit matrix T' , and noise vector δ' (see Fig. 5).

$$v_b = T'u_b + \delta' \tag{33}$$

with

$$T' = T_{ba}(I - TT_{aa})^{-1}TT_{ab} + T_{bb} \tag{34}$$

and

$$\delta' = T_{ba}(I - TT_{aa})^{-1}\delta, \tag{35}$$

where I is the identity matrix.

To determine the effect of imbedding upon the noise measure (29), we have to determine its effect upon $\delta\delta^{\dagger}$ and $P - TPT^{\dagger}$. First, from (35), it follows that

$$\delta'\delta'^{\dagger} = Q\delta\delta^{\dagger}Q^{\dagger}, \tag{36}$$

where

$$Q = T_{ba}(I - TT_{aa})^{-1}. \tag{37}$$

Next, from (34) and (37), we have

$$P - T'PT'^{\dagger} = P - (QT_{ab} + T_{bb})P(T_{bb}^{\dagger} + T_{ab}^{\dagger}T^{\dagger}Q^{\dagger}) = Q[Q^{-1}PQ^{-1\dagger} - (TT_{ab} + Q^{-1}T_{bb})P(T_{bb}^{\dagger}Q^{-1\dagger} + T_{ab}^{\dagger}T^{\dagger})]Q^{\dagger}. \tag{38}$$

Now, since the imbedding network is lossless under our present assumptions, the factor within square brackets

(38) may be transformed by the conditions of losslessness [(64) in Appendix I]. Using them to eliminate T_{bb} and T_{ab} from the brackets in (38), we find that

$$P - T'PT'^{\dagger} = Q[P - TPT^{\dagger}]Q^{\dagger}. \quad (39)$$

That is, under a lossless transformation the matrices $\overline{\delta\delta}^{\dagger}$ and $P - TPT^{\dagger}$ transform in exactly the same manner!

Consider the noise measure, as given by (29), of an amplifier network (T, δ) fed by a source of internal impedance Z_S . If the amplifier is imbedded in a lossless network in the manner of Fig. 5, the resulting new amplifier (T', δ') will have the new noise measure

$$M_e' = \frac{y^{\dagger}Q\overline{\delta\delta}^{\dagger}Q^{\dagger}y}{y^{\dagger}Q[P - TPT^{\dagger}]Q^{\dagger}y} \left(\frac{1}{2kT\Delta f} \right), \quad (40)$$

in view of (36) and (39). When the lossless network is varied through all possible forms, Q might be expected to vary accordingly. The surprising fact is that $Q = T_{ba}(I - TT_{aa})^{-1}$ is unrestricted by the conditions of losslessness [(64) in Appendix I]. Indeed, T_{ba} can be chosen quite arbitrarily for a lossless network, and (64) will only serve to determine T_{aa} , T_{bb} , and T_{ab} .

As Q is varied, M_e' may assume various values, depending upon the forms of $\overline{\delta\delta}^{\dagger}$ and $P - TPT^{\dagger}$. As mentioned previously, the noise spectral matrix $\overline{\delta\delta}^{\dagger}$ is positive (semi) definite. But, as far as the matrix $P - TPT^{\dagger}$ is concerned, three cases have to be distinguished (see Appendix I):

- 1) $P - TPT^{\dagger}$ is positive (semi) definite; T is the general-circuit matrix of a negative-resistance network; $M_e' \geq 0$.
- 2) $P - TPT^{\dagger}$ is negative (semi) definite; T is the general-circuit matrix of a passive network; $M_e' \leq 0$.
- 3) $P - TPT^{\dagger}$ is indefinite; T is the general-circuit matrix of a network capable of absorption, as well as delivery of power; $M_e' \geq 0$.

When Q in (40) is varied through all possible values, it is shown in Appendix II that M_e' reaches two extrema which are the two eigenvalues of the "characteristic noise matrix"

$$N = \frac{1}{2}[P - TPT^{\dagger}]^{-1}\overline{\delta\delta}^{\dagger} \quad (41)$$

divided by $kT\Delta f$.

With the aid of (36) and (39) it is easy to show that N undergoes a similarity transformation,

$$N' = (Q^{\dagger})^{-1}NQ^{\dagger},$$

under a lossless imbedding of the network. The eigenvalues of N remain unchanged. These extrema limit the range of values of M_e' , as shown in Fig. 6, for the three cases.

Now, the situations of most practical importance concern the noise performance of amplifiers driven from sources that have an internal impedance with positive

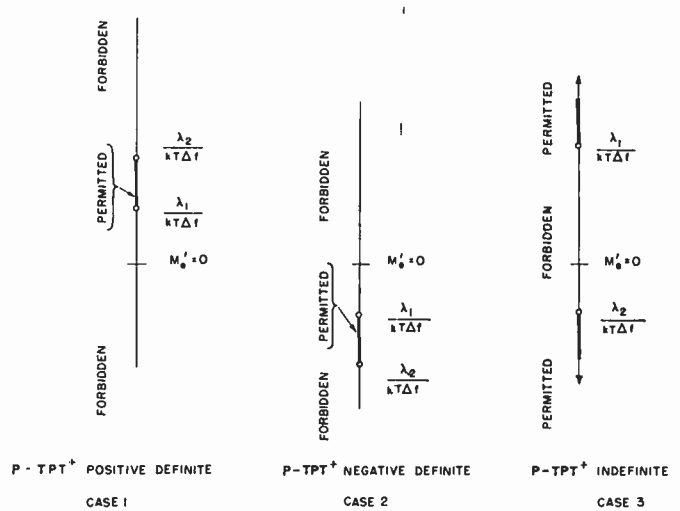


Fig. 6—Schematic of permitted values of M_e' for two-terminal-pair network.

real part. According to Table I, the noise measure is positive when $R_S > 0$ in all cases except $R_0 > 0, 0 < G_e < 1$. This case does not correspond to an amplifier. Hence we shall be interested in achieving only positive values of M_e' , which occur in cases 1 and 3 of Fig. 6. These cases both have an available gain, G , in the conventional sense, greater than unity ($G = G_e$, if $G_e > 1$; $G = \infty$, if $G_e < 0$).

Observe from (40) that the numerator is never negative. Therefore changes in sign of M_e' occur with those of the denominator. In case 3, which includes most conventional amplifiers, M_e' changes sign only at a zero of the denominator.¹ Thus, the values of M_e' cannot lie between $\lambda_1/kT\Delta f$ and $\lambda_2/kT\Delta f$.

The two cases of interest, cases 1 and 3 of Fig. 6, have a least positive eigenvalue of N which we call $\lambda_1 > 0$. We have therefore proved the following theorem.

Theorem 1

Consider the set of lossless transformations that carry a two-terminal-pair amplifier into a new two-terminal-pair amplifier with a conventional available gain, G , greater than one. When driven from a source that has an internal impedance with positive real part, the noise measure of the transformed amplifier cannot be less than $\lambda_1/kT\Delta f$, where λ_1 is the smallest positive eigenvalue of the characteristic noise matrix of the original amplifier.

The fact that $M_e' \geq \lambda_1/kT\Delta f$ also puts a lower limit upon the excess noise figure. Suppose that the amplifier is imbedded in a lossless network, and then connected to a source with an internal impedance having a positive real part. Let the resulting exchangeable power gain be G_e . Then, the excess noise figure of the resulting amplifier has to fulfill the inequality

$$F_e - 1 \geq \frac{\lambda_1}{kT\Delta f} \left(1 - \frac{1}{G_e} \right). \quad (42)$$

¹ The elements of T are assumed to be finite. Any difficulties with this assumption [3] can always be avoided by a formulation of the networks in another matrix form.

Thus, an amplifier has a definite lower limit imposed upon its excess noise figure which depends upon the exchangeable power gain achieved in the particular connection.

If $G_e > 0$, *i.e.*, the output impedance of the amplifier has a positive real part, the excess noise figure can be less than $\lambda_1/kT\Delta f$ only to the extent of the gain-dependent factor $(1 - 1/G_e)$.

If $G_e < 0$, *i.e.*, the output impedance has a negative real part, the lower limit to the excess noise figure is higher than $\lambda_1/kT\Delta f$ by $(1 + |1/G_e|)$.

Thus, if there exist two amplifiers with the same eigenvalues of their characteristic noise matrices, (41), one with a positive output impedance, and the other with a negative output impedance, the minimum excess noise figure of the latter cannot be less than that of the former.

Eq. (42) has established a lower bound for the excess noise figure achievable with lossless imbeddings of an amplifier. Several questions still remain unanswered.

- 1) Can this lower bound actually be realized with every amplifier?
- 2) Can this lower bound be achieved with a positive output impedance?
- 3) What is the best noise figure at large gain achievable by using amplifiers of different types?
- 4) How is the minimum noise figure at large gain affected by the use of lossy imbedding networks?

VI. GENERALIZATION OF THE NOISE MEASURE FOR 2n-TERMINAL-PAIR NETWORKS

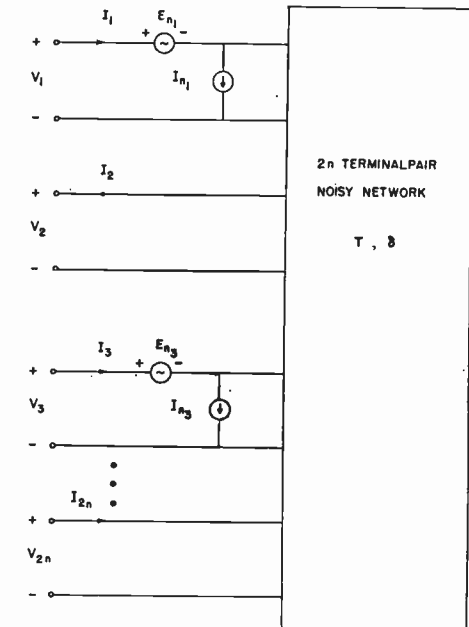
In order to answer the ambitious questions posed at the end of the preceding section we have to make use of a formal generalization of the noise-measure concept to 2n-terminal-pair networks. This generalization is suggested by the matrix notation developed in (29). Characterize the 2n-terminal-pair network of Fig. 7 by the general-circuit equation

$$v = Tu + \delta, \tag{43}$$

where v , u , and δ are all column vectors of 2nth order. The general-circuit matrix T is a square matrix of 2nth order. The column vector u characterizes the voltages and currents at one set of n -terminal pairs regarded as "output," while the column vector v characterizes the voltages and currents at the other set of n -terminal pairs regarded as "input." The choice of the terminal pairs is in general arbitrary, but is often dictated by expediency. Similarly, the order in which the voltages and currents are assigned to the terminal pairs is arbitrary.

The permutation matrix P_n of the 2n-terminal-pair network follows from the requirement that the term $-v^\dagger P_n v + u^\dagger P_n u$ represents the power generated in the network (see Appendix I). For the particular case of the network illustrated in Fig. 15, the permutation matrix is given in (59) of Appendix I.

We now define the generalized noise measure as a formal extension of (29) in terms of an arbitrary column



$$u = \begin{bmatrix} v_2 \\ I_2 \\ v_4 \\ I_4 \\ \vdots \\ v_{2n} \\ I_{2n} \end{bmatrix}; \quad v = \begin{bmatrix} v_1 \\ I_1 \\ v_3 \\ I_3 \\ \vdots \\ v_{2n-1} \\ I_{2n-1} \end{bmatrix}; \quad \delta = \begin{bmatrix} E_{n1} \\ I_{n1} \\ E_{n3} \\ I_{n3} \\ \vdots \\ (E_n)_{2n-1} \\ (I_n)_{2n-1} \end{bmatrix}$$

Fig. 7—2n-terminal-pair noisy network.

vector y of 2nth order:

$$M_e \equiv \frac{y^\dagger \delta \delta^\dagger y}{y^\dagger (P_n - T P_n T^\dagger) y} \left(\frac{1}{2kT\Delta f} \right). \tag{44}$$

We may study again the change of the value of M_e when the 2n-terminal-pair network is subjected to a lossless transformation. By virtue of the matrix formalism used in Section V, the findings of that section can be generalized immediately to a 2n-terminal-pair network (see Fig. 8). If the general-circuit matrix T of the 4n-terminal-pair imbedding network is split into an array of four matrices of 2nth order, the transformation between the various voltages and currents at input and output of the 4n-terminal-pair network can be written

$$\begin{aligned} v_a &= T_{aa}u_a + T_{ab}u_b \\ v_b &= T_{ba}u_a + T_{bb}u_b. \end{aligned} \tag{45}$$

Fig. 8 serves as an illustration of the way in which the excitation vectors v and u can be split into subvectors v_a , v_b , u_a , and u_b . Applying transformation (45) to the noise measure (44), and using the requirement of losslessness for the imbedding network, (64), we find that the value of M_e after the transformation is

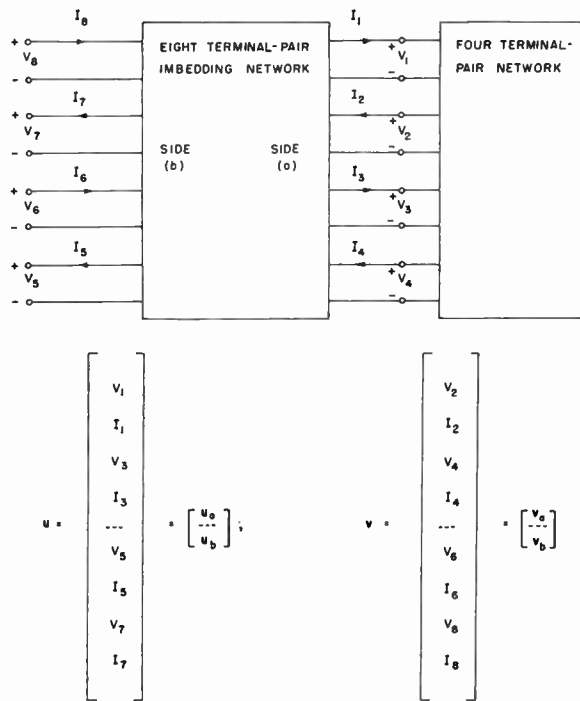


Fig. 8—Imbedding of a four-terminal-pair network. Column vectors u and v represent "output" and "inputs" with reference to the eight-terminal-pair imbedding network.

$$M_s' = \frac{y^t Q \overline{\delta \delta^t} Q^t y}{y^t Q (P_n - T P_n T^+) Q^t y} \left(\frac{1}{2kT\Delta f} \right). \quad (46)$$

[Compare with (36)–(40) for the two-terminal-pair network.]

It is shown in Appendix II that a quantity of the form of (46) has $2n$ values which are stationary with regard to arbitrary changes of the matrix Q . These values are again proportional, by the factor $kT\Delta f$, to the eigenvalues of the characteristic noise matrix,

$$N = \frac{1}{2} (P_n - T P_n T^+)^{-1} \overline{\delta \delta^t}, \quad (47)$$

which are invariant to a lossless transformation. Again we must distinguish three cases, according to the character of $P_n - T P_n T^+$. The distribution of eigenvalues for each case is shown in Fig. 9. Once more, in case 3 the forbidden range of M_s' between positive and negative extrema arises because (46) reverses sign only when the denominator passes through zero.

VII. ARBITRARY LOSSLESS INTERCONNECTION OF AMPLIFIERS

The foregoing results can now be applied to the proof of the following theorem.

Theorem 2

Consider a general lossless interconnection of an arbitrary number of different and independently noisy two-terminal-pair amplifiers that results in a two-terminal-pair network with an available gain, G , greater than one. When the amplifier is driven from a source that has an internal impedance with positive real part, the noise meas-

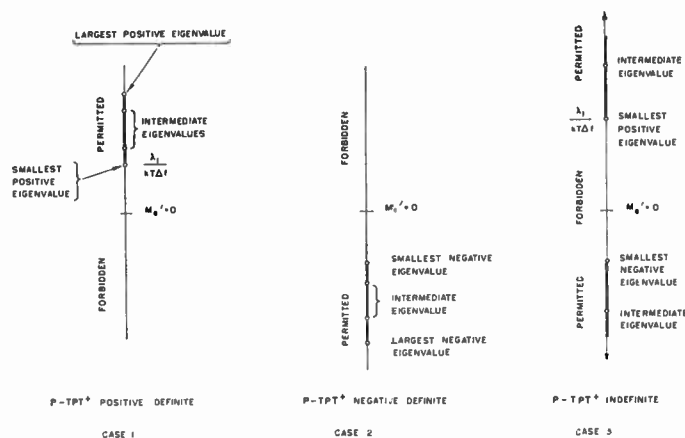


Fig. 9—Schematic of permitted values of M_s' for four-terminal-pair networks.

ure of the resulting two-terminal-pair network cannot be less than the optimum noise measure of the best amplifier; i.e., the amplifier with the least positive eigenvalue of its characteristic noise matrix.

Let us turn to the n two-terminal-pair networks of Fig. 10. They have the general circuit matrices $T_{(i)}$ and the noise column vectors $\delta_{(i)}$, with i going from 1 to n . The networks can be arranged in an array so as to form a $2n$ -terminal-pair network. The resulting $2n$ -terminal-pair network has a T matrix which consists of a diagonal array of the individual $T_{(i)}$

$$T = \text{diag} (T_{(1)}, T_{(2)}, \dots, T_{(n)}). \quad (48)$$

If the noises in the different amplifiers are uncorrelated, the correlation matrix $\overline{\delta \delta^t}$ of the over-all amplifier splits into a diagonal array of correlation matrices of second order of the n amplifiers

$$\overline{\delta \delta^t} = \text{diag} (\overline{\delta \delta^t}_{(1)}, \overline{\delta \delta^t}_{(2)}, \dots, \overline{\delta \delta^t}_{(n)}). \quad (49)$$

Similarly, the matrix $P_n - T P_n T^+$ of the over-all network also splits into a diagonal array of second-order submatrices.

$$P_n - T P_n T^+ = \text{diag} [(P - T_{(1)} P T_{(1)}^+), \dots, (P - T_{(n)} P T_{(n)}^+)]. \quad (50)$$

Thus, the characteristic noise matrix N of the $2n$ -terminal-pair network, on the right-hand side of Fig. 10, a matrix of $2n$ th order, splits into a diagonal array of the $N_{(i)}$'s, the characteristic noise matrices of the individual amplifiers,

$$N = \text{diag} (N_{(1)}, N_{(2)}, \dots, N_{(n)}). \quad (51)$$

The eigenvalues of N are identical with the $2n$ eigenvalues of the n noise matrices $N_{(1)}$ to $N_{(n)}$. Thus, if the n two-terminal-pair networks are imbedded in a $4n$ -terminal-pair lossless network (which preserves the eigenvalues), a new $2n$ -terminal-pair network results that has a characteristic noise matrix with $2n$ eigenvalues that are equal to the eigenvalues of the second-order N matrices of the n amplifiers.

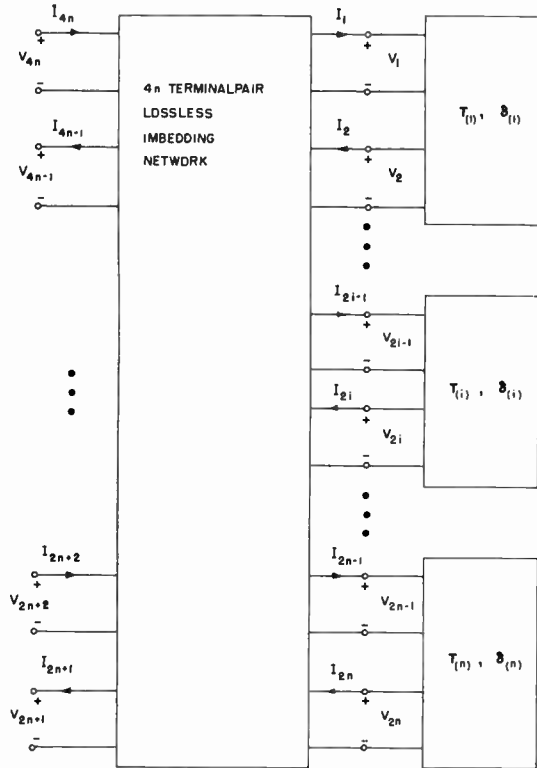


Fig. 10—Lossless interconnection of several amplifiers.

A two-terminal-pair network is obtained from the $2n$ -terminal-pair network if all but 2 terminal pairs are open-circuited. This represents the most general (lossless) way in which n networks can be interconnected to form a single two-terminal-pair network. Let the resulting two-terminal-pair network have the circuit matrix T_r and the noise vector δ_r . In Appendix III it is shown that the noise measure $(M_e)_r$ of the resulting network,

$$(M_e)_r = \frac{y_r^\dagger \bar{\delta}_r \delta_r^\dagger y_r}{y_r^\dagger (P - T_r P T_r^\dagger) y_r} \frac{1}{2kT\Delta f}, \quad (52)$$

is a special case of the noise measure M_e of the $2n$ -terminal-pair network, as given in (44). $(M_e)_r$ is obtained from M_e by a special choice of the vector y of $2n$ th order. This shows that $(M_e)_r$ can vary only within the limits imposed upon M_e . In particular, if the smallest positive eigenvalue among the $2n$ eigenvalues of N is denoted by λ_1 , we have, for positive $(M_e)_r$,

$$(M_e)_r \geq \lambda_1/kT\Delta f.$$

But, λ_1 is the optimum noise measure of the best amplifier among the n original amplifiers used. This proves Theorem 2.

VIII. LOSSY IMBEDDING OF AN AMPLIFIER

Theorem 2 can be extended to the following theorem.

Theorem 3

Passive lossy interconnections of amplifiers cannot lead to a positive noise measure lower than that achievable with lossless interconnections.

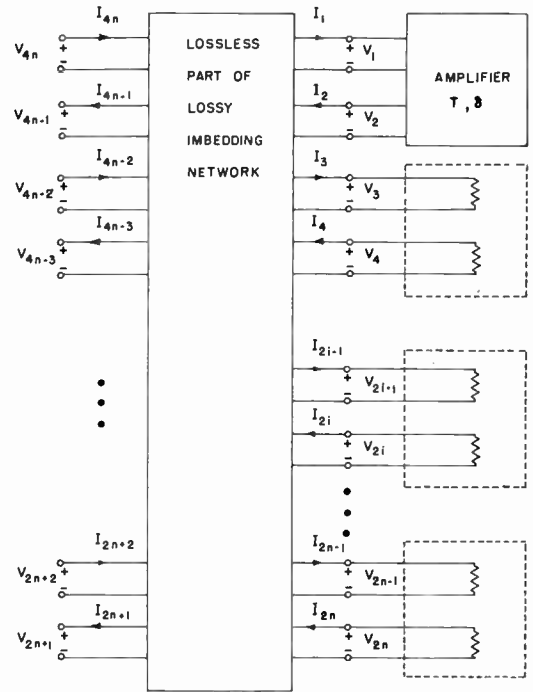


Fig. 11—Lossy imbedding of an amplifier.

Let us suppose first that we have found a lossy reciprocal transformation network for a two-terminal-pair amplifier which yields the lowest positive two-terminal-pair noise measure. Draw out each resistor of the resulting transformation network as a new terminal pair, and assume, for convenience, that there are an even number, $2n-2$, of resistances, which we place on the right-hand side of Fig. 11. Add an equal number of dummy terminal pairs on the left-hand side of the network, thereby creating $2n$ accessible terminal pairs on the left. Denote the original input and output-terminal pairs of the transformed amplifier by $4n$ and $4n-1$, respectively. The amplifier and the $2n-2$ resistances on the right-hand side comprise a $2n$ -terminal-pair network (similar to Fig. 10) with a characteristic noise matrix with $2n$ eigenvalues. Two of these pertain to the amplifier. The others pertain to two-terminal-pair passive (resistive) networks at equilibrium temperature T .

In Section II we have shown that the noise measure of any passive two-terminal-pair network at thermal equilibrium is always -1 . Thus, if a given passive two-terminal-pair network at equilibrium temperature T is imbedded in a variable, lossless, four-terminal-pair network, the resulting two-terminal-pair must always have the noise measure $M_e = -1$. Since the range of M_e is limited by the two (negative) eigenvalues of the corresponding characteristic noise matrix, as shown in Fig. 6, case 2, we conclude that *both eigenvalues* must be $-kT\Delta f$.

Referring again to Fig. 11, it follows that both eigenvalues of $N_{(k)}$ for the k th pair of resistances are equal to $-kT\Delta f$. The lossless $4n$ -terminal-pair network leaves the eigenvalues of N invariant (see Section V). Thus, the over-all $2n$ -terminal-pair network of Fig. 11 has the

same eigenvalues, namely $-kT\Delta f$. The only *positive* eigenvalue(s) is (are) contributed by the amplifier. The positive values of the generalized noise measure, (44), of this $2n$ -terminal-pair network have to lie (see Section VI) in the range *above* the least positive eigenvalue $\lambda_1/kT\Delta f$, as shown in Fig. 9. If all dummy terminal pairs $(2n+1)$ to $(4n-2)$ are now open-circuited, we obtain the original transformed two-terminal-pair amplifier with a particular noise measure. This noise measure is, according to Section VII, a special case of the generalized noise measure, (44). Accordingly, its value must lie within the allowed range of the generalized noise measure; hence it cannot be less than $\lambda_1/kT\Delta f$. Thus, the noise measure of the amplifier imbedded in the assumed lossy network cannot have a positive value lower than that which could have been achieved with a lossless imbedding network. This argument remains valid even when the temperature of the lossy imbedding network is lowered so that the eigenvalues of N arising from the resistance networks approach zero ever so closely, because they do so from the negative side.

The above result can be extended to the case in which the transformation network contains an odd number of resistances or, indeed, any passive (possibly non-reciprocal) networks of known noise performance. Use is made of the "canonical" form of such networks, mentioned in Section IX-B, and treated generally in Haus and Adler [6] and Mason [7].

IX. REALIZATION OF THE OPTIMUM NOISE MEASURE

The preceding sections were devoted to the demonstration of the properties of noise measure. In particular, it has been shown that the optimum noise measure of an amplifier determines the lower bound to the excess noise figure at high gain ($G_e \rightarrow \infty$) of a particular type of amplifier. This includes the use of either a single amplifier, or of a passive interconnection of amplifiers of the same type.

It now becomes important to know precisely how, by external network operations upon any given two-terminal-pair amplifier, its minimum positive noise measure can actually be achieved. Unfortunately, space limitations imposed upon this paper have made it necessary to discuss elsewhere [8] the detailed proofs pertinent to this question. Nevertheless, the form of the external networks used to realize optimum noise performance illuminates so much the relationship between the preceding rather abstract general theory and the procedures in current practice, that at least a brief presentation of the results must be included here.

In the realizations which will be presented, the source impedance and the amplifier output impedance (with the source connected) will always have positive real parts. It follows that, by cascading identical optimized amplifiers with appropriate lossless impedance transformation networks, arbitrarily high gain can be achieved at the optimized noise measure, and minimum

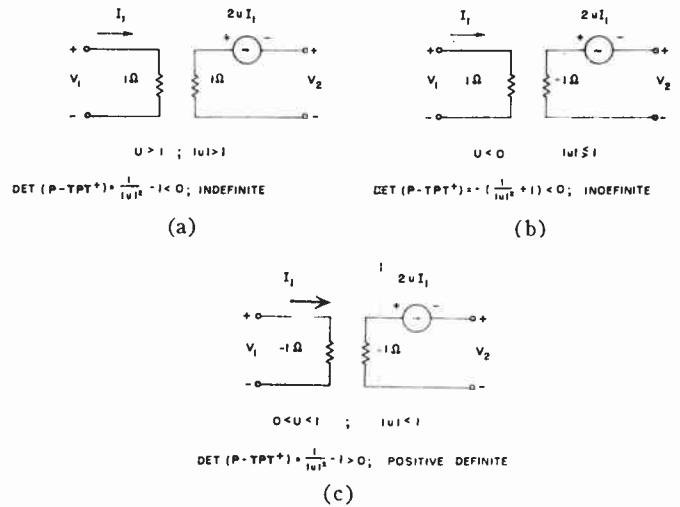


Fig. 12—Classes of amplifiers.

noise figure at high gain can, thereby, be realized.

The noise performance optimization problem is solved conveniently by referring to a more detailed classification of nonpassive two-terminal-pair networks (*i.e.*, amplifiers) than we have used so far. In particular, Mason [7] has shown that every such network can be reduced by lossless *reciprocal* imbedding to one of the three basic types shown in Fig. 12. His classification is based primarily upon the range of values of the *unilateral gain* U

$$U = \frac{|Z_{21} - Z_{12}|^2}{4(R_{11}R_{22} - R_{12}R_{21})} \tag{53}$$

where the R 's are the real parts of the impedance matrix elements. Since the numerical value of U is invariant to lossless *reciprocal* transformations [7], none of the three types can be carried into any other by such transformations.

The first type [Fig. 12(a)], with $U > 1$, is by far the most common. The majority of vacuum tube and transistor amplifiers belong to this class. The second type [Fig. 12(b)], $U < 0$, is less common. It does, however, share one important property with the first; namely both have

$$\det (P - TPT^*) < 0 \tag{54a}$$

which means that they can absorb, as well as deliver, power. It is perhaps not surprising, therefore, that with lossless *nonreciprocal* transformations amplifiers of the type of Fig. 12(b) can be carried into the form shown in Fig. 12(a) [8].

The amplifier in Fig. 12(c), however, has

$$\det (P - TPT^*) > 0 \tag{54b}$$

and cannot, under any terminal condition, absorb power. Obviously it cannot be reduced to any of the other forms by any *lossless* transformation whatsoever. It is a "negative-resistance" amplifier.

Recalling from (40) and subsequent equations that the optimum noise measure is not changed by any loss-

less transformation, we conclude that noise performance optimization of amplifiers need only be carried out on networks of the specific forms Fig. 12(a) and Fig. 12(c), and this will be sufficient to cover all nonpassive cases.

A. Optimization of Amplifier with $\det(P - TPT^\dagger) < 0$

The key point in achieving optimum noise performance of amplifiers obeying condition (54a) is contained in the theorem [8]:

The optimum noise measure of the amplifier of Fig. 12(a) can be achieved with a positive source resistance by using only a suitable lossless reciprocal mismatching network at the input. The output impedance remains 1Ω .

The value of the optimum noise measure is [8]

$$(M_e)_{opt} = \frac{\lambda_1}{kT\Delta f} = \frac{1}{8kT\Delta f} \left\{ \left[\frac{|E_{n1}|^2 + |I_{n1}|^2}{|u|^2 - 1} + \frac{2|u|^2 - 1}{|u|^2 - 1} 2 \operatorname{Re} \overline{E_{n1}I_{n1}^*} \right] + \sqrt{\left[\frac{|E_{n1}|^2 + |I_{n1}|^2}{|u|^2 - 1} + \frac{2|u|^2 - 1}{|u|^2 - 1} 2 \operatorname{Re} (\overline{E_{n1}I_{n1}^*}) \right]^2 + 16 \frac{|u|^2}{|u|^2 - 1} [|E_{n1}|^2 |I_{n1}|^2 - |E_{n1}I_{n1}^*|^2]} \right\} \quad (55)$$

which upon cascading of many identical optimized stages becomes the excess noise figure of the cascade at high gain. Observe that (55) checks with standard noise figure theory [1], [5] only if the gain per stage ($|u|^2$) is large. The same is true of the optimum effective source impedance.

Since all two-terminal-pair amplifiers obeying (54a) can be converted to Fig. 12(a) by lossless imbedding, the foregoing theorem is sufficient. The following detailed corollaries [8] are, however, of some obvious practical importance.

- 1) Any unilateral amplifier with $U > 1$ may be optimized with input mismatch alone.
- 2) A nonunilateral amplifier with $U > 1$, which is also stable for all passive source and load impedances, may be optimized with input mismatch alone.
- 3) Any amplifier with $U > 1$ may be optimized by first making it unilateral, using lossless reciprocal networks, and subsequently employing input mismatch.

The word *optimized* means achieving $(M_e)_{opt}$ with a source impedance and a resulting output impedance having positive real parts.

B. Optimization of Negative-Resistance Amplifiers, $\det(P - TPT^\dagger) > 0$

Two-terminal-pair negative-resistance amplifiers, obeying condition (54b) can always be optimized by lossless reciprocal imbedding. This method is rather uninteresting. Another method, actually valid for all the amplifier classes, is especially significant in the negative-resistance case. It stems from the theorem [6], [8]:

By lossless (nonreciprocal) transformation, any n -terminal-pair linear noisy network can be reduced to a "canonic" form of n isolated (positive or negative) resistors, each in series with a noise voltage generator uncorrelated with all the others. Moreover, the exchangeable power from each such isolated source is the negative of one of the n eigenvalues of the characteristic noise matrix N .

The canonic form for a two-terminal-pair amplifier appears in Fig. 13, opposite. Let the smallest positive eigenvalue of N be

$$\lambda_1 = - \frac{|E_{n1}|^2}{4R_1} > 0. \quad (55a)$$

Then it can be shown that [8]:

Connecting the terminal pair (E_{n1}, R_1) into a lossless ideal circulator with a positive (1Ω) balancing resistor at temperature T_0 , as shown in Fig. 14, achieves the optimum noise measure $(M_e)_{min} = \lambda_1/kT\Delta f$, with positive source and output impedance.

This is a general optimization result, valid in particular for the negative resistance amplifier class of interest here [*i.e.*, of the type shown in Fig. 12(c)].

Now, one form of maser amplifier (the only form actually built and tested to date) is representable as a one-terminal-pair negative resistance R_1 in series with a noise voltage generator E_{n1} [8], [9], [11]. Consider for a moment that the maser and some arbitrary positive resistor represent the canonic form of a two-terminal-pair network. The only positive eigenvalue of N for this network is

$$\lambda_1 = \frac{|E_{n1}|^2}{4|R_1|} > 0. \quad (55b)$$

It follows as a corollary of the result stated above in connection with Fig. 14 that:

The noise performance of a one-terminal-pair noisy negative resistance (like one form of the maser) is optimized by employing it in one arm of an ideal circulator, as shown in Fig. 14.

The results of Section IX lead directly to the last of our required theorems.

Theorem 4

The minimum noise figure F_{min} at arbitrarily high gain can be achieved with external passive network operations

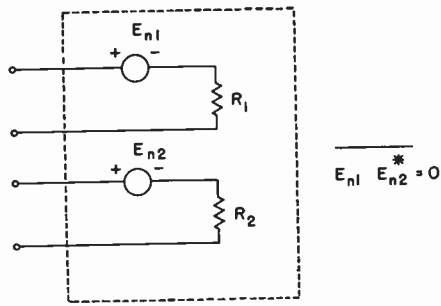


Fig. 13—"Canonic" form of two-terminal-pair amplifier.

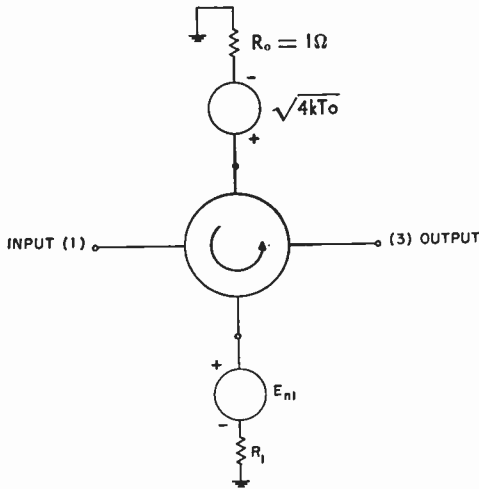


Fig. 14—Realization of optimum amplifier noise performance from "canonic" form of the amplifier.

for all amplifier types, with source and resulting output impedances that have positive real part.

X. CONCLUSION

Our discussion started from the premise that the (excess) noise figure is a reasonable measure of amplifier noise performance if the gain of the amplifier is high. It was natural to suppose at the outset that the quality of an amplifier with regard to noise performance should be measured in terms of the lowest (excess) noise figure at high gain that can be achieved with this amplifier, whether used singly, or in an arbitrary lossless interconnection of amplifiers of the same type. The lowest excess noise figure was found to be equal to the optimum noise measure, a number characteristic of the amplifier alone. The optimum noise measure was then adopted as a measure of amplifier quality (with regard to noise performance). The correctness of this choice was confirmed by the following demonstrations:

- 1a) The optimum noise measure of any amplifier can actually be achieved with a positive source impedance, positive output impedance, and an available gain $G > 1$.
- 1b) By cascading an arbitrary number of the foregoing optimized amplifiers, an arbitrarily high

gain can be achieved with the same noise measure. The excess noise figure, $F - 1$, of the resulting cascade is equal to this noise measure.

- 2) The use of lossy interconnecting networks cannot lead to an excess noise figure at high gain that is lower than that achievable through lossless interconnections.
- 3) Interconnection of amplifiers of different types cannot lead to an excess noise figure at high gain that is better than that achievable with amplifiers of the "best" class alone. The "best" amplifiers are those with the lowest optimum noise measure.

In a design of a practical system we may either try to actually achieve the lower limit for M_e , or we may use it as a guide to establish the point where further improvement is only achievable with diminishing returns.

This paper thus establishes a limit for the best noise performance achievable with any given amplifier type.

APPENDIX I

CLASSIFICATION OF SOURCE-FREE LINEAR NETWORKS

Consider the linear $2n$ -terminal-pair source-free network of Fig. 15 described in terms of an "input" column vector (matrix) v and "output" column vector u , and a general-circuit matrix T . These matrices are all of order $2n$, and they express the network equations in the form

$$v = Tu. \tag{56}$$

We wish to classify the network according to its ability to generate or absorb power.

The net time-average power P flowing out of the network (for $n=4$) is

$$P = -\frac{1}{2} \{ [V_1 I_1^* + V_1^* I_1 + V_3 I_3^* + V_3^* I_3 + V_5 I_5^* + V_5^* I_5 + V_7 I_7^* + V_7^* I_7] - [V_2 I_2^* + V_2^* I_2 + V_4 I_4^* + V_4^* I_4 + V_6 I_6^* + V_6^* I_6 + V_8 I_8^* + V_8^* I_8] \}, \tag{57}$$

which can be written more simply in matrix form as

$$P = \frac{1}{2} \{ u^t P_4 u - v^t P_4 v \}, \tag{58}$$

if the "permutation" matrix P_4 is given by

$$P_4 = \begin{pmatrix} 0 & 1 & 0 & 0 & 0 & 0 & 0 & 0 \\ 1 & 0 & 0 & 0 & 0 & 0 & 0 & 0 \\ \hline 0 & 0 & 0 & 1 & 0 & 0 & 0 & 0 \\ 0 & 0 & 1 & 0 & 0 & 0 & 0 & 0 \\ \hline 0 & 0 & 0 & 0 & 0 & 1 & 0 & 0 \\ 0 & 0 & 0 & 0 & 1 & 0 & 0 & 0 \\ \hline 0 & 0 & 0 & 0 & 0 & 0 & 0 & 1 \\ 0 & 0 & 0 & 0 & 0 & 0 & 1 & 0 \end{pmatrix}, \tag{59}$$

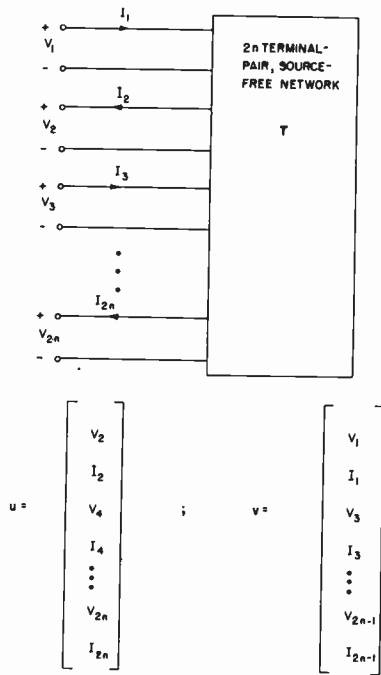


Fig. 15—2n-terminal-pair source-free network.

which is a logical extension of the matrix defined in (16), and has the same two properties.

The subscript “4” refers to the four square matrices

$$P = \begin{bmatrix} 0 & 1 \\ 1 & 0 \end{bmatrix}$$

that were defined in (16), and appear along the main diagonal of (59). A 2n-terminal-pair network with “input” and “output” variables arranged in their column vectors, specifically as shown in Fig. 15, will always have a “permutation” matrix P_n with n P matrices on its diagonal. (Other arrangements of the variables within their respective column matrices lead to different “permutation” matrices, as discussed in Appendix III.)

In view of (56), however, from (58), for a general 2n-terminal-pair network, we find

$$P = \frac{1}{2} \mathbf{u}^\dagger \{ P_n - T^\dagger P_n T \} \mathbf{u}. \tag{60}$$

This leads us to distinguish four cases:

- 1) The network is passive. It cannot generate any power. Then $P < 0$ for all \mathbf{u} , and $P_n - T^\dagger P_n T$ is negative definite (or semidefinite).
- 2) The network is incapable of absorbing power (negative-resistance network); $P > 0$ for all \mathbf{u} , and $P_n - T^\dagger P_n T$ is positive (semi) definite.
- 3) The network can either absorb or generate power (most conventional amplifiers are in this class). $P \geq 0$ depending upon \mathbf{u} , and $P_n - T^\dagger P_n T$ is indefinite.
- 4) The network is lossless. $P = 0$ for all \mathbf{u} , and

$$P_n - T^\dagger P_n T = 0. \tag{61}$$

In connection with noise measure, (29), we need a different form of condition (61) for a lossless network. Pre-multiplying (61) by $P_n(T^\dagger)^{-1}$, and postmultiplying it by $P_n T^\dagger$, we find

$$P_n - T P_n T^\dagger = 0, \tag{62}$$

since $P_n = P_n^{-1}$. For the special four-terminal-pair embedding network of Fig. 5, we want to express this condition in terms of the partitioned T matrix appearing in (30) and (31). We, therefore, write

$$T = \begin{bmatrix} T_{aa} & | & T_{ab} \\ T_{ba} & | & T_{bb} \end{bmatrix}$$

$$P_2 = \begin{bmatrix} 0 & 1 & | & 0 & 0 \\ 1 & 0 & | & 0 & 0 \\ 0 & 0 & | & 0 & 1 \\ 0 & 0 & | & 1 & 0 \end{bmatrix} = \begin{bmatrix} P & | & 0 \\ 0 & | & P \end{bmatrix} \tag{63}$$

and find four matrix relations of second order:

$$P - T_{aa} P T_{aa}^\dagger - T_{ab} P T_{ab}^\dagger = 0 \tag{64a}$$

$$T_{aa} P T_{ba}^\dagger + T_{ab} P T_{bb}^\dagger = 0 \tag{64b}$$

$$T_{ba} P T_{aa}^\dagger + T_{bb} P T_{ab}^\dagger = 0 \tag{64c}$$

$$P - T_{bb} P T_{bb}^\dagger - T_{ba} P T_{ba}^\dagger = 0. \tag{64d}$$

Eqs. (64b) and (64c) are redundant. This follows directly from them, and the fact that $P = P^\dagger$. Thus, (64) constitutes only three matrix relations among the four matrices T_{aa} , T_{bb} , T_{ab} , T_{ba} .

We shall also need another form of classification (1–3) for networks that are *not* lossless. The desired result is contained in the statement that the matrices

$$P_n - T P_n T^\dagger \text{ and } P_n - T^\dagger P_n T \tag{65}$$

have the same definite or semidefinite character. The proof depends directly upon a result obtained by Robinson [11], to which one may appeal directly by converting the matrices in (65) to their forms in terms of the wave-matrix variables by the methods of Appendix III. Therefore, the classification of networks becomes alternatively

- 1) $P_n - T P_n T^\dagger$ negative (semi) definite (passive),
- 2) $P_n - T P_n T^\dagger$ positive (semi) definite (negative resistance),
- 3) $P_n - T P_n T^\dagger$ indefinite (conventional amplifier),
- 4) $P_n - T P_n T^\dagger$ zero definite (lossless),

and it is in this form that it appears in the noise measure.

APPENDIX II

EXTREMA OF NOISE MEASURE

The search for extrema of the noise measure [(40) and (46)] is equivalent to the study of the extrema of the expression

$$kT\Delta f M_e' = \frac{x^\dagger A x}{x^\dagger B x},$$

under arbitrary variations of the x vector, where

$$\begin{aligned} Q^\dagger y &= x \\ \overline{\delta\delta}^\dagger &= A \\ 2(P_n - TP_n T^\dagger) &= B. \end{aligned}$$

The matrix A is positive (semi) definite, and B is Hermitian. The extrema (or stationary) values of M_e' may be found equivalently as the extrema (or stationary) values of $x^\dagger B x$, subject to the constraint $x^\dagger A x = \text{constant}$. Therefore, introduction of the Lagrange multiplier λ^{-1} and recognition that M_e' may be regarded as a function either of the components x_i^* of x^\dagger or of the components x_i of x leads to

$$\frac{\partial}{\partial x_i^*} (x^\dagger A x - \lambda x^\dagger B x) = 0; \quad i = 1, 2, \dots, n$$

or

$$A x - \lambda B x = (A - \lambda B)x = \mathbf{0}. \quad (66)$$

The values of λ are fixed by the requirement

$$\det(A - \lambda B) = 0 = \det(B^{-1}A - \lambda I). \quad (67)$$

The multipliers λ are therefore the eigenvalues of

$$B^{-1}A = \frac{1}{2}(P_n - TP_n T^\dagger)^{-1} \overline{\delta\delta}^\dagger. \quad (68)$$

Let λ_s be one of the eigenvalues of $B^{-1}A$ and $x^{(s)}$ the corresponding solution (eigenvector) of (66). Then premultiplication of (66) by $x^{(s)\dagger}$ yields

$$x^{(s)\dagger} A x^{(s)} = \lambda_s x^{(s)\dagger} B x^{(s)}$$

or

$$\lambda_s = \frac{x^{(s)\dagger} A x^{(s)}}{x^{(s)\dagger} B x^{(s)}} = (M_e') kT\Delta f$$

which is real.

It follows that the stationary values of the noise measure are the eigenvalues of the matrix $\frac{1}{2}(P_n - TP_n T^\dagger)^{-1} \overline{\delta\delta}^\dagger$ divided by $kT\Delta f$.

APPENDIX III

REARRANGEMENT OF VARIABLES AND REDUCTION TO TWO-TERMINAL-PAIRS

We shall study first how a permutation of the voltages and currents within the column matrices v and u of our network description can be taken into account in the analytical formulation of the network equations and the noise measure. Such a permutation obviously does not change the physics of the problem, and therefore should leave the numerical value of any physical quantity like power P or noise measure M_e unchanged. It does, however, alter the general algebraic expressions for these quantities in a manner that will be discussed below.

If in a $2n$ th-order column vector v we wish to exchange the order of the j th and k th elements v_j and v_k (counted from the top down), we must premultiply it by a $2n$ th-order identity matrix in which the j th and k th rows have been interchanged. Denote by R_{jk} such a rearranged unit matrix. For example, a sixth-order identity matrix, with rows 3 and 5 interchanged, becomes

$$R_{35} = \begin{pmatrix} 1 & 0 & 0 & 0 & 0 & 0 \\ 0 & 1 & 0 & 0 & 0 & 0 \\ 0 & 0 & 0 & 0 & 1 & 0 \\ 0 & 0 & 0 & 1 & 0 & 0 \\ 0 & 0 & 1 & 0 & 0 & 0 \\ 0 & 0 & 0 & 0 & 0 & 1 \end{pmatrix}. \quad (69)$$

The general rule is that in the identity matrix of appropriate order the jj th (one) and jk th (zero) elements are interchanged, and the kk th (one) and kj th (zero) elements are interchanged. The new column vector v' , arising from the exchange of elements v_j and v_k in v , is given by the product

$$v' = R_{jk} v. \quad (70)$$

Thus, if we introduce into our general-circuit matrix description of a noisy network the new "input" vector v' of (70), and a corresponding new "output" vector,

$$u' = R_{jk} u. \quad (71)$$

and observe by inspection that

$$R_{jk} R_{jk} = I, \quad (72)$$

the new network equations become

$$v' = R_{jk} T R_{jk} u' + R_{jk} \delta. \quad (73)$$

Eq. (73) characterizes a "new" network with a noise vector δ' and a general-circuit matrix T' with the property that

$$\delta' = R_{jk} \delta \quad (74a)$$

$$T' = R_{jk} T R_{jk} \quad (74b)$$

The new form of the "permutation" matrix ${}_p P_n$ for a $2n$ -terminal-pair system is found from the power-invariance requirement that, for all v ,

$$v^\dagger P_n v = v'^\dagger P_n v'. \quad (75)$$

Thus, from (70), and from the fact that $R_{jk} = R_{jk}^\dagger$, we find that

$${}_p P_n = R_{jk} P_n R_{jk}. \quad (76)$$

The quantities of interest in the noise measure may now be expressed by using (74) and (76), and the properties of R_{jk} .

$$\overline{\delta'\delta'}^\dagger = R_{jk} \overline{\delta\delta}^\dagger R_{jk} \quad (77a)$$

$${}_p P_n - T' {}_p P_n T'^\dagger = R_{jk} (P_n - TP_n T^\dagger) R_{jk}. \quad (77b)$$

But the noise measure is

$$M_e = \frac{y^\dagger \delta \delta^\dagger y}{y^\dagger (P_n - T P_n T^\dagger) y} \left(\frac{1}{2kT\Delta f} \right) = \frac{(y^\dagger R_{jk}^\dagger) \delta' \delta'^\dagger (R_{jk} y)}{(y^\dagger R_{jk}^\dagger) [{}_p P_n - T' {}_p P_n T'^\dagger] (R_{jk} y)} \left(\frac{1}{2kT\Delta f} \right), \quad (78)$$

which shows that if we set

$$y' = R_{jk} y, \quad (79)$$

the general definition of M_e in (44) can be applied with any rearranged form of the "input" and "output" variables, provided that the appropriate ${}_p P_n$ is used with the corresponding T' and δ' .

The extrema of M_e , with respect to lossless imbedding, are obviously unchanged on account of (78). This follows also from the fact that the new characteristic noise matrix N' is

$$N' = ({}_p P_n - T' {}_p P_n T'^\dagger)^{-1} \delta' \delta'^\dagger = R_{jk}^{-1} N R_{jk}, \quad (80)$$

which is a similarity transformation of N and has, therefore, the same eigenvalues.

Consider a general $2n$ -terminal-pair network with the general-circuit matrix T and the "noise vector" δ . If all but two terminal pairs of the $2n$ -terminal-pair network are left open-circuited, a two-terminal-pair network is effectively obtained. Here we shall show that the noise measure of the resulting two-terminal-pair network is always obtainable from the general $2n$ -terminal-pair definition (44) by an appropriate special choice of the column vector y .

The excitation vectors v and u , which are both of $2n$ th order, can be rearranged and subdivided into "input" subvectors $v_a, v_b',$ and v_c' , and "output" subvectors $u_a, u_b',$ and u_c' , respectively. The vectors v_a and u_a comprise the input and output on the two terminal pairs that are to be retained as the terminals of the resulting two-terminal-pair network terminals 1 and 2 in Fig. 7. The "input" vectors v_b', v_c' and the "output" vectors u_b' and u_c' are all of $(n-1)$ th order and comprise the remaining voltages and currents of Fig. 7 rearranged and separated as follows:

$$\left. \begin{aligned} u_a &= \begin{bmatrix} V_2 \\ I_2 \end{bmatrix}; & v_a &= \begin{bmatrix} V_1 \\ I_1 \end{bmatrix}; & \delta_a &= \begin{bmatrix} E_{n1} \\ I_{n1} \end{bmatrix} \\ u_b' &= \begin{bmatrix} I_4 \\ I_6 \\ I_8 \\ \vdots \\ I_{2n} \end{bmatrix}; & v_b' &= \begin{bmatrix} I_3 \\ I_5 \\ I_7 \\ \vdots \\ I_{2n-1} \end{bmatrix}; & \delta_b' &= \begin{bmatrix} I_{n3} \\ I_{n5} \\ I_{n7} \\ \vdots \\ (I_n)_{2n-1} \end{bmatrix} \\ u_c' &= \begin{bmatrix} V_4 \\ V_6 \\ V_8 \\ \vdots \\ V_{2n} \end{bmatrix}; & v_c' &= \begin{bmatrix} V_3 \\ V_5 \\ V_7 \\ \vdots \\ V_{2n-1} \end{bmatrix}; & \delta_c' &= \begin{bmatrix} V_{n3} \\ V_{n5} \\ V_{n7} \\ \vdots \\ (V_n)_{2n-1} \end{bmatrix} \end{aligned} \right\} \quad (81)$$

The purpose of the rearrangement in (81) is to separate the voltages and currents of the terminal pairs that will be open-circuited. Corresponding to the foregoing rearrangement of the excitation vectors, the network matrix T and the noise vector δ must also be rearranged to form T' and δ' , as shown in (74a) and (74b). The rearranged form δ' is contained in (81). The rearranged network relations can now be written in the separated form:

$$\begin{aligned} v_a &= T_{aa} u_a + T_{ab'} u_b' + T_{ac'} u_c' + \delta_a \\ v_b' &= T_{ba'} u_a + T_{bb'} u_b' + T_{bc'} u_c' + \delta_b' \\ v_c' &= T_{ca'} u_a + T_{cb'} u_b' + T_{cc'} u_c' + \delta_c'. \end{aligned} \quad (82)$$

The new permutation matrix ${}_p P_n$ for the rearranged permuted currents and voltages is found from the requirement that the power output P of the network be given by

$$P = - [v_a^\dagger v_b'^\dagger v_c'^\dagger] {}_p P_n \begin{bmatrix} v_a \\ v_b' \\ v_c' \end{bmatrix} + [u_a^\dagger u_b'^\dagger u_c'^\dagger] {}_p P_n \begin{bmatrix} u_a \\ u_b' \\ u_c' \end{bmatrix}.$$

By inspection, we confirm that ${}_p P_n$ is given by

$${}_p P_n = \begin{bmatrix} P & 0 & 0 \\ 0 & 0 & I \\ 0 & I & 0 \end{bmatrix}, \quad (83)$$

where P is given by (16) of the text. If we open-circuit all terminal pairs except the two corresponding to v_a and u_a , we have

$$u_b' = 0; \quad v_b' = 0. \quad (84)$$

Introducing (84) into (82), we find the equation for the resulting two-terminal-pair network:

$$v_a = T_r u_a + \delta_r, \quad (85)$$

and

$$\begin{aligned} T_r &= T_{aa} - T_{ac'} T_{bc'}^{-1} T_{ba'} \\ \delta_r &= \delta_a - T_{ac'} T_{bc'}^{-1} \delta_b'. \end{aligned} \quad (86)$$

From (86) we find by matrix multiplication

$$T_r P T_r^\dagger = M T' {}_p P_n T'^\dagger M^\dagger \quad (87)$$

and

$$\overline{\delta_r \delta_r^\dagger} = \overline{M \delta' \delta'^\dagger M^\dagger}$$

where

$$M = [I; -T_{ac'} T_{bc'}^{-1}; 0]. \quad (88)$$

The noise measure $(M_e)_r$ of the resulting two-terminal-pair network connected to a source with the impedance Z_S [see Section IV, (12) and (29)] is defined by

$$(M_e)_r = \frac{x^\dagger \delta_r \delta_r^\dagger x}{x^\dagger [P - T_r P T_r^\dagger] x} \left(\frac{1}{2kT\Delta f} \right) \quad (89)$$

with

$$\mathbf{x} = \begin{bmatrix} 1 \\ Z_S^* \end{bmatrix}.$$

With the aid of (87) and (88), we can write $(M_e)_r$ in the form

$$(M_e)_r = \frac{(\mathbf{x}^\dagger \mathbf{M}) \overline{\delta' \delta'^\dagger} (\mathbf{M}^\dagger \mathbf{x})}{(\mathbf{x}^\dagger \mathbf{M}) (P_p P_n - T_p' P_n T_p') (\mathbf{M}^\dagger \mathbf{x})} \left(\frac{1}{2kT\Delta f} \right). \quad (90)$$

In (90) we have used the fact that

$$P = M_p P_n M^\dagger,$$

as can be easily checked from (83) and (88). Comparison of (90) with (78) and (44) shows that the noise measure $(M_e)_r$ is indeed a special case of the general noise measure definition, (44), corresponding to the particular choice of \mathbf{y} ,

$$\mathbf{y} = \mathbf{M}^\dagger \mathbf{x}. \quad (91)$$

That is what we set out to prove.

ACKNOWLEDGMENT

The authors are especially grateful to Prof. L. N. Howard, of the Department of Mathematics, M.I.T., who made possible for them the matrix eigenvalue for-

mulation of the problem. They are also indebted to D. L. Bobroff, of Raytheon Manufacturing Company, who noticed in their early results a possible connection with available power.

BIBLIOGRAPHY

- [1] van der Ziel, A. *Noise*, New York: Prentice-Hall, 1954.
- [2] Haus, H. A. and Adler, R. B. "Invariants of Linear Networks," 1956 IRE CONVENTION RECORD, pt. 2, pp. 53-67.
- [3] Haus, H. A., and Adler, R. B. "Limitations on Noise Performance of Linear Amplifiers," paper presented at the Congress International Tubes Hyperfrequencies, Paris, June, 1956; to be published in *L'Onde Electrique*.
- [4] Haus, H. A., and Adler, R. B. "An Extension of the Noise Figure Definition," PROCEEDINGS OF THE IRE, Vol. 45 (May, 1957), pp. 690-691.
- [5] Rothe, H., and Dahlke, W. "Theory of Noisy Four-Poles," PROCEEDINGS OF THE IRE, Vol. 44 (June, 1956), pp. 811-817.
- [6] Haus, H. A., and Adler, R. B. "Canonic Form of Linear Noisy Networks," submitted for publication to IRE TRANSACTIONS ON CIRCUIT THEORY.
- [7] Mason, S. J., "Power Gain in Feedback Amplifiers," Research Laboratory of Electronics, Massachusetts Institute of Technology, Cambridge, Mass., Technical Report 257, August 25, 1953.
- [8] Adler, R. B., and Haus, H. A. "Network Realization of Optimum Amplifier Noise Performance," submitted for publication to IRE TRANSACTIONS ON CIRCUIT THEORY.
- [9] Wittke, J. P. "Molecular Amplification and Generation of Microwaves," PROCEEDINGS OF THE IRE, Vol. 45 (March, 1957), pp. 291-316.
- [10] Muller, M. W., "Noise in a Molecular Amplifier," *Physical Review*, Vol. 106 (April 1, 1957), pp. 8-12.
- [11] Robinson, F. N. H., and Haus, H. A. "Analysis of Noise in Electron Beams," *Journal of Electronics*, Vol. 4 (January, 1956), pp. 373-384.

CORRECTION

G. Bemski, author of "Recombination in Semiconductors," which appeared on pages 990-1004 of the June, 1958 issue of PROCEEDINGS, has informed the editors that Figs. 4-6, on pages 995 and 998, were incorrectly numbered. The two figures on page 995 should be Fig. 6 and Fig. 4 instead of Fig. 4 and Fig. 5, and the graph on page 998 should be Fig. 5.

Also, on page 998, on the sixth line of the second paragraph, the word "copper" should be "nickel."

Correspondence

Observations of the U. S. Satellites Explorers I and III by CW Reflection*

The detection of Sputniks I and II by CW reflection at The Ohio State University Radio Observatory has been reported.¹⁻³ The purpose of this communication is to report that numerous observations have also been made of the U. S. satellites Explorers I and III using the same CW reflection method. In connection with these observations, it is of particular interest that on many occasions the Explorers were detected at heights of the order of 1000 miles. In our earlier Sputnik observations, the satellites were always at heights of less than 500 miles. In order to observe the CW reflections, ionized regions of considerable area are required and, accordingly, the Explorer observations provide evidence of significant ion density occurring at heights of the order of 1000 miles.

The CW reflections were observed by recording 20- or 25-mc signals from WWV. Simultaneous recordings were made on 108 mc of the transmissions from the Explorers. By comparing the WWV and 108-mc records it was noted that numerous WWV bursts occurred during the passages of the Explorers. For example, Fig. 1 shows two recordings taken simultaneously on March 11, 1958. The upper trace is the 20-mc record with deflections due to momentary bursts of WWV signal and the lower trace is the 108-mc record due to the signals of Explorer I. Between 0539 and 0548 there is a deflection on the 108-mc record due to the signals of Explorer I. At 0543 and 0544 on the 20-mc record, there are small signal bursts of 15 to 30 seconds duration followed at about 0545 by a very large deflection which ended abruptly about 12 seconds later when WWV went off the air for its hourly 4-minute silent period. This signal burst is the largest obtained in weeks of recording and is several times the daytime level of WWV. It is probable that this burst and also the smaller ones at 0543 and 0544 were caused by reflection of WWV signals from ionization produced by Explorer I. At this time Explorer I was believed to be at a height of only a few hundred miles.

Evidence of WWV reflections from greater heights is presented by the sample records of Fig. 2. The upper pair of traces show the 25-mc WWV signal and 108-mc Explorer I record taken simultaneously on the evening of April 13, 1958; the lower pair show the 25-mc WWV signal and the 108-mc Explorer III record about 6 hours later on the morning of April 14, 1958. During these observations the 108-mc receiver was

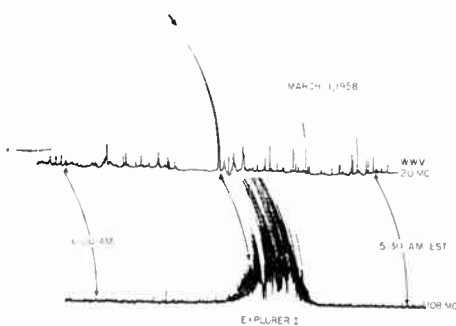


Fig. 1—Simultaneous recordings on March 11, 1958 of Explorer I transmissions on 108-mc (lower) and 20-mc signals from WWV (upper) with large burst of WWV signal occurring during passage of Explorer I. Time is indicated on both traces at 5:30 and 6:00 A.M. by the curved lines which coincide with the curved coordinates of the recorder.

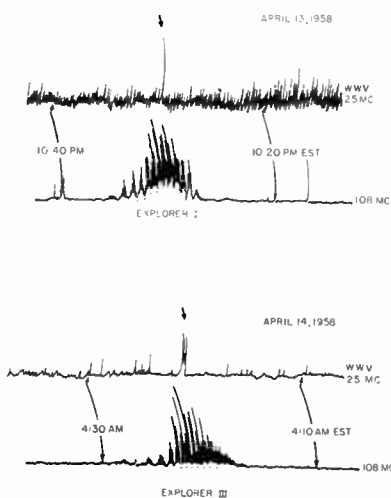


Fig. 2—Recordings of Explorer I and III 108-mc transmissions on the night of April 13-14, 1958, with simultaneous records of 25-mc WWV signals. In both cases bursts of WWV signal, as indicated by the arrows, occur within less than one minute of the meridian transit of the Explorer satellite.

connected to a pair of spaced antennas acting as an interferometer, the lobes of the pattern being evident in the records. (Only one antenna of the pair was connected during the record of Fig. 1.) In both examples in Fig. 2 a sizable burst of the WWV signal occurred within one minute of the meridian transit of an Explorer satellite. The time of the signal burst corresponds in each case very closely with the time of nearest approach of the satellite. During the entire night from 9 P.M. April 13 to 5 A.M. April 14, there was only one other significant WWV burst. This occurred at 10:10 P.M. and was presumably associated with Sputnik II. What may have been the same object was reported to have been seen from Denver, Colo., at 10:12 P.M. EST. Accordingly, the probability is very small that the bursts in Fig. 2 are due to a random process. Taking into consideration also the close correlation between Explorer passes and

WWV bursts on other nights, the probability of a random process being responsible becomes vanishingly small.

From the interferometer patterns of the 108-mc records, calculations indicate that the Explorers in both cases were at heights of the order of 1000 miles. Although the magnitudes of the WWV signal bursts in these and other Explorer observations are large, the duration in all cases is less than one-half minute. This would seem to indicate that the conditions required for observing a reflection are highly critical.

J. D. KRAUS

R. C. HIGGY

J. S. ALBUS

Radio Observatory

Dept. of Elec. Eng.

The Ohio State University
Columbus 10, Ohio

WWV Standard Frequency Transmissions*

Since October 9, 1957, the National Bureau of Standards radio stations WWV and WWVH have been maintained as constant as possible with respect to atomic frequency standards maintained and operated by the Boulder Laboratories, National Bureau of Standards. On October 9, 1957, the U.S.A. Frequency Standard was 1.4 parts in 10^9 high with respect to the frequency derived from the UT 2 second (provisional value) as determined by the U. S. Naval Observatory. The atomic frequency standards remain constant and are known to be constant to 1 part in 10^9 or better. The broadcast frequency can be further corrected with respect to the U.S.A. Frequency Standard as indicated in the table below. This correction is *not* with respect to the current value of frequency based on UT 2. A minus sign indicates that the broadcast frequency was low.

The WWV and WWVH time signals are synchronized; however, they may gradually depart from UT 2 (mean solar time corrected for polar variation and annual fluctuation in the rotation of the earth). Corrections are determined and published by the U. S. Naval Observatory.

WWV and WWVH time signals are maintained in close agreement with UT 2 by making step adjustments in time of precisely plus or minus 20 msec on Wednesdays at 1900 UT when necessary; no step adjustment was made at WWV or WWVH during the month.

* Received by the IRE, June 16, 1958.

* Received by the IRE, May 8, 1958.

¹ J. D. Kraus, "Detection of Sputnik I and II by CW reflection," *Proc. IRE*, vol. 46, pp. 611-612; March, 1958.

² J. D. Kraus, "The last days of Sputnik I," *Proc. IRE*, vol. 46, pp. 612-614; March, 1958.

³ J. D. Kraus and E. E. Dreese, "Sputnik I's last days in orbit," submitted for publication to *Proc. IRE*.

WWV Frequency†

May, 1958 1500 UT	Parts in 10 ⁹
1	-3.6
2	-3.5
3	-3.3
4	-3.2
5	-3.1
6	-2.9
7	-2.8
8	-2.6
9	-2.5
10	-2.4
11	-2.3
12	-2.2
13	-2.1
14	-2.0
15	-1.8
16	-1.6
17	-1.4
18	-1.2
19	-1.1
20	-1.1
21	-1.1†
22	-1.2†
23	-1.4†
24	-1.6†
25	-1.8†
26	-2.2†
27	-2.5
28	-2.9
29	-3.2†
30	-3.5
31	-3.6

† WWVH frequency is synchronized with that of WWV.

‡ Decrease in frequency of 0.5×10^{-9} at 1900 UT at WWV.

W. D. GEORGE
Radio Standards Lab.
Natl. Bur. of Standards
Boulder, Colo.



Fig. 1—Sample of relative phase of 40-mc signals received on two antennas spaced 1000 feet (bottom traces on each section) and relative amplitude of signal from one antenna (upper traces). First section represents approximate time of nearest approach, second section, early part of passage (satellite approaching from NW), and third section, approaching end of passage.

Continuous Phase Difference Measurements of Earth Satellites*

Numerous investigations have been made on the two earth satellites successfully launched to date using interferometric techniques of radio astronomy. The Radio Propagation Engineering Division of the National Bureau of Standards, Boulder Laboratories, conducted a series of observations of both satellites using a continuous phase-difference measuring technique developed earlier for studying atmospheric turbulence in the troposphere.¹

In a conventional interferometer, phase detection is accomplished by vectorial summing before detection. The detector output is thus a function of the amplitude of received signals and the cosine of their relative phase, and only discrete values of output (nulls) are chosen as significant for phase determination.

To remove this limitation on the total usable information in such records, measurements may be made in which the phase detection is performed in a manner which provides essentially constant sensitivity and signal-to-noise ratio.

The general technique used is that described in Herbstreit and Thompson¹ and, in

this case, consists of two similar Hammarlund SP-600 receivers operating on 20 (or 40) mc. The local oscillator signals for all three frequency conversions are obtained from one of the receivers to maintain coherence. The phase detector consists of an electronic phasemeter² which compares the af tones from the two receivers.

Within the practical limitations of the electronic phasemeters available, the following desirable features are obtained:

1) The output is a linear function of relative phase thus giving constant sensitivity for all phase angles.

2) The phase detector output as a function of signal strength saturates rapidly (at about $1 \mu\text{V}$ in the system used) and thus may be considered essentially a function of phase only.

3) The phasemeter is capable of detecting phase modulation components as high as the order of 100 cps and thus can respond to the fine structure which undoubtedly exists in the ionosphere.

Consequently, the records of this type contain not only much more information on gross phenomena such as orbit and refraction but also much more in the nature of the fine structure of the received signals.

The instrumentation and its maintenance and calibration are quite straightforward. Samples of records are illustrated in Fig. 1.

The records in general contain information on two types of mechanisms. One is the effect of gross geometrical changes (which account for the lobe structure of the simple

interferometer) and the second is the relatively irregular effect of ionospheric turbulence. For considerations of orbit or refraction the former are to be emphasized, while for the study of the latter the geometric effects should be minimized. This choice is made by the orientation of the antenna base line. Since the primary concern for these observations was with turbulence, the base line was chosen to be as feasible as possible, normal to the orbits to be observed. The result is to eliminate largely any "lobe" structure during nearly overhead passes. In the sample record of Fig. 1, the orientation was such that only 5 "lobes" were observed instead of the 80 which would have been expected using a baseline of 40λ . In addition to the first-order geometrical and turbulence effects noted above, the records many times indicated the presence of a variety of multipath effects. These produced correlated effects (as would be expected) on both phase difference and amplitude (of single signal). That this correlation was not the result of amplitude-phase interaction in the equipment was borne out by visual observations of the Lissajou figure during the recording period. Lack of time has prevented a more thorough analysis of the data to date but the techniques appear to have certain attractive features.

These measurements were the result of a joint effort involving a number of personnel of the Radio Propagation Engineering Division.

J. W. HERBSTREIT
M. C. THOMPSON, JR.
Radio Propagation Engineer Div.
Boulder Laboratories
National Bureau of Standards
Boulder, Colo.

* Received by the IRE, January 24, 1958.

¹ J. W. Herbstreit and M. C. Thompson, "Measurements of the phase of radio waves received over transmission paths with electrical lengths varying as a result of atmospheric turbulence," *Proc. IRE*, vol. 43, pp. 1391-1401; October, 1955.

² E. Florman and A. Tait, "An electronic phasemeter," *Proc. IRE*, vol. 37, pp. 207-210; February, 1949.

Semiconductor P - N Junction Radiation Counter*

Semiconductor p - n junction diodes that have a reverse breakdown voltage in excess of about 10 volts often exhibit an anomalous region in their reverse current vs voltage characteristic. Such an anomalous region can be readily observed in a current vs voltage display obtained by means of a dynamic tracer.¹ The region is usually located at the onset of avalanche breakdown and is marked by a gap or by multiple traces. On either side of the region the current vs voltage trace is single valued and well defined.

If a diode whose characteristic exhibits such a region is connected in series with a bias voltage and resistance, the values of which are such that the dc load line passes through the anomalous region, pulses will be observed on the voltage vs time display of an oscilloscope connected across the diode or resistance. The times of occurrence of the pulses and their widths are randomly distributed. The pulses are uniformly flat-topped, and have extremely short rise and decay times. With a series resistance of 5000 ohms, the pulse amplitude is typically 0.25 volt.²

These pulses have their origin in electrons and holes that are thermally generated within a diffusion length of the depletion layer, or local regions thereof. The thermally-generated carriers that traverse the region of high electric field set up by the bias voltage are multiplied by cumulative collision ionization, in a manner similar to that which takes place in a Geiger counter. The random pulse count rate can be determined by substituting a count-rate meter for the oscilloscope. This thermally-generated count rate, which constitutes a background count, decreases rapidly with temperature,³ usually as $\exp(-W/T)$, where T is the absolute diode temperature and W is the characteristic temperature of the thermal generation process.

When the diode is exposed to visible light, or other sufficiently energetic radiation, additional carriers are generated and the count rate increases. The additional count is found to be proportional to the incident radiation flux, up to extremely high count rates. The device is thus a true radiation detector and counter. Because of the relatively large amplitude flat-topped pulses that are obtained, it differs from conductivity-pulse crystal counters and from semiconductor diode counters previously reported^{4,5} in much the same way as a Geiger counter differs from an ionization chamber or from a proportional counter.

Our work was initially devoted to verifying that the device is indeed capable of

detecting and counting radiation. Such verification was obtained by using as incident radiation the photons of visible light, and also beta particles from a 40-microcurie $\text{Sr}^{90}\text{-Y}^{90}$ metal tab. With the latter source we found it necessary to operate the diode at reduced temperature to decrease its thermal background count. Our first successful experiment in detecting and counting betas from this source used a Hughes type 6008 diode operated at about 230 volts and -78 degrees C. In later experiments we have detected and counted betas from the same source with commercial diodes at lower voltages and higher temperatures. For example, we have detected and counted betas with a Hoffman type IN209 diode operated at about 60 volts and 0 degrees C. We believe that diodes can be made to detect and count radiation from weaker sources at room temperature, or higher, and with lower bias voltage.

The work described above was begun by K. Bewig and B. Salzberg at Naval Research Laboratory, and continued later under present auspices. We wish to thank Mr. Bewig for his participation in the early work. In connection with the more recent work we wish to acknowledge the beneficial comments of Drs. E. G. Fubini and K. C. Speh, and the experimental help of Dr. M. J. Zucker.

B. SALZBERG

K. SIEGEL

Airborne Instruments Lab., Inc.
Mineola, N. Y.

Observed Bunched Electron Current in a Velocity-Modulated Beam*

Space charge bunching problems of velocity-modulated electron beams occupy the attention of many research workers. In experimental studies of velocity-modulated beams, there are two kinds of useful microwave oscillography techniques. One of these is VonFoerster's uhf beam analyzer,¹ and the other is the traveling-wave cathode-ray oscilloscope. Using a beam analyzer, VonFoerster and his coworkers at Illinois University, succeeded in showing a picture of velocity distribution of the bunched electrons at a given point of interest along the beam. On the other hand, several kinds of traveling-wave cathode-ray-tubes (tw crt), which are suitable for recording uhf waveforms or high-speed transients, have already been developed. The author studied fundamental properties of the traveling-wave electron deflection system² and tried to utilize the tw crt for the waveform ob-

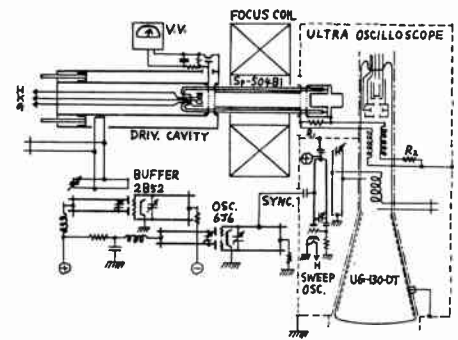


Fig. 1—Circuit diagram for the waveform observation of the bunched electron current in a velocity-modulated tube.

servation of the vhf electron current. In an experimental study of long beam, some typical waveforms of the bunched electron current in a velocity-modulated beam were directly obtained for the first time by oscillograms. They have only been estimated by the electron ballistic theory, and have not been found in an oscillogram.

As shown in Fig. 1, an observing apparatus, named the Ultra Oscilloscope, utilized the tw crt (UG-130-DT) and a sinusoidal horizontal sweep oscillator synchronously locked to the external signal. The tw crt has parallel cylindrical helices as the vertical deflecting line, and its frequency response of phase velocity (2.5×10^7 meters per second) is flat up to about 1500 mc. The axial length of the vertical deflecting line is 50 mm, and the phase shift angle on the line is about 1.3 radian at 100 mc, so that the observed distortion by end reflection is negligible. The experimental velocity-modulated tube (Sp-504B1) was designed by scaling for low-frequency and low-voltage operation. A vacuum-tube voltmeter was attached near the input gap for the purpose of indicating the gap voltage which derives the bunching parameter at operation. Connecting the fourth grid to the collector and loading the output gap with the resistance R_1 , made from graphite film, the bunched electron current flowing in R_1 is introduced to the vertical deflecting line of the tw crt.

Fig. 2 shows photographs of typical waveforms of the bunched electron current corresponding to the several values of the bunching parameter X . X is equal to $(\omega l_0 K/v_0)$ where $K = V_1/2V_0$, l_0 is the drift-tube length, v_0 is the beam velocity, V_0 is the accelerating voltage and V_1 is the buncher's gap voltage. Fig. 2(a) is for $X=0.67$, where the electron bunching is considerable, but the electrical angle of the bunched current in a cycle is not so narrow. In Fig. 2(b), where $X=1.14$ (condition for optimum bunching), it is found that many of the electrons are sharply focused into a small angle range of about 60° . Fig. 2(c), which corresponds to $X=1.4$, shows a condition of overbunching, where the waveform is double-humped. The photograph clearly shows that in the small-signal operation of the velocity modulation the electron bunching effect is sinusoidal, and the electron wave theory is appropriately applicable. But in the large signal operation (cases for optimum and overbunching), the bunched electron current contains comparatively many har-

* Received by the IRE, April 23, 1958.

¹ G. L. Pearson and B. Sawyer, "Silicon p - n junction alloy diodes," *Proc. IRE*, vol. 40, pp. 1348-1351; November, 1952.

² K. G. McKay, "Avalanche breakdown in silicon," *Phys. Rev.*, vol. 94, pp. 877-884; May, 1954.

³ J. E. Scobey, W. A. White, and B. Salzberg, "Fast switching with junction diodes," *Proc. IRE*, vol. 44, pp. 1880-1881; December, 1956.

⁴ K. G. McKay, "A germanium counter," *Phys. Rev.*, vol. 76, pp. 1537-1538; November, 1949.

⁵ C. Orman, H. Y. Fan, G. J. Goldsmith, and K. Lark-Horowitz, "Germanium p - n barriers as counters," *Phys. Rev.*, vol. 78, pp. 646-647; June, 1950.

* Received by the IRE, March 6, 1958.

¹ L. R. Bloom and H. M. Von Foerster, "Ultra-high frequency beam analyzer," *Rev. Sci. Instr.*, vol. 25, pp. 649-653; July, 1954.

² H. Maeda and K. Miyaji, "Electron deflection system of traveling-wave cathode-ray tubes," presented at Congress on Tube Hyper-frequencies, Paris, France; May, 1956; *Le Vide*, No. 67; pp. 128-140; January-February, 1957.

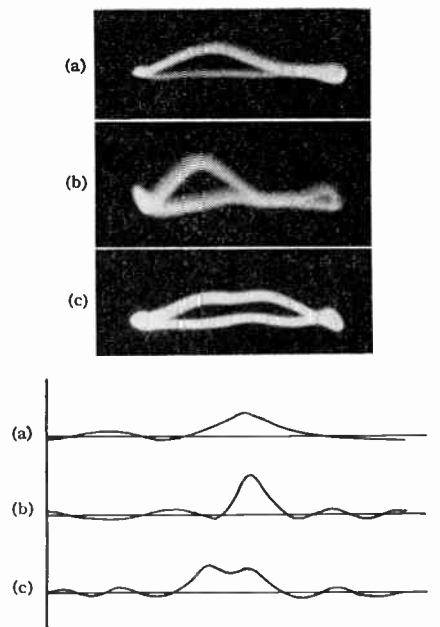


Fig. 2—Observed waveforms of the bunched electron current corresponding to the several values of the bunching parameter X . (a) $X=0.67$, $V_0=500v$, $K=0.14$, $I_0=15$ ma, (b) $X=1.14$, $V_0=500v$, $K=0.4$, $I_0=18$ ma, (c) $X=1.4$, $V_0=500v$, $K=0.29$, $I_0=18$ ma, where I_0 is the beam current.

monic components, where the electron ballistic phenomena seem to be predominant, as shown by the beam analyzer. The oscillograms shown here will introduce further profitable use of the tw crt in experimental study of the operation of other long-beam-tubes.

The author wishes to acknowledge the helpful counsel of Drs. A. Yamashita, H. Kuroda, and K. Miyaji, N.H.K., and the helpful suggestions on the experimental work given by Prof. Y. Koike of To-hoku University, and Dr. K. Owaki of Kobe Kogyo Co.

HARUO MAEDA
Japan Broadcasting Corp.
Tokyo, Japan

Design of Transistor Regulated Power Supplies*

The Angle Computer Company, Inc., has done extensive work in the field dealt with by Middlebrook.¹ A super-regulated transistorized power supply, Type 95710, which incorporates to a very great extent many features described by Middlebrook in his article, and which also has some additional new features, has been developed. This power supply was developed for Northrop Aircraft, Inc. early in 1957, with the first production unit being completed in April, 1957.

* Received by the IRE, January 24, 1958.
¹ R. P. Middlebrook, "Design of transistor regulated power supplies," Proc. IRE, vol. 45, pp. 1502-1509; November, 1957.

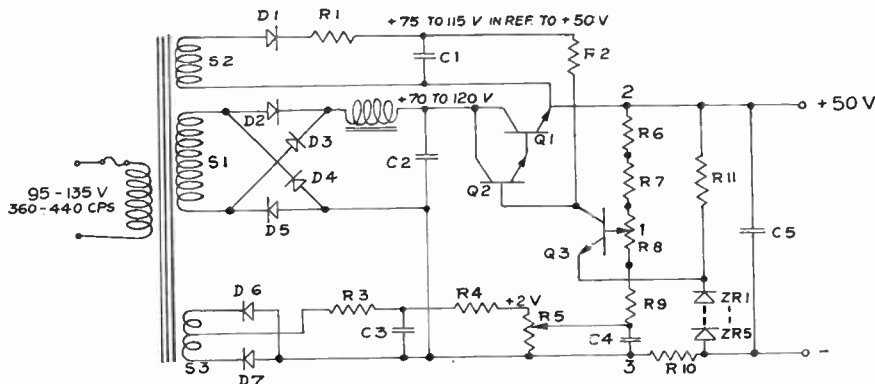


Fig. 1—Schematic diagram.

The basic differences between this power supply and the one described by Middlebrook are as follows:

- 1) Model 95710 power supply is designated to work at an ambient temperature of up to 100°C, hence silicon transistors are used.
- 2) Maximum required output current is 50 ma, which at that time was limited also by a shortage in the proper silicon power transistors with higher current capacity.
- 3) The additional voltage to supply the collector current of Q3 is not regulated.
- 4) Special compensation of output voltage changes caused by line voltage changes is incorporated.
- 5) Output voltage changes caused by temperature changes are compensated.

The details and operation of this power supply, in general, will not be discussed because it is basically discussed in detail in Middlebrook's article. I would like only to discuss briefly the compensation of output voltage changes caused by line voltage changes.

Assuming

- E_0 = output voltage,
- E_R = reference voltage on the zener diodes,
- E_A = voltage between points 2 and 1,
- E_B = voltage between points 1 and 3,

we find the output voltage E_0 from

$$E_0 = E_R \left(1 + \frac{E_A}{E_B} \right) \quad (1)$$

Further if

- R_B = the resistance between points 1 and 3 formed by part of R_8 and part of R_5 and R_9 ,
- R_A = the resistance formed by rest of R_8 , R_7 , and R_6 ,
- E_C = unregulated compensating voltage generated on part of R_5 by supply S_3 ,

the current drawn by the base of Q3 is negligible. We find that

$$\frac{E_A}{E_B} = \frac{1}{\frac{E_C}{E_0 - E_C} \frac{R_A + R_B}{R_A} + \frac{R_B}{R_A}} \quad (2)$$

From (1) and (2)

$$E_0 = E_R \left\{ 1 + \frac{1}{\frac{E_C}{E_0 - E_C} \frac{R_A + R_B}{R_A} + \frac{R_B}{R_A}} \right\} \quad (3)$$

From (3) we see that E_0 will decrease if E_C

increases. Since E_C is proportional to the line voltage, output voltage change caused by line voltage change can be compensated by proper value of E_C which primarily is determined by the basic regulation degree of the power supply.

The additional low power supply S_3 , supplying collector of Q3, has its minus connected to plus output voltage which increases the over-all regulation of the voltage applied to the collector at Q3 in reference to common minus.

The final characteristic of the Model 95710 power supply (average production unit) is as follows:

Input voltage range	95-135 v
Input frequency	400 cps ± 10 per cent
Output voltage	50 v adjustable ± 5 per cent
Line voltage regulation for ± 10 per cent line voltage change	± 0.003 per cent (± 1.5 mv)
Load regulation	0.006 per cent (3 mv)
Output impedance	0.02 ohm
Ripple	0.02 per cent (10 mv)
Output voltage temperature stability	-0.7 mv (0.0015 per cent) per 1°C.

Line voltage regulation, load regulation, and output impedance can be made positive, zero, or negative by adjusting R_5 and R_{10} .

Temperature influence is compensated by R_6 which is made of copper wire. A little higher value of this resistor would improve thermal stability of the output voltage.

LIST OF COMPONENTS

D1-D5	Silicon rectifier 3DS1, International Rectifier Company
D6-D7	Diode 1N298
ZR-ZR5	Zener reference element IN430A, National Semiconductor Co.
R1	1 kohm $\frac{1}{4}$ W ± 10 per cent carbon
R2	39 kohm $\frac{1}{4}$ W ± 10 per cent carbon
R3	1 kohm ± 10 per cent W.W.
R4	600 ohm ± 10 per cent W.W.
R5	500-ohm trimpot
R6	70-ohm temperature compensating resistor made of copper wire
R7	600 ohms ± 2 per cent W.W.
R8	500-ohm trimpot
R9	3900 ohms ± 2 per cent W.W.
R10	2.5- to 3-ohm W.W. positive feedback resistor (load change compensation)
R11	900 ohms ± 2 per cent W.W.
C1, C2, C4	1- μ f 200 VDCW
C3	4- μ f 6 VDCW tantalum capacitor
C5	80- μ f 60 V tantalum capacitor
Q1	970 } Texas Instrument Company.
Q2	953 } silicon transistors
Q3	951 }

T. F. KOPACZEK
Angle Computer Co., Inc.
Glendale, Calif.

Use of Microwave Ferrite Toroids to Eliminate External Magnets and Reduce Switching Power*

In most microwave ferrite devices, the ferrite element must be situated in a strong, constant magnetic field for proper operation. In the traverse field type of device, this magnetic bias is commonly supplied by a heavy electromagnet or permanent magnet which usually dwarfs the microwave structure. If the traverse field ferrite device under consideration is a circulator, then the ports of the circulator between which there is complete transmission or rejection may be rearranged or switched by reversing the biasing magnetic field. There are two rather serious difficulties with this procedure. The first difficulty is the high value of power needed to perform the switching. Uebele¹ estimates this power at 1800 watts for a one-microsecond switching time. The second difficulty is the problem of propagating the pulse through the conducting walls of the waveguide. Since a one-tenth microsecond pulse contains frequencies up to 10 mc, this problem is quite serious in going to higher switching speeds.

To solve the problems mentioned above, the use of microwave ferrite toroids has been proposed in three ferrite devices. Two of these devices have been constructed and experimental verification has been obtained. How ferrite toroids may be used to replace ferrite slabs in two nonreciprocal phase shifters is shown in Fig. 1. In Fig. 1(a) is shown the end view of a rectangular waveguide nonreciprocal phase shifter using two slabs oppositely magnetized² by an external magnetic structure, which is not shown. Fig. 1(b) shows how these slabs may be replaced by ferrite toroids. A single wire is shown going through the center of the toroids. It is through this single wire that the switching pulse is passed. The coaxial phase shifter,³ shown with ferrite slabs in Fig. 1(c) and with ferrite toroids in Fig. 1(d), may be switched by passing the switching pulse through the center conductor. A coupled wave type circulator⁴ and its toroid counterpart are shown in Fig. 2.

Besides reducing the switching power and the elimination of the external magnet, there are additional advantages which accrue from the use of toroids. Since the toroid is essentially a magnetic circuit with a zero demagnetizing factor, the magnetizing current through the central wire may be reduced to zero and the flux density in the toroid will remain at the remanence value. If the ferrite material has a reasonably square hysteresis loop, then the remanence value will be close to the saturation value and there will be no need to maintain the magnetizing current. Thus, besides eliminating the external magnet, the magnetizing current may be eliminated.

* Received by the IRE, February 28, 1958.

¹ G. S. Uebele, "High-speed ferrite microwave switch," 1957 IRE NATIONAL CONVENTION RECORD, pt. 1, pp. 227-234.

² B. Lax, K. J. Button, and L. M. Roth, "Ferrite phase shifters in rectangular wave guide," *J. Appl. Phys.*, vol. 25, pp. 1413-1421; November, 1954.

³ Max Sucher and H. J. Carlin, "Coaxial line nonreciprocal phase shifters," *J. Appl. Phys.*, vol. 38, pp. 921-922; August, 1957.

⁴ H. J. Carlin, "Nonreciprocal network theory applied to ferrite microwave devices," *Proc. IRE*, vol. 104, pt. B, supplement no. 6; June, 1957.

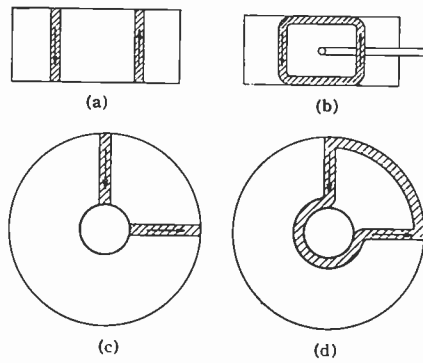


Fig. 1

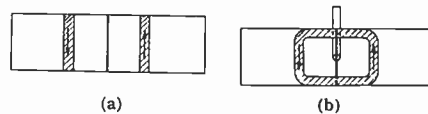


Fig. 2

Another advantage results in the fact that the two sides of the toroid may be brought much closer together than the two slabs used in the nontoroidal geometries. With an external magnet, as the slabs of ferrite are brought closer together, the *N* and *S* poles of the external magnet approach each other and the flux is shunted directly across the poles with very little going through the ferrites. A toroid may be made very narrow before shunting difficulties arise. The microwave advantages of using narrow toroids result from the fact that in all three cases shown above, more differential phase shift per unit length may be obtained as the slabs approach each other.²⁻⁴ Therefore, shorter waveguide structures will result.

Of the three devices mentioned above, the two rectangular geometries have been constructed and tested with ferrite toroids made in our own laboratory. The construction of the coaxial geometry has been delayed by the odd shape toroids required, which are now in the process of being fabricated by ultrasonic techniques. It was found possible to switch both the rectangular waveguide circulator and the coupled wave circulator in less than one tenth microsecond. The peak power of the switching pulse used was approximately 50 watts. However the ferrite saturates at much lower power. This peak power was required only to get a steep front edge for switching and very probably the power can be considerably reduced when a pulse with a shorter rise time is used.

In another series of experiments the nonreciprocal phase shift in the rectangular phase shifter of Fig. 1(b) was measured with the current on and off. The results indicated in one case that the nonreciprocal phase shift was 40° with the current on and 30° with the current off. This gives what might be called a "microwave squareness factor" of 0.75. No change in the 30° figure was observed even after the toroids were allowed to stand for several days without application of current. This tends to indicate that the remanence value of the flux density in the toroids was retained. Preliminary results, with ferrite material fabricated in our laboratory for this specific application, were

very encouraging since they indicated that improvement in the microwave squareness factor was feasible.

The authors wish to acknowledge the support of the Evans Signal Laboratory of the U. S. Army Signal Engineering Laboratories under Contract No. DA-36-039 SC-72327.

M. A. TREUHAFT
L. M. SILBER
Microwave Res. Inst.
Polytechnic Inst. of Brooklyn
Brooklyn, N. Y.

A Theorem for Dissipationless Networks*

I believe it is worthwhile mentioning that the theorem of Jones and Cohn¹ concerning insertion loss is a special case of a more general one, and is obtainable in a much simpler and more physical way.

Let us suppose that a dissipationless resistance-terminated network consists of two (not necessarily identical) networks *N*_a and *N*_b in tandem (see Fig. 1). According to Thévenin's theorem this can be substituted by the network in Fig. 2 at least as far as the central voltage and current are concerned, where *E*' is the open-circuit voltage at the terminals 22'. Evidently

$$I = \frac{E'}{Z_1 + Z_2} \quad (1)$$

and the power dissipated by *Z*₂ is given by:

$$P_2 = |I|^2 \text{Re}(Z_2) = \frac{1}{2} |I|^2 (Z_2 + Z_2^*) \quad (2)$$

where (*) means conjugation. This power is certainly equal to that dissipated by the termination *R*_L because this is the only resistive element in *Z*₂ which can dissipate power.

Now the equivalent generator of Fig. 2 with open-circuit voltage *E*' and impedance *Z*₁ is capable of delivering a maximum power which is obtainable if we terminate this generator with the conjugate impedance *Z*₁*:

$$P_{1 \max} = \frac{|E'|^2}{4 \text{Re}(Z_1)} = \frac{|E'|^2}{2(Z_1 + Z_1^*)} \quad (3)$$

It is easy to prove by elementary methods that this power is the maximum obtainable power which can be furnished by the original generator with open-circuit voltage *E* and impedance *R*_g. This is due to the fact that if we terminate *N*_a on terminals 22' by *Z*₁* the generator will see a termination on terminals 11' exactly equal to *R*_g. Under these circumstances however, the generator actually delivers the maximum possible power into its termination which can be dissipated only by the real part of *Z*₁* which is the only resistance in the network facing the generator.

Finally the inverse square of the modulus of the transfer coefficient is given by the

* Received by the IRE, February 14, 1958.

¹ E. M. T. Jones and S. B. Cohn, "Two theorems for dissipationless symmetrical networks," *Proc. IRE*, vol. 45, p. 1016; July, 1957.

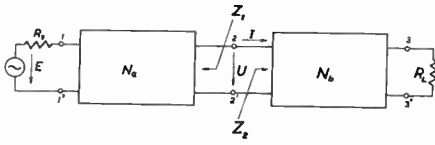


Fig. 1

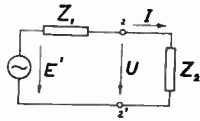


Fig. 2

ratio of these two power expressions, which results after substituting (1) into (2):

$$\frac{1}{|T|^2} = \frac{P_{1max}}{P_2} = \frac{|Z_1 + Z_2|^2}{(Z_1 + Z_1^*)(Z_2 + Z_2^*)} = 1 + \frac{(R_1 - R_2)^2 + (X_1 + X_2)^2}{4R_1R_2} \quad (4)$$

if we use the notation $Z_1 = R_1 + jX_1$ and $Z_2 = R_2 + jX_2$. This is the general theorem and a series of known results can be obtained from it in particular cases. The special expressions concerning the symmetrical and antimetrical configurations which have some significance in certain design methods, were known before the cited date of Jones and Cohn² and an equation similar to (4) but expressed as a transfer impedance was known as early as 1948.³

G. SZENTIRMAI
Standard Telephones and Cables Ltd.
London, Eng.

² E. A. Guillemin, "Synthesis of Passive Networks," John Wiley & Sons, Ltd., New York, N. Y. ch. 11, art. 6; 1957.
³ *Ibid.*, ch. 13, art. 5.

Cutoff Voltage Characteristics of TV Picture Tubes*

The cutoff voltage, *i.e.*, the voltage on the first grid (or cathode) of a crt required for visual extinction of the picture on the screen, represents an important design parameter. The maximally available emission current increases with increasing cutoff voltage while the average transconductance decreases at the same time. The cutoff voltage determines also the maximally required video signal. The "gamma" of the tube is correlated with the cutoff voltage; this correlation is important for achieving a monochromatic gray scale in tricolor picture tubes.¹

The cutoff voltage for *grid modulation* (the *positive* video signal is applied to the first grid) is given by:²

$$V_c = DV_{g2} \quad (1)$$

with D = penetration factor for the second grid voltage, V_{g2} = second grid voltage (with respect to ground), and where D is expressed by:

$$D = K_1 \frac{D_{g1}^3}{d_{g1}d_{g2}} \quad (2)$$

with

- D_{g1} = diameter of the first grid aperture,
- d_{g1} = spacing between cathode and (outside of) first grid,
- d_{g2} = spacing between first and second grid,
- K_1 = constant.

Note, that (2) is not valid for $d_{g1} < \frac{1}{2}D_{g1}$ (see below).

The cutoff voltage characteristic for *cathode modulation* (the *negative* video signal is applied to the cathode and the first grid is grounded) can be obtained from (1) by substituting: $V_{g2} \rightarrow V_{g2} - V_c$, the potential difference between cathode and second grid in the cutoff point of the current characteristic. We obtain then:³

$$V_c = \frac{D}{D+1} V_{g2} \quad (3)$$

While (2) expresses proportionality between the cutoff voltage and the penetration factor for grid modulation, (3) states that the cutoff voltage as function of D approaches a finite maximal value with D increasing. This conclusion can be verified easily by forming the first and second derivatives of (3) after D . We obtain:

$$\left. \begin{aligned} \frac{\partial V_c}{\partial D} &= V_{g2} \frac{1}{(1+D)^2} > 0 \\ \frac{\partial^2 V_c}{\partial D^2} &= V_{g2} \frac{1}{(1+D)^3} > 0 \end{aligned} \right\} \quad (4)$$

The saturation effect expressed by (4) is of practical importance for tubes having a penetration factor of $\frac{2}{3}$ or larger. Such a high penetration value may be conveniently obtained by decreasing the cathode-first grid spacing ($d_{g1} < \frac{1}{2}D_{g1}$). As mentioned above, (2) expressing the penetration factor as function of gun design parameters is not valid for $d_{g1} < \frac{1}{2}D_{g1}$ as an analysis of Klemperer's experimental results indicates.⁴ The penetration factor now has to be expressed by:

$$D = K_2 \frac{D_{g1}^{5/2}}{d_{g1}^{3/4}d_{g2}^{3/4}} \quad (5)$$

K_2 is a constant. Substituting (3) into (5) leads to

$$V_c = \frac{K_2 D_{g1}^{5/2}}{K_2 D_{g1}^{5/2} + d_{g1}^{3/4}d_{g2}^{3/4}} V_{g2} \quad (6)$$

Eq. (6) states that the cutoff voltage as a function of the cathode-grid spacing shows pronounced saturation with decreasing cathode-grid spacing values. In other words, V_c approaches a finite value for $d_{g1} \rightarrow 0$ and $D_{g1} \rightarrow \infty$.

From the above expression it follows that tubes employing a small cathode-first

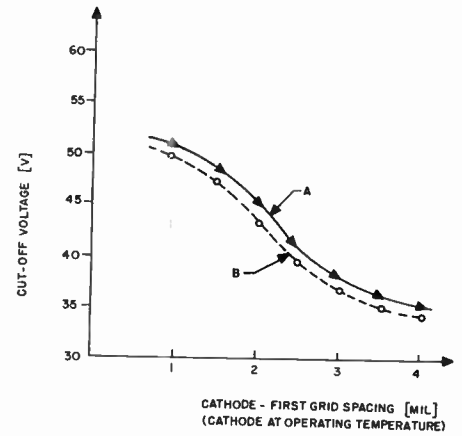


Fig. 1—Cutoff voltage in cathode modulation as function of the cathode-first grid spacing.

grid spacing and a high penetration factor are self-regulating on the upper limit of the cutoff voltage range if operated in cathode modulation.

The cutoff voltage at constant second grid voltage is depicted as function of the cathode-first grid spacing in Fig. 1. Curve A shows the theoretical results, calculated according to (6) with a numerical value for K_2 determined experimentally for the gun design considered here. Curve B shows the experimental results. It can readily be seen that the cutoff voltage approaches a finite value for the cathode-first grid spacing approaching zero.

W. F. NIKLAS
The Rauland Corp.
Chicago, Ill.

A Study of Earth Currents Near a VLF Monopole Antenna with a Radial Wire Ground System*

The efficiency of antennas for very low radio frequencies is determined to a large extent by the ohmic losses in the soil near the base of the antenna. It is customary to install a radial wire ground system buried just below the surface of the earth. The purpose of this wire grid is to provide a low-loss return path for the antenna base current in an effort to improve the efficiency of transmission.

The rules for ground system design in the past have been usually empirical and based on the results of experiments on existing installations. The first attempt to design an optimum system was carried out by Abbott.¹ Extensive calculations of the input resistance of a monopole with a radial wire ground system have been carried out by

* Received by the IRE, February 24, 1958.
¹ W. F. Niklas, "Some considerations concerning the gamma of tri-color picture tubes," *J. SMPTE*, vol. 65, pp. 546-551; October, 1956.
² H. Moss, "The electron gun of the cathode ray tube," *J. Brit. IRE*, vol. 6, pp. 99-124; June, 1946.

³ W. F. Niklas, C. S. Szegho, and J. Wimpffen, "Fernsehbildrochre fuer Kathodensteuerung mit erhoehter effektiver Perveanz," *Arch. Uebertr.*, vol. 12, pp. 54-60; February, 1958.
⁴ O. Klemperer, "Electron Optics," Cambridge University Press, Cambridge, Eng., p. 266; 1953.

* Received by the IRE, March 11, 1958.
¹ F. R. Abbott and C. J. Fisher, "Design of Ground System of Radial Conductors for a VLF Transmitter," U. S. Navy Electronics Lab. Rep. No. 105; February 10, 1949.

Wait and Pope.^{2,3} It should be emphasized that in this latter work no attempt was made to evaluate the losses associated with high-voltage insulators, tuning coils, and copper losses. The attention was devoted to the ohmic losses in soil and their dependence on number and length of radial wires. Furthermore, the radial wires were assumed to be in intimate contact with the soil being located just below the air-earth interface. The working formula for the component of the input resistance, ΔR , due to ohmic losses in the soil is given by

$$\Delta R \cong \text{real part of } \frac{1}{I_0^2} \int_0^\infty [H_t^\infty]^2 Z(\rho) 2\pi\rho d\rho \quad (1)$$

where I_0 is the base current of the antenna, H_t^∞ is the tangential magnetic field of the antenna assuming a perfectly conducting ground plane, ρ is the distance measured along the ground plane from the base of the antenna, and $Z(\rho)$ is the effective surface impedance of the actual ground plane. $Z(\rho)$ was taken to be equal to the intrinsic impedance of the soil, η , in parallel with the surface impedance of the radial wire grid, Z_s . That is,

$$Z(\rho) = \frac{\eta Z_s}{\eta + Z_s} \quad \text{for } \rho < a$$

$$= \eta \quad \text{for } \rho > a \quad (2)$$

where

$$\eta = \left[\frac{i\mu\omega}{\sigma + i\omega\epsilon} \right]^{1/2} \cong \left[\frac{i\mu\omega}{\sigma} \right]^{1/2}$$

and

$$Z_s = \frac{i\mu\omega d}{2\pi} \ln \frac{d}{2\pi c}$$

where a is the length of the radial wires, μ is the permeability of the ground ($\cong 4\pi \times 10^{-7}$), ω is the angular frequency, σ is the ground conductivity in mhos/meter, ϵ is the dielectric constant of the ground, c is the radius of the radial wires, and d is the spacing between the wires. (If there are N radial wires equally spaced about the base of the antenna, $d \cong 2\pi\rho/N$.)

The validity of (2) for the composite surface impedance was not established in the above mentioned work. The expression used for Z_s , the equivalent shunt impedance for a wire grid, was taken to be the same as that for an infinite parallel wire grid in free space. A recent analysis indicates that the equivalent shunt impedance for an infinite wire grid in the plane interface of two homogeneous media is indeed almost identical to Z_s for the isolated grid if the interwire spacing, d , is always much less than a wavelength in the electrically denser medium.⁴ In the present situation, this restriction is equivalent to stating that d should be somewhat less than an electrical skin depth in the soil, that is $d \ll (2/\sigma\mu\omega)^{1/2}$. In most practical cases this condition is met. A question also rises as to

the applicability of the formula for surface impedance of a parallel wire grid to a radial wire grid system where the wire spacing is not constant. Furthermore, the wires are not of infinite length being terminated by rods or some other means at a finite distance from the base of the antenna. The assumption that the radial wire behaves locally as a parallel infinite wire grid would seem to be very difficult to justify on purely theoretical grounds. It could be expected, however, that, if the length of the radial wires is large compared to a skin depth in the soil, the wave reflected from the end of the radial wires would be highly attenuated.

As a check of the wire grid theory for antenna ground loss calculations, an experimental test was carried out in Cutler, Me., which is the proposed site of a high-power (1-megw) vlf transmitter for the U. S. Navy. A small test antenna was erected on the site and radial wires were installed in the same manner as in a permanent installation. The actual currents carried by the wires were measured using a small loop pickup placed in proximity to the wires. The average currents carried by the ground were also measured. Now the ratio of the total current carried by the wires, I_w , to the current in the soil, I_s , is equal to the ratio of the surface impedance, η , of the soil to the surface impedance, Z_s , of the grid.² Therefore, such a test of the splitting of the current between the radial wires and the ground is a good check on the validity of the theory.

Before discussing the experimental results⁵ calculations of I_w are presented for pertinent values of the parameters. Denoting the effective antenna height by h , the tangential magnetic field, H_t^∞ , on the ground plane at distance ρ from the base is given by

$$H_t^\infty \cong \frac{I_0}{2\pi} \frac{h}{\sqrt{\rho^2 + h^2}}$$

for $\rho \ll \text{wavelength}$. Actually, H_t^∞ is the radial current density in amperes per meter emanating from the antenna for an idealized perfectly conducting ground plane. In the case of the imperfect conducting ground with the radial wire ground system present, the total ground current, I_t , is essentially numerically equal to H_t^∞ and is composed of two parts, I_s , the total earth current and, I_w , the total wire current. We can now write, for purposes of computation,

$$X = \left| \frac{I_w}{I_t} \right| = \left| \frac{1}{1 + \eta/Z_s} \right|$$

$$= \frac{\sqrt{2}p}{[p^2 + (p+q)^2]^{1/2}}$$

where

$$p = 120\pi\delta/\sqrt{2} \quad \delta = (\epsilon_0\omega/\sigma)^{1/2}$$

and

$$q = \frac{240\pi^2 P}{N} \ln \frac{P}{NC}$$

$C = c/\lambda$, $P = \rho/\lambda$. The amplitude of the current in one radial wire, I_w , is then given by

$$I_w = \frac{I_t}{N} = \frac{I_0}{2\pi N} \frac{h}{\sqrt{\rho^2 + h^2}} X$$

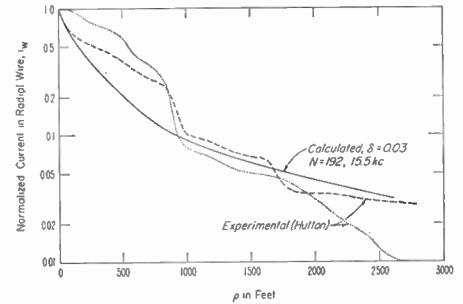


Fig. 1—Decay of current in radial wire as a function of distance ρ from base of antenna.

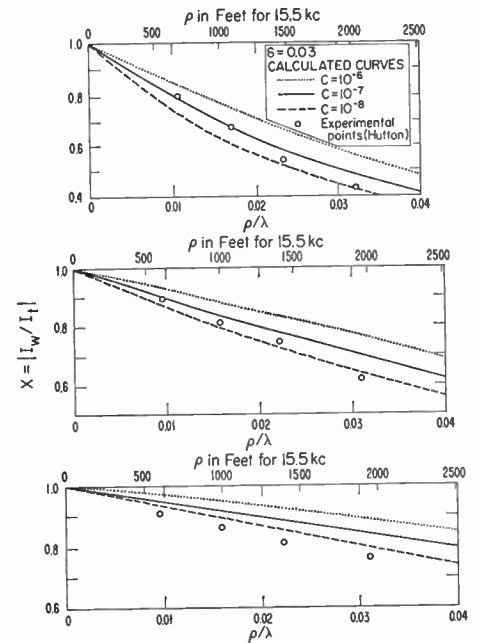


Fig. 2—Comparison of calculated and observed currents in radial wire, for $N=48, 96$, and 192 reading from top to bottom.

In Fig. 1 the computed current, I_w , normalized to unity at $\rho=0$, is shown plotted as a function of ρ in feet for $h=100$ feet, $\lambda=63,400$ feet (15.5 kc), $N=192$, $\delta=0.03$ ($\sigma=1$ milli-mho/meter), $C \cong 10^{-7}$ (no. 8 wire, awg at 15.5 kc). In Fig. 2, computed values of X are shown plotted as a function of ρ/λ for $N=48, 96$, and 192 , respectively. Various values of C are indicated on the curves.

In the experimental setup, the antenna was a monopole with a height of 100 feet with a circular capacity hat with a radius of about 200 feet. In view of the difficulty in clearing land in the heavily wooded and rocky terrain of Maine, it was not feasible to employ many radials emanating in all directions from the antenna. To effect a compromise three radials at azimuth angles of $0^\circ, 180^\circ$, and 270° were installed. The sector between about 60° and 100° was then selected as the region for further tests. In case 1, this sector was filled with radials at an angular separation of 7.5° , in case 2 it was 3.75° , and in case 3 it was 1.88° . For these three separations the equivalent value of N would be 48, 96, and 192 respectively.

The indicated points in Fig. 1 are measured current values in two of the central

² J. R. Wait and W. A. Pope, "The characteristics of a vertical antenna with a radial conductor ground system," *Appl. Sci. Res.*, B, vol. 4, pp. 177-195; 1954.

³ J. R. Wait and W. A. Pope, "Input resistance of l. f. unipole aerials," *Wireless Eng.*, vol. 32, pp. 131-138; May, 1955.

⁴ J. R. Wait, "On the theory of reflection from a wire grid parallel to an interface between homogeneous media," *Appl. Sci. Res.*, B, vol. 6, pp. 259-275; 1956.

⁵ W. G. Hutton and C. E. Smith, "Navy VLF Site Location Project," Final Rep., Smith Electronics Inc., Cleveland, Ohio; 1957.

wires of the fan as a function of ρ . The ordinates are normalized to unity at $\rho=0$. In this case the base current of the antenna was kept constant at about 1.0 ampere. There is a general agreement with the calculated curve. Discrepancies could be ascribed to the varying nature of the soil conductivity along the radial wires. Measurements of soil conductivity by the four-probe method indicated a random variation of 50 per cent about 1.0 milli-mho/meter. The abnormally large measured values of i_w for the smaller values of ρ in Fig. 1 might be ascribed to the asymmetrical variation of the total earth current resulting from using a fan of radials rather than a complete array equally spaced for 360°.

A more appealing experiment which overcomes to some extent the asymmetry of the experimental setup is carried out as follows. The receiving coil is moved in a direction transverse to the radial wires at a constant height and constant distance ρ . The measured magnetic field is then essentially constant for the region between the wires and rises to rather pronounced maxima over the wires. The ratio of the maximum field to that between the wires is denoted by B which is given by the relation

$$B \cong \frac{|I_w|/2\pi s}{|I_0|/d}$$

where s is the height of the receiving or pickup coil above the wire and d is their separation. Now, since the current in the wire lags the current in the ground by 45°, it follows that³

$$\frac{I_w}{I_0} = \frac{2\pi s}{d} B e^{-i\pi/4}$$

or

$$X = \left| \frac{I_w}{I_0 + I_w} \right| = \left[\frac{2A^2}{1 + 2A + 2A^2} \right]^{1/2}$$

with

$$A = \frac{\sqrt{2\pi s}}{d} B.$$

Values of X calculated from the experimental data are shown plotted in Fig. 2, for $N=48, 96$, and 192 respectively for $s=4$ feet and $d=2\pi\rho/N$. The agreement between the experimental points and the calculated curve for $C=10^{-7}$ (no. 8 wire at 15.5 kc) is quite good for the two cases of $N=48$ and 96 . The departure for the case $N=192$ can be attributed to contribution from the current in the wires to the measured field in the minimal position.

In general, one may say that satisfactory agreement between theory and experiment has been reached. Therefore, further justification is given to the validity of the published calculations of the ground loss component of the base resistance of a monopole with a radial conductor ground system. It should be mentioned, however, that the present study has not considered losses within the aperture or near the base of the antenna. Recent studies by Gustafson, Devaney, and Smith⁶ indicate that these

losses may be quite large in special antennas for high-power vlf installations.

The author wishes to thank A. D. Watt and T. E. Devaney for helpful advice, C. E. Smith and W. G. Hutton for permission to quote their experimental results, and Anabeth Murphy for assistance with the calculations.

JAMES R. WATT
Nat. Bur. of Standards
Boulder, Colo.

Design of Video Amplifiers with Stringent Electrical and Mechanical Requirements*

In the special pulse application where high gain, large dynamic range, wide pulses, and fast rise times must be handled simultaneously at low input signal levels, 10 mv or less, prior limiting is not practical. The most applicable circuit, to date, is the inverse feedback pair.¹ However, if, in addition, one wishes to reduce the effects of severe mechanical environment to a minimum, low microphonic tubes must be utilized (Sylvania's new line of ruggedized tubes 6943-44, etc.). However, the g_m of these tubes is notoriously low—about half a nonruggedized tube. Rather than use the standard feedback pair circuit where every other tube is biased, the number of envelopes and, consequently, the space and weight, may be reduced by the circuit in Fig. 1 which has a higher average g_m throughout several stages.

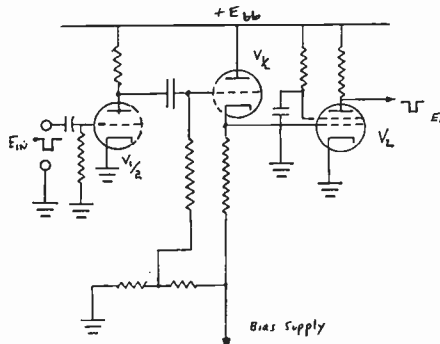


Fig. 1.

By use of this circuit as a basic building block, an amplifier was built which had zero recovery time² after a 10- μ sec pulse and met the following specifications:

Voltage Gain	3500
Dynamic Range	40 db (voltage)
Pulse Width	1 to 50 μ sec
Rise Time+Delay Time	0.08 μ sec (10 per cent input to 90 per cent output)
Minimum Signal	10 mvs
Ambient Temperature	-55° C to 71° C

* Received by the IRE, March 24, 1958.

¹ Valley and Wallman, "Vacuum Tube Amplifiers," McGraw-Hill Book Co. Inc., New York, N. Y., M.I.T. Rad. Lab. Ser., vol. 18, p. 134; 1948.

² Time to recover original sensitivity after largest signal input.

It can be noted that every amplifier tube in the circuit is running at, or near, zero bias, a condition of maximum g_m . The normal coupling capacitors may be balanced with decoupling networks to yield minimum overshoot for pulse widths of concern. The low gain/stage permits use of dual triodes without appreciable Miller effect. The total power consumed in this circuit is less than a feedback pair with the same specifications.

J. A. DEVELET, JR.
The Ramo-Wooldridge Corp.
Los Angeles, Calif.

Networks of Fixed and Variable Resistors*

Recently, Levenstein has discussed the properties of a network of linear rheostats, all fixed to one shaft.¹ These properties, as functions of the shaft rotation, are similar in form to the properties of a network of resistors and inductors as functions of frequency.

It is interesting to apply these ideas to networks of resistors, some of which are fixed while the others have their resistance controllable by some influence other than a shaft rotation. One might have, for instance, a network of fixed resistors and thermistors, the controlling influence being the temperature.² Similarly, there might be networks of fixed resistors and of photosensitive resistors, or of fixed resistors and magnetically controlled resistors.³

Thus the networks would consist of two types of resistors; one whose resistance was constant, the other having a resistance proportional to some quantity x . For the thermistors, for instance, x would be of the form $x_0 \exp(\phi/kT)$, x_0 and ϕ being constants, k Boltzmann's constant, and T the temperature.² For the photoresistors, x would be of the form $x_0 - aI$, a being a constant and I the intensity of illumination, and for the magnetically controlled devices one would expect x of the form $x_0(1 + \mu^2 B^2)$, μ being the carrier mobility and B the applied magnetic field.³ All these cases are simpler than that of the rheostats in that there will be no resistance varying as $1-x$. Accordingly, one may adapt Levenstein's first and second propositions directly, ρ being replaced by x , so that:

- 1) The driving-point impedance of the network under consideration is a rational function of x , the degree of the numerator being equal to or one more than the degree of the denominator. The zeros and poles are simple, real, and negative, and they alternate. The singularity closest to the origin is a zero.

* Received by the IRE, February 20, 1958.

¹ H. Levenstein, "Theory of networks of linearly variable resistances," Proc. IRE, vol. 46, pp. 486-493; February, 1958.

² A. van der Ziel, "Solid State Physical Electronics," Prentice-Hall Inc., New York, N. Y., sec. 19.3; 1957.

³ R. K. Willardson and A. C. Beer, "Magnetoresistance—new tool for electrical control circuits," Elec Mfg., vol. 57, pp. 79-84; January, 1956.

⁶ W. E. Gustafson, T. E. Devaney, and A. N. Smith, "Ground System Studies of High Power V.L.F. Antennas," paper no. 38, Record of the VLF Symposium, Boulder, Colo.; January 23-25, 1957.

2) The transfer function is a rational function of x , the order of the numerator being equal to or less than that of the denominator. The poles are simple real, and negative; the zeros may occur anywhere in complex conjugate pairs.

It would be possible to use this theory to obtain, e.g., a prescribed response in measuring devices. Thus, a network approximating the function $(\ln x)^{-1}$, made up of thermistors and resistors, might give a result linear in temperature.

Incidentally, in Levenstein's treatment, elements of resistance proportional to x and to $1-x$ (x being shaft rotation) are involved. An artifice reduces the problem to one in which there is only the variable $p = (1-x)/x$. It is suggested that this is done to avoid the difficulties of dealing with three kinds of element. The writer would suggest that another way of looking at the reason behind the substitution is as follows. The elements of the Z matrix could consist of constant terms, terms proportional to x , and terms proportional to $1-x$. Thus the coefficient of x in any element might be either positive or negative, according to the various values. This is in contrast to the usual network theory of elements which are functions of p , the complex frequency, where the coefficients of p are inherently positive.

Thus, in order to get a theory analogous to that of frequency-dependent elements, one must ensure that the coefficients be positive, and the substitution $(1-x)/x = p$ accomplishes just that.

H. L. ARMSTRONG
Pacific Semiconductors, Inc.
Culver City, Calif.

Space-Charge Grid High-Transconductance Guns*

There are two possible ways of using cathode-ray tubes in transistorized television receivers. In one approach a high enough drive voltage is obtained, in spite of the low supply voltage, by means of special circuitry. In the other approach a high-transconductance gun, i.e., a gun with low-voltage drive requirements, is used. The high-transconductance gun should deliver a (phosphor) screen current of the order of 500 μ a at a drive voltage of about 7 volts or less. A brief description is given now of the development which led to a design for a gun satisfying the requirements.

Most of the earlier high-transconductance guns required very close spacings. The resulting resolution was usually inferior to conventional guns. One of the approaches to a high-transconductance gun is to use a space-charge grid.^{1,2} The main increase in transconductance results from the move-

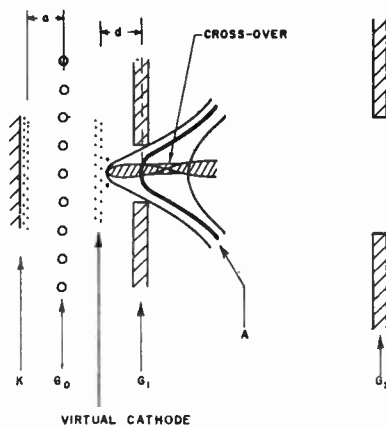


Fig. 1—Current control structure of space-charge grid gun.

ment of a virtual cathode, which serves as the electron source, toward the "anode" as the anode voltage of the "equivalent diode" is increased. The equivalent diode is defined by the virtual cathode and the anode. From Child-Langmuir's Law,

$$i = K \frac{V^{3/2}}{d^2}, \quad (1)$$

one can see that the current increases faster than with the three-half power of the anode voltage since the distance d between the virtual cathode and the anode decreases with increasing anode voltage.

The first design studied (Fig. 1) had a wire-mesh space-charge grid G_0 at a constant positive potential. Part of the current is injected through this grid into the space-charge grid (G_0)-control grid (G_1) space. G_1 is formed by an apertured disk. Electrons are drawn out by the accelerating field penetrating through G_1 . From available curves,³ one can see that maximum transconductance can be obtained when the following conditions are satisfied: 1) at maximum (phosphor) screen current i_{max} , i.e., at $V_{G_1} = 0$, the space-charge grid voltage V_{G_0} is equal to the potential of equipotential A , penetrating through G_1 ; and 2) equipotential A is located twice the cathode (K) space-charge grid (G_0) distance a . An increase of transconductance of 69 per cent results. A further increase of transconductance results from the movement of equipotential A during modulation. From an analysis one finds that the maximum possible total increase of transconductance is about 2.2. This result is for the case of equal cutoff voltage in a conventional gun and the space-charge grid gun. It should be kept in mind that the transconductance in a conventional gun increases with decreasing cutoff voltage. The characteristics are shown in Fig. 2. At 14,000-volt screen voltage blooming occurs at about 100 μ a screen current and, therefore, the first design does not satisfy present requirements.

The development led to a gun which fully satisfies the set requirements. In this

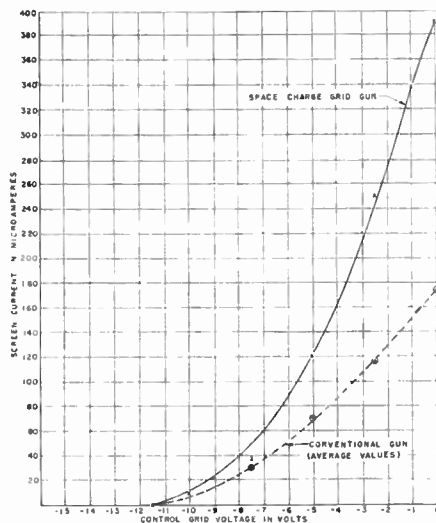


Fig. 2—Characteristic of first design of space-charge grid gun and average characteristic of conventional gun.

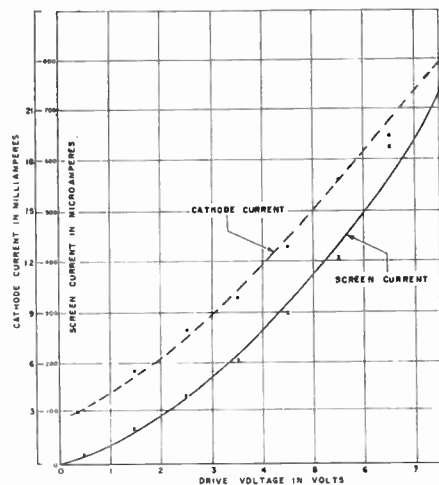


Fig. 3—Characteristics of second design of space-charge grid gun.

gun the space-charge grid which is at a positive potential is modulated. The phosphor screen current is a function of the supplied current to the virtual cathode as shown in the characteristics of Fig. 3. G_1 has primarily electron-optical functions. For this purpose G_1 is negatively biased. Should one maintain G_1 at a potential close to cathode potential, the virtual cathode could not exist any longer when approaching current cutoff and no proper crossover formation could take place. To minimize the reduction of transconductance by the negative bias at G_1 , this grid is modulated simultaneously with G_0 using cathode drive.

The resolution in a 17-inch, 90-degree tube at 14,000 volts was as good as in any conventional tube. Depth of focus was very good. When comparing the performance of such guns with that of conventional guns mounted in identical television sets, it was found that only about one-tenth drive voltage was required. At 7.5-volt drive voltage a screen current of about 700 μ a is obtained.

PAUL H. GLEICHAUF
General Electric Co.
Syracuse, N. Y.

* Received by the IRE, March 24, 1958.
¹ G. E. Condlife, I. Shoenberg, and W. F. Tedham, British Patent No. 431,327.
² British Patent No. 525,601.

³ C. E. Fay, A. L. Samuel, and W. Shockley, "On the theory of space charge between parallel plane electrodes," *Bell Sys. Tech. J.*, vol. 17, pp. 49-79; January, 1938.

Contributors

Richard B. Adler (A'44-SM'53) was born in New York, N. Y., on May 9, 1922. He received the B.S. and Sc.D. degrees in electrical engineering from the Massachusetts Institute of Technology, Cambridge in 1943 and 1949, respectively.

During the years 1944 to 1946 he was in the United States Naval Reserve assigned as instructor at the M.I.T. Radar School. After his discharge he became a part-time staff member at the Research Laboratory of Electronics, M.I.T., and since then he has been at M.I.T. in both a teaching and research capacity. His major interests have been in circuit theory, microwave field theory, and semiconductor devices. From 1951 to 1953 Dr. Adler was group leader of the M.I.T. Lincoln Laboratory Solid-State and Transistor Group. At present he is associate professor of electrical engineering at M.I.T.

Dr. Adler is a member of Sigma Xi and Eta Kappa Nu.

S. V. Chandrashekhar Aiya, for a photograph and biography please see p. 619 of the March, 1958, issue of PROCEEDINGS.

Dr. Helmut Brueckmann (SM'49-F'58) was born in Frankfort on Main, Germany, in 1906. He received the Dipl. Eng. degree in electrical engineering in 1930 from the Technical University of Berlin and the Doctor of Engineer degree in 1935 from the same university. From 1930 to 1937 he was a scientific consultant with the Central Technical Department of the German Reichspost. When the Research

Institute of the German Reichspost was founded in 1937, he headed a section there until the end of the war.

After an interim period as Chief Transmitter Engineer of Radio Frankfort, he joined the newly organized technical institute of the broadcast stations in the western zones of Germany as head of the Broadcast Transmitter Branch.

Since 1948 Dr. Brueckmann has been a consultant with the U. S. Army Signal Research and Development Laboratories, Fort Monmouth, N. J.

Edward A. Day was born in Saginaw, Mich., on March 4, 1919. He received the Bachelor of Science degree in mechanical engineering from the University of Michigan, Ann Arbor, Mich., in 1942.

From 1942 to 1946 Mr. Day served with the U. S. Navy. In 1946 he became associated with the Radiation Laboratory of the University of California, Berkeley, Calif. as a mechanical engineer.

From 1949 to 1956 Mr. Day was a research associate at the Department of Physics, University of Minnesota, Minneapolis, Minn.

Since 1956, he has been a mechanical engineer with the Midwestern Universities Research Association, Madison, Wis.

Richard Glicksman was born on October 3, 1924, in New York, N. Y. He received the B.S., M.S., and Ph.D. degrees in chemistry in 1948, 1949, and 1953, respectively, from New York University. At N.Y.U., Dr. Glicksman studied the kinetics of diffusion controlled reactions for his thesis problem; he also investigated metal-metal ion exchange and adsorption with the use of radioactive silver, under an Atomic Energy Commission Contract (1951-1952).

He also held a graduate assistantship at N.Y.U. from 1950-1952.

Prior to his work at N.Y.U., Dr. Glicksman spent three and one-half years in the service, during which time he studied meteorology at the Massachusetts Institute of Technology, Cambridge, Mass.

He was a weather officer in the Army Air Force, and attained the rank of First Lieutenant.

Dr. Glicksman joined RCA Laboratories, Princeton, N. J., in January, 1953, and since that time he has been actively engaged in electrochemical research. His work has covered a wide range of topics, including corrosion, battery, and electrochemical polarization phenomena.

Dr. Glicksman is a member of the American Chemical Society, Electrochemical Society, Sigma Xi, and Phi Lambda Upsilon. He recently was recipient of a 1957 RCA Achievement Award for outstanding research.

Hermann A. Haus was born in Ljubljana, Yugoslavia, in 1925. He attended the Technische Hochschule in Graz, Austria, from 1946 to 1948 and studied one term at the Technische Hochschule in Vienna. He attended Union College, Schenectady, N. Y., receiving the B.S. degree in 1949. He received the M.S. degree from the Rensselaer Polytechnic Institute, Troy, N. Y., in 1951 and the Sc.D. degree from the Massachusetts Institute of Technology Cambridge, in 1954.

He is now engaged in microwave tube research at the Research Laboratory of Electronics, M.I.T., and is also associate professor of electrical engineering.

Dr. Haus is a member of Sigma Xi.

Eugene E. Lampi was born on April 19, 1917 in Chisholm, Minn. He attended the Hibbing Junior College, majoring in electrical engineering. He received the B.E.E. degree in 1940, and the M.S. degree in physics in 1941, both from the University of Minnesota.

He was associated with the Naval Ordnance Laboratory, White Oak, Md., from 1941 to 1946, working on magnetic and acoustic instrumentation problems. He joined the Physics Department, University of Minnesota, as a research fellow in 1946. He received the Ph.D. degree in physics from that university in 1949.

From 1950 to 1957, he was a member of the Proton Linear Accelerator Group as a research associate. In 1957, Dr. Lampi joined the Bell Telephone Laboratories at the Allentown Laboratory as a member of the technical staff working on semiconductor diode development.

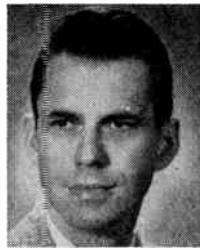
Dr. Lampi is a member of Eta Kappa Nu and Sigma Xi, and is a fellow of the American Physical Society.

Gerald S. Lozier was born on October 3, 1930, in Londonville, Ohio. He received the B.S. and M.S. degrees in chemistry in 1952 and 1953, respectively, and the Ph.D. degree in 1956, all from Western Reserve University, Cleveland, Ohio.

Dr. Lozier held a teaching fellowship



R. B. ADLER



E. A. DAY



H. A. HAUS



R. GLICKSMAN



E. E. LAMPI



H. BRUECKMANN

from September, 1950 to September, 1953, and received the Electrochemistry Society, Cleveland Section, Award for the most out-



G. S. LOZIER

standing student in Electrochemistry in the Cleveland Section area. From September, 1952 to December, 1954 he participated in ONR research at the Ultrasonic and Electrochemistry Research Laboratory of Western Reserve University on the investigation of ultrasonic effects on electrode processes. He joined RCA Laboratories in January, 1955, and has been doing battery research for the past two years.

Dr. Lozier is a member of the American Chemical Society and Electrochemical Society. He recently was recipient of a 1957 RCA Achievement Award for outstanding research.



George H. Millman (SM'53) was born in Boston, Mass., on June 2, 1919. He received the B.S. degree in physics from the University of Massachusetts in 1947, and the M.S. and Ph.D. degrees in physics, from Pennsylvania State University in 1949 and 1952, respectively.



G. H. MILLMAN

From 1942 to 1946, he was an electronics-radar officer in the United States Army Air Force, serving as officer-in-charge of an experimental radar project for the Far East Air Force. Military education consisted of communication training at Yale University and radar training at the Harvard-M.I.T. radar schools.

While at Pennsylvania State University, he was employed as a teaching and research assistant by the Department of Physics from 1947 to 1950, and as an instructor of engineering research by the Ionosphere Research Laboratory from 1950 to 1952

where he was engaged in the investigation of turbulence and wind movements in the ionosphere. In 1952, Dr. Millman became associated with the General Electric Company, working on problems related to airborne and ground radar systems analysis and radar antijamming research. Since 1955, he has been involved in experimental and theoretical studies in the field of electromagnetic-atmospheric propagation.

Dr. Millman is a member of the American Physical Society, American Association of Physics Teachers, Phi Kappa Phi, Sigma Pi Sigma, Pi Mu Epsilon, and Sigma Xi.



C. K. Morehouse was born in Boston, Mass., on April 8, 1917. He received the B.S. degree in chemistry in 1939 from Tufts College and the M.S. degree in chemistry from McGill University in 1940. He was a teaching fellow in chemistry at Tufts College from 1938-1939 and at Massachusetts Institute of Technology from 1946-1947. He was employed at the National Bureau of Standards as a research chemist in the field of electrochemistry. He received the Ph.D. degree from M.I.T. in February, 1947.



C. K. MOREHOUSE

From 1947 to 1949, he was a supervisor in charge of battery research at the Western Cartridge Plant of Olin Industries. From 1949 to 1951, he was assistant director of research of the Electrical Division, Olin Industries, and from 1951 to 1953, he was research and development manager of that division. Dr. Morehouse joined the technical staff of RCA Laboratories, Princeton, N. J. in January, 1953 and since then has been in charge of battery research in the Physical and Chemical Research Laboratory. He has been issued seven patents.

Dr. Morehouse is a member of the American Chemical Society, Sigma Xi, Electrochemical Society, and Alpha Chi Sigma. He was recipient of a 1957 RCA Laboratories Achievement Award for outstanding research and was elected to the Executive Committee of the Battery Division of the Electrochemical Society for 1956-1958.

Dr. Morehouse is a member of the American Chemical Society, Sigma Xi, Electrochemical Society, and Alpha Chi Sigma. He was recipient of a 1957 RCA Laboratories Achievement Award for outstanding research and was elected to the Executive Committee of the Battery Division of the Electrochemical Society for 1956-1958.

Harry J. Schulte was born in Newark, N. J. in 1925. He received the B.S. degree in physics from Rensselaer Polytechnic Institute in 1948. During the period of his graduate work at the University of Rochester he worked on and with the 130-inch cyclotron, and participated in the early work on X rays from mesonic atoms. He received the Ph.D. degree in physics from that institution in 1953.



H. J. SCHULTE

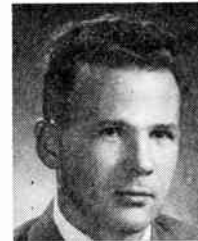
He was a research associate in physics at the University of Minnesota for the ensuing two years, participating in the construction of the 68-MEV Linear Accelerator.

Since July, 1955, Dr. Schulte has been a member of the technical staff at Bell Telephone Laboratories, Murray Hill, N. J., working on switching devices and digital computer systems.

Dr. Schulte is a member of the American Physical Society, Tau Beta Pi, and Sigma Xi.



Edmund B. Tucker was born in Wolfville, Nova Scotia, on May 6, 1922. His undergraduate work was completed in 1943 at Mount Allison University, Sackville, New Brunswick. After spending two years in the Royal Canadian Navy Volunteer Reserve as a radar officer he attended Oxford University, Oxford, England, and received the Ph.D. degree from Yale University in 1951.



E. B. TUCKER

For five years Dr. Tucker was a member of the Linear Accelerator group at the University of Minnesota. In mid-1955 he joined the staff of the General Electric Research Laboratory, Schenectady, N. Y., where he is presently employed.

Dr. Tucker is a member of the American Physical Society and Sigma Xi.



Scanning the Transactions

Push-button electronic classrooms are being proposed in which automatic teaching devices would perform many of the more routine teaching activities, thus freeing the teacher for matters requiring greater skill. In this hypothetical classroom of the future the student would sit at a chair equipped with a special set of push buttons. A teaching machine would present the lesson by means of motion pictures or tape recordings, asking questions of the student at each stage of the lesson. The student would answer by pushing one of several buttons. Based on the student's response the machine would repeat or enlarge on the material just covered, or go on to the next part of the lesson. A master control unit would adjust the speed with which the machine took the student through the lesson to the ability of the individual student to comprehend, at the same time recording his progress for later study by the teacher, who could then bring his full skills to bear on the particular need of each student during supplemental sessions.

Are proposals such as this pipe dreams? The answer is not too important. What is important is that we live in an age of technological revolution, and in applying our newly found skills we should not overlook the important field of teaching aids. Electronics is supposed to be the branch of technology that specializes in the transmission and processing of information. Surely somewhere in its vast storehouse of new techniques and devices there must be some that, if properly applied, would greatly increase the efficiency and effectiveness of the educational process. (S. Ramo, "A new technique of education," IRE TRANS. ON EDUCATION, June, 1958; P. K. Weiner, "A proposed 'automatic' teaching device," *ibid.*)

The Medical Electronics Center of the Rockefeller Institute, under the direction of Dr. V. K. Zworykin, has just completed preparation of a document which must be regarded as a major publication milestone in the young and sprawling field of medical electronics. We have reference to an extensive bibliography covering 2200 articles dealing with the application of the various branches of electronics, such as acoustics, communications, television techniques, spectrophotometry and dielectric heating, to the many problems of biological and medical research, therapy, public health and related fields. With the increasing pace of scientific investigation, the localization of information pertinent to any specialized branch of investigation becomes increasingly difficult. In a poorly defined interdisciplinary field such as medical electronics, this problem is all the more difficult. The bibliography, which includes both a subject and author index, for the first time makes readily accessible a major fraction of the work that has been done to date in this vitally important field. It has just been published by the IRE Professional Group on Medical Electronics, and is now available from IRE headquarters at \$2.50 per copy. ("Bibliography on Medical Electronics," published by PGME, June, 1958.)

Ceramics are usually thought of as insulators or dielectric materials. It may, therefore, surprise some to know there is one group of ceramics which may be classed as semiconductors or even conductors at room temperature. It is characteristic of these materials that as temperature increases their conductivity also increases, which is opposite to the effect found in metallic materials. The application of conductive ceramics to electronics is a wide-open field. These materials are only now in the embryo stage of development, research is moving very slowly, and the literature is practically void of any information on electronic applications. Among the most common ceramics in this class are the zinc, zirconium and tin oxides. Others in the group include various borides, carbides, nitrides and silicides. To date these materials have been used chiefly, as far as their electrical properties are concerned, as high-temperature resistance heating elements. However, they offer

many interesting possibilities in the realm of temperature compensating devices, the fabrication of high-temperature waveguides, and indeed in a wide variety of applications involving high temperature conditions. The electronics industry stands much to gain by investigating these unexploited new materials. (Z. A. Post and P. E. Ritt, "Conductive ceramics," IRE TRANS. ON COMPONENT PARTS, June, 1958.)

Unmanned space ships capable of orbiting about the moon have passed from the realm of science fiction and are now an acknowledged goal of the near future. If we wish to place instruments on board and telemeter information back to earth, what will be the requirements for the radio system? If we figure on a 10 watt transmitter aboard the vehicle operating at 2250 mc, a 500 kc bandwidth receiver, and make certain reasonable assumptions concerning the characteristics of other parts of the system, it turns out we can readily span the 260,000 miles with a 4.8 foot antenna on the vehicle and a 60 foot receiving antenna on earth. However, if the same ship is to orbit about a nearby planet some 100 million miles away, the problem becomes more formidable. The transmitting antenna will have to be increased to 60 feet in diameter, the receiving antenna to 84 feet, and the receiver bandwidth reduced to one kilocycle. These and other requirements imposed on the system probably could not be met by presently realizable techniques. However, there seems little doubt that the kinds of improvements that are needed to make a planetary telemetry system feasible will be well within our capabilities in the near future. (H. Scharla-Nielsen, "Space ship telemetry," IRE TRANS. ON TELEMETRY AND REMOTE CONTROL, June, 1958.)

Photomultiplier tubes have become an important tool for measuring extremely short time intervals. The accuracy of such measurements, however, is limited by small differences in the transit times of electrons in the tube caused by variations in their initial velocities and path lengths. An ingenious scheme for determining the extent of these differences has been developed by making the tube take a picture of its own performance. By presenting the output pulse on an oscilloscope and comparing its length with the known length of the test input pulse, it has been determined that the transit time deviations of commercial photomultipliers is on the order of one millimicrosecond. While this may seem trivial, it is a significant time interval to such people as nuclear physicists who wish to measure radioactive phenomena in the millimicrosecond range. (M. H. Greenblatt, "On the measurement of transit time dispersion in multiplier phototubes," IRE TRANS. ON NUCLEAR SCIENCE, June, 1958.)

The future of electronics lies to a great degree in its many applications to industrial processes. A brief glimpse of the diversity, as well as the growing importance, of this still-young branch of electronics is afforded by the program of last fall's annual Industrial Electronics Symposium. A glance at the menu of 16 papers reveals a veritable technical smorgasbord, from which we have culled the following sample tidbits: (1) a transistorized telemetering device for transmitting torque data from the rotors of high-speed machinery, (2) automatic machine tool control, (3) magnetic pickups for counting metal parts, (4) electrolytic method of counting and analyzing the size of minute particles, (5) gas analyzer based on speed of sound measurements, (6) electronic sorting of mail, (7) photoelectric control for automatic registration in multi-color printing, and (8) industrial measurements with X rays. (IRE TRANS. ON INDUSTRIAL ELECTRONICS, May, 1958.)

The semiconductor is making steady inroads into TV receiver circuits, judging from the latest issue of Broadcast and Television Receivers TRANSACTIONS. All three papers in the issue were devoted to one aspect or another of the subject.

Reverse biased junction diodes, which act as voltage variable capacitors, are proving to be practical for fine tuning and FM automatic frequency control circuits. Meanwhile, investigations into transistorized horizontal deflection, high voltage, and sound sections show a number of important advantages over the corresponding tube circuits, while the few remaining disadvantages are awaiting only the arrival of improved transistors before they, too, are overcome. (IRE TRANS. ON BROADCAST AND TELEVISION RECEIVERS, June, 1958.)

Electronic simulators, which have been used for a number of years to solve complex problems in the design and operation of various systems, are now finding important use in the study of heat transfer systems in nuclear power plants. Thus, electronics is placing still another important instrument at the disposal of the nuclear engineer, the analog computer. (S. O. Johnson, *et al.*, "Simulation of hot channel boiling in water-cooled reactors," IRE TRANS. ON NUCLEAR SCIENCE, June, 1958.)

Books

Physique Electronique des Gaz et des Solides by Michel Bayet

Published (1958) by Masson et Cie, Editeurs, 120 Boulevard Saint-Germain, Paris 6, France. 220 pages +21 appendix pages +2 index pages +1 bibliography page. 81 figures. 9½ × 6¼. 4,900 fr.

This book by Professor Bayet is intended for the graduate student and the specialist interested in the kinetics of electrons in the presence of other bodies. It is a text book for an advanced course in electronics.

The book starts with a review of fundamental concepts of statistical mechanics and of the two-body problem in classical mechanics. Then the author deals with the kinetic theory of gases involving up to three different types of particles. In Chapters III and IV Professor Bayet develops in detail the more sophisticated theories pertaining to a Lorentz gas and to the electromagnetic properties of plasmas. Then, for the sake of completeness, the multitudinous phenomena which can occur in ionized gases are covered in a brief description. The last two chapters are devoted to free electrons in metals and semiconductors. The book concludes with a set of appendices giving valuable relations for frequently used mathematical operations.

Those who only wish to get acquainted with the physical principles of gaseous electronics will appreciate the brevity of the book and regret that it is not available in English. About one hundred fifty pages are devoted to the explanation of various phenomena. Nowhere does the author dwell on experimental or technological detail. For experimental data (and for an extensive bibliography) the reader is referred to pertinent selections of the vast literature in this field.

The introductory chapter is somewhat sketchy because fundamental relations are introduced without derivation—more elementary texts are available for this. On the other hand, the advanced reader unfamiliar with the symbolism may not be able to start with the more advanced chapters without first browsing through the beginning of the book in search of definitions.

The distinguishing feature of this book is its exclusive concern with the kinetics of the electron gas with or without the interac-

tion of other particles (ions, molecules, holes or periodic structures).

M. Bayet is the product of France's outstanding school for physicists, the Physics Laboratories of the Ecole Normale Supérieure of Paris whose director, Professor Y. Rocard, has written the preface.

J. I. PANKOVE
RCA Labs.
Princeton, N. J.

The Exploration of Space by Radio by R. H. Brown and A. C. B. Lovell

Published (1958) by John Wiley & Sons, Inc., 440 Fourth Ave., N. Y. 16, N. Y. 201 pages +5 index pages +xii pages. 132 figures. 9½ × 6. \$6.50.

Considering the temper of the times it is not surprising that a book which is essentially a revision of *Radio Astronomy* by A. C. B. Lovell and J. A. Clegg, published in 1952, should now appear with the above title. Its appearance is timely not only for the great surge of interest in space research, as astronomy is now called, but because it has been three years now since the last book was published in English on the same general subject: *Radio Astronomy* by J. L. Pawsey and R. N. Bracewell. During these years several important advances and discoveries have been made.

The authors of *The Exploration of Space by Radio* are both eminent radio astronomers. Dr. Lovell is the Director of the Jodrell Bank Experimental Station of the University of Manchester, England. His foresight and courage are largely responsible for the erection of the world's largest steerable radio telescope, a 250-foot diameter reflector which has been nearly a decade in the making. His specialty is radio meteor astronomy; he is the author of the comprehensive treatise, *Meteor Astronomy* (Oxford, 1954). R. Hanbury Brown is noted for his outstanding ability in both electronics and astronomical research. His principle field of investigation has been the mapping of galactic radio emissions using the 218-foot fixed parabolic reflector at Manchester. In recent years he has collaborated with R. Q. Twiss in developing and exploiting a radically new method of measuring the size of both radio "stars" and optical stars using their principle of a correlation interferometer.

Their book is to be compared with *Radio*

Astronomy by Lovell and Clegg which appeared six years ago. An appreciable fraction of the figures and many pages of text in the book under review are taken directly from the book by Lovell and Clegg. Both books were written for the layman interested in radio or astronomy. The treatment is non-mathematical and clearly descriptive but is less adaptable for classroom use than is the text by Pawsey and Bracewell.

An outstanding feature of the book under review is the excellent reproduction of 27 photographs; ten are related to the 250-foot radio telescope. The last nine pages of the book are devoted to a description of this impressive instrument, to its general design and construction, to its observational program and its use as a radar antenna. The longest section covered is on radar studies of meteors. The second longest chapter is on techniques of radio astronomy. The radio engineer should be cautioned that he will find only block diagrams of the various arrangements of simple radio telescopes, interferometers, multi-antenna systems, radio spectrographs and polarimeters. This chapter is clearly written and is a pleasure to read. However, may I point out that in Figure 33, on page 48, the interference fringes should be drawn up and down, not slanted. The next topics covered, in the order of space allocated to them, are: continuum radio emission from the galaxy, solar radio emission, some properties of radio waves, the moon, the earth satellite and planets, a review of astronomy, hydrogen line radiation, scintillation of radio stars, and radio emission and reflection from aurora.

To the reviewer it was disappointing to find that the treatment of solar radio emission was not up to the high standard of the chapters on meteors and radio techniques. The over-all treatment of solar radio emission is a revised version of that given in the book by Lovell and Clegg, but was not brought up to date. The only new feature is the inclusion of a two-page discussion of cosmic radio wave emission from the sun during the great February 23, 1956 solar flare event. There is a one-sentence mention of dynamic spectra of solar bursts; a development in the early 1950's by Paul Wild which has made possible a major advance in the

understanding of radio emission from the sun. There is no mention of polarization of solar bursts, of the size of bursts, their spectrum or any recent work on the generation of radio waves from the sun. The occultation of the crab nebula by the solar corona is briefly mentioned.

A book of this nature is usually balanced in favor of the interests of the authors but it is regrettable that no mention is made of investigations in France, Japan, Germany, the Scandinavian countries and, with the exception of the theoretical work by Shklovsky and Ginzburg, Russia. The coverage of radio astronomy in England, Canada, United States and Australia is more complete than in the earlier book by Lovell and Clegg.

The book is very attractively arranged and put together. Although it is not entirely up to date in several areas, it is easy to read and is a good summary of much of the material treated.

The authors are to be congratulated in writing this popular book on radio astronomy. It is widely hoped that they will follow this up with a treatise on radio astronomy techniques.

F. T. HADDOCK
Univ. of Michigan
Ann Arbor, Mich.

Principles of Electrical Measurements by H. Buckingham and E. M. Price

Published (1957) by Philosophical Library, Inc., 15 E. 40 St., N. Y. 16, N. Y. 592 pages+8 index pages+xxiii pages. 418 figures. 8½×6. \$15.00.

This book covers the field of electrical measurements by breaking the various methods and instruments down into specific methods such as deflection instruments, deflection methods, potentiometer measurements, bridge methods, methods using thermionic valves, resonance and heterodyne methods, and so on. At places this division breaks down in favor of a division by usage, chapters such as the one on power system measurements or the one on the measurement of some non-electrical quantities cut across a variety of measuring systems and methods.

The book is not designed specifically as a text, although, it could be used by students in the advanced phases of electrical engineering as a text. By and large the flavor of the book is that of the standard type of measurements book giving the greatest emphasis to d-c and low frequency a-c measurements with only relative small part of the book on the high frequency measurements. Nothing at all is included on measurements in traveling wave systems such as wave guides or coaxial lines. The book covers 592 pages with 13 chapters of which a little over two chapters are devoted to radio frequency work. These chapters comprise approximately 130 pages.

The work on radio frequency measurements is really very well done, even though it is sketchy at times. For example electronic accounting, including scalars, gets a treatment two pages long. The development of the electron tube voltmeter is done very well and throughout this section of the book there are small examples of the importance of the magnitudes of the quantities involved done in small type. A person studying these

really should get a very good background in the principles described. The reviewer differs with the authors in regard to their discussion of input resistance of thermionic voltmeters since the authors do this in terms of the amount of power absorbed by the voltmeter whereas the reviewer prefers to think of the resistance as something which because of the input impedance of the source being measured will cause the voltmeter reading to be less than it should be. These two concepts are not always the same.

The introduction to the resonance circuit theory is exceedingly well done. In this chapter quartz crystals are discussed and in a few pages the authors cover the fundamental and basic characteristics of the crystal in a very excellent manner.

The rest of the book devoted primarily to dc and low frequency measurements is quite thorough and quite well written. In the section on deflection instruments the discussion of torque equations and scale shapes is most excellent and a student can learn well the theory of operation of these instruments from this book.

There are practically no references in this book to original work or to other books. This might be viewed as a defect inasmuch as a reader wishing to pursue a particular point might like to go beyond the boundaries of the book and explore the situation in greater detail.

If a reader does not already have in his library a basic book on electrical measurements, this would be an excellent book for that spot on the bookshelf.

G. B. HOADLEY
North Carolina State College
Raleigh, N. C.

An Introduction to the Theory of Random Signals and Noise by W. B. Davenport, Jr. and W. L. Root

Published (1958) by McGraw-Hill Book Co., Inc., 330 W. 42 St., N. Y. 36, N. Y. 382 pages+17 appendix pages+6 bibliography pages+3 index pages+ix pages. Illus. 9½×6½. \$10.00.

This well-planned and carefully-executed book is an expansion of notes prepared some years ago by Dr. Davenport for a one-semester graduate electrical engineering course at M.I.T. The book is divided roughly into two parts. The first half deals with the "development of those elements of probability theory and statistics which are particularly pertinent to a study of random signals and noises in communications systems." The second half is devoted to applications.

Specifically, the first half begins with a discussion of probability functions and random variables, and continues with averages, correlation, laws of large numbers, and spectral analysis. The first half concludes with careful treatments of two random processes—shot noise in vacuum tubes and the Gaussian process. The applications section starts with the analysis of the performance of linear systems with random inputs, including the derivation of some optimum linear systems for smoothing, prediction, etc. The following chapters discuss the performance of certain non-linear systems, specifically square-law detectors or vth-law devices (including ideal limiters). The book concludes with an excellent short introduction to the statistical

detection of signals, with examples from radar and communications applications.

The book is clearly intended for the theoretically-inclined engineer and not for the mathematical specialist. The specific prerequisites assumed are "some electrical network theory and an advanced engineering calculus course containing Fourier series and integrals," but what would really seem necessary is not so much a knowledge of particular topics as a degree of mathematical sophistication. The authors disavow any attempt at rigor, but they have not allowed their concern for lucidity to tempt them into easy rationalizations, careless arguments, or false generalizations. For example, consistent use is made of the Karhunen-Loève expansion of a random function over a finite interval, rather than the more familiar but less satisfactory trigonometric expansion. As a result the average engineering graduate student will likely find parts of the book rather difficult, but for the most part these sections can be skipped in a first course without serious loss in continuity. On the other hand, the more advanced reader will appreciate the numerous specific references to the literature and the excellent bibliography and index. A number of problems, both illustrating and extending the text, are provided for each chapter.

This book is certain to receive an enthusiastic welcome from both students and teachers seeking a readable yet careful introduction to what often appears to be a confusing and esoteric subject. But it should prove equally useful to the industrial research engineer who is dissatisfied with *ad hoc* methods of handling random signals and who desires a more orderly treatment.

W. M. SIEBERT
M.I.T.
Cambridge 39, Mass.

Atmospheric Explorations, ed. by H. G. Houghton

Published (1958) by The Technology Press of M. I. T. and John Wiley & Sons, Inc., 440 Fourth Ave., N. Y., 16, N. Y. 125 pages+x pages. Illus. 9½×6. \$6.50.

This book is a collection of five papers on subjects relating to the atmosphere which were presented at the Benjamin Franklin Memorial Symposium of the American Academy of Arts and Sciences in 1956. The choice and treatment of the subjects in the papers are selective rather than comprehensive. This approach was chosen in keeping with the spirit of the celebration of Franklin's two hundred and fiftieth birthday as illustrative of the keen analytical approach which would be expected of him if he were living.

The authors are eminently qualified to present the interpretation of their own work and the work of others in their particular fields. The belated publication of the papers in book form has reduced the significance of the articles as original contributions, but these distinctive papers are a fitting tribute to one of America's greatest scientists.

The first three papers discussing various phases of atmospheric electricity are as follows: *The Electrification of Clouds and Raindrops* by Ross Gunn, Director, Office of Physical Research, U. S. Weather Bureau; *The Formation of Electrical Charges*

in *Thunderstorms* by J. P. Kuettner, Geophysical Research Directorate, Air Force Cambridge Research Center; and *Positive Streamer Spark in Air in Relation to the Lightning Stroke* by L. B. Loeb, Professor of Physics, the University of California, Berkeley.

Dr. Gunn discusses ionization in the clear atmosphere and in water droplet clouds, and presents experimental results of charge distribution measurements by the Weather Bureau in a cloud chamber. He compares these results with his theory of the ionization of water drops.

Dr. Kuettner, starting from the original observation of Franklin and the English physicist Wilson concerning the polarity of clouds, discusses the processes for segregation of charges in thunderstorms.

As a logical extension of the first two papers, Dr. Loeb describes work relating to the discharge of clouds through lightning strokes with emphasis on the positive streamer spark.

The last two papers deal with two views of the upper atmosphere and are as follows: *A Meteorologist Looks at the Upper Atmosphere*, by Harry Wexler, Director of Meteorological Research, U. S. Weather Bureau; and *Phenomena of Radio Scattering in the Ionosphere* by H. G. Booker, Professor of Electrical Engineering, Cornell University.

Dr. Wexler discusses meteorological processes in the upper atmosphere with emphasis on the upward and downward propagation of storms as extensions of the more routinely used low level development and horizontal movements of storms. Some efforts are made to discuss possible direct linkages between solar and atmospheric phenomena.

Dr. Booker's approach to the upper atmosphere is through the use of vertical soundings with radar and long range radio communications. Improved measurement techniques and extension of frequency ranges have made possible a more complete understanding of the ionosphere.

Although this book is recommended neither as a text nor as a reference, it serves admirably to chronicle the spirit of scientific history in the making.

A. W. STRAITON
Univ. of Texas
Austin, Tex.

Soviet Education for Science and Technology by A. G. Korol

Published (1957) by The Technology Press of M.I.T. and John Wiley & Sons, Inc., 440 Fourth Ave., N. Y. 16, N. Y. 417 pages+47 appendix pages+16 bibliography pages+26 index pages+xxv pages. 9½×6½. \$8.50.

This very competent and cautious book on the Soviet educational system derives from a project which was begun by the Center for International Studies of the Massachusetts Institute of Technology in 1953 and was continued after 1955 under a grant from the Carnegie Corporation of New York. In addition to the staff of the Center, many faculty members of M.I.T. assisted in the evaluation of the documentary material, such as Soviet textbooks, examination questions, and specific curricula details. Much of the quantitative informa-

tion could appear as astounding progress in broad general education; but fortunately, Mr. Korol in many places points out significant qualitative factors to set the total program into the proper perspective. Though the over 400 pages of text, supported by 3 charts and 56 tables and many appendices might give the impression of elaborate presentation of facts that in many other places have been so simply summarized, it should be emphasized that the simpler presentations have often given completely wrong impressions and have led to alarming conclusions. Anyone interested in Soviet education in the fields of science and technology will be well rewarded in reading this rather comprehensive treatise. In particular, attention should be directed to the author's comments and reflections which represent his own evaluation of the comparative advantages and disadvantages of the Soviet educational system. And system, indeed, it is, centrally directed and supervised with the objective of careful and forceful indoctrination in the Communist doctrines, giving education not as we understand it in the Western World, but as a planned activity fitting into the over-all pattern of a planned economy.

The major part of the book, Chapters 5 to 10 inclusive, is devoted to the Soviet counterpart of undergraduate college education in science and technology. In particular, historical data are given concerning growth of the university and institute patterns and the successive changes in emphasis. In 1955, the last year of complete data available for inclusion into this book, the enrollment in all technical professional schools was 450,000 full-time students, 100,000 evening students, and 100,000 correspondence course students, representing a total of 35 per cent of the entire registration in higher education. It is this great emphasis upon one phase of higher education which has given rise to the warnings. Yet, if we follow the author's qualitative comments and realize the rigidity of curricula and the extreme specialization, we learn to attach different significance to these numbers. Individually, the chapters carry the self-explanatory titles: the institutional system; selection, enrollment, and graduation; the academic plan; sample curricula in mechanical engineering, in physics, and in mathematics (at a teacher's college); teachers, textbooks, and facilities; the teaching process.

To illustrate the preparation for college, Chapters 2 and 3 deal with the ten-year school roughly equivalent to our elementary and high school periods, though more strenuous and with much emphasis on mathematics and the sciences. Again, the author examines in detail organization and curriculum, instruction, textbooks, and examinations. There appears little doubt that the rigorous schedule and program of this 10-year school is a very direct and effective preparation for college.

Chapter 4 is devoted to the secondary engineering (industrial) technical schools, so-called *technikums*, which furnish well-trained technicians in much larger numbers than available in this country. The course runs for 2½ years and the enrollment has increased from 187,000 in 1940-1941 to

843,000 in 1955-1956, a trend that is probably most significant in any comparison of relative technical training in this country and in Soviet Russia.

The first chapter gives a general introduction to the Soviet system of mass education, and outlines all phases of general and secondary education together with the "State Labor Reserve" and its training programs.

For anyone really interested in the serious comparison of Soviet vs U.S.A. education, this book is practically imperative reading since it points out so ably the different atmospheres out of which objectives of education have been formulated.

ERNST WEBER
Polytechnic Inst. of Brooklyn
Brooklyn, N. Y.

An Introduction to Digital Computers by R. K. Livesley

Published (1957) by Cambridge University Press, 32 E. 57 St., N. Y. 22, N. Y. 52 pages+1 bibliography page+viii pages. Illus. 8½×5½. \$1.75.

This is a brief introduction to the basic principles of operation of digital computers and to the types of routine problems which can be solved with such machines. The book is intended primarily for the engineer or other person who is more interested in the possible applications of digital computers than in the detailed design of computing circuits. For this reason, emphasis is placed on programming and on over-all system operation. The equipment, devices, and circuitry which can be used to construct digital computers are discussed only where necessary to help explain the general operation. The author has avoided detailed discussions of mathematical techniques and comprehensive descriptions of the idiosyncrasies of particular machines.

The book contains four chapters. In the first chapter, *The Elements of Programming*, the author explains the fundamentals of digital computer operation and the use of a program of machine instructions by illustrating how a simple mathematical problem can be mechanized and solved. The discussion of elementary programming is continued to include jump instructions, address modification, and some information about the instruction codes used in real machines.

Some of the "hardware" used in the construction of actual machines is described in Chapter 2, titled *Input, Storage and Output of Numbers*. This chapter contains brief descriptions of the most widely used binary storage systems and types of input-output equipment. A short discussion of decimal and binary systems of numbers is also included. The reviewer feels that some discussion of the devices and techniques used in the computing circuits should have been included in this chapter. For instance, the use of semiconductors and vacuum tubes is barely mentioned. Also, the author makes a statement in the second paragraph on page 19 which gives an erroneous impression of the speeds obtainable with modern digital computers. He states that the access time of the high speed stores of most modern computers is of the order of a millisecond, whereas a more correct figure would be tens of microseconds.

The third chapter, *The Organization of Programmes*, describes the way in which large programs are usually constructed, and considers some of the techniques which make programming easier.

In the final chapter, *The Solution of Engineering Problems*, the author discusses in very general terms some of the problems which can be solved with digital computers. These include problems in linear and non-linear algebra, ordinary and partial differential equations, and function tabulation.

Although this book is very short, the author has managed to present a broad picture of the outstanding features of digital computers in such simple language that the nonspecialist should find it easy to read and understand. Coverage on programming and general system operation is especially good.

W. B. CAGLE
Bell Telephone Labs.
Whippany, N. J.

Principles of Electronic Instruments by G. R. Partridge

Published (1958) by Prentice-Hall, Inc., 70 Fifth Ave., N. Y. 11, N. Y. 383 pages +9 index pages +xiv pages. Illus. 9½ X 6½. \$11.00.

As stated by the author in the preface, the book is essentially the result of teaching a course in electronic instrumentation and measurements. This field has become so extensive that it would of course be well nigh impossible to cover it in even reasonable detail in one lecture course, or one book of some 380 pages, as the present one. In such condensed presentations the subjects covered will not all receive the same degree of condensation, since any teacher or writer will have a special interest in certain areas, which will then necessarily receive a more detailed treatment than others. When such a book is used as a text in a lecture course, this is not a serious handicap, since the primary purpose of education should not, and cannot be to cover every detail and application, but rather to show the student the principles involved and let him then apply this knowledge to other problems of a similar nature. A practicing engineer, on the other hand, who hopes to find a reference book on electronic instrumentation and methods, might be disappointed; his chances of finding a description of just the instrument or method he may be interested in at the moment, are naturally rather slim. However, it should be stated that the literature references at the end of each chapter are of decided help in this respect.

The book can be divided into roughly two parts. The first 12 chapters, representing about 60% of the text, deal with electronic instruments. There are three chapters on dc and ac vacuum tube voltmeters, in the course of which such well known instruments as the Ballantine and Hewlett-Packard meters are described in detail. One chapter—good reading for any electrical engineer—deals with that perennial favorite subject of confusion: rms responsive, average value responsive and peak responsive instruments. Other chapters deal with electrometer tubes, electronic wattmeters, frequency measurements, phase meters, Q-meters, Z-angle meters and digital displays.

The second part of the book deals with the application of electronic measurement

techniques in the field of non-electrical quantities. A number of the better known transducers, such as SR-4 strain gages, linear variable differential transformers and accelerometers are discussed briefly. Other chapters deal with the measurement of velocity of gases or liquids, of time, measurements in the field of sound, light, pressure, temperature and radio activity. While these chapters are also far from complete, they give a valuable birds-eye view of what electronic instrumentation can accomplish. The reader desiring more detailed information will again find the references at the end of each chapter of help. Incidentally, in the lists of references on pages 191, 210 and 255, the designation "Communications and Electronics" should read: "Transactions of the AIEE, Part I, Communications and Electronics."

The book can be recommended to the teacher planning a course in the field of electronic instrumentation. It will also be of value to a person who wishes to obtain a general picture of this field.

WALTHER RICHTER
Consulting Electrical Engineer
Milwaukee 17, Wis.

Zone Melting by W. G. Pfann

Published (1958) by John Wiley & Sons, Inc., 440 Fourth Ave., N. Y. 16, N. Y. 208 pages +21 appendix pages +6 index pages +xvi pages. Illus. 9½ X 6. \$7.50.

It is fortunate that the world-authority on zone-melting, W. G. Pfann, was able to publish this important book, before less qualified authors "made hay" of the urgent need for such a volume, as has often happened in other fields. Although Kapitza, as well as Andrade and Roscoe, had made use of the zone-melting process years before World War II, it was not until Pfann pioneered in the many varied applications of this technique, particularly in semiconductor purification, that its potentialities were realized.

The book is singularly comprehensive covering every aspect of zone-melting from the fundamental principles to the many ingenious applications. Most of the new ideas in this volume were originally conceived and tested by the author and his co-workers, which gives him an intimate familiarity with the subject.

The introduction (first chapter) outlines the principle of zone-melting and scans the contents of each chapter in a few sentences; a most effective way of familiarizing the reader with the pertinent terminology. The second chapter treats the process of freezing and the associated segregation of solutes which leads to the definition of the "distribution coefficient" and methods of its determination. The "Theory of Zone Refining" is briefly and concisely presented in the third chapter; easy to understand without sacrificing details or accuracy.

The most outstanding chapter is the fourth on "Techniques of Zone Refining" where little is left to the imagination of the reader. Every conceivable modification of the zone refining principle seems to be described, so that it should prove most valuable to the reader interested in the practical application of this process. The fifth chapter on the "Application of Zone Refining" gives a few examples of materials which have been

successfully purified by zone melting. Chapter Six on "Continuous Zone Refining" is of particular interest for the production-oriented reader. Many heretofore unpublished methods are described together with their theoretical foundation. "Zone Leveling and Single Crystal Growth" are dealt with in the seventh chapter with a section on "Dislocations and Crystalline Perfection."

The eighth chapter, "Methods of Perturbing the Concentration," goes into metallurgical and diffusion techniques for the control of the concentration distribution of the solute, such as impurities in semiconductors. The text deals primarily with semiconductor examples, among them Pfann's remelt method of producing *p-n* junctions and *p-n-p* transistor structures.

"Temperature Gradient Zone Melting," discussed in the last chapter, is probably the most intriguing extension of the zone melting principle. This technique produces motion of a finite molten volume within a solid body in the direction of a constant temperature gradient. It can be used for *p-n* junction fabrication, single crystal growth and even the determination of diffusivities in liquids.

An appendix with twenty generalized curves of solute concentration versus distance along a zone-refined ingot for different distribution coefficients will be invaluable for the reader interested in the quantitative appraisal of zone-melting for specific purposes.

The terminology seems somewhat arbitrary in spots and certain headings are not entirely clear, at least to the non-metallurgist. Although this does not impair the general usefulness of the book, it is a minor blemish in view of the expected broad readership from many different fields.

Zone Melting is an outstanding book for engineers, physicists, chemists and metallurgists generally interested or directly concerned with metallurgical methods. Emphasis on the application to semiconductor problems render it "a must" for anybody engaged in work on semiconductor materials and devices. This relatively small volume contains a surprising amount of new and practical information.

D. A. JENNY
RCA Labs.
Princeton, N. J.

Feedback Control Systems by O. J. M. Smith

Published (1958) by McGraw-Hill Book Co., Inc., 330 W. 42 St., N. Y. 36, N. Y. 643 pages +12 appendix pages +35 index pages +xviii pages. Illus. 9½ X 6½. \$13.50.

This is an advanced book which will be most useful for these with some experience in the field of automatic control. The variety of material covered is impressive, the approach to various techniques of analysis and synthesis is unique, and the enthusiasm of the author in developing his ideas is clearly apparent.

The introductory chapter, though short, explains the general principles of feedback in terms of the author's philosophy, and varied examples of application such as those in production, inventory, transportation, economic, and society control are given. This is significant because reference to these various fields is made throughout the book to make

the reader constantly aware of the versatility of automatic control.

A number of contributions to techniques of analysis and synthesis of control systems are presented for the first time in a textbook. One of the first that is introduced is the L plane which is essentially a log magnitude-phase angle diagram with the gain in nepers and the phase in radians. The important point is that the scales are arranged to have one neper equal to one radian. With this scale selection, vector lengths on the chart have meaning, and the relation between the frequency response plot and the locations of the critical closed loop poles in the s plane can be established from the corresponding complex vector margin and the vector attenuation rate on the L plane.

The author stresses his belief that the basis for understanding the operation and performance of a feedback control system must be obtained from a study of the relationships between the open and closed loop roots in the s plane. To illustrate this relationship, a number of elaborate open and closed-loop pole-zero plots with contours of constant phase and magnitude are shown. The importance of the s -plane saddle points in factoring polynomials in plotting root loci, and in the relation between open and closed loop roots is frequently discussed. This subject is further emphasized in Chapter 3, S -Plane Analogs, where the details of constructing, calibrating, and using potential analogs, conducting paper, and electrolytic tanks, as well as geometric analogs are discussed in unusual detail.

A large portion of the book is based on the use and manipulation of block diagrams, and this topic is introduced in a chapter on multiple loops. A complete discussion of unilateral, bilateral, reciprocal, and linear elements is given as a foundation for transforming circuits and equations into block diagrams and blocks into different types of systems.

Another chapter, Power Spectra, introduces the concept of random signals and this is explained in terms familiar to electrical engineers. This practical interpretation may be of particular interest to those who have only a mathematical acquaintance with random signals. A particularly noteworthy section explains how different random signals are combined and used when they are correlated. This is a subject which is usually omitted from most papers and texts.

This chapter, Power Spectra, concludes the first part of the book titled "Linear Analysis." There are three other parts: "Linear Synthesis," "Steady-State Nonlinear Analysis," and "Nonlinear Synthesis."

The last three parts of the book are as informative and thought provoking as the first. Optimum linear synthesis based on minimizing the mean square error is considered both from a rigorous and heuristic viewpoint. In fact, several different interpretations of the optimum filter philosophy are given in practical engineering terms. The theoretically optimum filter is converted into practical feedback system configurations which minimize nonlinear component effects by block diagram manipulations.

Practical considerations such as selecting components, networks, and tolerances, and distributing power and locating components in the loops are discussed.

Methods of analyzing and synthesizing systems with distributed parameters and transportation lags are treated thoroughly in a separate chapter, but sampled data systems are not included.

The fundamental concepts of nonlinear control are introduced in a study of relay operation where the describing function is derived for triangular and gaussian inputs as well as for sinusoidal inputs. Subsequently, the nonlinear analysis is developed to include deadzone, different types of hysteresis, backlash, and coulomb friction. Actually, 150 pages are devoted to the subject of nonlinear analysis and another 100 are concerned with nonlinear synthesis.

Nonlinear synthesis with prediction control, or switching functions, is based on phase plane analyses and this is extended in concept to phase space. The nonlinear switching control is extended to systems with saturation, complex poles, dead time, and multiple saturations.

The last chapter in the book concerns the analysis, synthesis, and realization problems in the construction of carrier frequency systems. The analysis is based on pole zero locations, and there is considerable discussion on components, modulators, demodulators, and various types of linear and nonlinear compensating networks.

It should be mentioned that each of the 18 chapters has an excellent introduction and summary, and that each chapter ends with 20 to 50 problems and a bibliography concerning the subject of the chapter.

There are several minor deficiencies that should be mentioned. One is that standard symbols and terminology as proposed or approved by automatic control committees have not been used. However, it is in keeping with the theme and philosophy of the book because the general approach to all of the subject matter is somewhat different from the conventional. Although some readers may object to different treatments of some of the techniques that are well established in other textbooks, others will find this book capable of stimulating new ideas.

It does seem, however, that another minor deficiency may be found in the style of writing. In his enthusiasm, the author frequently dashes from one idea to another, and it is not always clear whether some of his conclusions and counsel are founded on a rigorous proof, experience, general philosophy, opinion, or imagination. In any case all of his viewpoints are interesting although it appears that a few of his original interpretations may be more complicated and inefficient than some which are more commonly known. However, whether or not the reader agrees with the author's philosophy, it is bound to be stimulating and challenging to graduate students and to experienced persons alike. Certainly, it is a book which will prove to be a valuable reference for all who are seriously interested in feedback control system analysis and design.

G. S. AXELBY
Westinghouse Elec. Corp.
Baltimore, Md.

Electronic Semiconductors by Eberhard Spenke, translated by D. Jenny, H. Kroemer, E. G. Ramberg, and A. H. Sommer

Published (1958) by McGraw-Hill Book Co., Inc., 330 W. 42 St., N. Y. 36, N. Y. 379 pages +14 appendix

pages+7 index pages+xxvi pages. Illus. 9½×6½. \$11.00.

This book is a translation of the second German edition of Eberhard Spenke's book *Elektronische Halbleiter* which appeared in the German edition several years ago. The translators have been true to the original spirit of the book; however, they have followed American practice with respect to nomenclature and symbols and have added a series of problems at the end of each chapter. This reviewer feels that the additions made by the translators have increased the value of the book which, in its present form, should make an excellent textbook in an introductory course to the fundamentals of semiconductor physics.

The book is divided into two main sections. The first five chapters deal with the conduction mechanism of electronic semiconductors and the physics of rectifiers and transistors; while the last five chapters deal with the fundamentals of semiconductor physics. In the first part the subjects considered are:

- I. The Conduction Mechanism in Electronic Semiconductors
 - II. The Nature, Models, and Reactions of Impurities and Imperfections
 - III. The Hole
 - IV. The Mechanism of Crystal Rectifiers
 - V. The Physical Mechanism of Crystal Amplifiers (Transistors).
- In the second part chapters are devoted to:
- VI. Approximation Methods in the Quantum Mechanics of the Hydrogen Molecule
 - VII. The Band Model
 - VIII. Fermi Statistics of the Electrons in a Crystal
 - IX. The Dynamic Approach to Impurity Equilibria and the Inertia of Impurity Reactions
 - X. Boundary Layers in Semiconductors and the Metal-Semiconductor Contact.

Dr. Spenke's treatment is for the most part clear and easy to follow. The bibliography, while not extensive, does nevertheless make adequate reference to the original literature for the purposes of a textbook.

In short, it seems to this reviewer that this book is an excellent introduction to the fundamentals of semiconductor physics. With regard to the treatment of semiconductor devices the book is not as complete as one might hope. This is largely due to the fact that the first German edition was written in 1952 and the revisions of the second edition of 1954 or thereabouts seemed principally in extending the references to the literature. Thus, since the field of semiconductor devices is a very rapidly moving one indeed, one regrets that some of the latest contributions could not have been included. Nevertheless, the book is recommended as an introductory text for those students who wish to learn something about semiconductor physics and particularly as applied to rectifier and transistor problems.

G. C. DACEY
Bell Tel. Labs.
Murray Hill, N. J.

Photosensors by W. Summer

Published (1958) by The Macmillan Co., 60 Fifth Ave., N. Y. 11, N. Y. 592 pages +61 bibliography

pages+2 appendix pages+18 index pages+xvi pages.
Illus. 8½×6. \$21.00.

This book contains a comprehensive review of photoelectric devices and their uses in industry, including two thousand references plus a list of patents in this field. Part I is devoted to a description of these devices and their characteristics, while Part II describes their industrial applications and the uses of related equipment.

Part I contains nine sections as follows:

1. Historical background.

2. Applications:

A comparison of visual against photoelectric reaction time; fatigue, etc.

3. Photosensor and the human eye to photoelectric devices, covering color, depth perception and spectral response.

4. Photosensors.

A description of the general characteristics of photoelectric devices as well as outline of the various types including photovoltaic cells.

5. Basic Circuits.

This covers amplifications, shielding, wheatstone bridges, etc.

6. Optical Equipment.

A fairly complete compilation of the physics of optics and light and its correlation to photosensors.

7. Sources of Radiant Energy.

A definition and description of various radiant energy sources such as light sources, monochromatic light sources, black body radiation, ultraviolet and infrared radiation sources, etc.

8. Color.

An outline of the physical properties of color, contrast, complementary colors, etc.

9. Optical Filters.

Fairly complete coverage is given optical filters, including a discussion of transmission, absorption and reflection properties, polarizing filters, and attenuation of radiation.

Part II is composed of twenty sections as follows:

10. Protective Devices.

Uses of photoelectric units as industrial safeguards such as fire prevention, detection of noxious gases, power presses, etc.

11. Production Control.

Uses of photoelectric devices in textile, painting, manufacture of steel, testing.

12. Assembly Control.

13. Luminescence.

Industrial uses in thermography, fluoroscopy, infrared image converters, etc.

14. Chemical Industry.

The chemical industry uses such as ultraviolet and X-ray absorption analysis, automatic titration, etc.

15. Combustion Control.

Control of fuel, flue gases and flames.

16. Temperature Control.

Thermostatic control systems, low temperature control, measurement of high frequency energy.

17. Mining.

Detection of fire-damp, dust in mines, and smoke.

18. Inspection of Mass-Produced Articles.

These devices may be used in statistical quality control, for detecting flaws or impurities, gauging, etc.

Other applications include: 19. Colorimetry; 20. Step Control of a Productive Process; 21. Limit Switches; 22. Level Indicators; 23. Counting Devices; 24. Synchronizers; 25. Door Openers; 26. Timing Devices; 27. Relays; 28. Recorders; 29. Installation, Maintenance and Servicing.

Although covering the same field as Zworykin's *Photoelectricity*, this book is more thorough and complete. Both theory and practical devices are well outlined, analyzing the advantages and disadvantages of each type of photoelectric device. It is recommended as a laboratory reference book on the subject of photoelectric devices and their applications.

FREDERICK KOURY
Sylvania Elec. Products, Inc.
Salem, Mass.

Control Engineer's Handbook, ed. by J. G. Truxal

Published (1958) by McGraw-Hill Book Co., Inc.
330 W. 42 St., New York 36, N. Y. 1048 pages+75
index pages+xiii pages. 1145 figures. 6×9. \$18.50.

In recent years the systems approach to problems has been elevated to primary significance. In this process the importance of available components and their characteristics has sometimes gotten less emphasis than desirable. A large number of books are available on control systems theory, much fewer on the nature and characteristics of components. It is this void that the *Control Engineer's Handbook* tends to fill and indeed fills quite well.

After covering the elements of control systems and analysis in a rather condensed fashion, the book concentrates on the description and analysis of control components. A desirable way of doing this is to: (1) discuss the underlying principles of the design and use of the component; (2) describe available components and their design; (3) summarize the theoretical tools used to describe these components; and (4) demonstrate the analysis and design of systems involving such components. In some of the sections this recipe is followed with excellent success; in other cases the treatment is not as complete. Perhaps the best example of an excellent treatment is the section on hydraulic controls (Section 15). But even where some aspects enumerated above may be weak or absent, the information present is most valuable. In certain cases this book appears to be the only comprehensive source of the subject from the point of view of the control engineer. The sections on magnetic amplifiers (Section 7), mechanical components (Section 13), clutches and brakes (Section 14), and signal transducer (Section 17) will prove to be invaluable, if not sole, sources for the practical control engineer.

The effort of condensing the analytical methodology has naturally resulted in some brief and one-sided coverage. For example, nonlinear system analysis in Section 2 covers numerical computations in one page, con-

centrating on one specific numerical method. Another example of such an omission is the treatment of sampled data system analysis in which digital computers are not mentioned. Fortunately, more effort is devoted to design techniques (Section 3) which is extensive and practical. In Section 4, specialized design techniques, an excellent summary of network synthesis is presented; yet this is a field which has been well covered in the literature. The relation of network synthesis to control design problems could be more heavily emphasized. In the same section the use of signal flow graphs is presented and constitutes a welcome addition to control theory. The examples, however, could have been extended to the analysis of whole systems in addition to circuit analysis. Also in this section the treatment of random functions and statistical methods as they apply to control systems is good but somewhat brief. A more extended treatment would have compensated for the relative dearth of appropriate text books.

The most complex components in control systems are computers which are dealt with in Section 5. The role of electronic analog computers in simulation and analysis of control problems is extremely well treated. But practically no mention is made of mechanical analog computers and of the role of analog computers as part of control systems. The treatment of digital computers is more balanced, and covers both simulation and control. This section could be correlated with sampled data theory by describing z-transforms of computer programs and by analyzing specific systems using digital computers.

As the preface mentions, the purpose of the handbook was not to cover every possible component but to give a thorough treatment of the approaches to their design and utilization. As an example solenoids are mentioned only incidentally and although relay characteristics (Section 10) are covered excellently no drawing or photograph of that component is shown. But in most cases the control components are thoroughly covered and copious design information supplied. This handbook then becomes an excellent collection of useful and unified information on a variety of important topics ranging from amplifiers through transistors, power supplies, electromechanical and mechanical items to hydraulic and pneumatic controls.

Altogether the book is a very welcome addition to the library of the control engineer and fills a real need which was begging to be filled in the control field.

J. M. SALZER
The Magnavox Research Labs.
Los Angeles 64, Calif.

Van Nostrand's Scientific Encyclopedia, 3rd ed.

Published (1958) by D. Van Nostrand Co., Inc.,
257 Fourth Ave., N. Y. 10, N. Y. 1839 pages+vi
pages. 1400 figures. 9×11½. \$30.00.

This book on the physical sciences, mathematics, engineering, and medicine covers twenty-three major subjects: chemistry, nuclear science and engineering, guided missiles, metallurgy, chemical engineering, physics, electrical engineering, mechanical engineering, electronics, astronomy, navigation, meteorology, photography, aeronau-

tics, civil engineering, statistics, mathematics, geology, mineralogy, radio and television, botany, zoology, and medicine. In an attempt to obtain unity, the publishers assigned to one authority the responsibility for the coverage of each field.

The encyclopedia defines and explains about 15,000 terms, which are arranged alphabetically. A useful feature is a cross referencing system that puts key words of the explanations in bold-face type. Each cross reference is itself explained and described in its alphabetical position. Thus, the original expository material is considerably amplified.

Any publication that is represented as an encyclopedia immediately becomes open to attack by critics who are piqued at the audacious implication of all-inclusiveness conveyed by such a work. For this reason most reviewers find it very difficult to be objective and fair when evaluating an encyclopedic work.

For this review a formula was sought for averaging out individual prejudices so that a valid opinion could be presented. The biological sciences were ignored since these are of secondary interest to the radio engineer. For the categories representing the physical sciences and engineering, workers in those areas were interviewed. Fortunately, it was possible to reach individuals in a wide variety of scientific pursuits, since they were conveniently found in the organization in which this reviewer is employed. Each individual was requested to sample a representative list of terms of his own choosing. When judging the adequacy with which each term was covered, he was requested to weigh the following:

- a. The completeness of the definition.
- b. The detail of definition that one should rightfully expect in an encyclopedic work of this size and scope.
- c. The usefulness and adequateness of the definitions to persons in the same field as well as to those in other scientific fields.

This reviewer must admit that he commenced this survey with the preconceived

idea that the results of the poll would not favor this book. With remarkably few exceptions this encyclopedia was found to be very satisfactory. Some of the entries were more comprehensive than one might expect considering the multiplicity of fields covered. Most of the persons who participated in this review commended the excellence of this encyclopedia and only two expressed any doubt as to its value.

Any work of this type is bound to have a few weaknesses as exemplified by the omissions that were uncovered by the survey. It would serve little purpose in this critical review to point out those omissions, since they were an insignificant per cent of the terms searched.

The flaws must be weighed against the merits of the book. This has been done, and *Van Nostrand's Scientific Encyclopedia*, 3rd edition, has not been found wanting. While the purchase price of \$30.00 might seriously strain the budget of an individual, certainly the benefit that is to be derived from this work makes it a worthwhile investment for libraries and organizations.

GUSTAVE SHAPIRO
National Bureau of Standards
Washington 25, D. C.

RECENT BOOKS

Frohlich, H., *Theory of Dielectrics*, 2nd ed. (identical to the first edition except for an addendum containing three paragraphs.) Oxford University Press, 114 Fifth Ave., N. Y. 11, N. Y. \$4.80.
 Jones, D. D., and Hilbourne, R. A., *Transistor A.F. Amplifiers*. Philosophical Library, Inc., 15 E. 40 St., N. Y. 16, N. Y. \$6.00.
 Landee, R. W., Davis, D. C., and Albrecht, A. P., *Electronic Designers' Handbook*. McGraw-Hill Book Co., Inc., 330 W. 42 St., N. Y. 36, N. Y. \$16.50.
 Murphy, G. J., *Basic Automatic Control Theory*. D. Van Nostrand Co., Inc., 257 Fourth Ave., N. Y. 10, N. Y. \$10.75.
 Peck, L. G., and Hazelwood, R. N., *Finite Queuing Tables*. John Wiley & Sons,

Inc., 440 Fourth Ave., N. Y. 16, N. Y. \$8.50.
 Perrine, J. O., *Physics and Mathematics in Electrical Communication*. John F. Rider, Inc., 116 W. 14th St., N. Y. 11, N. Y. \$7.50.
 Platt, Sidney, *Industrial Control Circuits*. John F. Rider, Inc., 116 W. 14th St., N. Y. 11, N. Y. \$3.90.
Proceedings of the EIA Conference on Maintainability of Electronic Equipment. Engineering Publishers, GPO Box 1151, N. Y. 1, N. Y. or Interscience Publishers, 250 Fifth Ave., N. Y. 1, N. Y. \$5.00.
Proceedings of the Fourth Annual Computer Applications Symposium. Armour Research Foundation of Illinois Institute of Technology, 10 W. 35th St., Chicago 16, Ill. \$3.00.
Proceedings of the 1957 National Electronics Conference—Vol. 13. R. E. Bard, National Electronics Conference Headquarters, 84 E. Randolph, Chicago, Ill. \$7.50.
Proceedings of the XIIth General Assembly, Volume XI, Part 1, Commission I on Radio Measurements and Standards. Secretary-General of U.R.S.I., 7, Place Emile Danco. Uccle-Brussels, Belgium. \$2.00.
 Richmond, A. E., *Calculus for Electronics*. McGraw-Hill Book Co., Inc., 330 W. 42 St., N. Y. 36, N. Y. \$8.25.
 Riordan, John, *An Introduction to Combinatorial Analysis*. John Wiley & Sons, Inc., 440 Fourth Ave., N. Y. 16, N. Y. \$8.50.
 Schure, A., *Impedance Matching*. John F. Rider, Inc., 116 W. 14 St., N. Y. 11, N. Y. \$2.90.
 Schure, A., *Vacuum Tube Rectifiers*. John F. Rider, Inc., 116 W. 14th St., N. Y. 11, N. Y. \$1.50.
The Direction of Research Establishments. Proceedings of a symposium held in 1956 in England. Philosophical Library, Inc., 15 E. 40 St., N. Y. 16, N. Y. \$12.00.
 Timbie, W. H., *Basic Electricity for Communications*, 2nd ed. Revised by F. J. Ricker. John Wiley & Sons, Inc., 440 Fourth Ave., N. Y. 16, N. Y. \$6.25.

Abstracts of IRE TRANSACTIONS

These issues of TRANSACTIONS have recently been published, and are now available from the Institute of Radio Engineers, Inc., 1 East 79 Street, New York 21, N. Y., at the prices indicated. The contents of each issue and, where available, abstracts of technical papers are given on the following pages.

Sponsoring Group	Publication	Group Members	IRE Members	Non-Members*	
Broadcast & TV	Receivers	Vol. BTR-4, No. 3	\$1.20	\$1.80	\$3.60
	Component Parts	Vol. CP-5, No. 2	1.65	2.50	4.95
	Education	Vol. E-1, No. 2	1.10	1.65	3.30
	Industrial Electronics	PGIE-6	2.00	3.00	6.00
	Nuclear Science	Vol. NS-5, No. 1	.80	1.20	2.40
	Telemetry & Remote Control	Vol. TRC-4, No. 1	.80	1.20	2.40

* Public libraries and colleges may purchase copies at IRE Member rates

Broadcast & TV Receivers

VOL. BTR-4, No. 3, JUNE, 1958

Gilbert E. Gustafson (p. 1)
 Look for More Troubles (p. 2)
 Minutes of the Meeting of the Administrative Committee of the IRE Professional Group on Broadcast and Television Receivers (p. 3)
 Chapter News Reports (p. 7)
 Call for Papers for Radio Fall Meeting (p. 9)
 Characteristics and Applications of Low Impedance Diodes Used as Voltage Variable Capacitors—W. F. Palmer and D. H. Rice (p. 10)

The use of germanium VLI diodes as voltage sensitive capacitors has been investigated. Data concerning the variation of diode capacitance with bias voltage is presented and circuit requirements for resonant circuits tuned with variable capacitance diodes are discussed.

Formulae and curves for Q and frequency control sensitivity are developed and discussed in view of VLI diode characteristics.

Two basic modes of diode operation are possible:

- (a) Self-bias operation
- (b) External-bias operation

Unexpectedly large values of diode capacitance have been encountered in self-bias operation and are explained. Large and small signal operations are also discussed.

Practical circuits for television fine tuning and FM automatic frequency control are presented and possible television automatic frequency control is discussed.

Transistorized TV Horizontal Deflection and High Voltage System—G. Schiess and W. Palmer (p. 19)

Design considerations for transistorized television horizontal-deflection circuits are given.

Deflection volt-ampere requirements for various picture tube sizes are tabulated and compared to the deflection power capabilities of presently available transistors.

An experimental deflection circuit for a small screen picture tube (8DP4) is described, consisting of transistor phase detector, blocking oscillator, driver, and transistor output stage.

Objective specifications are given for horizontal deflection transistors for use with picture tubes of various screen sizes and deflection angles.

Transistorized Sound Section for TV Receivers—George Schiess and William Palmer (p. 36)

Two circuits for transistorized sound sections for use in hybrid or all-transistor TV receivers are described. Both circuits consist of transistor sound i-f amplifier, ratio detector and transistor audio amplifier. Performance data are given for both circuits.

Calendar of Coming Events and Authors' Deadlines (p. 42)

1957 Award of the PGBTR (p. 44)

Component Parts

VOL. CP-5, No. 2, JUNE, 1958

Information for Authors (p. 71)
 Recent Advances in the Solid-State Electrolytic Capacitor—A. V. Fraioli (p. 72)

The tremendous interest in the solid-state capacitor is due to the combination of superior technical characteristics with very small size and large "bulk" capacity. Present literature shows 35 vdc and 85°C voltage and temperature limitations.

Through the analysis of units made to operate at the extended limits of 100 vdc and

150°C, a model has been proposed which serves to explain four sets of anomalous and apparently unrelated electrical characteristics found in this type of unit.

Some Problems Associated with the Charging of Dry Batteries—P. H. Adams (p. 76)

The effects of the periodic application of a reverse emf to dry batteries, with the object of increasing their service life, are discussed and the optimum conditions to minimize the possibility of damage to both flat and round cells are laid down. The application of this process in ac battery portable radio receivers is examined and it is shown that the extent to which battery service life is likely to be increased is dependent on the conditions of use of the receiver in question.

Conductive Ceramics—Z. A. Post and P. E. Ritt (p. 81)

This paper describes a representative selection of materials from the general class known as conductive ceramics. Specifically, the materials discussed are tin oxide, zirconium oxide, silicon carbide, and molybdenum disilicide. A table of some of the more pertinent physical, thermal and electrical properties of each material is included. Some of the present applications of the materials are discussed and other uses are proposed. A graph of the specific resistivity of tin oxide vs absolute temperature is given, and a figure shows the effect of impurities on the specific resistivity of tin oxide vs absolute temperature. A discussion of the results of a preliminary investigation to determine the feasibility of electroplating various metals on the surface of tin oxide is presented.

The Symmetrical Transfer Characteristics of the Narrow-Bandwidth Four-Crystal Lattice Filter—T. R. O'Meara (p. 84)

The conventional four-crystal lattice filter is analyzed, without recourse to image parameter theory, in order to obtain an (approximate) expression for a general symmetrical insertion-loss characteristic. The resulting expression is given as an equivalent low-pass transfer function which is the ratio of two polynomials of the second degree in complex frequency. These in turn have coefficients which are functions of three parameters:

- 1) shunt capacitance ratio;
- 2) fractional-bandwidth, crystal-Q products;
- 3) fractional stagger of the inner critical frequencies of the crystal.

Numerous curves illustrate the effect on the insertion-loss characteristic of the three design parameters.

Where comparison is possible, the approximate equations reached in this paper are shown to agree with the corresponding approximate image parameter equations of Kosowsky. Also, a variety of responses are shown to result which were not discovered by previous image parameter techniques.

The approximations involved are equivalent to ignoring critical frequencies of the impedance elements (and hence of the transfer function) when these are far removed from the filter center frequency. Thus the representation is only valid near the filter center frequency. However, the error involved in the approximation is typically less than 0.1 db to the 40-db attenuation points, with narrow-band filters.

Transient Response of Phosphors—G. I. Cohn and H. M. Musal (p. 90)

The transient behavior of cathode-ray tube phosphors is of considerable interest in many applications, such as the improvement of the signal-to-noise ratio in radars. Although material appears in the literature concerning the decay characteristics a short time after the excitation is switched off, very little appears regarding the buildup characteristics or the decay characteristics immediately following removal of the excitation. The analysis of a phosphor model which covers the entire

buildup and decay range is presented in this paper. The analysis shows that under certain conditions the transient behavior of phosphor brightness buildup and decay can be accurately expressed in a relatively simple form during the excitation period and immediately after the excitation is removed. The transient behavior and time constants involved are determined by the number of different types of imperfection centers present and their excitation and decay probability time densities.

Prediction of Temperatures in Forced-Convection Cooled Electronic Equipment—Lawrence Fried (p. 102)

In electronic equipment, the life, reliability, and operating characteristics of component parts (tubes, resistors, capacitors, motors, etc.) to a large extent are determined by temperature conditions within the parts. In practical cases, these internal conditions are best represented by one or more temperatures on the surface of each part. In special cases, with precautions, even large items such as pressurized equipment may be regarded as component parts, and their internal temperature conditions may be related to case temperatures.

There is great need to be able to predict the surface temperatures of component parts without performing an endless series of tests, the results of which are ambiguous in many instances.

The analysis presented is limited to prediction of surface temperatures of component parts which are cooled primarily by forced convection. In this case, conductive and radiative cooling would be relatively small. This limitation is not a major one, however, because it is expected that most electronic equipment, especially airborne equipment, will be forced-convection cooled. The heat dissipated by component parts by means other than convection will often appear at some other surface and be removed by convection.

Evaluating the Thermal Stability and Radiation Resistance of Silicone Dielectrics—D. F. Christensen (p. 107)

This paper, directed toward the designers of electronic equipment, deals with the aspects of thermal stability and radiation resistance of silicone dielectrics. Information is included which indicates how designers can utilize the maximum thermal stability and radiation resistance inherent in the silicone molecule. It points out that the useful life of silicone electrical insulation subjected to these environments is largely dependent upon physical rather than electrical property changes.

Contributors (p. 116)

Education

VOL. E-1, No. 2, JUNE, 1958

The Laboratory (p. 33)
 Whither Electrical Engineering Education—Samuel Seely (p. 34)

Changes have been occurring in the character of the present-day engineering product which require a review of the education for such engineering. A number of studies and reports have been made which seek to assess the needs and to suggest ideas for meeting the real challenge that exists. A separate study has been conducted by a group at the Case Institute of Technology along these same lines. This paper discusses the general educational problems and the broad philosophy which have been established to guide our subsequent curriculum development. The result is the need for a complete reappraisal of the existing curricula, with a degree of depth and integration along subject matter far beyond anything that has heretofore been attempted.

A New Technique of Education—Simon Ramo (p. 37)

The rapid advance of science and technology in today's world threatens to heighten, rather than minimize, the coming crisis in education. This paper advocates that the technological advances now possible must include advances also in the method of education. Those now engaged in modern engineering and science must apply their ingenuity and resources to major creative efforts in the art of teaching. As with all other intellectual tasks in the coming period, the educational process must also be visualized as a "man-machine" process. The brain and sense of the human teacher must be extended by new engineering systems. This paper discusses specific examples, including feedback as a concept in automatic or semi-automatic lecturing, and stresses that by removing from the duties of the teacher those tasks which can be done as well or better by machines the teacher is elevated to those tasks requiring the superior intelligence and sensitivity of a trained human being.

A High-School Science Teacher Views Industry-Education Cooperation—T. D. Miner (p. 43)

Teachers actively engaged in the classrooms do not agree that today's science education is a failure. Schools are expressions of our culture, and their deficiencies have much deeper roots than most current analysis recognize. Fundamental rather than superficial remedies are indicated. Industry, in its approach to education must recognize the central importance of the teacher himself as an expert in the job to be done, and try to adjust its efforts to the special conditions of the classroom. Certain of the steps now being taken by industry in the field of secondary education are noted, and suggestions for their improvement are offered. It is necessary to put intellectual interests in a favorable competitive position with respect to more glamorous teen-age activities, and a possible action in this direction is suggested.

Improvement of the economic and social status of the teaching profession would be the single most powerful development in bringing about better secondary education.

Teaching Aids for Laboratory Courses in Electrical Circuits and Electronics—Dale Rummel (p. 46)

As more and more material becomes relevant for laboratory work in the undergraduate curriculum in electrical engineering, it becomes increasingly important to find more efficient systems for setting up the equipment for laboratory experiments. Any such system should result in a neat, easily followed arrangement when assembled, should be flexible with respect to the experiments which can be performed, and should not result in stereotyped experiments.

This paper describes a system which has been evolved utilizing chassis upon which are mounted an array of banana jacks on three-quarter inch centers. Many different circuits can be assembled easily and quickly by plugging in components which are mounted on double banana plugs. Different chassis are arranged for different circuits such as a dual triode, single pentode, and push-pull power amplifier.

A Proposed "Automatic" Teaching Device—P. K. Weimer (p. 51)

Teaching devices capable of directing the study of a student in accordance with his individual needs and capabilities offer exciting possibilities for the schools of the future. An "automatic" teaching device is one which incorporates both the presentation of information and the testing of the student in a controlled feedback relationship. This paper presents the case for "automatic" teaching devices along with some proposals for the construction of such machines.

Crisis in Engineering Education—J. L. Stewart (p. 54)

It is contended that engineering education in the United States is and has always been backward and of low quality compared to that in other countries, particularly Russia. Consequent low quality raises serious questions regarding ability to compete with the Communist world.

Historical reasons for low quality are scrutinized as created by personality factors, financial matters, university policies, and federal policies. Significant differences between educators and practitioners in science and engineering are discussed. Specific practical proposals for action by federal and university agencies are given which can aid in reducing the serious shortage of well-trained engineers.

Contributors (p. 62)

Call for Letters to the Editor (p. 63)

Industrial Electronics

PGIE-6, MAY, 1958

(Sixth Annual Industrial Electronics Symposium, Chicago, Ill., September 23-24, 1957)

Message from the Publications Chairman (p. 2)

Transmission of Signal Data from High Speed Machines—E. S. Shepard (p. 3)

This paper deals with the development of a completely transistorized and encapsulated telemetering device capable of transmitting signal data from high-speed machines at speeds up to 54,000 rpm. The need for this type of telemetering arose from the simple fact that in many instances it was not convenient to install contacting devices of a permanent nature on certain types of turbine machinery and the like, due to space limitations and limitations in the maximum number of information channels.

The Inductosyn, Its Uses and Applications to Machine Control—J. L. Winget (p. 14)

Magnetic and Eddy Current Type Transducers for Use in Industrial Electronics—D. L. Elam (p. 29)

The characteristics of magnetic pickups are discussed with regard to practical application. The principles of operation are discussed briefly and the output voltages illustrated are taken under actual operating conditions at various speeds. The mechanical construction is covered in progressive steps. Various models for both low and high temperature applications are described.

A brief description of the principle of operation of the eddy current of proximity pickup is presented. The operating clearance range is given for various models. A description is given of the use of proximity pickups for counting work parts, for controlling feed and for initiating steps of operation in automated factories.

A Classification System for Measurement and Control—E. A. Keller (p. 38)

This paper describes a new approach for the classification of instruments for measurement and control.

Most of the previous classifications grouped the instruments according to their input and output characteristics, this new classification groups the instruments in terms of precision, dynamic behavior, shelf life, reliability of operation and purchase characteristics; such as cost, availability and volume. Each characteristic is specified by a decimal digit. Each digit number defines the performance of instruments for a specific quality within one order of magnitude.

This classification serves the systems engineers for a selection of compatible instruments to solve a specific problem of measurement or control.

A perforated card system is described permitting the selection of suitable instruments once the performance parameters for a specific problem has been established.

This classification was established for and with the cooperation of the Institute of Radio Engineers Subcommittee 10.3 on Industrial Electronics.

Rapid Volumetric Particle Size Analysis via Electronics—R. H. Berg (p. 46)

A basically new method for sub-sieve particle size analysis is described, with emphasis on the three dimensional nature of the measurement principle. Previous methods are comparatively reviewed, and the role played by electronics in enabling speed and accuracy of the new method is discussed.

By suspending particles in a conductive liquid and causing the suspension to flow through an immersed aperture with electrodes on either side, a series of voltage pulses is produced by the passages of individual particles. This series of pulses is electronically scaled and counted.

Various aspects of basic response, effects of coincident passages and calibration methods are discussed. Applications to a variety of materials are covered, with extension to different forms of data presentation for process control purposes. A number of specific examples are included.

Technique for Automatic Testing Electronic Components—V. W. Walter and S. W. Nelson (p. 53)

The technique for automatic testing of electronic components must be adapted to the requirements for each individual test program. This paper describes the methods employed in instrumenting two test programs. The first involves approximately 75,000 components of four types—resistors, diodes, transistors and capacitors—all being tested for an extended period under environmental and electrical load conditions. The second program, in contrast, describes the parameter measurements which have to be made on small quantities of semiconductor devices under nuclear radiation conditions.

Sonic Gas Analyzers and Their Industrial Uses—Dale I. Steele and Michael Kniazuk (p. 64)

The theory of operation is given for a gas analyzer utilizing the speed of sound for its operation. Sensitivities to traces of common gases in both air and helium are given. When suitable gas chromatography tubes are used with the analyzer, the quantitative analysis of some gas mixtures can be made using peak readings of the analyzer.

The Importance of High-Speed Voltage-to-Digital Translation Equipment for Industrial Data Control—J. F. LaFontaine (p. 68)

There are two basic arguments for the importance of high-speed voltage-to-digital translation equipment in an industrial control system. The first is that early voltage-to-digital conversion is an important step toward overall system reliability. Second, in a system where such equipment is used, in many applications system accuracy can be achieved only through the use of a high-speed converter. The first argument—the one for system reliability—is the more well-known of the two and is therefore considered only briefly. The second argument—system accuracy via high-speed digitization—is treated more fully and is exemplified by descriptions of specific applications of high-speed conversion devices.

Industrial Digital Systems—E. J. Otis (p. 73)

This paper discusses some of the basic reasons why digital equipment, rather than analog equipment, is preferable for logging and control systems. Characteristics of system components such as input multiplexer and digitizer, digital computer, and output devices are

discussed as parts of an integrated, flexible, and reliable industrial data handling and control system. In discussing the functional role played by each of the above system components, broad design criteria are developed for their construction, and operation is demonstrated when controlled by a general-purpose digital computer.

An Electronic Approach to Sortation Control—R. W. Burness (p. 80)

Various sorting operations, such as the sorting of sacked mail in terminals throughout the country, become very complex operations. In order to meet the requirements of complex systems such as these, a rugged, trouble free control system has been developed around computer techniques which give an extremely high degree of versatility. This article describes such a system which has been installed and is now operating in Philadelphia.

Photo-Electric Registration Control Systems—J. C. Frommer (p. 86)

Pulse-Width Control of Transistors—J. N. Van Scoyoc and R. W. Bull (p. 95)

Duty cycle, or pulse width, modulation can be used to advantage in transistor circuits where the desired output is a direct current or slowly varying voltage such as required in proportional control systems. For a prescribed transistor dissipation, several times greater load power can be controlled by this technique than with class A operation. Conversely, for a given load power, the transistor can be operated at lower dissipation and thus at higher temperatures than is permissible with conventional modes of operation. Circuits have been devised for several different types of load circuits and also for signal generation. Combination of the duty-cycle modulation generation and output circuits yields a unique direct current amplifier.

Obtaining Optimum Performance from a Magnetic Thermocouple Amplifier—W. E. Nesbitt (p. 101)

An instrument-type magnetic amplifier is operated with positive feedback to produce high gain. A negative feedback loop then trades this gain to achieve high effective input impedance. The resultant circuit presents negligible loading to a low-impedance thermocouple for use in temperature sensing and control equipments.

Two circuits are analyzed to determine conditions for optimum performance. One circuit has a single-stage amplifier; the other circuit uses a two-stage magnetic amplifier. Amplifier operation is analyzed and the behavior is predicted from the resulting equations. Predicted performance compares favorably with measured performance. The analytical results are used to optimize amplifier parameters and to anticipate the best amplifier for a given circuit.

A typical practical circuit is found to have an error of about 2 per cent when adjusted for an optimum gain of 262.

Design and Development of the Alinco Electronic Integrating System—G. W. Harrison and Harry Stern (p. 115)

The area beneath an analog curve (integral) is often a useful measurement in a host of different fields. However, resolution, inertia, response, and general performance of integrating devices has until now precluded their use in the study of transient and dynamic phenomena. The ALINCO Model 270 Integrating System is an all-electronic integrator invented by Charles M. Minke, ALINCO Production Manager. The heart of the system is a reactance tube oscillator tuned to 100 kc. Using suitable mixers, gates, and programming circuitry, the Model 270 displays elapsed time and total integral on decimal counter units

with high resolution and linearity. Counting begins by preset signal level or by closing contacts, and stops by signal decay, preset time, or by closing contacts.

For transient phenomena, 100 milliseconds would provide 1000 counts for a readability of 0.1%. For long-term phenomena (over 100 seconds), provision has been made for hook-up of accessory counters to count beyond the capacity of the instrument.

In data reduction where analog signals or records are integrated, the Model 270 represents a fast, direct, and more accurate solution, especially where short rise times and rapidly changing amplitudes exist.

Industrial Measurements with X-Rays—J. E. Bigelow (p. 121)

A review is made of the application of x-ray photoelectric effect and scattering to diverse problems of measurement. The basis of operation of thickness and coating weight gages, spectrographic analyzers, diffraction apparatus, and inspection equipment will thereby be shown. It is recognized that many of the measurements now being made with X rays could be made in no other way; thus, it is especially hoped that a useful solution may be suggested for yet unsolved problems.

IRE Professional Group on Industrial Electronics Membership Directory (as of 1 April 1958) (p. 128)

Transducers for Machine Control—J. K. Snell (p. 6)

The paper presents a discussion of the types of analog transducers in use today for the automatic control of machine tools. Mentioned are comparator type transducers as used in tracer heads as well as direct measuring type transducers used for numerical positioning and numerical contouring controls. Types of transducers are classified and discussed from the standpoint of application and expected accuracy.

Nuclear Science

VOL. NS-5, No. 1, JUNE, 1958

Simulation of Hot Channel Boiling in Water-Cooled Reactors—S. O. Johnson, N. J. Curlee, and J. V. Reihing (p. 1)

The problems encountered in a study of the transient response of a heat transfer system in which the coolant experiences a phase change are discussed. The differential equations which govern the system are presented. The analog computer circuit is developed from the equations and the peculiarities of the circuit are described. Analog results of a typical coolant flow transient are presented.

Instrumentation for Fast Neutron Time-of-Flight Studies—R. V. Smith (p. 10)

In connection with a continuing program of fundamental research concerning the scattering of fast neutrons, instrumentation has been developed for measuring the energies of 1-4 mev neutrons by means of their flight time over a one-meter path. Some problems involved in measuring the resultant 30-70 μ sec time intervals with an accuracy of a few per cent are discussed, together with the limitations imposed by intensity considerations, presently available photomultipliers, and known electronic recording techniques. Some results are given showing the spectra of neutrons scattered from a primary energy of 4.3 mev by zirconium, carbon, nickel, aluminum, and chromium.

On the Measurement of Transit Time Dispersion in Multiplier Phototubes—M. H. Greenblatt (p. 13)

In the use of a multiplier phototube to measure short time intervals, the accuracy of the measurement is limited by the statistical deviations in the output pulse from the phototube. These deviations arise from variations in the electron transit time in the phototube. This paper reports a technique by which the transit time dispersion in the tube structure can be measured. A beam of electrons is deflected through an aperture onto the first dynode of the photomultiplier by an rf sweep voltage. The output pulse resulting is examined using the sweep voltage as a time base. Values of the order of 1 μ sec were obtained using three commercial type photomultiplier tubes.

Technique and Measurement of Radiation Background in Albuquerque, New Mexico, During and After the Teapot Series—H. H. Sander and T. B. Cook, Jr. (p. 17)

Radiation background intensity has been monitored in Albuquerque, New Mexico, on a continuous, 24-hour basis since February 1, 1955. This paper describes the techniques used in the measurements. As an example, the increase in total dose received in Albuquerque due to the Teapot tests (atomic test series in Nevada, spring of 1955), over what the dose would have been had there been no tests, is determined to be 4.5 milliroentgens (mr).

Telemetry & Remote Control

VOL. TRC-4, No. 1, JUNE, 1958

The Chairman's Message (p. 1)

A Survey of Progress Reported in 1956 and 1957 in Telemetry and Remote Control—F. E. Rock (p. 2)

Progress in the fields of telemetry and remote control reported during 1956 and 1957 is summarized under the headings: data processing, data storage, digital transmission equipment, millivolt telemeter equipment, multiplexing methods and equipment, radio transmission and systems, remote control, theory and analysis, transducers, and transistorized telemeter equipment.

Correction (p. 9)

A Bibliography of Telemetry—M. V. Kiebert (p. 10)

Space Ship Telemetry—H. Scharla-Nielsen (p. 20)

Application of the Phase-Locked Loop to Telemetry as a Discriminator or Tracking Filter—C. E. Gilchrist (p. 36)

This paper studies a system of FM detection suggested by work done in optimum-demodulation theory, and a summary of the problems of ordinary discriminators is made so that possible improvement may be demonstrated readily. This summary points out an important defect of FM discriminators which affects the data accuracy of the telemeter but which is rarely recognized. The system study deals with generalized optimum filtering for transient signals applicable to commutated signals and operators such as discrimination. The solution for particular applications with respect to the phase-locked loop or optimum-demodulation system is offered. With these applications available, noise and transient signals are studied to see how the system fits the practical system. Normalized charts are made which may be applied to any standard telemetering channel that may be designed. A comparison of this system with ordinary discriminators shows a large threshold improvement and a reduction in over-all system error. Graphs of the comparison of these effects are also included. Heuristic suggestions of application are offered for further study.

Abstracts and References

Compiled by the Radio Research Organization of the Department of Scientific and Industrial Research, London, England, and Published by Arrangement with that Department and the *Electronic and Radio Engineer*, incorporating *Wireless Engineer*, London, England

NOTE: The Institute of Radio Engineers does not have available copies of the publications mentioned in these pages, nor does it have reprints of the articles abstracted. Correspondence regarding these articles and requests for their procurement should be addressed to the individual publications, not to the IRE.

Acoustics and Audio Frequencies.....	1556
Antennas and Transmission Lines.....	1557
Automatic Computers.....	1557
Circuits and Circuit Elements.....	1558
General Physics.....	1560
Geophysical and Extraterrestrial Phenomena.....	1562
Location and Aids to Navigation.....	1562
Materials and Subsidiary Techniques..	1562
Mathematics.....	1566
Measurements and Test Gear.....	1566
Other Applications of Radio and Electronics.....	1566
Propagation of Waves.....	1567
Reception.....	1567
Stations and Communication Systems..	1567
Subsidiary Apparatus.....	1568
Television and Phototelegraphy.....	1569
Transmission.....	1569
Tubes and Thermionics.....	1569

The number in heavy type at the upper left of each Abstract is its Universal Decimal Classification number and is not to be confused with the Decimal Classification used by the United States National Bureau of Standards. The number in heavy type at the top right is the serial number of the Abstract. D.C. numbers marked with a dagger (†) must be regarded as provisional.

ACOUSTICS AND AUDIO FREQUENCIES

- 534.2** 1942
The Scattering of Sound Waves in Inhomogeneous Waveguides—A. D. Lapin. (*Doklady Akad. Nauk S.S.S.R.*, vol. 118, pp. 55-58; January 1, 1958.) Mathematical analysis for a waveguide filled with an inhomogeneous medium which has an average refractive index of about unity. Waveguides with rough interior walls are also examined. See also 3002 of 1957 (Isakovich).
- 534.232-14-8:534.133** 1943
Amplitude of a Quartz Plate Vibrating in Liquids—S. Parthasarathy and Harkrishan Singh. (*Nature, London*, vol. 181, p. 260; January 25, 1958.) The amplitude of vibration of a quartz crystal plate in various liquids calculated according to Vigoureux's formula is compared with the amplitude of the resulting sound wave determined experimentally by a calorimetric method. See 1602 of 1956 (Parthasarathy and Narasimhan).
- 534.41:621.372.543.2** 1944
Active, Adjustable Audio Band-Pass Filter—J. R. Macdonald. (*J. Acoust. Soc. Amer.*, vol. 29, pp. 1348-1356; December, 1957.) A filter having seventh-order Butterworth attenuation characteristics (42 db/octave slopes) is described. Six miniature double triodes and no inductors are used.
- 534.612:061.3** 1945
Sound Level Meter Symposium—(*J. Acoust. Soc. Amer.*, vol. 29, pp. 1330-1341; December, 1957.) A summary is given of 10 papers read at a symposium held by the Acoustical Society of America in New York, May 23-25, 1957, in connection with Com-

The Index to the Abstracts and References published in the PROC. IRE from February, 1957 through January, 1958 is published by the PROC. IRE, May, 1958, Part II. It is also published by *Electronic and Radio Engineer*, incorporating *Wireless Engineer*, and included in the March, 1958 issue of that journal. Included with the Index is a selected list of journals scanned for abstracting with publishers' addresses.

mittee Z24-W-18 of the American Standards Association.

- 534.75** 1946
Comparison of the Auditory Threshold as Measured by Individual Pure Tone and by Békésy Audiometry—W. Burns and R. Hincliffe. (*J. Acoust. Soc. Amer.*, vol. 29, pp. 1274-1277; December, 1957.)
- 534.75** 1947
Threshold of Hearing and Equal-Loudness Relations for Pure Tones, and the Loudness Function—D. W. Robinson and R. S. Dadson. (*J. Acoust. Soc. Amer.*, vol. 29, pp. 1284-1288; December, 1957.) "In connection with standards for audiometry, measurements have been made of the threshold of hearing for pure tones by earphone listening, and these have since been extended to the case of listening in free field. Latterly a redetermination of the equal-loudness relations for pure tones has been completed aimed at resolving discrepancies between former determinations and providing an improved basis for the establishment of a standard set of contours. These results apply to a large team of otologically normal observers, and cover the range from 25-15,000 cps and up to 130 db in sound pressure level."
- 534.75** 1948
Further Observations on Pitch associated with a Time Difference between Two Pulse Trains—W. R. Thurlow. (*J. Acoust. Soc. Amer.*, vol. 29, pp. 1310-1311; December, 1957.) Changing the time separation between two trains of filtered pulses, each at the same basic repetition rate, makes it evident that there is a pitch which is correlated with the magnitude of the time separation. See also 1855 of 1955 (Thurlow and Small).
- 534.76** 1949
An Unexpected Effect in Sound Localization—D. H. Holding and J. P. Dennis. (*Nature, London*, vol. 180, pp. 1471-1472; December 28, 1957.) Tests at 1 kc show that sound localization by human subjects is improved by the wearing of a light cloth cap.
- 534.78** 1950
Further Test of the Constant-Ratio Rule in Speech Communication—F. R. Clarke and C. D. Anderson. (*J. Acoust. Soc. Amer.*, vol. 29, pp. 1318-1320; December, 1957.) "The use of the constant-ratio rule to predict the confusion matrices for each of two five-item subsets given the confusion matrix for a ten-item master set is tested with naive subjects." See also 10 of 1958 (Clarke).

534.78 1951
Effects of Ambient Noise on Speaker Intelligibility for Words and Phrases—J. J. Dreher and J. J. O'Neill. (*J. Acoust. Soc. Amer.*, vol. 29, pp. 1320-1323; December, 1957.) Report of experiments based on a "voice-reflex" effect whereby a speaker with normal hearing unconsciously raises his voice and changes the characteristics of his speech to compensate for the level of noise in which he is speaking.

534.78 1952
Effect of Noise and Filtering on Speech Intelligibility at High Levels—I. Pollack and J. M. Pickett. (*J. Acoust. Soc. Amer.*, vol. 29, pp. 1328-1329; December, 1957.) The effects of a high level of background noise on intelligibility are compared with the effects of filtering.

534.78:621.39 1953
Signal Theory in Speech Transmission—E. E. David, Jr. (IRE TRANS. ON CIRCUIT THEORY, vol. CT-3, pp. 232-244; December, 1956. Abstract, PROC. IRE, vol. 45, pp. 716-717; May, 1957.)

534.78:621.395.623.54 1954
Speech Communication at High Noise Levels: the Roles of a Noise-Operated Automatic Gain Control System and Hearing Protection—I. Pollack. (*J. Acoust. Soc. Amer.*, vol. 29, pp. 1324-1327; December, 1957.) Two aids for hearing conservation, a noise-operated automatic gain control system and an insert ear protection, were evaluated in terms of their effect upon speech intelligibility. At high noise levels, these aids not only do not interfere with the speech intelligibility, they may substantially improve speech intelligibility while affording hearing protection.

534.78:621.395.625.3 1955
Intelligibility Measurements on Transmission Systems using German Logatoms Recorded on Magnetic Tape—W. Wisch. (*Nachricht. Z.*, vol. 7, pp. 342-345; August, 1957.) A method of forming German logatoms is described. The use of tape recordings for subjective tests appears to be advantageous.

534.78:681.188:8.03 1956
Vowel Recognition in Clipped Speech—R. Ahmed. (*Nature, London*, vol. 181, p. 210; January 18, 1958.) In the course of work on speech-input devices for a translation machine a pulse count analysis has been made of vowel sounds in clipped speech. The consistency of the results is illustrated.

534.84 1957
Acoustical Field at Normal Modes in Rooms—T. S. Korn and R. Van de Plas. (*J. Acoust. Soc. Amer.*, vol. 29, pp. 1267-1270; December, 1957.) "The physical form of the acoustical field at normal complex modes in rooms can be represented as a set of elementary curvilinear ducts, each carrying a single stationary wave, satisfying individually the boundary conditions at the walls. In spite of the differences in their lengths, all the ducts resonate at the same nominal frequency."

534.844/.845 1958
Design and Performance of a New Reverberation Room at Armour Research Foundation, Chicago, Illinois—D. R. McAuliffe. (*J. Acoust. Soc. Amer.*, vol. 29, pp. 1270-1273; December, 1957.) The room has a volume of approximately 3000 ft³ and a reverberation time of about 5 seconds. The four walls and ceiling of the room have been splayed. Measurements indicate that the room has a relatively uniform reverberation time with respect to frequency.

534.88 1959
Analysis of a Multiple-Receiver Correlation System—M. J. Jacobson. (*J. Acoust. Soc. Amer.*, vol. 29, pp. 1342-1347; December, 1957.) A theoretical study is made of an acoustic receiving system consisting of two arrays of omnidirectional receivers and one correlator.

621.395.614:546.431.824+31 1960
Laboratory Standard Ceramic Microphone—W. Newitt. (*J. Acoust. Soc. Amer.*, vol. 29, pp. 1356-1365; December, 1957.) Microphones using BaTiO₃ disk ceramics in conjunction with a split-tube diaphragm are adaptable for use at high sound pressures, and for sound measurements in liquids as well as in air. Sensitivities from -86 to -88 db referred to 1 volt per dyne/cm² were obtained and the frequency response was uniform within ±1 db from 10 cps to 30 kc.

621.395.623.74 1961
Principles of Loudspeaker Design and Operation—J. Chernof. (*IRE TRANS. ON AUDIO*, vol. AU-5, pp. 117-127; September/October, 1957. Abstract, *Proc. IRE*, vol. 46, p. 800; April, 1958.)

621.395.625:621.317.76 1962
"Wow" and "Flutter"—Bennett and Currie. (See 2190.)

621.395.625.3:621.397.5 1963
Television Tape Recorder—(See 2244.)

621.395.625.3:621.397.5 1964
Television Recording on Magnetic Tape by the Ampex Method—Braunmühl and Schmidbauer. (See 2245.)

ANTENNAS AND TRANSMISSION LINES

621.315.212.029.63/.64 1965
Variations of Characteristic Impedance along Short Coaxial Cables—J. Allison. (*Proc. IEE*, pt. C, vol. 105, pp. 169-176; March, 1958.) The measured deviations from a harmonic series of the resonance frequencies of a short length of open or short-circuited cable are used to calculate the coefficients of a Fourier series describing the impedance variations along the length of the cable.

621.372.2 1966
Outline of a Theory of Nonuniform Transmission Lines—B. G. Kazansky. (*Proc. IEE*, pt. C, vol. 105, pp. 126-138; March, 1958.) Families of complex differential equations are analyzed and the corresponding two-param-

eter solution curves investigated. The relationship between singular points of the differential equations for the normalized impedance and the nonreflective impedances of the corresponding nonuniform line are established.

621.372.2:621.3.012 1967
Transformation of the Smith Chart through Lossless Junctions—H. V. Shurmer. (*Proc. IEE*, pt. C, vol. 105, pp. 177-182; March, 1958.) The relation between the Smith chart representations of the impedances on either side of a lossless junction is analyzed using complex variables. A chart is derived for transforming circles of constant voltage SWR relating to any plane on one side of the junction, into corresponding circles relating to the corresponding plane on the other side.

621.372.21:621.396.65.029.6 1968
Cable and Radio Links for the Microwave Range—O. Zinke. (*Nachricht. Z.*, vol. 10, pp. 425-430; September, 1957.) A comparison of the suitability and cost of coaxial and waveguide transmission lines for the various frequency ranges used in radio links. The performance of single-wire lines in the range 30-3000 mc is discussed in detail. The alternatives examined are the plain wire (Sommerfeld), the dielectric coated (Goubau) straight line, and helical plain and coated lines.

621.372.8 1969
A Contribution to the Theory of Probes in Waveguides—L. Lewin. (*Proc. IEE*, pt. C, vol. 105, pp. 109-116; March, 1958.) The theory of a probe spanning a rectangular guide and fed by a coaxial line is analyzed in detail in two cases: a) the short-circuit case considering the probe both as a top-short-circuited antenna and also as a waveguide post terminated by the cable impedance; b) a top-loaded probe, terminated by means of a tuning plunger.

621.372.821:621.3.095 1970
Parallel-Plate Transmission Lines and Equivalent Radiators—A. B. Hillan. (*Electronic and Radio Engr.*, vol. 35, pp. 170-173; May, 1958.) It is shown that an infinite plane current sheet has no induction field, and that the radiated field is a faithful reproduction of the current density.

621.372.826+621.396.677 1971
Excitation of Surface Waves—B. Friedinan and W. E. Williams. (*Proc. IEE*, pt. C, vol. 105, pp. 252-258; March, 1958.) "It is shown how to locate a dipole source above a dielectric surface so as either to produce as pure a surface wave as possible or to maximize the amount of energy carried by the surface wave."

621.372.837.3:621.318.134 1972
Some Applications of Ferrites to Microwave Switches, Phasers and Isolators—A. C. Brown, R. S. Cole, and W. N. Honeyman. (*Proc. IRE*, vol. 46, pp. 722-727; April, 1958.) A switch is described which is matched in both states, and also one which can be used at a high repetition rate. The scaling of isolator designs is examined.

621.372.85:537.226:621.315.612.4 1973
Vacuum Breakdown in Dielectric-Loaded Waveguides—G. B. Walker and E. L. Lewis. (*Nature, London*, vol. 181, pp. 38-39; January 4, 1958.) Experiments of the type reported earlier [see 2560 of 1957 (Shersby-Harvie et al.)] were continued with the aim of studying breakdown in TiO₂ dielectric disks. Lead borate enamel is found to be very effective in preventing breakdown.

621.372.85:621.318.134 1974
Cut-Off Phenomena in Transversely Magnetized Ferrites—R. F. Soohoo. (*Proc. IRE*, vol. 46, pp. 788-789; April, 1958.) The cut-off

frequencies are determined for a rectangular waveguide loaded with a lossless ferrite slab, and are checked by experiment.

621.396.67.095.1 1975
Transmission between Aerials of Any Type—K. Baur. (*Frequenz*, vol. 11, pp. 308-312; October, 1957.) Summary of practical formulas for evaluating received power together with definitions of various antenna parameters, covering reception in linearly and elliptically polarized fields.

621.396.673 1976
The Effect of the Ground Constants, and of an Earth System, on the Performance of a Vertical Medium-Wave Aerial—G. D. Monteath. (*Proc. IEE*, pt. C, vol. 105, pp. 292-306; March, 1958.) The compensation theory is used to examine the effect of ground conductivity and of an earth system upon the input impedance, the ground-wave field strength for a given antenna current, and the vertical radiation pattern. If the effective height of the antenna exceeds 0.1λ, an earth system of 0.2λ radius is sufficient for ground of high conductivity and of 0.3-0.4λ radius if of low conductivity. The vertical radiation pattern is not materially affected by the earth system.

621.396.677.029.63 1977
The Design of Decimetre-Wave Wide-Band Directional Aerials with Extremely Small Reflection Coefficient—H. P. Wolff. (*Optik*, vol. 14, pp. 458-473; October, 1957.) Two designs of radiating elements for use at 2 kmc with a bandwidth amounting to 10 per cent of midband frequency and a reflection coefficient less than 2½ per cent are considered. In one design a paraboloidal reflector 3 meters in diameter is fed from a full-wave dipole with the reflector feedback cancelled; in the other a half-wave dipole is fitted but the feedback of the paraboloid is used to match the impedance of the radiator to that of the feeder.

621.396.677.3 1978
A Simplified Derivation of the Fourier Coefficients for Tchebysheff Patterns—J. L. Brown, Jr. (*Proc. IEE*, pt. C, vol. 105, pp. 167-168; March, 1958.) An alternative derivation of Salzer's result (350 of 1957).

621.396.677.6:621.396.933.2 1979
Study of the Feasibility of Airborne H.F. Direction-Finding Antenna Systems—Carter. (See 2096.)

621.372.2 1980
Transmission-Line Theory [Book Review]—R. W. P. King. Publishers: McGraw-Hill Book Co., Inc., London, Eng. 509 pp.; 1955. (*Nature, London*, vol. 180, p. 1443; December 28, 1957.)

AUTOMATIC COMPUTERS

681.142 1981
Digital Codes in Data-Processing Systems—M. P. Atkinson. (*Trans. Soc. Instrum. Tech.*, vol. 9, pp. 124-130; December, 1957.) The design of digital coding systems including error-detecting and error-correcting codes is discussed.

681.142 1982
A New Cycle-Counting Instruction for a Three-Address Electronic Digital Computer—L. Lunelli. (*Ricerca sci.*, vol. 27, pp. 3381-3394; November, 1957.) See also 3757 of 1957 (Dadda).

681.142 1983
An Electrical Apparatus for Solving Polynomial Equations—H. Adler. (*Nachricht. Z.*, vol. 7, pp. 335-342; August, 1957.) The analog equipment described can be used for solv-

ing equations of up to 8th degree with real coefficients.

681.142.:514 1984
Computation of Arc Tan N for $-\infty < N < +\infty$ using an Electronic Computer—E. G. Kogbetliantz. (*IBM J. Res. Dev.*, vol. 2, pp. 43–53; January, 1958.)

681.142:538.221 1985
The Application of Square-Hysteresis-Loop Materials in Digital Computer Circuits—A. D. Holt. (*Electronic Eng.*, vol. 30, pp. 196–199; April, 1958.) "Theories and the practical design of shifting registers are explained. Core matrix storage systems are reviewed. A description is given of a store in which a shifting register is used to convert the parallel output into serial form; this register is also used during the writing process."

681.142:621.374.32 1986
A Decimal Product Accumulator—R. R. Hoge. (*J. Brit. IRE*, vol. 18, pp. 125–132; February, 1958. Discussion, p. 133.) Dekatrons enable the correlation between two series of numbers to be found if all terms are positive. Given pairs of numbers of two decimal digits each, the machine accumulates 100 products per minute.

681.142(410) 1987
British-Built Computers—(*Overseas Engr.*, vol. 31, pp. 167–173; December, 1957.) A review of digital and analog computers with details of specifications, special features, and applications.

CIRCUITS AND CIRCUIT ELEMENTS

621.3.018.7:[621.314.6+621.375.2] 1988
Analysis of Current Pulses—F. G. Heymann. (*Electronic and Radio Engr.*, vol. 35, pp. 165–167; May, 1958.) An approximate method of analysis used earlier (2439 of 1955) is extended to include nonlinear characteristics, and its application to a class-C amplifier circuit is described.

621.3.049.75:621.375.1 1989
Printed Circuits and High-Quality Amplifiers—(*Point to Point Telecommun.*, vol. 2, pp. 18–24; February, 1958.) Printed circuits are suited to equipment where standardization is essential. Inherent in this type of circuitry is improved performance; special production methods are needed to ensure reliability.

621.3.049.75:621.397.62:535.623 1990
Etched I.F. Amplifier Pares Colour TV Cost—Ruth. (See 2248.)

621.311.62:621.3.072.2 1991
Simple Variable-Voltage Power Supply—J. M. Macintosh. (*Short Wave Mag.*, vol. 15, pp. 568–571; January, 1958.) Design details of a circuit giving an output of 0–200 volts at currents up to 60 ma.

621.318.42:538.221:538.566 1992
Electromagnetic Fields in a Ferromagnetic Medium, with Particular Reference to Harmonic Distortion due to Hysteresis—V. G. Welsby. (*Proc. IEE*, pt. C, vol. 105, pp. 218–229; March, 1958.) The frequency dependence of the third-order distortion factor of an inductor at low flux densities is studied theoretically. An analog method is described which enables the study to be extended experimentally to large flux densities and complex input waveforms.

621.318.5 1993
A Numerical-Graphical Method for Synthesizing Switching Circuits—A. H. Scheinman. (*Commun. & Electronics*, no. 34, pp. 687–689; January, 1958.) Economical circuit arrangements can be rapidly developed by systematic

application of three simple rules to a numerical representation of a Boolean function. Simple examples are given.

621.318.57 1994
Minimum-Energy Triggering Signals—L. A. Beattie. (*Proc. IRE*, vol. 46, pp. 751–757; April, 1958.) The optimum signal is defined as that which produces a given current through, or a voltage across, a resistive output element at a given time, while requiring a minimum of energy from the generator. The solution of this problem is discussed and illustrated by a simple case.

621.318.57:621.314.7 1995
Controlled Saturation in Transistors and its Application in Trigger Circuit Design—N. F. Moody. (*Electronic Eng.*, vol. 30, pp. 121–127 and 200–204; March and April, 1958.) Carrier storage of charge in transistors has a maximum which is defined as controlled saturation; this depends only on the base current. This idea is used to develop a trigger circuit of good resolving time whose output terminal is able to handle heavy currents and presents a low impedance.

621.318.57:621.314.7 1996
Fast Transistor Relay—D. L. Anderson. (*Electronics*, vol. 31, p. 145; March 14, 1958.) Describes a push-pull switching circuit incorporating Zener diodes having a rise time of 50 μ sec and capable of handling currents up to 10 a.

621.372.011.1 1997
Generalized Operators for the Approximate Steady-State Analysis of Linear and Nonlinear Circuits—A. J. O. Cruickshank. (*Proc. IEE*, pt. C, vol. 105, pp. 76–87; March, 1958.) The method is a periodic analog of the time-series technique by which waveforms are represented by an n -component operator giving values at each of n ordinates. A shift operator translates any waveform by $1/n$ th of the appropriate sample period. For linear circuits the method is advantageous where the periodic input is known and a similar description of the output is required without recourse to Fourier analysis. For nonlinear circuits the output is obtained by a series of approximations applied to the steady-state condition.

621.372.012:621.391 1998
Signal Theory—W. H. Huggins. (*IRE TRANS. ON CIRCUIT THEORY*, vol. CT-3, pp. 210–216; December, 1956. Abstract, *Proc. IRE*, vol. 45, p. 716; May, 1957.)

621.372.012:621.391 1999
System Theory as an Extension of Circuit Theory—W. K. Linvill. (*IRE TRANS. ON CIRCUIT THEORY*, vol. CT-3, pp. 217–223; December, 1956. Abstract, *Proc. IRE*, vol. 45, p. 716; May, 1957.)

621.372.09 2000
Derivation of the Phase Characteristic from the Attenuation Curve in Minimum-Phase Systems—E. A. Graham. (*Alta Frequenza*, vol. 26, pp. 563–576; October, 1957.) The graphical method described is illustrated by numerical examples.

621.372.412:621.372.54 2001
Stable Crystal Filter is Parallel Resonant—J. C. Seddon. (*Electronics*, vol. 31, pp. 155–157; March 14, 1958.) A high- Q , unbalanced crystal circuit is similar to a parallel-tuned circuit with a low LC ratio over an appreciable frequency range. It is readily adaptable for use in FM oscillators, signal generators and variable-bandwidth filters.

621.372.413 2002
The Concept of Heterogeneous Surface Impedance and its Application to Cylindrical

Cavity Resonators—A. E. Karbowiak. (*Proc. IEE*, pt. C, vol. 105, pp. 1–12; March, 1958.) Formulas are developed relating the Q -factor and the resonant frequency of a cavity to its dimensions and the Fourier components of the surface impedance function. The cases of circumferential and axial heterogeneity are analyzed in detail. In general, a unique value of surface impedance cannot apply to an unbounded periodic sheet unless the period is small compared with λ .

621.372.5 2003
Synthesis of Tchebycheff Impedance-Matching Networks, Filters and Interstages—G. L. Matthaei. (*IRE TRANS. ON CIRCUIT THEORY*, vol. CT-3, pp. 163–172; September, 1956. Abstract, *Proc. IRE*, vol. 45, p. 253; February, 1957.)

621.372.5 2004
Two Theorems Concerning Group Delay with Practical Application to Delay Correction—G. G. Gouriet. (*Proc. IEE*, pt. C, vol. 105, pp. 240–244; March, 1958.) "Two theorems are stated which enable properties of group delay to be expressed directly in terms of the transfer function of a linear transmission system. Examples are given to show how the results might be usefully applied to certain problems of delay correction."

621.372.5:621.374.3 2005
Linear Pulse-Forming Circuits—W. C. Gore and T. Larsen. (*IRE TRANS. ON CIRCUIT THEORY*, vol. CT-3, pp. 182–188; September, 1956. Abstract, *Proc. IRE*, vol. 45, p. 253; February, 1957.)

621.372.5:621.396.96 2006
Synthesis of Delay-Line Networks—D. A. Linden and B. D. Steinberg. (*IRE TRANS., ON AERONAUTICAL AND NAVIGATIONAL ELECTRONICS*, vol. ANE-4, pp. 34–39; March, 1957. Abstract, *Proc. IRE*, vol. 45, p. 1034; July, 1957.) Description of synthesis procedure for delay systems used in processing continuous-trace radar information.

621.372.54 2007
The Network Synthesis on the Insertion-Loss Basis—J. Zdunek. (*Proc. IEE*, pt. C, vol. 105, pp. 259–291; March, 1958.) Methods of synthesis of most important network functions are derived in terms of the steady-state network performance; realization procedures are explained and expressed in explicit formulas for direct application to the design of conventional ladder structures with an arbitrary number of branches. The symmetrical and the inverse-impedance low-pass networks are solved in detail.

621.372.54:621.318.4 2008
Exact Ladder Network Design using Low- Q Coils—L. Weinberg. (*Proc. IRE*, vol. 46, pp. 739–750; April, 1958.)

621.372.6 2009
Conditions for the Impedance and Admittance Matrices of n -Ports without Ideal Transformers—I. Cederbaum. (*Proc. IEE*, pt. C, vol. 105, pp. 245–251; March, 1958.)

621.372.6.012.8:621.396.822 2010
Equivalent Circuits of Noisy Networks—L. Young. (*Electronic Eng.*, vol. 30, pp. 205–207; April, 1958.) Equivalent circuits for a combination of amplifiers, attenuators, and terminations are presented and a new method for the precision measurement of noise figure is described.

621.372.622 2011
Small-Signal Heterodyne Mixers with Excessive Injection Amplitudes—J. F. Cline. (*Commun. & Electronics*, no. 34, pp. 739–745;

- January, 1958.) The theory of small-signal heterodyne mixers operating with very large injection potentials is described. The mixer properties investigated are the conversion transconductance, the relative amplitudes of the difference-frequency and injection-frequency components in the output, and the amplitude of the injection modulation-frequency component in the output in the case where the injection potential is amplitude-modulated to a small degree. A set of universal performance curves is obtained for mixers of a particular class chosen to illustrate the method.
- 621.373.421.13** 2012
VXO—a Variable Crystal Oscillator—H. Shall. (*QST*, vol. 42, pp. 11–15; January 1958.) Description of a stable oscillator which covers the range 3500–4000 kc and uses six crystals.
- 621.373.431.1** 2013
Flip-Flop Stability—T. G. Clark. (*Wireless World*, vol. 64, pp. 212–213; May, 1958.) Modifications to the circuit described earlier (716 of 1958), including the use of a different type of tube, do not affect its stability in respect to pulse duration.
- 621.373.444:621.314.7** 2014
Transient Processes in a Trigger Circuit with a Transistor—N. I. Brodovich. (*Avtomat. i Telemekh.*, vol. 18, pp. 273–279; March, 1957.) Transient processes in a common-base circuit using a point-contact transistor are considered. Expressions for the currents are derived and the speed of operation of the circuit is estimated. Requirements are formulated for point-contact transistors to be used in high-speed trigger circuits. See also 2381 of 1957 (Kuz'min).
- 621.373.444:621.314.7** 2015
High-Sensitivity Transistor Pulse Trigger Circuit—E. Zaglio. (*Nuovo Cimento*, vol. 6, pp. 512–515; September 1, 1957.) (In English.) A Ge diode and a differential negative resistance of high stability consisting of a transistor amplifier with positive feedback is used.
- 621.373.52** 2016
Transistorized RC Phase-Shift Power Oscillator—L. J. Giacoletti. (*IRE TRANS. ON AUDIO*, vol. AU-5, pp. 59–62; May/June, 1957.) Data on the performance of a RC phase-shift circuit operating at frequencies around 1 kc are given.
- 621.375.1:621.396.822** 2017
A Theorem concerning Noise Figures—A. G. Bose and S. D. Pezaris. (*IRE TRANS. ON CIRCUIT THEORY*, vol. CT-3, pp. 190–196; September, 1956. Abstract, *PROC. IRE*, vol. 45, p. 254; February, 1957.)
- 621.375.121.1** 2018
Stagger-Tuned Band-Pass Amplifiers—Y. Peless. (*Electronic and Radio Eng.*, vol. 35, pp. 175–178; May, 1958.) A procedure is given for designing narrow-band amplifiers with specified gain and overshoot when either bandwidth or rise time is specified. Data are included for single-tuned cascades with up to five stages. See also 3774 of 1957 (Peless and Murakami).
- 621.375.126.016.35** 2019
Stability and the Effects of Valve Input Conductance in Wide-Band I.F. Amplifiers—F. Carassa. (*Alla Frequenza*, vol. 26, pp. 550–562; October, 1957.) An analysis of the effects of small variations of circuit parameters and of tube input conductance on amplitude and group-delay response of double-tuned inter-stage amplifiers. See also 2368 of 1957.
- 621.375.13:621.376.23** 2020
Some Studies on Delayed Feedback Circuits—H. Seki. (*Proc. IRE*, vol. 46, pp. 758–763; April, 1958.) By inserting delayed signals along with the main signal to be observed, an improvement in signal/noise ratio can be achieved. Other applications of this circuit are for producing artificial reverberation [see 3476 of 1955 (Axon *et al.*)], as a narrow-band filter, and as a short-time storage circuit.
- 621.375.2:621.317.725** 2021
Bootstrapped Differential Amplifier with Reduced Common-Mode Effects—R. J. Blume. (*Rev. Sci. Instr.*, vol. 29, pp. 122–124; February 1958.) A common-mode signal of ± 35 volts changes the differential gain of the circuit by 0.5 per cent or less. Full-scale deflection can be obtained on a 1-ma 1.5-k Ω recorder with 0.2-volt dc input.
- 621.375.2.029.3** 2022
Push-Pull Audio Amplifier Theory—M. A. Melehy. (*IRE TRANS. ON AUDIO*, vol. AU-5, pp. 86–89; July/August, 1957.) A mathematical analysis is given applicable to all classes of operation of the push-pull amplifier assuming nonlinear tube characteristics.
- 621.375.2.029.3** 2023
Two-Valve Pre-amplifier—C. Hardcastle. (*Mullard Tech. Commun.*, vol. 3, pp. 254–256; January, 1958.) The performance of the amplifier is discussed when used with magnetic and crystal pickups, tape recorder play-back heads, and microphone and radio inputs.
- 621.375.2.029.63** 2024
Straight P.A. for 70 Centimetres—J. A. Plowman. (*Short Wave Mag.*, vol. 15, pp. 595–597; January, 1958.) Design and operating details for a RF amplifier on 430 mc using a double tetrode.
- 621.375.23.029.3** 2025
A Nonlinear Low-Frequency Instability Phenomenon in Audio Amplifiers—T. Usher, Jr. (*Commun. & Electronics*, no. 34, pp. 698–701; January, 1958.) Under certain conditions, AF amplifiers with feedback may show instability at low frequencies, which is not predictable by conventional linear analysis. The problem is analyzed theoretically with supporting experimental results and a technique given for reducing the nonlinear effect.
- 621.375.232.3** 2026
Some Augmented Cathode-Follower Circuits—J. R. Macdonald. (*IRE TRANS. ON AUDIO*, vol. AU-5, pp. 63–70; May/June, 1957.) Direct-coupled cathode-follower circuits with very high input and low output impedance are described, suitable for driver stages (see, *e.g.*, 2888 of 1955), buffer stages and frequency-selective amplifiers.
- 621.375.3** 2027
Magnetic Amplifiers: Basic Principles and Applications—L. W. Stammerjohn. (*Bell Lab. Record*, vol. 36, pp. 16–20; January, 1958.) A basic qualitative description of the principles of operation.
- 621.375.4:621.317.3** 2028
1-kc/s Transistor High-Gain Tuned Amplifier—R. A. Hall. (*Electronic Eng.*, vol. 30, pp. 192–195; April, 1958.) "Particular attention has been paid to stability of gain and bandwidth against transistor variations; over a period of 12 months the maximum gain of about 125 db has changed by only 1.5 db with no measurable change in bandwidth. The amplifier has been designed principally for use as a bridge detector and general-purpose amplifier, but provision has also been made for transistor noise-figure measurements by the addition of a stage at the input in which the transistor under test provides sufficient gain to make the effective noise figure of the amplifier negligible for most purposes."
- 621.375.4.029.3** 2029
A Stable-Gain Transformer-Coupled Transistor A.F. Amplifier—H. Kemhadjian. (*Mullard Tech. Commun.*, vol. 3, pp. 245–251; January, 1958.) The amplifier is designed primarily for use with dc choppers giving a square-wave output at 400 cps. Circuit diagrams are given and the performance is illustrated by graphs. Changes in the transformer design for use at other frequencies are discussed.
- 621.375.4.029.3:621.314.7** 2030
A Transistorized Decade Amplifier for Low-Level Audio-Frequency Applications—A. B. Bereskin. (*IRE TRANS. ON AUDIO*, vol. AU-5, pp. 138–142; September/October, 1957. Abstract, *PROC. IRE*, vol. 46, pp. 800–801; April, 1958.) 1957 National Electronics Conference paper.
- 621.375.4.072** 2031
A Generalized Theory of Transistor Bias Circuits—H. Hellerman. (*Commun. & Electronics*, no. 34, pp. 694–697; January, 1958.) A general method of analyzing bias circuits is presented. Almost all three-terminal bias circuits can be reduced to the same standard form for which the analysis is given. An example from current practice shows the unifying concepts resulting from the general theory.
- 621.375.4.123** 2032
Transistor Amplifier Stages Operating from 6, 9 and 12 V—O. J. Edwards. (*Mullard Tech. Commun.*, vol. 3, pp. 251–253; January, 1958.) A description of low-level stages using a Type-OC71 transistor which can be used to build RC-coupled amplifiers operating in ambient temperatures up to 45°C.
- 621.375.422.029.3** 2033
Direct-Coupled Transistor Audio Amplifier—D. A. G. Tait. (*Wireless World*, vol. 64, pp. 237–239; May, 1958.) Description of a design procedure for a three-stage amplifier in which the collector of one stage is directly connected to the base of the following stage. See 627 of 1958 (Milnes).
- 621.375.9:538.569.4:538.221** 2034
Parametric Amplification using Low-Frequency Pumping—S. Bloom and K. K. N. Chang. (*J. Appl. Phys.*, vol. 29, p. 594; March, 1958.) Describes how low-frequency pumping is possible if two pumping sources are used in conjunction with a nonlinear reactance having an odd-order nonlinearity. An analysis of the equivalent circuit is given.
- 621.375.9:538.569.4:538.221** 2035
A Traveling-Wave Ferromagnetic Amplifier—P. K. Tien and H. Suhl. (*PROC. IRE*, vol. 46, pp. 700–706; April, 1958.) Amplification of signal power can be obtained in a propagating structure which is partially or totally embedded in a ferromagnetic medium. It is shown that one form of the structure possesses two propagating modes and can also support a traveling wave supplied by a local oscillator which provides through the magnetic changes a time-varying coupling between the two propagating modes. The principle of operation is illustrated by a simple transmission-line model.
- 621.375.9:538.569.4.029.64** 2036
Contribution to the Theory of the Molecular Generator—Yu. L. Klimontovich and R. V. Khokhlov. (*Zh. Eksp. Teor. Fiz.*, vol. 32, pp. 1150–1155; May, 1957.) The resonance interaction between an electromagnetic field and a molecular beam, and self-oscillatory processes in a molecular oscillator are investigated for the case of a single-velocity beam. Results obtained taking account of "nonmonochromatic" molecules in the beam are considered qualitatively.

621.375.9:538.569.4.029.64 2037
 Operation of a Three-Level Solid-State Maser at 21 cm—J. O. Artman, N. Bloembergen, and S. Shapiro. (*Phys. Rev.*, vol. 109, pp. 1392–1393; February 15, 1958.) A three-level paramagnetic solid-state maser has been operated both as an amplifier and as an oscillator at 1373 mc. A single crystal of about 1 cm³ of K₃Co(CN)₆ containing 0.5 per cent K₂Cr(CN)₆ as active element is used.

621.375.9:621.385.029.64:537.533 2038
 Parametric Amplification of Space-Charge Waves—Louisell and Quate. (See 2273.)

621.376.2:621.318.134 2039
 The Magnetic Ring Modulator and Demodulator—R. Elsner and L. Pungs. (*Nachricht. Z.*, vol. 10, pp. 436–438; September, 1957.) Advantages and disadvantages are outlined with reference to the equivalent circuit and to a practical modulator for use with a 10-kc carrier frequency.

621.376.32 2040
 Multiplication of Frequency-Modulated Oscillations over an Extremely Wide Frequency Range—H. Schönfelder. (*Frequenz.*, vol. 11, pp. 274–278; September, 1957.) The problem of multiplying in a ratio 1:1000 with a fundamental frequency of 100 kc is discussed with reference to the performance of a serrasoid modulator (279 of 1954). See also 1378 of 1958.

621.376.32:621.318.134 2041
 Frequency Modulation by Inductance Variation: a Magnetically Stable Ferrite Modulator—F. Slater. (*J. Brit. IRE*, vol. 18, pp. 189–204; March, 1958.) The operation of modulators incorporating a reactance tube or a variable inductance is summarized. The losses in the magnetic core of the inductance modulator are considerably reduced by using magnetic ferrites, and details of this type of modulator are given. It can be used in simple variable-frequency circuits up to 500 mc.

621.376.32:621.318.134 2042
 Simple Circuit Stabilizes Ferrite F.M. Modulator—A. B. Przedpelski. (*Electronic Ind.*, vol. 17, pp. 56–57; February, 1958.) Stabilization over a range of frequencies is achieved by the use of an auxiliary fixed-frequency oscillator and associated feedback control circuit.

621.374.32:621.387.4 2043
 Multichannel Pulse Height Analysers [Book Review]—H. W. Koch and R. W. Johnston, eds. Publishers: National Academy of Sciences—National Research Council, Washington, D. C., 1957, 205 pp. (*Nature, London*, vol. 180, p. 1381; December 21, 1957.) Proceedings of an informal conference held at Gatlinburg, Tennessee, September 26–28, 1956.

621.375.4.029.3 2044
 Transistor A.F. Amplifiers [Book Review]—D. D. Jones and R. A. Hilbourne. Publishers: Iliffe & Sons, London, 1957, 152 pp. (*J. Electronics Control*, vol. 4, p. 96; January, 1958.)

GENERAL PHYSICS

530.12 2045
 A Variational Principle for Classical Field Theories—J. Pachner. (*Ann. Physik.*, vol. 19, pp. 353–368; May 10, 1957.)

530.12:537.21 2046
 The Definition of Current Charge and Electric Force in the Unified Field Theory—H. Treder. (*Ann. Physik.*, vol. 19, pp. 369–380; May 10, 1957.)

535.13 2047
 On the Deduction of the Lorentz-Einstein Transformation from Maxwell's Electromagnetic Field Equations—K. Stiegler. (*Proc.*

Phys. Soc., London, vol. 71, pp. 512–513; March 1, 1958.)

535.223:538.566.029.65 2048
 Precision Determination of the Velocity of Electromagnetic Waves—K. D. Froome. (*Nature, London*, vol. 181, p. 258; January 25, 1958.) Using an interferometer of improved performance operating at 72 kmc a value $c_0 = 299,792.50 \pm 0.10$ km has been obtained.

535.376:546.26-1 2049
 Investigations by Microscope and Oscilloscope of the Electroluminescence of Non-conducting Diamonds—E. Krautz and G. Zollfrank. (*Optik, Stuttgart*, vol. 14, pp. 446–457; October, 1957.) The electroluminescence is investigated at field strengths above 10⁶ v/cm. With very strong fields and high current densities graphite whiskers form in the diamond at the electrodes and the electroluminescence is thereby enhanced. Oscillograms indicate that recombination processes are a contributory cause of electroluminescence.

537.12:538.1 2050
 Magnetic Interaction of Electrons and Anomalous Diamagnetism—V. T. Geilikman. (*Zh. Eksp. Teor. Fiz.*, vol. 32, pp. 1206–1211; May, 1957.)

537.311.62 2051
 On the Theory of Skin Effect in Metals—M. Ya. Azbel'. (*Zh. Eksp. Teor. Fiz.*, vol. 32, p. 1259; May, 1957.) The coefficient of electromagnetic wave transmission through a sufficiently thick film is calculated taking into account a small slowly damped addition derived from the evaluation of the spin magnetic moment.

537.312.62 2052
 Critical Current for Superconducting Films—V. L. Ginzburg. (*Doklady Akad. Nauk S.S.S.R.* vol. 118, pp. 464–467; January 21, 1958.) Mathematical analysis of critical currents for superconducting films 10⁻²–10⁻⁶ cm thick.

537.525.6 2053
 Emission Mechanism of Cold-Cathode Arcs—K. G. Hernqvist. (*Phys. Rev.*, vol. 109, pp. 636–646; February 1, 1958.) A new theory is proposed in which excited atoms play a predominant role as a source for ion generation in the vicinity of the cathode surface. The processes of resonance ionization and of ionization in the strong electric field at the cathode surface are considered.

537.533:621.385.032.269.1 2054
 A General Theorem for Dense Electron Beams—A. R. Lucas, B. Meltzer, and G. A. Stuart. (*J. Electronics Control*, vol. 4, pp. 160–164; February, 1958.) A sufficient condition for the existence of any particular set of trajectories is derived for Pierce-type dense electron beams.

537.533.79:537.226.3:538.561 2055
 Energy Loss by a Charged Particle Passing through a Laminar Dielectric: Part 1—Ya. B. Fainberg and N. A. Khizhryak. (*Zh. Eksp. Teor. Fiz.*, vol. 32, pp. 883–895; April, 1957.) A general expression has been obtained for losses of a particle moving in an unbounded laminar medium or a waveguide filled with a dielectric. Polarization losses are examined and an expression for the spectral distribution of parametric Cherenkov radiation is derived.

537.56 2056
 Electron-Electron Interaction and Heat Conduction in Gaseous Plasmas—L. Goldstein and T. Sekiguchi. (*Phys. Rev.*, vol. 109, pp. 625–630; February 1, 1958.) The thermal

conductivity in low-gas-pressure Ne and Xe plasmas has been shown experimentally to be determined chiefly by heat flow in the electron gas of the plasma. The experimentally determined values of the thermal conductivity are in agreement, within less than one order of magnitude, with those given by the theory of Spitzer and Härm (*ibid.*, vol. 89, pp. 977–981; March 1, 1953.)

537.56 2057
 Energy Exchange Between Electron and Ion Gases through Coulomb Collisions in Plasmas—A. A. Dougal and L. Goldstein. (*Phys. Rev.*, vol. 109, pp. 615–624; February 1, 1958.) The general aspects of energy exchange between the electron, ion, and molecular constituent gases and their energy transfer to the boundary have been examined experimentally for a partially ionized gas. Coulomb collisions between electrons and ions are shown to contribute significantly to thermal energy transfer from the electron gas, even in weakly ionized gases. In a plasma produced in Ne gas at 2.25 mm Hg at 300°K, the characteristic time for equipartition of excess mean electron energy with the ion gas varies from 11 to 5μs as the ion concentration increases from 1.6 to 5.8 × 10¹¹ cm⁻³.

537.56 2058
 Theory of Electric Waves in Inhomogeneous Plasmas—K. Kischel. (*Ann. Physik.*, vol. 19, pp. 309–321; May 10, 1957.) Dispersion functions are derived for longitudinal waves in plasmas of variable electron density. The special case of a quasi-neutral electron beam of spatially variable density is discussed.

537.56 2059
 Simplification of Equations for the Distribution Function of Electrons in a Plasma—A. V. Gurevich. (*Zh. Eksp. Teor. Fiz.*, vol. 32, pp. 1237–1238; May, 1957.) An analysis based on the Boltzmann kinetic equation, considering initially a spatially homogeneous plasma located in electric and magnetic fields.

537.56 2060
 Contribution to the Theory of Transport Processes in a Plasma Located in a Magnetic Field—E. S. Fradkin. (*Zh. Eksp. Teor. Fiz.*, vol. 32, pp. 1176–1187; May, 1957.) The mean statistical characteristics such as velocity, heat flow, and stress tensor are determined.

537.56 2061
 Space-Charge, Field Emission and the Ionic Condenser—H. Ritow. (*J. Electronics Control*, vol. 4, pp. 97–110; February, 1958.) High electrostatic fields measured at the electrodes during gas discharge experiments in H indicate that the mechanism initiating a flash of intermittent glow is field emission from the cathode or from the negative space charge. The hypothesis is applied to the experimental results of other workers and is confirmed. It is shown to provide simple explanations for many gas discharge phenomena. It is suggested that the measured high fields are due to concentrated space charges forming ionic condensers with the electrodes or within the gas itself in the form of stationary striations.

537.56:535.33 2062
 Statistical Broadening of Spectral Lines Emitted by Ions in a Plasma—M. Lewis and H. Margenau. (*Phys. Rev.*, vol. 109, pp. 842–845; February 1, 1958.)

537.56:538.566 2063
 Ponderomotive Force in Localized Plasma in the Electromagnetic Field of a Plane Wave—V. V. Yankov. (*Zh. Eksp. Teor. Fiz.*, vol. 32, pp. 926–927; April, 1957.) A sphere of uni-

formly ionized gas is considered as a rough model of localized plasma. The radius of this sphere is smaller than the wavelength of the field in vacuum or in plasma. Expressions for the internal and surface intensities of the ponderomotive force are derived.

537.56:538.566 2064

Excitation of Plasma Oscillations and Growing Plasma Waves—G. D. Boyd, L. M. Field, and R. W. Gould. (*Phys. Rev.*, vol. 109, pp. 1393-1394; February 15, 1958.) Report of preliminary results of a new experiment in which the beam is modulated by a microwave signal before it interacts with the plasma. A very strong interaction is observed which shows essentially the theoretically predicted form of behavior.

537.56:538.63 2065

Movements of Rarefied Plasma in an Alternating Magnetic Field—Ya. P. Terletskii. (*Zh. Eksp. Teor. Fiz.*, vol. 32, pp. 927-928; April, 1957.) An expression is derived showing that even with constant current the energy of rotation of plasma particles can increase many times in consequence of the decrease of the radius.

538.114 2066

Contribution to the Theory of Anisotropy of Ferromagnetic Single Crystals—N. A. Potapkov. (*Doklady Akad. Nauk S.S.S.R.*, vol. 118, pp. 269-272; January 11, 1958.) A mathematical analysis based on Dyson's theory of spin-wave interaction (3696 of 1956) is applied to the investigation of anisotropic ferromagnets of hexagonal symmetry.

538.22:538.569.4 2067

Paramagnetic Resonance and Polarization of Nuclei in Metals—M. Ya. Azbel', V. I. Geraskimenko, and I. M. Lifshits. (*Zh. Eksp. Teor. Fiz.*, vol. 32, pp. 1212-1225; May, 1957.) A theory of paramagnetic resonance is proposed based on simultaneous solutions of Maxwell's equations and the kinetic equation for the density operator. It is shown that the polarization varies with depth and also that the paramagnetic resonance gives rise to selective transparency in metallic films.

538.249 2068

Basic Features of Néel's Theory of Impurity Atom After-Effects—F. Schreiber. (*Z. angew. Phys.*, vol. 9, pp. 203-212; April, 1957.) Exposition in simple terms of Néel's theory of magnetic diffusion after-effects (3072 of 1952). The equivalent circuit of a Bloch wall is derived which allows for the influence of impurity atoms. Thirty-three references.

583:550.38 2069

Two-Dimensional Problems of the Decay of Magnetic Fields in Magnetohydrodynamics—T. G. Cowling and A. Hare. (*Quart. J. Mech. Appl. Math.*, vol. 10, pt. 4, pp. 385-405; November, 1957.) The normal modes of decay of magnetic fields in conducting fluids are studied for different classes of steady motion. See 1328 of 1955 (Bullard and Gellman).

538.56.029.64:531.61 2070

On a Macroscopic Measurement of the Spin of Electromagnetic Radiation—G. Toraldo di Francia. (*Nuovo Cimento*, vol. 6, pp. 150-167; July 1, 1957.) (In English.) The spin of electromagnetic radiation may be deduced from the torque exerted at microwave frequencies by a circularly polarized wave upon a screen which can conduct current only parallel to a given direction [see 354 of 1950 (Carrara)]. Calculations are made of the angular-momentum and scattering cross-sections of the screen, and the feasibility of an accurate experiment is discussed.

538.561:537.122 2071

The Cherenkov Effect in Composite (Isotropic) Media—A. M. Sayied. (*Proc. Phys. Soc., London*, vol. 71, pp. 398-404; March 1, 1958.) A theoretical investigation based on the invariance of Maxwell's equations. The case of two coaxial dielectrics and permeable cylinders with a common cylindrical interface, and a charged particle moving along their common axis is considered. Results are discussed with particular reference to Cherenkov radiation at radio and microwave frequencies. The effect of coherence on the output of the emitted radiation is outlined.

538.561:537.533 2072

Radiation from a Point Charge Moving Uniformly along the Surface of an Isotropic Medium—A. I. Morozov. (*Zh. Eksp. Teor. Fiz.*, vol. 32, pp. 1260-1261; May, 1957.) Energy emitted per unit of time by a particle moving along a surface in a nondispersive medium is calculated. Expressions are derived for relativistic and nonrelativistic conditions and for magnetic and ferrite-type media. See also 1628 of 1955 (Danos).

538.566:535.42 2073

Diffraction by Cylindrical Reflectors—R. Plonsey. (*Proc. IEE*, pt. C, vol. 105, pp. 312-318; March, 1958.) Measurements of the near-zone diffracted field of a cylindrical reflector with a line source at the center agree with calculations using geometrical-optics current. The equivalent line currents give slightly better agreement.

538.566:537.562 2074

The Propagation of Slow Electromagnetic Waves along Inhomogeneous Plasma Layers—W. Oehrl. (*Z. angew. Phys.*, vol. 9, pp. 164-171; April, 1957.) On the basis of Schumann's work (sec. e.g., 712 of 1953) the special case of surface waves in the plasma and the adjoining layers of air is considered.

538.569.4 2075

Molecular-Beam Resonances in Oscillatory Fields of Nonuniform Amplitudes and Phases—N. F. Ramsey. (*Phys. Rev.*, vol. 109, pp. 822-825; February 1, 1958.) The transition probability equations are reduced to forms which are suitable for digital computer calculations. A computer program for the calculation of the shapes of the resonances is described.

538.63 2076

Quantum Theory of Galvanomagnetic Effects—P. N. Argyres. (*Phys. Rev.*, vol. 109, pp. 1115-1128; February 15, 1958.) A study is made of the effect of the quantization of the electron orbits in a magnetic field on the galvanomagnetic properties of an isotropic semiconductor or semimetal in the phonon-scattering range. The conductivity tensor is calculated using the quantum-mechanical density operator. The Hall coefficient and transverse resistivity are studied for a number of different sets of conditions for electron density, magnetic field, and temperature.

539.2 2077

Theoretical Investigation of the Electronic Energy Band Structure of Solids—F. Herman. (*Rev. Mod. Phys.*, vol. 30, pp. 102-121; January, 1958.) A review including sections dealing with a) the elements of energy-band theory, b) the uses of group theory and perturbation theory c) a survey of numerical methods for solving the crystal wave equation, d) examples illustrating complex energy-band structures. A representative list of about 200 references is given. Experimental techniques are discussed by Lax (2078 below).

539.2 2078

Experimental Investigations of the Electronic Band Structure of Solids—B. Lax. (*Rev.*

Mod. Phys., vol. 30, pp. 122-154; January, 1958.) Experiments are discussed which have been of value in contributing to current knowledge of the band structure of many materials of importance at present. The experiments mentioned include those involving the de Haas-van Alphen effect, cyclotron resonance, the galvanomagnetic effect, and infrared absorption. One hundred and seventy-two references.

539.2 2079

Electron Interaction in Solids. General Formulation—P. Nozières and D. Pines. (*Phys. Rev.*, vol. 109, pp. 741-761; February 1, 1958.) A general Hamiltonian formalism is developed to treat from first principles the motion of electrons in solids, including their mutual Coulomb interaction. It is shown that, under suitable circumstances, plasmons (the quanta of the plasma oscillations) represent a well-defined elementary excitation of the solid. The "existence criterion" for plasmons is found to be a high electronic polarizability. After the plasmon modes are separated out, the remaining electron interaction is found to be screened, with a range of the order of the interelectron spacing. The usefulness of this effective Hamiltonian for the calculation of the electronic energy levels and cohesive energy in solids is discussed briefly.

539.2 2080

Electron Interaction in Solids. Collective Approach to the Dielectric Constant—P. Nozières and D. Pines. (*Phys. Rev.*, vol. 109, pp. 762-777; February 1, 1958.) A quantum theory of the dielectric constant for solids of both low and high polarizability is developed from first principles. In the latter case, the approach used is collective in that the long-range part of the electron interaction is described by the plasmon field. Both the static and frequency-dependent dielectric constant are derived. It is shown that the interaction between electrons may be described in terms of the dielectric constant of the solid provided the electrons in question form a small minority group which can be isolated from the much larger majority electron group.

539.2 2081

Electron Interaction in Solids. The Nature of Elementary Excitations—P. Nozières and D. Pines. (*Phys. Rev.*, vol. 109, pp. 1062-1074; February 15, 1958.) Possible elementary excitations in solids are studied with the aid of the general theoretical approach developed in the preceding papers of this series (2079 and 2080 above). Particular attention is paid to the basic theoretical justification for the individual-particle-like elementary excitation ("effective" electrons). It is concluded that good qualitative arguments could now be given for the existence of effective electrons in solids. The presence of an energy gap is shown to be a necessary condition for the existence of strong spatial correlations between minority carriers in solids; and the nature of such correlated minority electron excitations is discussed.

539.2:538.221:621.318.134 2082

Approximate Theory of Ferrimagnetic Spin Waves—T. A. Kaplan. (*Phys. Rev.*, vol. 109, pp. 782-787; February 1, 1958.) "The wave functions and the energy spectrum for the spin-wave problem in a normal spinel are found by means of a straightforward extension of Anderson's approach to antiferromagnetism (*ibid.*, vol. 86, pp. 694-701; June 1, 1952.). Only A-B exchange is assumed to exist, and the calculation is carried to second order in the magnitude of the propagation vector, k . Five distinct energy surfaces (E vs k) are found, two of which are identical, in the classical limit, to the ones previously reported by H. Kaplan (*ibid.*, vol. 86, p. 121; April 1, 1952.)."

GEOPHYSICAL AND EXTRATERRESTRIAL PHENOMENA

- 523.164.3:621.396.11 2083
Propagation of Radio Waves from Cosmical Sources—E. Chvojková. (*Nature, London*, vol. 181, p. 105; January 11, 1958.) A formula is given for the refraction of radio waves reaching the earth's atmosphere from outside. The formula may be applied to waves from artificial earth satellites.
- 523.164.32:523.75 2084
A New Spectral Characteristic in Solar Radio Emission—A. Maxwell and G. Swarup. (*Nature, London*, vol. 181, pp. 36–38; January 4, 1958.) Equipment at Fort Davis, Texas, covers the band 100–580 mc and comprises a 28-foot-diameter parabolic antenna with three broad-band primary arrays coaxially mounted at its focus [see 1126(l) of 1958 (Maxwell, et al.)]. A new type of fast burst having a frequency/time graph in the form of an inverted U and of duration 3–10 seconds is reported, and the possible origin of these bursts is discussed.
- 550.38:523.165 2085
Effective Magnetic Meridian for Cosmic Rays—J. R. Storey, A. G. Fenton, and K. G. McCracken. (*Nature, London*, vol. 181, p. 34; January 4, 1958.) Observations of the cosmic-ray meridian made with neutron intensity monitors at Melbourne, Australia, are reported. Doubts are expressed about the equivalent-dipole theory of the earth's magnetic field [see, e.g., 3721 of 1956 (Simpson et al.)].
- 550.389.2:629.19 2086
Scientific Observations of the Artificial Earth Satellites and their Analysis—H. S. W. Massey and R. L. F. Boyd. (*Nature, London*, vol. 181, pp. 78–80; January 11, 1958.) Report of a discussion held by the Royal Society on November 29, 1957.
- 550.389.2:629.19 2087
Lifetime of an Artificial Russian Satellite—J. A. Fejer. (*Nature, London*, vol. 180, p. 1413; December 21, 1957.) A simple formula for the calculation of lifetime from data on the initial orbit is given. It was applied to observations made at Johannesburg of the Doppler effect on signals received at 40.002 mc from the first Russian satellite.
- 550.389.2:629.19 2088
Interception of Radio Signals Transmitted by the Satellite 'Sputnik I'—P. F. Checacci, V. Russo, and C. Carreri. (*Ricerca sci.*, vol. 27, pp. 3252–3260; November, 1957.) Brief outline of apparatus and methods used; some recordings of the 20 and 40-mc transmissions obtained in Florence are reproduced.
- 550.389.2:629.19 2089
Observations in Australia of Radio Transmissions from the First Artificial Earth Satellite—G. H. Muuro and R. B. White. (*Nature, London*, vol. 181, p. 104; January 11, 1958.) Observations of the strength of 20 and 40-mc signals were made at Bringelly, near Sydney, Australia. The rate of fading appears to be a minimum when the direction of propagation of the wave is nearly perpendicular to the earth's magnetic field.
- 551.510.535 2090
Ionospheric Drift in the F₂ Region near the Magnetic Equator—B. W. Purslow. (*Nature, London*, vol. 181, pp. 35–36; January 4, 1958.) Graphs of the diurnal variations of drift in the F₂ layer based on observations made at Singapore from September, 1953 to August, 1956 suggest that the drift is predominantly in an E-W direction and has a maximum value of about 90 meters per second.
- 551.594.5:621.396.11:551.510.535 2091
Artificial Aurora—(*Electronic and Radio Engr.*, vol. 35, pp. 168–170; May, 1958.) The Luxembourg effect is explained, and the possibility of using it to produce a luminous discharge in the E layer is discussed.
- 551.594.5:621.396.96 2092
Determination of Auroral Height by Radar—R. S. Unwin and M. Gadsden. (*Nature, London*, vol. 180, pp. 1469–1470; December 28, 1957.) Preliminary report of observations made during the I.G.Y. at a radar station erected at 885 feet above sea level at Bluff in the South Island of New Zealand. Echoes have been recorded at 55 mc from heights of about 110 km and ranges up to about 1250 km to the south.
- 551.594.6:621.317.3 2093
Atmospheric Radio Noise—Harwood and Nicolson. (See 2176.)
- LOCATION AND AIDS TO NAVIGATION
- 621.396.663 2094
Cable Symmetry Requirements for Two-Channel Direction Finders—G. Ziehm. (*Frequenz*, vol. 11, pp. 287–294; September, 1957.) The effects of differences in length of the cables connecting d.f. antenna systems to the receiver are investigated. Tolerances for these differences and for matching antennas to the receiver input are evaluated.
- 621.396.93+621.396.96].061.3 2095
Radio Navigational Aids—(*Wireless World*, vol. 64, pp. 210–211; May, 1958.) Digest of papers presented at an IEE Convention held in London, March 27–28, 1958.
- 621.396.933.2:621.396.677.6 2096
Study of the Feasibility of Airborne H.F. Direction-Finding Antenna Systems—P. S. Carter, Jr. (IRE TRANS. ON AERONAUTICAL AND NAVIGATIONAL ELECTRONICS, vol. ANE-4, pp. 19–23; March, 1957. Abstract, PROC. IRE, vol. 45, p. 1034; July, 1957.)
- 621.396.96:621.372.5 2097
Synthesis of Delay-Line Networks—Linden and Steinberg. (See 2006.)
- 621.396.96:621.396.665 2098
The Design of Automatic-Gain-Control Systems for Auto-tracking Radar Receivers—J. C. G. Field. (*Proc. IEE*, pt C, vol. 105, pp. 93–108; March, 1958.) The AGC requirements for conical-scanning-type radars and practical methods of control are reviewed. Design methods are illustrated by a description of the development of a system for a particular fire-control radar and the results of operational trials are briefly described.
- 621.396.969:629.13 2099
Effect of Precipitation on the Design of Radio Altimeters—R. K. Moore. (IRE TRANS. ON AERONAUTICAL AND NAVIGATIONAL ELECTRONICS, vol. ANE-4, pp. 24–29; March, 1957. Abstract, PROC. IRE, vol. 45, p. 1034; July, 1957.) See also 1457 of 1957 (Moore and Williams).
- 621.396.969.3 2100
Atmospheric Angels Mimic Radar Echoes—V. G. Plank. (*Electronics*, vol. 31, pp. 140–144; March 14, 1958.) The false echoes due to atmospheric conditions, insects, or birds are discussed. Echoes due to layers, clouds, wind-carried and other sources are considered, together with meteorological data. Unexplained traces which move rapidly across the screen and then disappear are also mentioned.
- 621.396.969.34:621.396.933.2 2101
The Air Traffic Control Radar Beacon System—D. S. Crippen. (IRE TRANS. ON
- AERONAUTICAL AND NAVIGATIONAL ELECTRONICS, vol. ANE-4, pp. 6–15; March, 1957. Abstract, PROC. IRE, vol. 45, p. 1034; July, 1957.)
- MATERIALS AND SUBSIDIARY TECHNIQUES
- 535.215:546.561 2102
Photoconductivity of Cuprite—A. N. Krongauz, V. K. Lyapidevskii, and Yu. S. Deev. (*Zh. Eksp. Teor. Fiz.*, vol. 32, pp. 1012–1017; May, 1957.) Investigations of the temperature dependence of photoconductivity indicate the occurrence of peaks for both positive and negative photoconductivity [see 2448 of 1954 (Krongauz and Lyapidevskii)]. The combined effects of X rays and visible light depend on the sequence of the illumination processes.
- 535.215:546.817.221:539.23 2103
Quantum Efficiency of Photoconductive Lead Sulphide Films—H. E. Spencer. (*Phys. Rev.*, vol. 109, pp. 1074–1075; February 15, 1958.) By using photoconductivity measurements it is shown that the quantum efficiency of lead sulphide films is almost unity. Mobilities calculated from photoconductivity data agree with mobilities obtained from noise and Hall measurements. It is concluded that noise at room temperature is not photon noise.
- 535.215:546.863.221 2104
Structural Characteristics of Antimony Sulphide Layers—V. N. Vertsner, B. V. Gorbunov, and Ya. A. Oksman. (*Zh. Eksp. Teor. Fiz.*, vol. 32, pp. 957–961; May, 1957.) An electron-diffraction investigation shows that when a layer condenses on a heated backing it consists of an amorphous mass of Sb₂S₃ and a thin surface film of Sb₂O₃. The photosensitivity appears to be determined by the crystalline oxide which acts as an additional trapping center for the current carriers.
- 535.37:[546.472.21+546.482.21]:535.215 2105
De-excitation of ZnS and ZnCdS Phosphors by Electric Fields—H. Kallmann, B. Kramer, and P. Mark. (*Phys. Rev.*, vol. 109, pp. 721–729; February 1, 1958.) The change of photoconductivity of power samples brought about by external ac and dc fields, applied both during and after excitation with ultraviolet light, is described and compared with impedance changes due to irradiation with infrared light. The de-excitation and recovery phenomena observed are explained by a consideration of the distribution of conduction electrons created by the application of the field.
- 535.37:548.52 2106
The Synthesis of Single Crystals of the Sulphites of Zinc, Cadmium and Mercury and of Mercuric Selenide by Vapour-Phase Methods—D. R. Hamilton. (*Brit. J. Appl. Phys.*, vol. 9, pp. 103–105; March, 1958.) Conditions of growth are examined in the light of recent theory.
- 535.376 2107
Electroluminescence of Zinc Sulphoselenide Phosphors with Copper Activator and Halide Coactivators—I. J. Hegyi, S. Larach, and R. E. Schrader. (*J. Electrochem. Soc.*, vol. 104, pp. 717–721; December, 1957.)
- 535.376 2108
Electroluminescence and Field Effects in Phosphors—H. F. Ivey. (*J. Electrochem. Soc.*, vol. 104, pp. 740–748; December, 1957.) A review of the effects of applied electric fields on phosphors with or without other means of excitation. Possible explanations are given in terms of solid-state and semiconductor theories. Eighty-one references.
- 535.376:546.681.18 2109
Grain Boundaries and Electroluminescence

- 537.311.33:546.28:669.046 2132
Heat Treatment of Silicon using Zone-Heating Techniques—H. C. Theuerer, J. M. Whelan, H. E. Bridgers, and E. Buehler. (*J. Electrochem. Soc.*, vol. 104, pp. 721-723; December, 1957.) Donor contamination and changes in lifetime are not necessarily introduced by heat treatment, but may be due to contaminants still left after normal etching and washing processes.
- 537.311.33:546.289 2133
Lifetime Measurements of Minority Carriers Across and Along a Dislocation Wall in a Germanium Crystal—R. R. Hasiguti and E. Matsuura. (*J. Phys. Soc. Japan*, vol. 12, pp. 1347-1351; December, 1957.) The spacing of dislocations in the wall was about 2×10^{-4} cm; the recombination diameter, 2.2×10^{-8} cm. The lifetime measured along the wall was 210 μ s in a sample of mean lifetime 70 μ s. It is suggested that the dislocation wall formed a thin *p*-type layer in an *n*-type crystal.
- 537.311.33:546.289 2134
Radial Variation of Minority-Carrier Lifetime in Vacuum-Grown Germanium Single Crystals—C. A. Hogarth and P. J. Hoyland. (*J. Electronics Control*, vol. 4, pp. 60-62; January, 1958.) Radial variation is found to exist with vacuum-grown crystals, but not with those grown in an inert gas; this has already been found in Si crystals.
- 537.311.33:546.289 2135
Lifetime of the O^+ Excited States in Ge^{70} —H. W. Kendall. (*Phys. Rev.*, vol. 109, pp. 861-862; February 1, 1958.)
- 537.311.33:546.289 2136
Lifetime Measurements of Minority Carriers in Deuteron-Irradiated Germanium Crystals—R. R. Hasiguti, E. Matsuura, and S. Ishino. (*J. Phys. Soc. Japan*, vol. 12, pp. 1351-1354; December, 1957.) Very long lifetimes were measured on the deuteron-irradiated surface of *n*-type crystals which, it is suggested, is due to the formation of a thin *p*-type layer.
- 537.311.33:546.289:538.63 2137
Investigation of the Longitudinal and Transverse Galvanomagnetic Effect in *n*-Type Germanium Single Crystals Cut along the Main Crystallographic Axes—R. G. Annaev and A. Allanazarov. (*Doklady Akad. Nauk S.S.S.R.*, vol. 118, pp. 47-50; January 1, 1958.) Experiments carried out at 29°C on pure *n*-type Ge single crystals show how the conductivity and the galvanomagnetic effect depend on the direction of the crystallographic axes. Results for crystals cut along [100], [110] and [111] axes are shown graphically.
- 537.311.33:546.36.87:539.23 2138
The Optical Absorption, the Photoelectric and Thermal Emission and the Temperature Dependence of the Conductivity of Caesium-Bismuth Layers of Differing Composition—H. G. Clerc and G. Wallis. (*Ann. Physik*, vol. 19, pp. 344-352; May 10, 1957.)
- 537.311.33:546.41.786 2139
Trap Distributions in Calcium Tungstate Single Crystals—J. R. Cook. (*Proc. Phys. Soc., London* 1, vol. 71, pp. 422-429; March 1, 1958.) Thermoluminescence and current "glow" curves were used in the investigation. The resulting trap distribution agrees reasonably well with the results of a theoretical analysis of the photocurrent and phosphorescence decays after irradiation with ultraviolet light or gamma rays from a Co^{60} source.
- 537.311.33:546.47-31 2140
The Influence of Hydrogen on the Electrical Conductivity at the Surface of Zinc Oxide Crystals—G. Heiland. (*Z. Physik*, vol. 148, pp. 15-27; March 4, 1957.) The formation under the influence of hydrogen of two types of high-conductivity layer on ZnO crystals is discussed. For experimental investigation of the influence of an oxygen atmosphere, see 1105 of 1956.
- 537.311.33:546.472.21:548.0 2141
Electronic Energy Bands in ZnS: Potential in Zincblende and Wurtzite—J. L. Birman. (*Phys. Rev.*, vol. 109, pp. 810-817; February 1, 1958.) The nature of the chemical bond in ZnS is discussed and evidence indicating mixed covalent and ionic bonding is reviewed. Calculation shows the crystal potential to be the same for both modifications in two corresponding prominent crystallographic directions.
- 537.311.33:546.472.21:548.0 2142
Electronic Energy Bands in ZnS: Preliminary Results—C. Shakin and J. Birman. (*Phys. Rev.*, vol. 109, pp. 818-819; February 1, 1958.) "Preliminary results of the cellular calculations of electronic energy bands in cubic ZnS have been obtained at three points in the Brillouin zone: Γ , X, A. These results indicate that there is a normal order of states in the valence band, and an energy gap of 6-8 v at $k=(0,0,0)$ corresponding to the $\Gamma_4' \rightarrow \Gamma_1'$ transition." See also 2141 above.
- 537.311.33:[546.623.86+546.682.86] 2143
Influence of the Surface Area on the Type of Conductivity in AlSb and InSb—V. F. Synorov. (*Doklady Akad. Nauk S.S.S.R.*, vol. 118, pp. 483-484 January 21, 1958.) The dependence of the conductivity on grain size is investigated. For grain sizes 2-3 μ the conductivity is very low and with a decrease in grain size conductivity changes from *n* type to *p* type.
- 537.311.33:[546.681.19+546.682.19] 2144
Nuclear Magnetic Resonance in Semiconductors: Part 3—Exchange Broadening in GaAs and InAs—R. G. Shulman, B. J. Wyluda, and H. J. Hrostowski. (*Phys. Rev.*, vol. 109, pp. 808-809; February 1, 1958.) "Nuclear magnetic resonance lines have been observed for the more abundant isotopes of the semiconductors GaAs and InAs. The resonances are broader than expected from nuclear dipolar widths alone. The additional broadening is explained by the indirect nuclear exchange mechanism and is consistent with previous measurements on the homologous semiconductors InSb and GaSb." Part 1: 1107 of 1956 (Shulman *et al.*).
- 537.311.33:546.681.19:546.289 2145
Some Properties of Gallium Arsenide-Germanium Mixtures—D. A. Jenny and R. Braunstein. (*J. Appl. Phys.*, vol. 29, pp. 596-597; March, 1958.) The solubility of Ge in GaAs is probably less than two atomic per cent in spite of the near identity of their crystal parameters. The presence of the maximum soluble amount of Ge reduces the band gap 1.35 ev by about 0.1 ev.
- 537.311.33:546.682.18 2146
Some Properties of Semiconducting Indium Phosphide—W. N. Reynolds, M. T. Lilburn, and R. M. Dell. (*Proc. Phys. Soc., London*, vol. 71, pp. 416-421; March 1, 1958.) "Pure polycrystalline samples of InP have been prepared. Point-contact experiments have shown useful rectification on both *n* and *p*-type samples, as well as transistor effects with power gains up to 20 times. The infrared transmission spectrum has been extended to 20 μ , and the effective mass of electrons has been estimated as 0.02*m*. Previous work on general properties has been revised and extended."
- 537.311.33 2147
The Indium-Selenium System—J. C. Brice, P. C. Newman, and H. C. Wright. (*Brit. J. Appl. Phys.*, vol. 9, pp. 110-111; March, 1958.) Polycrystalline specimens of In_2Se_3 , InSe, and In_2Se were prepared by direct fusion, and their resistivity and spectral absorption characteristics were measured. The first two were found to be semiconductors, but single-phase specimens of the last were not achieved.
- 537.311.33:546.682.86 2148
Avalanche Multiplication and Electron Mobility in Indium Antimonide at High Electric Fields—A. C. Prior. (*J. Electronics Control*, vol. 4, pp. 165-169; February, 1958.) The *I/v* characteristic of InSb has been measured up to field strengths of 800 v/cm. Avalanche multiplication was found to occur at values above 150 v/cm. No variation of electron mobility was found.
- 537.311.33:546.682.86:537.312.8 2149
Magnetoresistance of *n*-Type InSb at 4.2°K—R. B. Broom. (*Proc. Phys. Soc., London*, vol. 71, pp. 470-475; March 1, 1958.) Investigations of specimens prepared by different techniques from single crystals of differing purity indicate that negative magnetoresistance is not a bulk property of the material but is largely due to the method of preparation. Oscillations in the magnetoresistance as a function of magnetic field have been observed in samples with a balanced donor concentration of less than 10^{16} cm $^{-3}$. Results are discussed in detail for two samples.
- 537.311.33:[546.812.241+546.812.231+546.682.87] 2150
Electrical Properties of SnTe, SnSe and InBi at Low Temperatures—K. Hashimoto. (*J. Phys. Soc. Japan*, vol. 12, p. 1423; December, 1957.)
- 537.311.33:546.873.241 2151
Galvanomagnetic Effects in *n*-Type Bismuth Telluride—J. R. Drabble, R. D. Groves, and R. Wolfe. (*Proc. Phys. Soc., London*, vol. 71, pp. 430-443; March 1, 1958.) The resistivity, Hall coefficients, and low-field magnetoresistance coefficients associated with current flow in the cleavage planes have been measured at 77°K, and over the range 100-300°K in the case of resistivity and Hall coefficients. Experimental results are reasonably consistent with a many-valley model of the band structure in which the energy minima are situated on the reflection planes. Evaluation of parameters of this model leads to relations between the two Hall coefficients and the density of carriers, which are used to obtain the conductivity mobility of electrons for current flow in the cleavage planes.
- 537.311.33:621.314.63:537.52 2152
Avalanche Breakdown Voltage in Hemispherical *p-n* Junctions—J. Shields. (*J. Electronics Control*, vol. 4, pp. 58-60; January, 1958.) This voltage is calculated and a critical radius found at which a difference from a plane junction sets in; curves are given for Si *p-n* junctions. See also 3681 of 1957 (Armstrong *et al.*), and 471 of 1956 (Miller).
- 537.32+536.2 2153
Thermal Conductivity and Thermoelectric Phenomena in Metals in a Magnetic Field—M. Ya. Azbel', M. I. Kaganov, and I. M. Lifshits. (*Zh. Eksp. Teor. Fiz.*, vol. 32, pp. 1188-1192; May, 1957.) Asymptotic expressions for the tensors of the thermal conductivity, and Thomson coefficients in a strong magnetic field are derived.
- 538.22 2154
Magnetic Properties of Oxide of Manganese at Temperatures from 20° to 300°K—A. S. Borovik-Romanov and M. P. Orlova. (*Zh. Eksp. Teor. Fiz.*, vol. 32, pp. 1255-1256;

May, 1957.) Graphs show the reciprocal of the magnetic susceptibility as a function of temperature for natural samples of Mn_2O_3 and Mn_3O_4 .

538.221+538.569.4:549.517.13 2155

Maser Action in Ruby—G. Makhov, C. Kikuchi, J. Lambe, and R. W. Terhune. (*Phys. Rev.*, vol. 109, pp. 1399-1400; February 15, 1958.) Brief report on the results of an investigation of the electron-spin resonance properties of ruby; evidence of oscillations and amplification was obtained.

538.221+621.318.1 2156

Conference on Magnetism and Magnetic Materials—(*J. Appl. Phys.*, vol. 29, pp. 237-548; March, 1958.) The texts are given of some 120 papers presented at the conference held in Washington, D.C., November 18-21, 1957, with abstracts of others and an index of authors. Papers are grouped under 13 headings including magnetization reversal and thin films, small particles and permanent magnets, ferromagnetic resonance, magnetic moments and crystal structure of oxides, applications and testing, anisotropy and magnetostriction, magnetization processes, and magnetic apparatus and techniques. Titles of some of the papers are given below; a few others are abstracted separately.

1) Spontaneous Magnetization of some Garnet Ferrites and the Aluminium-Substituted Garnet Ferrites—R. Pauthenet. (pp. 253-255.)

2) Magnetic Resonance of Ferrites with a Compensation Temperature—J. Pauleve. (pp. 259-263.)

3) Static and Dynamic Behaviour of Thin Permalloy Films—D. O. Smith. (pp. 264-273.)

4) Flux Reversal in Thin Films of 82% Ni, 18% Fe—C. D. Olson and A. V. Pohm. (pp. 274-282.)

5) Transverse Flux Change in Soft Ferromagnetics—F. B. Humphrey. (pp. 284-285.)

6) Effects of Heat Treatment of Thin Ferromagnetic Films at Intermediate Temperatures—E. N. Mitchell. (pp. 286-287.)

7) Reversible Rotation in Magnetic Films—R. M. Sanders and T. D. Rossing. (pp. 288-289.)

8) Steady-State and Pulse Measurement Techniques for Thin Magnetic Films in the V.H.F.-U.H.F. Range—D. O. Smith and G. P. Weiss. (pp. 290-291.)

9) Ferromagnetic Resonance and Non-linear Effects in Yttrium Iron Garnet—R. C. LeCraw, E. G. Spencer, and C. S. Porter. (pp. 326-327.)

10) Substitution for Iron in Ferrimagnetic Yttrium-Iron Garnet—M. A. Gilleo and S. Geller. (pp. 380-381.)

11) Measurement of Losses of Magnetic Materials at High Inductions at Frequencies up to 100 Megacycles—I. Bady. (pp. 393-394.)

12) Behaviour of the TE Nodes in Ferrite-Loaded Rectangular Waveguide in the Region of Ferrimagnetic Resonance—W. J. Crowe. (pp. 397-398.)

13) Energy Distribution in Partially Ferrite-Filled Waveguides—J. E. Tompkins. (pp. 399-400.)

14) Miniaturized Resonant Antenna using Ferrites—D. M. Grimes. (pp. 401-402.)

15) Appraisal of Permanent-Magnet Materials for Magnetic Focusing of Electron Beams—M. S. Glass. (pp. 403-404.)

16) Origin and Use of Instabilities in Ferromagnetic Resonance—H. Suhl. (pp. 416-421.)

17) Microwave Frequency-Conversion Studies in Magnetized Ferrites—E. N. Skomal and M. A. Medina. (pp. 423-424.)

18) Spin-Lattice Relaxation Time in Yttrium Iron Garnet—R. T. Farrar. (pp. 425-426.)

19) Ferrimagnetic Resonance in Gado-

linium Iron Garnet—B. A. Calhoun, W. V. Smith, and J. Overmeyer. (pp. 427-428.)

20) Ferromagnetic Resonance in Yttrium Iron Garnet at Low Frequencies—E. G. Spencer, R. C. LeCraw, and C. S. Porter. (pp. 429-430.)

21) Microwave Properties of Polycrystalline Rare-Earth Garnets—M. H. Sirvetz and J. E. Zneimer. (pp. 431-433.)

22) Temperature Dependence of Microwave Permeabilities for Polycrystalline Ferrite and Garnet Materials—J. Nemanich and J. C. Cacheris. (pp. 474-476.)

23) Effect of Cobalt on the Relaxation Frequency of Nickel-Zinc Ferrite—F. J. Schnettler and F. R. Monforte. (pp. 477-478.)

24) Switching Properties of Permalloy Cores of Varying Coercivity—T. D. Rossing and V. J. Korkowski. (pp. 479-480.)

25) Operating Range of a Memory using Two Ferrite Plate Apertures per Bit—M. M. Kaufman and V. L. Newhouse. (pp. 487-488.)

26) Further Development of the Vibrating-Coil Magnetometer—K. Dwight, N. Menyuk, and D. Smith. (pp. 491-492.)

27) Improved Torque Magnetometer—W. S. Byrnes and R. G. Crawford. (pp. 493-495.)

28) Transparent Ferromagnetic Light Modulator using Yttrium Iron Garnet—C. S. Porter, E. G. Spencer, and R. C. LeCraw. (pp. 495-496.)

29) Design of Optimum Inductors using Magnetically Hard Ferrites in Combination with Magnetically Soft Materials—J. T. Ludwig. (pp. 497-499.)

30) Pulse Generator based on High Shock Demagnetization of Ferromagnetic Material—R. W. Kulterman, F. W. Neilson, and W. B. Benedick. (pp. 500-501.)

31) New Magnetic Core Loss Comparator—R. E. Tompkins, L. H. Stauffer, and A. Kaplan. (pp. 502-503.)

32) Skullcap Method for Magnetizing Bowl-Shaped Neutron Magnets—F. X. MacDonough. (pp. 506-507.)

33) Magnetization Reversal by Rotation—P. R. Gillette and K. Oshima. (pp. 529-531.)

34) Optical Properties of Several Ferrimagnetic Garnets—J. F. Dillon, Jr. (pp. 539-541.)

538.221 2157

Domain Wall Motion in Metals—R. W. DeBlois. (*J. Appl. Phys.*, vol. 29, pp. 459-467; March, 1958.) Ferromagnetic domain wall theory is reviewed and a description is given of experimental results of an extension of the Sixtus-Tonks experiment to axial domain wall velocities over 50 km, made possible by use of nearly perfect iron whiskers. Plots of axial velocity vs applied field are nonlinear and in some cases show velocity discontinuities.

538.221 2158

The Effect of Added Titanium and Aluminium on the Magnetic Behaviour of α Ferric Oxide—G. Haigh. (*Phil. Mag.*, vol. 2, pp. 505-520; April, 1957.) The antiferromagnetic transition at -15°C is still observed in synthesized materials for relatively large impurity contents (~ 10 per cent). The magnetic properties of these materials are compared with those of naturally occurring hematites.

538.221 2159

Magnetic Domains in Manganese-Antimony—R. Perthel and W. Andrä. (*Ann. Physik*, vol. 19, pp. 265-267; May 10, 1957.) Domain patterns in Mn_2Sb and $MnSb$ obtained by the Bitter method are reproduced.

538.221 2160

Magnetic Scattering of Thermal Neutrons of a Ferromagnetic or Antiferromagnetic Material near the Curie Point—M. A. Krivoglaз. (*Doklady Akad. Nauk S.S.S.R.*, vol. 118, pp. 51-54; January/February, 1958.) Mathemati-

cal treatment of the thermodynamic theory of magnetic scattering of neutrons.

538.221 2161

Electron-Microscopic Investigation of Magnetic Powder Patterns—W. Schwartze. (*Ann. Physik*, vol. 19, pp. 322-328; May 10, 1957.) The relation of magnetic structure to powder pattern is investigated and a method of preparing specimens is described.

538.221 2162

A Magnetic Heating Effect in Oxidized Nickel Wires—C. Schwink. (*Naturwissenschaften*, vol. 44, pp. 485-486; September, 1957.) An application of the electron-optical shadow technique (1515 of 1956) showing the variation of the position of the effective magnetic pole in Ni wires under strain, after heating with and without an alternating field at temperatures below the Curie point.

538.221:537.312.8 2163

Magnetoresistance Coefficients and their Temperature Dependence in Iron and Silicon-Steel—E. Tatsumoto. (*Phys. Rev.*, vol. 109, pp. 658-662; February 1, 1958.)

538.221:538.569.4 2164

Resonant Modes of Ferromagnetic Spheroids—L. R. Walker. (*J. Appl. Phys.*, vol. 29, pp. 318-323; March, 1958.) The spectrum of modes of oscillation of a ferromagnetic spheroid situated in a uniform dc magnetic field is discussed. It is shown that, for samples of normal size, a part of the spectrum consists of magneto-static modes for which exchange and propagation may be ignored. The analysis presented satisfactorily describes the observed absorption curves.

538.221:538.632 2165

Hall Effect in Ni_3Mn and Fe-Co as a Function of Order—S. Foner, F. E. Allison, and E. M. Pugh. (*Phys. Rev.*, vol. 109, pp. 1129-1133; February 15, 1958.) In Ni_3Mn the values of R_0^* were found to change uniformly from a negative value for a well-ordered sample to a positive value for a disordered sample. This dependence is associated with a Curie-point anomaly. In Fe-Co the values of R_0^* were found insensitive to the degree of atomic ordering and were related to the band structure.

538.221:538.652 2166

A Highly Elastic Magnetostrictive Material—O. Henkel. (*Nachricht. Z.*, vol. 7, pp. 346-350; August, 1957.) Report of investigations on cylindrical specimens consisting of Fe particles suspended in rubber-like substances.

538.221:538.652:539.37 2167

Plastic Deformation and Magnetostriction—G. Rieder. (*Z. angew. Phys.*, vol. 9, pp. 187-202; April, 1957.) A combined theory covering internal stresses due to plastic deformation and magnetostriction is developed. Its practical application with reference to investigations of magnetic properties [e.g., 1825 of 1957 (Kersten) and 2215 of 1957 (Dietrich and Kneller)] gives satisfactory results. Thirty-two references.

538.221:539.1 2168

Polarization of Positrons and Annihilation in Ferromagnetic Materials—S. S. Hanna and R. S. Preston. (*Phys. Rev.*, vol. 109, pp. 716-720; February 1, 1958.) The angular correlation of two-quantum radiation from annihilation of positrons in ferromagnetic media has been investigated as a function of the direction of magnetization. The observed changes in the correlations are attributed to the polarization of positrons emitted from an unpolarized source.

538.221:[621.318.124+621.318.134] 2169

Theory of Magnetostriction and g-factor in

- Ferrites**—N. Tsuya. (*Sci. Rep. Res. Inst. Tohoku Univ., Ser. B*, vol. 8, pp. 161–255; March, 1957.) The theory is based on the Heitler-London approximation. The conclusions are that four mechanisms are mainly responsible for magnetostriction: a) the interplay of spin-orbit interaction with the strain potential; b) classical dipolar interaction; c) the interplay of anisotropic exchange interaction with the strain potential; d) the interplay of intra-spin-spin interaction with the strain potential. The relative importance of the different mechanisms in various ferrites is discussed. Sixty-nine references.
- 538.221:621.318.124** 2170
The Temperature Dependence of the Magnetic Properties of Barium Ferrite—E. Schwabe. (*Z. angew. Phys.*, vol. 9, pp. 183–187; April, 1957.) The characteristics of magnets composed of anisotropic $\text{BaO} \cdot 6\text{Fe}_2\text{O}_3$ are investigated. Tests were made on a loud speaker magnet assembly to determine the demagnetizing forces and to derive the means of minimizing the effects of low-temperature storage on operation. See also 506 of 1957 (Sixtus *et al.*).
- 538.222:538.569.4** 2171
Paramagnetic Absorption at Very High Frequencies of some Mn Salts Located in Parallel Fields—A. I. Kurushin. (*Zh. Eksp. Teor. Fiz.*, vol. 32, pp. 938–939; April, 1957.)
- 538.222:538.569.4** 2172
Paramagnetic Absorption at High Frequencies in Gadolinium Salts in Parallel Fields—A. I. Kurushin. (*Zh. Eksp. Teor. Fiz.*, vol. 32, pp. 727–730; April, 1957.) The internal field constant, the isothermal spin relaxation time, and the dependence of the absorption coefficient on the stationary field strength are derived.
- 548.0:53** 2173
Electrical, Optical and Elastic Properties of Diamond-Type Crystals: Part 2—V. S. Mashkevich. (*Zh. Eksp. Teor. Fiz.*, vol. 32, pp. 866–873; April, 1957.) The vibration spectrum for long waves is investigated. Part 1: 3940 of 1957 (Mashkevich and Tolpygo).
- 621.315.616:539.56** 2174
Brittleness in Polyethylene—I. L. Hopkins. (*Bell Lab. Record*, vol. 36, pp. 5–8; January, 1958.) A qualitative description of the molecular structure responsible for brittleness, and of tests designed to measure material characteristics as the rupture point is approached.
- MATHEMATICS**
- 517.5** 2175
Coefficients for "Decomposition" of Functions into Laguerre-Function Series—J. W. Head and G. M. Oulton. (*Proc. IEE*, pt C, vol. 105, pp. 55–56; March, 1958.) For certain functions a 10-term Laguerre-series approximation may be written down in terms of the value of the function at times proportional to the 10 zeros of the Laguerre function of order 10.
- MEASUREMENTS AND TEST GEAR**
- 621.317.3:551.594.6** 2176
Atmospheric Radio Noise—J. Harwood and C. Nicolson. (*Electronic and Radio Eng.*, vol. 35, pp. 183–190; May, 1958.) Equipment incorporating recent modifications is described for the measurement of the characteristics of atmospheric noise, with main emphasis on very low frequencies. Parameters measured include the average voltage of the noise envelope, the fraction of time for which various voltages are exceeded by the envelope, and the number of excursions of the envelope above various voltage levels.
- 621.317.3:621.314.7** 2177
A Transistor Tester for the Experimental Lab—R. A. Hempel. (*Electronic Ind.*, vol. 17, pp. 58–61; February, 1958.)
- 621.317.3:621.314.7** 2178
A Method for Measuring Transistor Current Gain at Radio Frequencies—F. J. Hyde. (*J. Sci. Instr.*, vol. 35, p. 115; March, 1958.) A null method of measuring complex values of α at frequencies up to tens of megacycles, using simple apparatus, is described.
- 621.317.3:621.314.7** 2179
Transistor Cut-Off Frequency Measurement—L. C. Cripps. (*Proc. IRE*, vol. 46, pp. 781–782; April, 1958.) Considerable advantage may be gained by measuring the alpha cut-off frequency by feeding signals to the base with the emitter grounded, since a value nearer to that for the intrinsic cut-off frequency is obtained.
- 621.317.3:621.396.822:621.372.54** 2180
A Tunable Filter for Use in the Measurement of Excess Noise from Local Oscillators—W. P. N. Court. (*Electronic Eng.*, vol. 30, pp. 208–209; April, 1958.) "A method of forming a filter from available microwave components is described. This filter is tunable over a wide band and need not be removed physically from the circuit when filter action is not required."
- 621.317.3:029.5:621.396.822** 2181
Bridge Method of Measuring Noise in Low-Noise Devices at Radio Frequencies—K. S. Champlin. (*Proc. IRE*, vol. 46, p. 779; April, 1958.) Noise resistances of several hundred ohms can be measured with an over-all error of less than 5 per cent. Errors due to stray coupling and pre-amplifier noise are minimized.
- 621.317.31(083.74)** 2182
Redetermination of the Standard Ampere—(*Tech. News Bull. Nat. Bur. Stand.*, vol. 42, pp. 21–23; February, 1958.) The National Bureau of Standards maintains permanent standards of voltage and resistance from which it is possible to calculate a standard ampere. A comparison with the absolute ampere has recently been made a) using a Pellat-type electro-dynamometer and b) using a current balance. The observed change since 1942 when the last comparison was made is so slight that it may be due to experimental error only.
- 621.317.316:621.372.413.029.64** 2183
Measuring Frequency of X-Band Standard Cavities—W. A. Gerard. (*Electronic Ind.*, vol. 17, pp. 66–70; February, 1958.) A flexible method of measuring cavity frequency is described and the determination of stability, temperature compensation, *etc.*, is discussed.
- 621.317.335.3:029.64** 2184
A Spectrometer Method for Measuring the Electrical Constants of Lossy Materials—J. S. Seeley. (*Proc. IEE*, pt C, vol. 105, pp. 18–26; March, 1958.) The analysis of the propagation of a plane wave at oblique incidence through a strip of lossy material is stated, the behavior being completely represented by the use of a complex refractive index and a complex reflection coefficient. A technique is described for measuring these constants by means of a 1-cm parallel-plate spectrometer.
- 621.317.4** 2185
High-Frequency Magnetic Permeability Measurements using Toroidal Coils—R. D. Harrington and R. C. Powell. (*Proc. IRE*, vol. 46, p. 784; April, 1958.) The results of a previous investigation [3625 of 1954 (Kostyshyn and Haas)] are discussed in relation to the conclusions reached by Schwartz (44 of 1958).
- 621.317.729:621.3.013.2** 2186
An Improved Electromagnetic Analogue—W. T. J. Atkins. (*Proc. IEE*, pt C, vol. 105, pp. 151–154; March, 1958.) A quantitative representation of symmetrical electromagnetic fields is possible enabling dynamic and static effects to be studied.
- 621.317.75:621.395.625.3** 2187
The Magnetic-Tape Oscillograph—W. Reinert. (*Elektrotech. Z.*, vol. 9, pp. 493–498; December 21, 1957.) By means of the process of boundary-displacement recording [1963 of 1952 (Daniels)] oscillograms can be produced on magnetic tape and made visible by the application of iron dust. The design and advantages of such a system are discussed.
- 621.317.755:621.318.57:621.387** 2188
Impulse Voltage Wave Chopping Circuit for Use with a Recurrent Surge Oscilloscope—J. W. Armitage. (*Electronic Eng.*, vol. 30, pp. 186–188; April, 1958.) A hydrogen-filled thyatron is used at voltages up to 2.5 kv.
- 621.317.755:621-526** 2189
An Error-Sampled Sweep-Position Control System—C. H. Knapp, E. Shapiro, and R. A. Thorpe. (*IBM J. Res. Dev.*, vol. 2, pp. 14–35; January, 1958.) Discusses the design of equipment developed for controlling the position of an instantaneous portion of a CRO trace with sufficient precision to permit accurate measurements.
- 621.317.76:621.395.625** 2190
"Wow" and "Flutter"—R. G. T. Bennett and R. L. Currie. (*Electronic and Radio Eng.*, vol. 35, pp. 162–164; May, 1958.) A method of measurement requiring only a stable oscillator and an oscilloscope.
- 621.317.77** 2191
Some Methods of Phase Measurement used in Transfer Function Analysis—D. J. Collins and J. E. Smith. (*Electronic Eng.*, vol. 30, pp. 182–186; April, 1958.) The more conventional systems of measurement are summarized and their limitations are indicated.
- 621.317.77:621.396.11.029.64** 2192
Single Path Phase Measuring System for Three-Centimetre Radio Waves—Thompson and Vetter. (See 2205 below.)
- 621.317.79.087.9:538.632:537.311.33** 2193
A Digital Recording System for Measuring the Electrical Properties of Semiconductors—R. H. A. Carter, D. J. Howarth, and D. H. Putley. (*J. Sci. Instr.*, vol. 35, pp. 115–116; March, 1958.) A modification of the self-balancing potentiometer system described earlier [see 3155 of 1956 (Putley)], whereby measurements can be recorded in digital form on teleprinter tape suitable for feeding directly into an electronic computer.
- OTHER APPLICATIONS OF RADIO AND ELECTRONICS**
- 621.319.2:535.215** 2194
Photoelectrets and the Formation of a Latent Electrophotographic Image—V. M. Fridkin. (*Doklady Akad. Nauk S.S.S.R.*, vol. 118, pp. 273–276; January 11, 1958.) A method similar to xerography using a polarized layer of polycrystalline sulphur 50μ thick is described. A graph shows that the polarization of the electrets after dropping to 40 per cent of its original value remains constant for several hundred hours.
- 621.384.612** 2195
Linear Theory of Synchrotron Oscillations: Part 2—Particle Losses during Acceleration and Tolerance Theory—L. L. Goldin and D. G. Koškarev. (*Nuovo Cimento*, vol. 6, pp. 286–298;

August 1, 1957.) (In English.) Part 1 of the paper is contained in an article on synchrotron oscillations in strong-focusing accelerators noted in 1839 of 1956. See also 2558 of 1957.

621.384.613 2196
Space-Charge Phenomena in a Betatron—H. W. Schmidt. (*Ann. Physik*, vol. 19, pp. 298–303; May 10, 1957.)

621.385.833 2197
The Use of the Electron-Microscope Shadow Method for Studying the Potential Distribution in $p-n$ Junctions—V. N. Vertsner and L. N. Malakhov. (*Doklady Akad. Nauk S.S.S.R.*, vol. 118, pp. 266–268; January 11, 1958.) A resolution of the order of 0.1μ is obtained.

621.398:629.19 2198
Earth-Satellite Telemetry Coding System—R. W. Rochelle. (*Elec. Eng.*, vol. 76, pp. 1062–1065; December, 1957.) Square-hysteresis-loop magnetic materials are used with transistors in magnetically coupled multivibrators. The encoder operates on a time sharing principle and controls AF multivibrators. The length of time these are on, the frequency of oscillation, and the length of time between oscillation periods give the required channels of information with no dead time in the transmitted signal. See also 1844 of 1958 (Matthews).

PROPAGATION OF WAVES

621.396.11 2199
On the Propagation of the Electromagnetic Waves in an Inhomogeneous Atmosphere: Part 2—Y. Nomura and K. Takaku. (*Sci. Rep. Res. Inst. Tohoku Univ., Ser. B*, vol. 8, pp. 61–96; September, 1956.) The integral representation for electromagnetic wave propagation (see Part 1: 250 of 1957) is transformed into the sum of residues at poles, and the intensity of diffracted waves in the geometric-optical shadow is calculated. The inhomogeneous atmosphere causes a marked change in the intensity of the diffracted waves as compared with the homogeneous atmosphere. Expressions are derived for diffracted waves at the boundaries where the medium changes continuously, as well as at the ordinary boundaries where the medium changes discontinuously. For a preliminary report of the work, see 545 of 1956.

621.396.11 2200
June—Vertical and Oblique Incidences—R. Gea Sacasa. (*Rev. Telecommunicación, Madrid*, vol. 11, pp. 2–13; September, 1957.) (In Spanish and English.) A further series of comparisons between IFRB forecasts and those based on the Gea method. See also 1241 of 1958.

523.164.3:621.396.11 2201
Propagation of Radio Waves from Cosmical Sources—Chvojková. (See 2083.)

621.396.11:551.510.535 2202
Single-Hop Propagation of Radio Waves to a Distance of 5300 km—E. Warren and E. L. Hagg. (*Nature, London*, vol. 181, pp. 34–35; January 4, 1958.) Single-hop propagation between Ottawa and Slough associated with reflection at apparent heights of 600–900 km, was observed, e.g., at 1800 GMT on September 11, 1957 for frequencies of 27–33 mc. Records indicate that the one-hop mode occurs with the same reliability as the two and three-hop modes at times between 1200 and 2020 GMT for similar distances and frequencies.

621.396.11.029.45:551.510.53 2203
Observations of Magneto-ionic Duct Propagation using Man-Made Signals of Very Low Frequency—R. A. Helliwell and E. Gehrels. (*Proc. IRE*, vol. 46, pp. 785–787; April, 1958.) Echoes of $\frac{1}{4}$ -second pulse signals from station

NSS in Annapolis, Maryland, on 15.5 kc have been detected with delays up to nearly 1 second at Cape Horn, South America, providing a controlled test of the Eckersley-Storey theory of "whistlers" (see, e.g., 142 of 1954). When observed, the echoes were 10–30 db weaker than the direct wave, and were subject to systematic fading and splitting.

621.396.11.029.62/.63 2204
Guglielmo Marconi and Communication beyond the Horizon—G. A. Isted. (*Point to Point Telecommun.*, vol. 2, pp. 5–17; February, 1958.) Marconi's work on propagation at 30 and 400 mc is reviewed. He showed conclusively that communication could be achieved beyond optical path limits using reflection in the lower atmosphere. His apparatus is described which, although primitive, seemed very effective.

621.396.11.029.64:621.317.77 2205
Single Path Phase Measuring System for Three-Centimetre Radio Waves—M. C. Thompson, Jr. and M. J. Vetter. (*Rev. Sci. Instr.*, vol. 29, pp. 148–150; February, 1958.) A practical system is described for making single-path phase measurements at X-band frequencies over ranges up to about 20 miles with instrumental noise of the order of a fraction of one degree. The techniques for obtaining the necessary transmitter frequency stability of $1:10^9$ are described. The use of such techniques to form a simple microwave repeater system with power gain of the order of 50 db is discussed.

621.396.8 2206
Asymmetry in Long-Distance W/T Circuits—A. M. Humby. (*Wireless World*, vol. 64, pp. 204–207; May, 1958.) An analysis has been made of hourly records of reception conditions on the Montreal-Melbourne circuit for the period 1935–1955, for which both short and long paths are mainly over sea. A seasonal asymmetry is noticed, resulting in a significant fall in performance in the direction which entails reception in local summer. No sharply defined hour of onset of this asymmetry is evident, as was reported for transequatorial land routes [see 3208 of 1956 (Humby and Minnis)].

RECEPTION

621.376.2/.3:621.372.5 2207
The Change of Amplitude Modulation into Frequency Modulation Caused by some Limiter Circuits—E. De Castro and E. Stanghellini. (*Alta Frequenza*, vol. 26, pp. 530–544; October, 1957.) Simple formulas for calculating output phase deviation corresponding to a given input modulation depth are derived. See also 2879 of 1956 (De Castro).

621.376.23:621.372.54 2208
Detection of Pulsed Signals in Noise—H. S. Heaps and A. T. Isaacs. (*Electronic and Radio Engr.*, vol. 35, pp. 190–193; May, 1958.) An analysis of the optimum design of a low-pass filter for the detection of rectangular pulses in a background of white noise. Results are shown graphically.

621.396.62:621.376.3:621.314.7 2209
A Transistorized 150-Mc/s F.M. Receiver—W. J. Giguere. (*Proc. IRE*, vol. 46, pp. 693–699; April, 1958.) A completely transistorized experimental fm communication receiver is described. Diffused-base transistors are used and its frequency range is 152–174 mc. Power consumption is 130 mw and adjacent-channel selectivity is better than 70 db for 60-kc channel spacing.

621.396.621.54 2210
Variable-Selectivity I. F. Stages in Communication Receivers—J. B. Dance. (*Short*

Wave Mag., vol. 15, pp. 572–578; January, 1958.) Design considerations for the construction of an IF unit of variable selectivity for use with an existing receiver.

621.396.662 2211
Sensitive Tuning Indicators—R. Oliver. (*Wireless World*, vol. 64, pp. 235–236; May, 1958.) A note on circuit arrangements for improving the performance of a "magic-eye" tuning indicator, particularly by connecting it to an appropriate screen-grid line or, in the case of fm receivers, in the limiter anode circuit.

621.396.82 2212
Radio Interference: Part 1—Introduction—D. A. Thorn. (*P.O. Elec. Engr. J.*, vol. 50, pt 4, pp. 226–227; January, 1958.) An introduction to a series of six articles which will present a general survey of the subject with emphasis on the telecommunications aspects.

621.396.82 2213
Radio Interference: Part 2—The Post Office Radio Interference System—G. A. C. R. Britton. (*P.O. Elec. Engr. J.*, vol. 50, pt 4, pp. 227–230; January, 1958.) The organization for dealing with interference complaints, the apparatus, and methods used for tracing the interference are described. The main types of apparatus that cause the interference are listed.

621.396.82:621.376.3 2214
Theory of Stronger-Signal Capture in F.M. Reception—E. J. Baghdady. (*Proc. IRE*, vol. 46, pp. 728–738; April, 1958.) The amplitude limiter in fm receivers spreads out the spectrum of the disturbing signals over a range which is often much greater than that of the message modulation. Hence limiting followed by filtering can suppress disturbances considerably ahead of the discriminator stage.

STATIONS AND COMMUNICATION SYSTEMS

621.391 2215
On Nonuniform Sampling of Bandwidth-Limited Signals—J. L. Yen. (*IRE TRANS. ON CIRCUIT THEORY*, vol. CT-3, pp. 251–257; December, 1956. Abstract, *Proc. IRE*, vol. 45, p. 717; May, 1957.)

621.391 2216
Definition of "Bandwidth" and "Time Duration" of Signals which are Connected by an Identity—D. G. Lampard. (*IRE TRANS. ON CIRCUIT THEORY*, vol. CT-3, pp. 286–288; December, 1956. Abstract, *Proc. IRE*, vol. 45, p. 717; May, 1957.)

621.391:519.2 2217
Systems Analysis of Discrete Markov Processes—R. W. Sittler. (*IRE TRANS. ON CIRCUIT THEORY*, vol. CT-3, pp. 257–266; December, 1956. Abstract, *Proc. IRE*, vol. 45, p. 717; May, 1957.) See also 1227 of 1957 (Huggins).

621.391:519.2 2218
Limiting Conditions on the Correlation Properties of Random Signals—G. Kraus and H. Pötzl. (*IRE TRANS. ON CIRCUIT THEORY*, vol. CT-3, pp. 282–285; December, 1956. Abstract, *Proc. IRE*, vol. 45, p. 717; May, 1957.)

621.391:621.376.2 2219
The Theory of Analytic Band-Limited Signals Applied to Carrier Systems—J. R. V. Oswald. (*IRE TRANS. ON CIRCUIT THEORY*, vol. CT-3, pp. 244–257; December, 1956. Abstract, *Proc. IRE*, vol. 45, p. 717; May, 1957.)

621.391:621.376.5 2220
A Study of Rough Amplitude Quantization by means of Nyquist Sampling Theory—B. Widrow. (*IRE TRANS. ON CIRCUIT THEORY*, vol. CT-3, pp. 266–267; December, 1956.

Abstract, Proc. IRE, vol. 45, p. 717; May, 1957.)

621.391:621.396.822 2221
The Penetration of Noise into Communication Channels in the Light of Information Theory—P. Neidhardt. (*Nachricht. Z.*, vol. 7, pp. 419–422; September, 1957.) The reduction of information content by noise is discussed in terms of communication theory particularly as derived by Shannon.

621.396.1 2222
On Channel Spacing—(*Point to Point Telecommun.*, vol. 2, pp. 19–23; October, 1957.) Channel separations of 50 kc are called for in the 80 and 160-mc bands in the United Kingdom. Some of the problems of this and possible smaller separations are discussed briefly.

621.396.2.029.6 2223
Standardizing Microwave Communication Systems—T. Clark. (*Electronic Ind.*, vol. 17, pp. 50–54; February, 1958.) Suggestions by a committee of the Electronic Industries Association for standardization and definition of terms for microwave communication systems.

621.396.3 2224
Automatic Error Correction on H. F. Telegraph Circuits—P. R. Keller. (*Point to Point Telecommun.*, vol. 2, pp. 25–48; February, 1958.) A seven-character three-mark code based on the Van Duuren system recommended by the CCIT is described with respect to error correction. The techniques involved and the basic block diagrams for circuitry are given. Emphasis is placed on the need for fully electronic equipment and an appendix is given on cold-cathode tube circuits.

621.396.3:621.376.4 2225
Kineplex, a Bandwidth-Efficient Binary Transmission System—R. R. Mosier and R. G. Clabaugh. (*Commun. & Electronics*, no. 34, pp. 723–727; January, 1958. Discussion, pp. 727–728.) Description of a high-capacity phase-shift data transmission system which will operate in a single telephone voice band of standard quality or equivalent, and will accept at its input, with suitable conversion, binary data from any source.

621.396.41:621.376.32 2226
F.M. Exciter for Sight or Scatter Systems—A. E. Anderson and H. D. Hern. (*Electronics*, vol. 31, pp. 148–151; March 14, 1958.) The exciter accepts multichannel output of the telephone terminal equipment as a modulating signal and produces an output power of 15 watts from 700 to 1200 mc, and 8 watts from 1700 to 2400 mc. The unit handles 132 voice channels in addition to an order-wire system.

621.396.41:621.396.65 2227
6000-Mc/s Radio Relay System for Broad-Band Long-Haul Service in the Bell System—M. B. McDavitt. (*Commun. & Electronics*, no. 34, pp. 715–722; January, 1958.) The system is designed to transmit telephone messages or color television signals over distances up to 4000 miles. Objectives and requisites of the system and its principal features are described. Details are given of some of the more interesting new components.

621.396.5:621.396.65 2228
An Introduction to "Rural Radio"—C. B. Wooster. (*Point to Point Telecommun.*, vol. 2, pp. 24–28; October, 1957.) Techniques are discussed which permit the full integration of single-channel VHF links with line telephone systems in areas where it is impracticable to erect landlines. The equipment is fairly simple and not very difficult to maintain. A wide range of signaling facilities is available. See 2294 of 1957.

621.396.65 2229
Convention on Radio Links—(*Alla Frequenza*, vol. 26, pp. 321–576; October, 1957.) First of a number of issues covering the proceedings of a convention held in Rome, June 5–8, 1957. Abstracts of some of the papers are given individually; titles of others are as follows:

- 1) The Trends of Telecommunications as Affected by Solid-State Electronic Instrumentation—M. J. Kelly. (pp. 333–345. In English. Discussion, pp. 346–348.)
- 2) Propagation with Horizontal and Vertical Polarization over the Paths Portofino-Monte Beigua and Portofino-Monte S. Nicolao-P. Quarta. (pp. 404–414.)
- 3) Tests of Radio Propagation beyond the Horizon over the Mediterranean—L. Niccolai. (pp. 415–418.)
- 4) Radio Link Italy—Spain for Tropospheric Propagation beyond the Horizon—L. Pallavicino. (pp. 419–427.)
- 5) 6000-Mc/s Radio Relay System for Broad-Band Long-Haul Service in the Bell System—M. B. McDavitt. (pp. 428–446. In English.) See 2227 above.
- 6) Some Problems Experienced in the Establishment of Radio Link Systems—A. W. Montgomery. (pp. 447–462. In English.)
- 7) The Planning of Tropospheric Scatter Systems—K. W. Pearson. (pp. 463–467. In English.)
- 8) Kineplex—P. J. Icenbice and S. R. Crawford. (pp. 468–473. In English.) See 2225 above.
- 9) Calculation of the Intermodulation Noise in F.M. Radio Links for Telephony—B. Peroni. (pp. 502–529.)
- 10) Possibilities and Limitations in the Use of Radio Links comprising Demodulation-Type Repeaters—R. B. Chau. (pp. 545–549. In French.)

621.396.65 2230
Radio Link Milan-Palermo for Sound and Telephony—B. Peroni. (*Alla Frequenza*, vol. 26, pp. 371–388; October, 1957.) Detailed description of the relay system for transmitting the television sound broadcasts of the RAI. Four two-way high-quality sound channels and 12 speech channels are available, and particular attention has been given to the reduction of cross-modulation and noise. For details of the television link, see 2254 below.

621.396.65:621.396.43:621.396.8 2231
The Calculation of Distortion Factors and Noise due to various Types of Distortion in Multichannel F.M. Radio Links—H. Marko. (*Nachricht. Z.*, vol. 10, pp. 450–457; September, 1957.) The discussion is based on the CCIR recommendations for radio-link systems. See also 2232 below.

621.396.65:621.396.43:621.396.822 2232
The Distribution of Noise in Radio Links for Multichannel Telephony Transmission—W. Mansfeld. (*Nachricht. Z.*, vol. 7, pp. 329–335 and 466–472; August and October, 1957.) The characteristics are outlined of a hypothetical 2500-km radio link intended as reference system and based on CCIR specifications. The various types of noise, their origin and elimination are discussed.

621.396.65:621.396.822 2233
Thermal Noise in Multisection Radio Links—B. B. Jacobsen. (*Proc. IEE*, pt C, vol. 105, pp. 139–150; March, 1958.) An investigation of methods for calculating thermal noise in a long radio link when the individual sections are subject to fading. A technique is described for combining the fading statistics from individual sections to obtain the first three moments for

the over-all circuit. This is expressed in terms of an "augmented log-normal distribution," which can readily be translated into the distribution of thermal noise in the complete path. A method is described for synthesizing an over-all circuit distribution from a number of sections with similar fading statistics.

621.396.931:621.395.3 2234
The Probability of Success of a Call over the Swiss Network for Calling Motor Vehicles—E. Wey. (*Tech. Mitt. PTT*, vol. 35, pp. 387–395; September 1, 1957.) Description of the system (see 1159 of 1955) and report on the efficiency of the service based on country-wide field-strength measurements.

SUBSIDIARY APPARATUS

621–52 2235
A Note on the Evaluation of the Response of a Nonlinear Element to Sinusoidal and Random Signals—J. L. Douce. (*Proc. IEE*, pt C, vol. 105, pp. 88–92; March, 1958.) A method is developed based upon a mathematical technique described by Lewis (*Trans. AIEE*, vol. 73, pt 1, pp. 693–700; 1954) which is particularly useful for the analysis of nonlinear control systems. Simple cursors may be constructed to determine the effective gain of the nonlinear unit. The application to hysteretic nonlinearities and the response to random signals is illustrated.

621–52:681.142 2236
Statistical Design Theory for Strictly Digital Sampled-Data Systems—S. S. L. Chang. (*Commun. & Electronics*, no. 34, pp. 702–708; January, 1958. Discussion, pp. 708–709.) Present design theories are based on system response to inputs of known shape, and little attention is given to situations in which only the statistical properties of the inputs are known. The basis of a statistical design theory is presented and applied to the optimum design of a strictly digital system. The new theory forms a close parallel to Wiener's theory of optimum filtering and prediction, and its various manifestations in applications to continuous feed-back control systems.

621–526 2237
A Correlation between the Transient and Frequency Responses in Servomechanisms—Z. J. Jelonek and G. I. Boomer. (*J. Brit. IRE*, vol. 18, pp. 101–114; February, 1958.) Statistical evidence is used to relate time and frequency-response parameters. These empirical relations, together with a new theoretical relation for the delay time, enable the step response to be sketched, given the open-loop response. Some nontypical closed-loop responses may be broken down into two subtransient step responses which are separately determinable.

621–526:519.2 2238
Fundamental Equations for the Application of Statistical Techniques to Feedback-Control Systems—G. A. Biernson. (*IRE TRANS. ON AUTOMATIC CONTROL*, vol. AC-2, pp. 56–78; February, 1957. Abstract, Proc. IRE, vol. 45, p. 572; April, 1957.)

621–526:621.375.4 2239
Direct-Drive Amplifier for Two-Speed Servos—B. E. Orr. (*Electronics*, vol. 31, pp. 146–147; March 14, 1958.) A five-transistor servo amplifier drives a standard motor without using an output transformer. For a two-speed system the amplifier contains a switching circuit incorporating Zener diodes, and a three-stage feedback network.

621.311.68 2240
Automatic Power Plant for Telecommunications Installations—K. J. Bladon. (*Point to Point Telecommun.*, vol. 2, pp. 5–18; October, 1957.) The development of multichannel radio-

telephone services capable of unattended operation for long periods has led to the need for automatic generators of electric power. Some of the factors in the design of Diesel power plants are considered. Both mains standby and dual alternator systems are discussed.

621.314.22 2241
Hot Transformers—(*Engineering, London*, vol. 184, p. 623; November 15, 1957.) Brief note on two experimental types of transformer designed for operation at 500°C. One, housed in an evacuated stainless-steel case, is rated 100 va at 1600 cps, the other is of open construction with a nominal rating of 50 va at 50 cps.

621.314.58:621.373.431.1 2242
Magnetic Inverter uses Tubes or Transistors—C. H. R. Campling. (*Electronics*, vol. 31, pp. 158–161; March 14, 1958.) A means of producing ac from dc. The collector and emitter coil windings of the "on" transistor of a multivibrator are differentially connected across the input voltage so that the drive winding partially determines the frequency of oscillation.

TELEVISION AND PHOTOTELEGRAPHY

621.397.5:535.623 2243
The Analogous Frequency of the Colour Sub-carrier in an Adaptation of the N.T.S.C. System to the 625-Line C.C.I.R. Standard—E. Schwartz. (*Rundfunktech. Mitt.*, vol. 1, pp. 191–195; October, 1957.) The various proposals for a suitable color subcarrier frequency are discussed. Calculation leads to a value of 4.17 ± 0.04 mc, so that 4.2109375 or 4.1015625 mc could be chosen. A symmetrical-sideband system can be adopted if a low subcarrier frequency is used. See also 1878 of 1956 (Below and Schwartz).

621.397.5:621.395.625.3 2244
Television Tape Recorder—(*Electronic and Radio Eng.*, vol. 35, pp. 193–195; May, 1958.) In the "vision electronic recording apparatus" of the BBC, a 20½-inch diameter reel of half-inch magnetic tape played at 200 inch per second provides 15 minutes of program. Three tracks are used simultaneously, two for the video signal and one for sound. The modulation system used, and some electrical and mechanical details, are described.

621.397.5:621.395.625.3 2245
Television Recording on Magnetic Tape by the Ampex Method—H. J. V. Braunmühl and O. Schmidbauer. (*Rundfunktech. Mitt.*, vol. 1, pp. 186–190; October, 1957.) See also 294 of January (Ginsburg).

621.397.6:621.314.7 2246
The Application of Transistors to Television—J. N. Barry and A. E. Jackets. (*J. Television Soc.*, vol. 8, pp. 318–334; October–December, 1957.) After a review of recent progress towards increasing the frequency and power range of transistors, their application to each of the main television circuits is discussed in detail with circuit diagrams. A short note on their suitability in color television apparatus is included, and possible future applications are discussed.

621.397.61.029.63 2247
B.B.C. Band-V Experimental Television Transmission—(*Engineer, London*, vol. 204, pp. 797–798; November 29, 1957.) Details of the transmitter equipment installed at Crystal Palace for tests in the range 470–960 mc, but particularly at a vision frequency of 654.25 mc. An initial series of tests on 405 lines will be followed by 625-line transmissions.

621.397.62:535.623:621.3.049.75 2248
Etched I.F. Amplifier Pares Colour TV Cost—L. Ruth. (*Electronics*, vol. 31, pp. 135–

137; March 14, 1958.) Vane-tuned inductances and rejection traps are etched on the same board as the wiring of a 41-mc IF strip. Design requirements, construction details and performance data are given.

621.397.62:621.314.7 2249
Transistor Television Circuits: Part 2—Scan Output Stages, Video and Signal-Frequency Amplifiers—J. N. Barry and G. W. Secker. (*Wireless World*, vol. 64, pp. 231–235; May, 1958.) Circuit details are given of a complete frame output section for a 17-inch receiver, and the operation of transistors in linear RF amplifiers is discussed. Part 1: 1889 of 1958.

621.397.62.029.63:621.372.632 2250
Television Reception on Band V—H. N. Gant. (*Wireless World*, vol. 64, pp. 244–246; May, 1958.) A converter for use with band-III receivers is described, which incorporates a UHF amplifier stage. A new type of tube with special electrode construction and low anode current is used and a noise factor of about 11 db for the converter is achieved.

621.397.621.2.002.1:535.623 2251
Development Problems of Colour-Television Picture Tubes—I. Bornemann. (*Nachricht. Z.*, vol. 7, pp. 399–404; September, 1957.) The differences in afterglow duration of phosphors for tricolor cathode ray tubes and their effect on color fringing are considered. See also 2930 of 1957.

621.397.7 2252
The New B.B.C. Television Studios in London—A. N. Thomas. (*Rundfunktech. Mitt.*, vol. 1, pp. 169–180; October, 1957.) Illustrated descriptions are given of the lay-out and the equipment of the Riverside studios [see 609 of 1958 (Nickels and Grubb)], the television theater at Shepherds Bush in operation since July, 1957, and the White City television center under construction.

621.397.7 2253
The New Television Studios of the R.A.I. in Rome—L. Sponzilli. (*Rundfunktech. Mitt.*, vol. 1, pp. 181–185; October, 1957.)

621.397.7 2254
Television Radio Link Milan—Palermo—F. Carassa. (*Alta Frequenza*, vol. 26, pp. 349–370; October, 1957.) The wide-band relay link described is 1640 km long and comprises 21 repeater and terminal stations.

621.397.7 2255
The Microwave Television Link Italy—Sardinia—F. Carassa. (*Alta Frequenza*, vol. 26, pp. 389–403; October, 1957.) The system described consists of an oversea link of 238 km length. As a result of propagation tests (1890 of 1957) a carrier frequency of 940 mc, that of the main television network, was chosen; this provides a large bandwidth and facilitates connection to the relay system on the mainland (2254 above).

621.397.7:621.3.018.78 2256
Waveform Distortion in F.M. Television Radio Links—F. Carassa. (*Alta Frequenza* vol. 26 pp. 474–501; October, 1957.) The waveform distortion due to small sinusoidal deviations from the ideal flat amplitude and group-delay response curves is interpreted in terms of echoes. The effect of various response conditions on the CCIR test waveform is investigated. Distortion can be reduced considerably, by means of a video-frequency low-pass filter following the demodulator.

621.397.8 2257
The Influence of Multipath Propagation on the Carrier-Frequency Spectrum of the Tele-

vision Signal—K. Bernath and H. Brand. (*Tech. Mitt. PTT*, vol. 35, pp. 401–412; October 1, 1957.) The case of ideal two-path reception is analyzed and the principal factors controlling the shape of the received spectrum are discussed. Experimental results are compared with computed spectra of received signals for two transmitters and various paths, including a case of almost ideal reflection from an intervening lake, and reception via a long mountainous path. The difficulties likely to arise in the reception of color television signals are examined in the light of statistical investigations of reception in built-up areas.

621.397.8:535.623 2258
The Definition of Picture Quality in Monochrome and Colour Television—P. Neidhardt. (*Nachricht. Z.*, vol. 7, pp. 389–398; September, 1957.) Detailed discussion of the means of assessing picture quality in clearly definable terms. By analogy with information theory the concept of detail entropy is derived and its application extended to the assessment of color image quality. Twenty-nine references.

TRANSMISSION

621.396.61:621.314.7 2259
Transistor Transmitter—L. F. Shaw. (*Wireless World*, vol. 64, pp. 241–243; May, 1958.) A portable all-transistor amateur transmitter for the 160-m band is described.

TUBES AND THERMIONICS

621.314.63:546.28 2260
Determination of the Diffusion Length L and the Inversion Density n_i from the Forward Characteristics of Silicon Alloy Junction-Type Rectifiers—A. Herlet. (*Z. angew. Phys.*, vol. 9, pp. 155–158; April, 1957.) A method of determining L and n_i is derived on the basis of a comparison of experimentally obtained characteristics with theory. See also 598 of 1956.

621.314.63.029.65:546.28 2261
Wafer-Type Rectifiers for Millimetre Waves—W. M. Sharpless. (*Bell Lab. Record* vol. 36, pp. 21–24; January, 1958.) See 1607 of 1957.

621.314.632.209.64:546.681.19 2262
A Gallium Arsenide Microwave Diode—D. A. Jenny. (*Proc. IRE*, vol. 46, pp. 717–722; April, 1958.) The semiconductor properties of GaAs, particularly the high electron mobility and forbidden band gap, besides favorable point-contact rectification characteristics, are of interest for microwave diode applications. Theoretically and experimentally GaAs is potentially superior to Ge and Si in point-contact diodes. Its mixer conversion loss is less, and it should operate at higher temperatures.

621.314.7 2263
Developments in Transistor Electronics—L. B. Valdes. (*J. Electronics Control*, vol. 4, pp. 1–16; January, 1958.) The design theory of point-contact and junction transistors is reviewed. Selected examples illustrate the small-signal and large-signal properties of junction transistors. These phenomena are related to the theory of $p-n$ junctions.

621.314.7 2264
On Carrier Accumulation, and the Properties of Certain Semiconductor Junctions—J. B. Gunn. (*J. Electronics Control*, vol. 4, pp. 17–50; January, 1958.) In a semiconductor near an electrode boundary a situation may arise in which minority carriers are drawn by the electric field towards the boundary, across which they can pass only with difficulty. Carrier accumulation will then develop. It is shown theoretically that where a junction exists between relatively pure and relatively impure

regions of a semiconductor, carrier accumulation should be observable in the lightly doped section. Such a junction is used in a class of devices known as conductance transistors, which can have a large current gain. This gain is calculated in a particular case, together with emitter and collector impedances.

621.314.7 2265

Effects of Low Temperatures on Transistor Characteristics—A. B. Credle. (*IBM J. Res. Dev.*, vol. 2, pp. 54–71; January, 1958.) Describes measurements on a group of similar *p-n-p* alloy-junction transistors made between 0.5 and 5 mc and from room temperature down to that of liquid N₂, leading to simple equivalent networks. Grounded-emitter pulse tests show that, for a given output pulse current, rise time decreases with temperature, and at the temperature of liquid N₂ rise time decreases as the output current pulse increases. A 30-mw, 3-mc transistor can then deliver a 1-a current pulse with a rise time of a few tenths of a microsecond, with a grounded-emitter gain of about 20. Theoretical expressions for the effect of temperature on transistor parameters are evaluated. See also 4041 of 1957 (Uda.)

621.314.7:621.317.3 2266

A Transistor Tester for the Experimental Lab.—Hempel. (See 2177.)

621.314.7:621.317.3 2267

A Method for Measuring Transistor Current Gain at Radio Frequencies—Hyde. (See 2178.)

621.314.7:621.317.3 2268

Transistor Cut-Off Frequency Measurement—Cripps. (See 2179.)

621.314.7:621.318.57 2269

Controlled Saturation in Transistors and its Application in Trigger Circuit Design—Moody. (See 1995.)

621.314.7:621.397.6 2270

The Application of Transistors to Television—Barry and Jackets. (See 2246.)

621.383.032.217.2 2271

Interference Photocathodes of Increased Yield with Freely Variable Maximum Spectral Response—K. Deutscher. (*Naturwissenschaften*, vol. 44, pp. 486–487; September, 1957.) A layer of SbCs₃ covers a wedge of MgF₂ mounted an ac mirror. By investigating this interference system under monochromatic light the relation of photocurrent to the reflecting power of the system was determined. The photoelectric yield is a maximum where the reflection is reduced to a minimum.

621.385.029.6 2272

Stability of an Electron Beam on a Slalom Orbit—J. S. Cook, W. H. Louisell, and W. H. Yocom. (*J. Appl. Phys.*, vol. 29, pp. 583–587; March, 1958.) A study of an electrostatic method of focusing an electron beam in a traveling-wave tube in which the beam traverses a slalom-like orbit between the wires of the slow-wave structure. The equations of motion are solved to find initial conditions for stable orbits. Good agreement is found between the computed and measured current transmitted.

621.385.029.64:537.533:621.375.9 2273

Parametric Amplification of Space-Charge Waves—W. H. Louisell and C. F. Quate. (*Proc. IRE*, vol. 46, pp. 707–716; April, 1958.)

The principle of using a variable reactance to obtain gain can be applied to an electron beam by modulating it at a frequency of twice the signal frequency. The normal space-charge wave breaks into two parts—one growing and one attenuated; either the “slow” or “fast” wave can be amplified. The beam can then be coupled to a slow-wave circuit, in which the “fast” wave can be amplified again. Noise theorems for previous microwave amplifiers deal with the “slow” wave and do not apply here. Lower values for the noise figure should in principle be achieved. See also 1606 of May (Bridges).

621.385.032.213.13 2274

The Conductivity of Oxide Cathodes—G. H. Metson. (*Proc. IEE*, pt C, vol. 105, pp. 183–188 and 189–195; March, 1958.)

Part 3—Movements of Electrolytic Oxygen in a Conventional Diode System—Negative oxygen ions from the cathode, if not completely absorbed at the anode, may return to the cathode and produce reactions analogous to the electrolytic actions of the S-type assembly.

Part 4—Electron Transfer Mechanisms—At temperatures between 850 and 1100° K all the electrons are thermionically emitted at the cathode-core surface and pass through the vacuum interstices of the oxide-cathode matrix; their energy is dissipated uniformly by successive non-elastic collisions with solid oxide particles. Between 290 and 600° K, the mechanism is one of solid-state semiconduction and no thermionic emission takes place. These deductions from experimental results agree with the hypothesis of Loosjes and Vink (3208 of 1950).

Parts 1 and 2: 4072 and 4073 of 1957. Please note change of U.D.C. number.